A neuroimaging study of the neural language network in the preterm infant brain

Salvan, Piergiorgio

Awarding institution:
King's College London

December 2016

King's College London

Division of Imaging Sciences & Biomedical Engineering

A neuroimaging study of the neural language network in the preterm infant brain

Piergiorgio Salvan

Degree

PhD in Neuroscience

Abstract

Language is uniquely human, and represents a fundamental feature of human cognition. However, whether the brain's language network is already present around time of normal birth, or emerges in parallel with the behavioural development of this cognitive function during childhood, remains unclear. Preterm children are at increased risk for cognitive, language, and behavioural impairment. Studying preterm born infants at the time of normal birth therefore represents an opportunity to test hypotheses regarding the ontogeny of the language brain network, and to shed new light on how premature environmental exposure may affect the emergence of neurolinguistic architecture.

Non-invasive in-vivo magnetic resonance imaging represents a powerful tool with which to study quantitatively the developing human brain. Previous neuroimaging studies have shown the presence around the time of normal birth of functional neural correlates of auditory speech processing, suggesting the presence of organized brain architecture at term. Current evidence also suggests that the human brain is particularly sensitive to developmental disruption occurring during the last trimester of gestation, with premature delivery having a long lasting signature on whole-brain architecture and later neurodevelopment.

This thesis aims to 1) test the hypothesis that an adult-like brain language network is already present at the time of normal birth and is linked to cognitive performance at two years; 2) assess the effect of early environmental exposure linked to the degree of prematurity at birth in the relationship between brain and behaviour.

Evidence is provided for the presence at term-equivalent age of adult-like functional/structural language brain features, linked to linguistic and cognitive abilities developed in early childhood, and independent of premature environmental

exposure. This is consistent with the idea that neurolinguistic development is strongly constrained by brain maturation, and depends on the interplay between an initial genetic endowment, driving brain development, and interactions in a favourable socioeconomic environment.

Declaration

This thesis and the work presented herein (with the exception of the complementary genetic analysis) are my own and were conducted at King's College London between October 2013 and December 2016. All sources are appropriately referenced.

Piergiorgio Salvan

Acknowledgements

Firstly and foremost, I would like to thank my supervisors, Professor Serena J Counsell, Professor A David Edwards and Dr Tomoki Arichi, for their guidance, insight and enthusiasm. Their support and encouragement have been fundamental over the years.

I am particularly thankful to the Medical Research Council (MRC) for funding my studies and allowing me to pursue a doctoral thesis. I would also like to express my thanks to the Oxford Centre for Functional MRI of the Brain (FMRIB) and its Graduate Programme that represented a fundamental part of my training.

I am grateful to the families, clinicians and investigators who made the ePrime study possible. I would also like to express my thanks to colleagues and friends at the Centre for the Developing Brain for their support and discussion.

Finally, special thanks to my family, who has been a constant source of support, and to Indy and Alessia for being part of this journey with me.

Contents

List of Figures

List of Tables

List of Abbreviations

ACC Anterior cingulate cortex

ADC Apparent diffusion coefficient

AFNI Analysis of functional neuroimages

ANTs Advanced normalization tools

ARD Automatic relevance determination

ATP Adenosine triphosphate

BOLD Blood oxygen level dependent

BSID Bayley scales of infant and toddler development

BT between-module

CCA Canonical correlation analysis

CSD Constrained spherical deconvolution

CSF Cerebro-spinal fluid

DTI Diffusion tensor imaging

DTI-TK Diffusion tensor imaging toolkit

DWI Diffusion-weighted imaging

DMN Default mode network

EPI Echo-planar imaging

EEG Electroencephalography

ePrime Evaluation of preterm imaging study

FA Fractional anisotropy

FIX FMRIB's ICA-based X-noiseifier

FLICA FSL’s linked ICA

fMRI Functional magnetic resonance imaging

FSL FMRIB’s software library

FWE Family-wise error

FWHM Full-width-at-half-maximum

GA Gestational age

GLH Germinal layer haemorrhage

GLM General linear model

GRE Gradient echo

GWAS Genome-wide association studies

HARDI High angular resolution diffusion imaging

Hb Haemoglobin / d-Hb deoxygenated haemoglobin

HMM Hidden Markov model

ICA Independent component analysis

ITG Inferior temporal gyrus

ITK-N4 Insight segmentation and registration toolkit-N4

IVH Intraventricular haemorrhage

JAG Joint association of genetic variants

MEG Magnetoencephalography

MFG middle frontal gyrus

MELODIC Multivariate exploratory linear optimized decomposition into independent components

M1S1 Primary sensori-motor cortex

MD Mean diffusivity

MR Magnetic resonance

MRI Magnetic resonance imaging

MSE mean-squared-error

MTG Middle temporal gyrus

NIRS Near-infrared spectroscopy

NMR Nuclear magnetic resonance

ODF Orientation density function

OLS Ordinary least squares

PARCAR Parent report of children's abilities revised

PCA Principal component analysis

PLS Partial least squares

PMA Postmenstrual age

PVL Periventricular leukomalacia

PT Planum temporale

RF Radio-frequency

RMS-FD Root mean square frame-wise displacement

RSN Resting-state network

ROI Region-of-interest

SD Standard deviation

SES Socioeconomic score

SLI Specific language impairment

SMA Supplementary motor area

SMG Supramarginal gyrus

SNP Single nucleotide polymorphism

SNR Signal-to-noise ratio

ST Strength

STG Superior temporal gyri

STS Superior temporal sulcus

SVZ Subventricular zone

TBSS Tract-based spatial statistics

TE Echo time

TR Repetition time

VZ Ventricular zone

WT within-module

Conference abstracts and Presentations

The work described in this thesis has been presented at the following meetings:

Salvan P., et al. “Language ability in children born preterm is associated with arcuate fasciculus microstructure at term equivalent.” 2016 Society for Neurobiology of Language in London, UK.

Salvan P., et al. “Temporal-spatial organization of the neonatal brain is associated with neurodevelopmental outcome.” 2016 Organization for Human Brain Mapping in Geneva, Switzerland.

Salvan P., et al. “Language ability in children born preterm is associated with arcuate fasciculus microstructure at term equivalent.” 2016 Paediatric Academic Societies Annual Meeting in Baltimore, MD.

Salvan P., et al. “Early maturation of the auditory resting state network in the neonatal period.” 2015 Paediatric Academic Societies Annual Meeting in San Diego, CA.

Salvan P., et al. “Functional and structural alterations to the learning and memory circuit in adults born very preterm." 2013 Paediatric Academic Societies Annual Meeting in Washington DC.

Chapter 1

Introduction

Background and motivation

This thesis focuses on the ontogeny of the language network in the human brain. In this work I study the functional and structural architecture of an adult-like language brain network in a cohort of preterm infants at the time of normal birth; the relationship with linguistic and cognitive abilities at 20 months corrected age; and the effect of premature environmental exposure on this relationship.

But why study language brain organization before the formal appearance of organised efficient speech? Language is uniquely human, and represents a fundamental evolutionary achievement of human cognition (Berwick *et al.*, 2013; Skeide and Friederici, 2016). Nevertheless the precise neural mechanisms that allow human infants to develop this high-order cognitive function remain unclear (Kuhl, 2004, 2010; Dehaene-Lambertz and Spelke, 2015; Skeide and Friederici, 2016). Understanding the typical developmental trajectory of the human brain's cognitive networks is important for computational models of real-life behaviour and cognitive development, and ultimately to understand how they are altered in disease.

Shortly after birth, infants already demonstrate basic linguistic abilities, including discriminating close phonemes (Dehaene-Lambertz and Pena, 2001) and sentences from different languages (Mehler *et al.*, 2002). Previous neuroimaging studies using task-based electroencephalography (EEG), functional-magnetic resonance imaging

(MRI), and near-infrared spectroscopy (NIRS) have focused on these acoustic-phonological features, highlighting how in early infancy the passive listening of speech evokes specific neural correlates (Dehaene-Lambertz *et al.*, 2006; Perani *et al.*, 2011; Gómez *et al.*, 2014). By showing that preterm infants imaged between 28–33 weeks of gestational age display some neural correlates similar to 'mismatch' responses in the temporal and frontal cortices (Mahmoudzadeh *et al.*, 2013), these studies have further provided evidence of the early onset of the human brain organization. The fact that consonant speech boundaries (lying at high frequencies starting at around 300 Hz) are strongly attenuated in utero (Partanen *et al.*, 2013; Gómez *et al.*, 2014), argues against the idea that early phonological skills are solely the result of prenatal environmental experience. These results thus suggest that the human brain possesses a certain experience-independent bias toward the auditory-perceptual processing of speech input, sensitivity that in turn is argued might facilitate later language development (Gervain *et al.*, 2008). However, whether an adult-like language network is already present in the neonatal brain remains unclear. Furthermore, whether its early architecture relates to the most remarkable accomplishments of human learning during the first two years of life, such as the efficient acquisition of the native language attributes and the mastering of the combinatorial properties of language (Dehaene-Lambertz and Spelke, 2015), remains unknown.

Preterm born children have impaired linguistic ability when compared to their term-born peers (Vohr, 2014); impairment that seems to persist as linguistic delay throughout childhood (van Noort-van der Spek *et al.*, 2012) but to catch-up in receptive vocabulary during adolescence (Luu *et al.*, 2009, 2011). Studying this population therefore provides a unique opportunity to test hypotheses concerning infant brain mechanisms linked to language acquisition and to assess the

environmental effects of early life exposure. Previous studies have shown that speech perception abilities in preterm infants are not more advanced than those of age-matched full-term infants at the end of the first year of life, suggesting that early environmental exposure does not accelerate speech emergence, and that human brain development represents a key constraint in the early stages of language acquisition (Peña *et al*., 2010, 2012). These findings indicate that the early sensitivity to the linguistic environment results from the presence of an experience-independent organization in the infant human brain, and that early linguistic exposure following premature birth does not accelerate the development of phonological skills.

However, one may suggest that focusing exclusively on the neural architecture responsible for early acoustic-phonological abilities may be suboptimal for understanding the emergence of language neural architecture as a whole. It may be argued that considering a more holistic approach, such as that of "developmental cognitive neuroscience" (Johnson and De Haan, 2015), would be more appropriate. In this perspective, possible trajectories of neurolinguistic development are defined by the joint influence of bidirectional environmental interactions and developmental constraints in the complex architecture of the whole-brain, and not just in a finite set of regions "active" during some task.

In this thesis I challenge previous models regarding the ontogeny of language in the human brain (Perani *et al.*, 2011; Skeide and Friederici, 2016). Specifically, I challenge the assumption that the early emergence of language abilities mainly relies on the bilateral organization of the temporal cortices, thus only enabling bottom-up processing up to the third year of life. I hypothesise the presence at the time of normal birth, of organized resting-state functional and structural connectivity between regions resembling an adult-like brain language network (such as between

temporal and prefrontal areas); and a relationship between these neural features and later complex language abilities. This model postulates the possibility of neonatal brain architecture allowing the development of top-down (as well as of bottom-up) processing from shortly after birth. The presence of a complex neural organization supporting top-down and bottom-up processing at the time of normal birth would enable the early and efficient development of auditory-verbal working memory and thus the mastering of symbolic representations.

I plan to test my hypothesis (formally summarised in the following sub-section) by combining computational quantitative neuroimaging of a cohort of preterm born infants at term equivalent age (using connectivity features based on resting-state functional-MRI and diffusion weighted-MRI) with neurodevelopmental assessments of linguistic, cognitive and motor abilities carried out at 20 months corrected age. This fresh approach allows me to exploit: 1) contemporary advances in neuroimaging research which have demonstrated the presence of large-scale dynamic neural systems both during task and at rest (Vincent *et al.*, 2007; Smith *et al.*, 2009); 2) the high spatial resolution of in-vivo non-invasive MRI techniques; 3) the dramatic behavioural development in linguistic abilities occurring around the second year of life (such as the mastering of symbolic representations, the exponential explosion of vocabulary starting just a few months earlier, and the first combinatorial capacities (Kuhl, 2004; Dehaene-Lambertz and Spelke, 2015)).

Hypothesis and aims

The work of this thesis was motivated by the need for a new understanding of the ontogeny of human brain cognitive function, and particularly of the infant brain mechanisms mediating the emergence of high-order linguistic abilities.

This thesis aims to test the following hypotheses:

- An organised adult-like brain language network is present at term-equivalent age in the studied cohort of premature infants, well before the emergence of natural language later in childhood.
- Resting-state functional connectivity of the auditory-motor brain network is significantly associated with later expressive linguistic ability at 20 months of corrected age.
- Inter-subject differences in composite linguistic skills at two years are associated with term equivalent fractional anisotropy of the left and right arcuate fasciculi.
- Term-equivalent dynamic brain network interaction is linked to inter-subject differences in cognitive and linguistic abilities in childhood.

This is conducted with the following aims:

- Reliably quantify resting-state functional-MRI connectivity in a cohort of preterm infants at term-equivalent age, robust to in-scanner head-motion, and to cardiac and respiratory artefacts; in order to calculate subject-specific functional connectivity and its dynamics across time of acquisition.
- Exploit constrained spherical deconvolution of high angular resolution diffusion-weighted neuroimaging data in a cohort of preterm infants at term-equivalent age; in order to perform probabilistic tractography on the bilateral arcuate fasciculi, connecting the superior temporal cortices to the inferior frontal gyri.
- Assess how the calculated brain connectivity metrics are related to linguistic and cognitive abilities at 20 months corrected age; and understand how the

identified brain-behaviour relations are modulated by extrinsic factors such as early environmental exposure linked to premature delivery.

Thesis outline

The rest of the thesis is summarised below:

Chapter 2: The Developing Brain and Preterm Birth. Describes the key steps of the last trimester of gestation with regard to brain development, and briefly defines the incidence, epidemiology and neurodevelopmental outcome of preterm birth as well as the most common forms of preterm brain injury. Particular attention is spent on t quantitative imaging of the preterm brain and discussion of the current knowledge of preterm brain development and injury is provided.

Chapter 3: The neurobiology of Language. Provides a description of the most influential theories and findings regarding language brain mechanisms. Particular attention is reserved for changes in neurolinguistic processing during development, from shortly after birth throughout childhood.

Chapter 4: Physics and Analysis. Provides an overview of the basis of functional- and diffusion weighted-magnetic resonance imaging, and a discussion of the state-of-the-art methods to analyse this data in order to quantify human brain function and architecture.

Chapter 5: Language ability in preterm children is associated with arcuate fasciculi microstructure at term. In the mature human brain, the arcuate fasciculus mediates verbal working memory, word learning and sub-lexical speech repetition. However, its contribution to early language acquisition remains unclear. Here, it is shown that term equivalent fractional anisotropy of the left and right arcuate fasciculi is

significantly associated with individual differences in composite linguistic abilities in early childhood, independent of degree of prematurity. It is also shown that increased prematurity at birth was associated with lower fractional anisotropy in the left arcuate fasciculus. These findings suggest that differences in arcuate fasciculi microstructure at the time of normal birth have a significant impact on language development and modulate the first stages of language learning.

Chapter 6: Acquisition of expressive language is mediated by genetically linked auditory–motor brain activity at the time of normal birth. Throughout childhood, the expressive-language brain network increases its functional integration within the auditory and sensori-motor systems. However, its role in infancy is unknown. Here, it is shown that left-lateralized correlated brain activity between the auditory and motor cortices is already present at term-equivalent age, and is significantly associated with expressive language abilities at 2 years, independent of degree of prematurity at birth. It is also shown that this language brain feature is associated with single nucleotide polymorphisms in genes within a meta-analytic linguistic gene-set. These results demonstrate that the functional network that supports expressive language processing is already present at the time of normal birth, has a genetic basis, and is relatively unaffected by early environmental influences.

Chapter 7: Time-resolved connectivity in the neonatal brain supports efficient linguistic and cognitive development through global network integration. In the mature brain large-scale neural systems are shown to alter their dynamics to meet goal-directed activities or to satisfy task demands, enabling humans to perform the complex cognitive functions necessary for everyday living. However, the psychological relevance of time-varying brain networks interaction during development is unknown. Here, it is shown that term-equivalent dynamics of resting

state functional connectivity are linked to later linguistic and cognitive abilities, independent of degree of prematurity at birth. It is further shown that these functional connectivity dynamics result in an increase of global network efficiency; and in the integration of a distributed network of connector hubs, suggesting a possible brain mechanism for the computational emergence of auditory-verbal working memory.

Chapter 8: Summary and limitations. Provides a summary of the work presented in this thesis, its limitations, and examines potential pathways for future study.

Chapter 2

The Developing Brain and Preterm Birth

Human Brain Development

During the period between 24-40 weeks of gestation the human brain undergoes a rapid and dramatic sequence of development, that is highly structured and programmed (Battin and Rutherford, 2002; de Graaf-Peters and Hadders-Algra, 2006). Formation of cerebral pathways is achieved through a combination of axonal growth, neuronal differentiation and synaptogenesis; with the correct timing and completion of these processes essential for healthy brain ontogeny (Figure 1) (Kostović and Jovanov-Milošević, 2006; Volpe, 2008; Kostović and Judaš, 2010). As a result of these developmental changes in morphology, organization, and function, much of the characteristic brain anatomy seen in the adult life is recognizable even at this early stage.

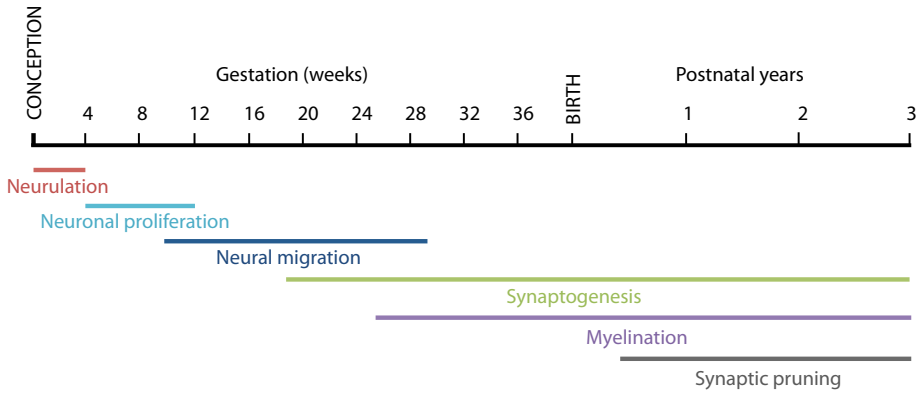

FIGURE 1 ILLUSTRATION OF THE ONSET TIME AND ACTIVITY OF DEVELOPMENTAL PROCESSES IN THE HUMAN CENTRAL NERVOUS SYSTEM. LINES DENOTE PERIODS OF GREATEST ACTIVITY.

There are several features during cortical brain development that differ from the development of other organs. The fact that none of its constituent neurons is generated within the cortex itself is the most remarkable (Rakic, 2009). By early gestation these key elements are generated in the proliferative transient embryonic zone: the ventricular zone (VZ), a germinal area formed by epithelial cells lining the wall of the closing neural tube (Mrzljak *et al.*, 1992; Bystron *et al.*, 2008; Volpe, 2008). The onset of all proliferative processes occurring during brain development starts here in the VZ around the 5th week of gestation, with multipotent radial glial cells prominently generated at this stage. In humans after the onset of neurogenesis and neuroblast differentiation around the 8th week of gestation, dividing cells start to appear at the basal border of the VZ creating a distinct new proliferative zone: the subventricular zone (SVZ), which contains an upper layer of mitotic neurogenic cells within which the rate of proliferation becomes preponderant in comparison to the adjacent VZ by 25 weeks of gestation (Bystron *et al.*, 2008). As the VZ and SVZ increase in size following neurogenesis, postmitotic cells start migrating along the radial scaffold forming transient, laminar structures in the developing neocortex

(Figure 2) (Hatten, 1999; Dhavan and Tsai, 2001; Bystron *et al.*, 2008). This phenomenon of migration, known as the 'inside-out gradient of neurogenesis', reaches its peak between 12 and 20 weeks of gestation and decays between 26 to 29 weeks (de Graaf-Peters and Hadders-Algra, 2006). From the VZ and SVZ, each subsequent wave of cells migrate along the radial glial fibres through the intermediate zone, subplate, and past earlier-born cortical plate neurons to settle below the marginal zone (Dhavan and Tsai, 2001; Bystron *et al.*, 2008). The end-point and function of the differentiating neuroblasts depend upon spatial position and exposure to several genetically determined molecular gradients (Rakic, 1990; Rakic *et al.*, 1994).

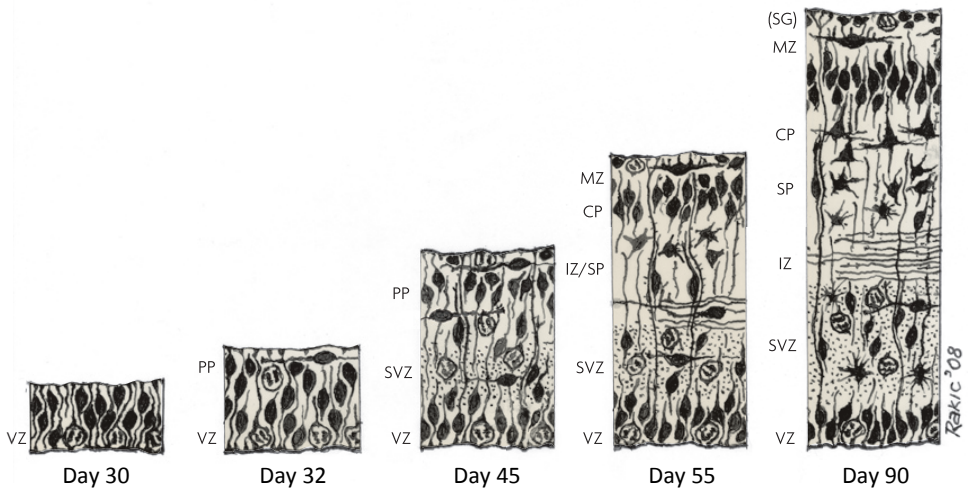

FIGURE 2 SCHEMATIC DIAGRAM OF THE LAMINAR STRUCTURE IN THE DEVELOPING NEOCORTEX

Sequence of development of the six major transient zones of the developing cortex between (approximately) 30 and 90 embryonic days. Each zone is characterised by a distinct cytoarchitecture and role during development. VZ = ventricular zone, PP = preplate, SVZ = subventricular zone, IZ = intermediate zone, SP = subplate, CP = cortical plate and MZ = marginal zone. Figure reproduced and adapted from (Bystron *et al.*, 2008).

By mid gestation synaptogenesis starts in the subplate as immature neurons sprout axons guided to their targets by chemo-attractive and repellent processes (Kostovic

and Rakic, 1990; de Graaf-Peters and Hadders-Algra, 2006; Kostović and Jovanov-Milošević, 2006; Kostović and Judaš, 2010). This area is of particular interest because it is thought to act as a major target for afferent sprouting axons originating from the thalamus, basal forebrain, and brainstem nuclei before they reach their cortical destination (Kostovic and Rakic, 1990; Allendoerfer and Shatz, 1994; Herrmann *et al.*, 1994; Kostović and Judaš, 2002; Kostović and Jovanov-Milošević, 2006). Around 29 weeks of gestation the subplate is at its thickest point and is clearly recognizable via MRI in both early preterm infants and foetuses in utero (Maas *et al.*, 2004; Perkins *et al.*, 2007; Dudink *et al.*, 2010). As the subplate is seen to gradually regress after the 31st gestational week (and then disappear completely by full term gestation), glial proliferation, dendritic differentiation and synaptic formation increases within the cortical plate. This activity marks the cortical layers, defining changes in the cortical cytoarchitecture as complex multi-directional fibre arrangements are formed (de Graaf-Peters and Hadders-Algra, 2006; Kostović and Jovanov-Milošević, 2006). The process of synaptogenesis continues postnatally up to approximately two years of age with the proliferation of cortico-cortical association and commissural fibres (Huttenlocher and Dabholkar, 1997).

Throughout gestation cortical gyri and sulci begin to form according to a specific spatiotemporal schedule, with the large interhemispheric (10-15 weeks) and sylvian (14-19 weeks) fissures forming first, and the secondary and tertiary gyri not seen until approximately 18-20 weeks (Chi *et al.*, 1977; Van der Knaap *et al.*, 1996; Battin and Rutherford, 2002; Volpe, 2008; Habas *et al.*, 2011). As the last trimester of gestation is approached, a far more complex pattern of folding is established, with the sulci progressively becoming deeper with the sidewalls gradually steepening (Battin and Rutherford, 2002; Jessica Dubois *et al.*, 2008). The interaction between these two processes of cortical growth leads to an exponential growth trajectory in

the brain's surface area between 24 to 36 weeks, in contrast to a linear increase in whole brain volume (Kapellou *et al.*, 2006). This allows us to see the characteristic folding pattern of the mature adult brain as early as the end of this gestational period (Figure 3).

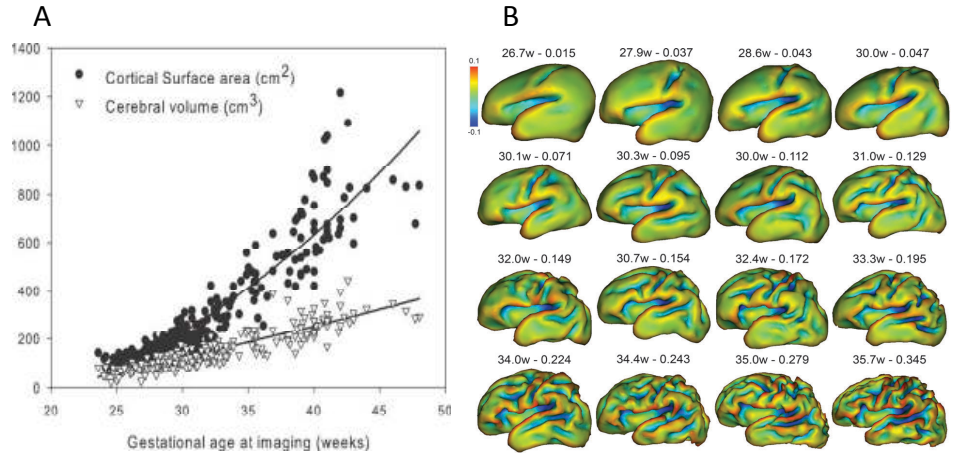

FIGURE 3 DEVELOPMENT OF CEREBRAL VOLUME AND CORTICAL SURFACE DURING THE THIRD TRIMESTER OF GESTATION

A) During this period the surface area of the human brain increases more rapidly than brain volume. Figure reproduced and adapted from (Kapellou *et al.*, 2006). B) Development of cortical folding from 26 to 36 weeks post-menstrual age. The rapid changes in gyrification and sulcation seen during the third trimester of human development are clearly evident on these inner cortical surface reconstructions derived from MRI data. At 26 weeks, the brain is relatively lissencephalic with the exception of the central sulci and sylvian fissures, in marked contrast to deeper and intricate (but still relatively immature) pattern of folding seen at 36 weeks. Figure reproduced and adapted from (Jessica Dubois *et al.*, 2008).

Another cornerstone of human neurodevelopment is myelination, which describes the processes underlying the establishment of the lipid myelin bilayer around neuronal axons. Its functional role is fundamental as it allows fast conduction of nerve impulses. Myelination predominantly occurs postnatally following the formation and maturation of oligodendrocytes, progressing in a posterior-to-anterior

and medial-to-lateral direction, with a gradient from the central regions to periphery, and continuing into adolescence and adulthood (Yakovlev and Lecours, 1967; Benes, 1989; Gilles *et al.*, 2013). Histological evidence indicates that myelinated fibres at birth are only present at the level of the pons, at the cerebral peduncles, and along the inferior sections of the posterior limb of the internal capsule (Yakovlev and Lecours, 1967). Preliminary investigations of white matter development between 3-11 months have noninvasively mapped myelin content throughout the brain in healthy infants, providing a quantitative visualization of brain myelination *in vivo* (Figure 4) (Deoni *et al.*, 2011). This has shown significant differences in the rate of myelination across different brain regions, with significant hemispheric differences observed in temporal, occipital and parietal lobe white matter. It was further shown that by comparing the temporal onset and rate of myelination, areas with early myelin deposition have slower rates of subsequent myelination than areas with later deposition. However, these observations originate from a single set of cross-sectional data; and therefore data from additional infants will be required before definitive conclusions can be reached.

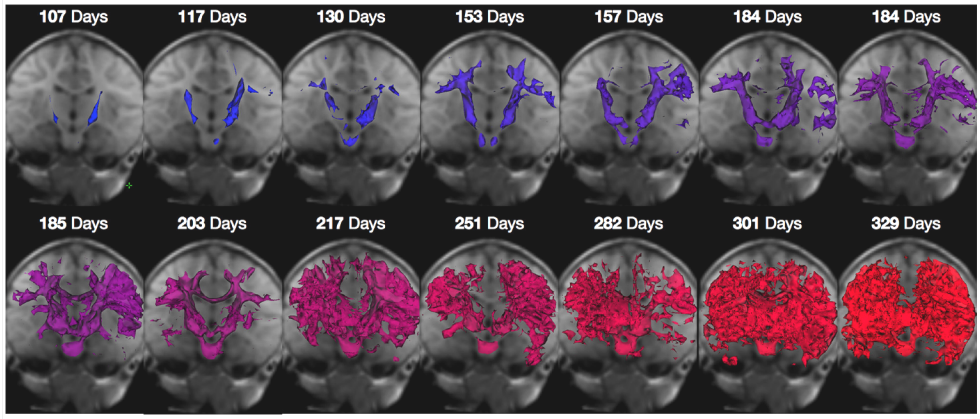

FIGURE 4 IN VIVO MRI MAPPING OF INFANT BRAIN MYELINATION BETWEEN 3-11 MONTHS OF AGE

Showing three-dimensional segmentations of myelinated white matter across different post-natal ages. The spatiotemporal progression from deep white matter (cerebellar, internal capsules) to superficial regions (optic radiations, corpus callosum and frontal white matter) corresponds with the histologically established sequence of myelination. Figure reproduced and adapted from (Deoni *et al.*, 2011).

Development of white matter fibres

Although during the second part of pregnancy the human brain undergoes a crucial overproduction and elimination of neurons, the precise tempo of these processes remains poorly understood. Neuronal and synaptic overproduction enables the formation of projection fibres first (such as thalamo-cortical connections), and subsequently of associative fibres (such as cortico-cortical connections) (Stiles and Jernigan, 2010). This initial tendency in increasing the number of connection is followed by cellular apoptosis, axonal retraction and (postnatal) synaptic pruning. This pruning stage is thought to subserve the elimination of redundant and inefficient connections in order to increase the sensitivity to environmental interactions (Kanold and Luhmann, 2010; Kostović and Judaš, 2010).

At the macroscopic level this processes result in the formation of what is known as the macro-scale structural brain network, a subcortical organisation of crossing long-/short-distance white matter bundles. Together with the postnatal myelination process, this characteristic is through to play a key role in the efficient organization of the human brain (Bullmore and Sporns, 2012). Indeed the differential development of the white matter network is mirrored by a regional asynchrony in white matter bundles myelination. Projection fibres (i.e. thalamo-cortical bundles; cortico-spinal tract; and the optic radiations) have faster maturation rates and myelination progression than associative fibres (i.e. cortico-cortical bundles; intra-hemispheric bundles; superior longitudinal fasciculus), highlighting an initial faster

developmental process for those white matter bundles underlying somatosensory, visual and auditory functions (Kinney *et al.*, 1988).

Epidemiology of Preterm Birth

Defined as birth after less than 37 weeks of completed gestation, every year around 13 million babies worldwide (10% of all births) are born preterm (Beck *et al.*, 2010). Preterm birth affects 7-8% of all babies born in the UK and this rate has increased steadily over the past two decades (Beck *et al.*, 2010). Although 60-70% of premature births occur spontaneously with no clear aetiology (Goldenberg *et al.*, 2008), various epidemiological and clinical risk factors have been associated with the incidence of preterm delivery (Slattery and Morrison, 2002). Of these, the most important are multiple pregnancies (Gardner *et al.*, 1995; Blondel and Kaminski, 2002); hypertensive disorders of pregnancy (Iannucci *et al.*, 1996); intrauterine growth restriction (Burke and Morrison, 2000); low socioeconomic status (Olsén *et al.*, 1995); ethnic origin (Ananth *et al.*, 2001; Steer, 2005); substance abuse (Offidani *et al.*, 1995); and maternal infection during pregnancy (Romero *et al.*, 2001). Moreover, multiple underlying biological pathways as well as possible genetic and epigenetic mechanisms of birth timing regulation have also been implicated (Vuadens *et al.*, 2003; Lockwood *et al.*, 2005; Roizen *et al.*, 2008; Tobi *et al.*, 2011).

However the rise towards higher reported rates of premature delivery and the associated health difficulties is an important matter of public-health concern. Preterm delivery can be a devastating event with great long-term health problems and social implications in childhood and beyond (Goldenberg and Rouse, 1998; Ananth *et al.*, 2001; Mattison *et al.*, 2001).

Neurodevelopmental Outcome Following Preterm Birth

Advances in neonatal care have led to two major effects regarding preterm born infants: decrease in mortality rate and increase in long-term morbidity (Horbar *et al.*, 2002; Slattery and Morrison, 2002; Wilson-Costello *et al.*, 2007). However, several studies have demonstrated the rise in morbidity and a high prevalence of neurological, cognitive and behavioural deficits in surviving preterm infants (Marlow *et al.*, 2005; Delobel-Ayoub *et al.*, 2009; Johnson *et al.*, 2009, 2010). Furthermore, it has become clear that, despite the overall improvement in perinatal care, the adverse functional and behavioural consequences seen in early infancy may persist into adolescence and early adulthood, with preterm birth engendering a very specific pathological phenotype of long-lasting neurobehavioral sequelae (Rushe *et al.*, 2001; Hille *et al.*, 2007; Allin *et al.*, 2008; Aarnoudse-Moens *et al.*, 2009).

Motor outcome

A particularly prevalent neurological condition in surviving preterm born infants is cerebral palsy. This represents a set of chronic motor system disorders such as spasticity, dyskinesia or ataxia, that disrupt movement and postural control with symptoms that can range from mild to severe (Bax, 1964; Bayley, 2006). The increased risk of developing cerebral palsy is strongly linked to lower gestational age (between 32 and 36 weeks of gestation prevalence is around 10 per 1000; before 32 weeks of gestation prevalence is between 40 and 100 per 1000; in term born infants prevalence is 1 per 1000), with the greatest difference in prevalence between term and preterm born infants when compared to other disabilities associated with preterm birth (Hagberg *et al.*, 1996; Marlow *et al.*, 2005; Vohr *et al.*, 2005; Platt *et al.*, 2007). Improvements in medical treatments have led to a significant decrease in the

incidence and severity of cerebral palsy in infants who were born before the 34th week of gestation (van Kooij *et al.*, 2012).

Motor impairment following premature birth may also occur in the absence of overt cerebral palsy. Although the impact of this type of deficit may be less severe, it would be likely to contribute to the poor scholastic outcome commonly seen in this population (Marlow *et al.*, 2007). The prevalence is of 30% for those infants who were born less then 32th weeks of gestation, with fine motor and coordination impairments (Goyen *et al.*, 1998; Huddy *et al.*, 2001; Bracewell and Marlow, 2002; Foulder-Hughes and Cooke, 2003; Goyen and Lui, 2009).

Cognitive outcome

Prematurity is known to have an adverse effect on cognitive abilities and educational outcome. When assessed in childhood and early adolescence, adverse neurocognitive development is commonly reported in preterm survivors, with a high prevalence (>20%) that has not changed over the last 2 decades (Bhutta *et al.*, 2002; Moore *et al.*, 2012; Wolke *et al.*, 2015). Indeed a universal nonlinear gestational age effect has been identified, linking lower intelligence and mathematical scores to increasing prematurity at birth for children born lower then 34 gestational weeks, with no clear statistical difference between whose children born between 34-41 weeks of gestation (Breslau *et al.*, 1994; McCarton *et al.*, 1997; Saigal *et al.*, 2000, 2003; Taylor *et al.*, 2000; Marlow *et al.*, 2005; Jaekel *et al.*, 2013; Wolke *et al.*, 2015). Recent findings have demonstrated considerable cross-cohort consistency of long-term cognitive impairment in preterm born survivors despite significant improvements in neonatal intensive care, suggesting that an increased survival rate does not provide indication of improved cognitive function across the whole population of children born moderately or very preterm (Wolke *et al.*, 2015). Although cognitive abilities and

attainment may be affected by socioeconomic score (SES), in general all of these studies together suggest that the longer the gestation, the better the long-term outcome.

Compared to matched controls, preterm children score lower on overall cognitive performance and more frequently have multiple problems in memory, reasoning, language processing and attention (Stephens and Vohr, 2009). By 2-3 years of age, prematurely born children already have lower standardized scores in all cognitive domains at the Bayley Scales of Infant and Toddler Development (Wood *et al.*, 2000; Bayley, 2006). Other cohorts of preterm children have shown significant deficits in memory (Rose and Feldman, 1996; de Haan *et al.*, 2000); composite executive functions (Harvey *et al.*, 1999; Anderson and Doyle, 2004); language development (Breslau *et al.*, 1996; Luoma, 1998); accompanied by a greater risk of developing behavioural problems such as attention deficit/hyperactivity disorder (Botting *et al.*, 1997; Bhutta *et al.*, 2002). In addition, the prevalence of psychiatric symptoms that may underlie disorders ranging from schizophrenia to autism is increased in preterm adolescents (Indredavik et al. 2004).

Language outcome

Preterm born children are at high risk of developing impaired linguistic function even in absence of brain injury or socioeconomic deprivation, with lasting effects and increased needs for speech therapy and educational support (Vohr, 2014). Delays in the acquisition of expressive language, receptive language processing, and articulation, and deficits in phonological short-term memory are common in preterm children, and are likely to impair the development of appropriate communication, joint attention, and social interaction skills (Caravale *et al.*, 2005; Ortiz-Mantilla *et al.*, 2008; Luu *et al.*, 2009, 2011; Foster-Cohen *et al.*, 2010; Van Noort - Van Der

Spek *et al.*, 2010; Barre *et al.*, 2011). When compared to their term-born peers, preterm children have significantly higher rates of problems in language processing (Wolke and Meyer, 1999; Van Noort - Van Der Spek *et al.*, 2010; Barre *et al.*, 2011). A recent meta-analysis investigated whether language difficulties in preterm-born children compared with term-born decrease, deteriorate, or remain stable between 9-12 years of age (Van Noort - Van Der Spek *et al.*, 2010). Preterm scores were significantly lower on simple, as well as on complex, language function tests throughout childhood, even in the absence of major disabilities and independent of SES. When analysing differences between the two groups, impairment in simple language function was constant over time. However, difficulties in complex language function increased during childhood. This is in accordance with the longitudinal study by Landry et al, where preterm-born children from 3 to 8 years of age showed lower levels and slower rates of complex language development (Landry *et al.*, 2002). Although there is a general agreement on the fact that preterm birth leads to impairment in linguistic abilities that seems to persist as linguistic delay throughout childhood (Franken et al., 2012; Vohr, 2014), some studies have also shown that in adolescence there may be a catch-up in receptive vocabulary (Luu et al., 2009, 2011).

Several studies have concluded that many of the language deficits in preterm-born children were more likely a result of general cognitive problems than evidence for specific language impairment (Wolke and Meyer, 1999; Barre *et al.*, 2011). Whilst other studies have reported significantly impaired phonological working memory, putting these children at risk for persisting language difficulties throughout life (Briscoe *et al.*, 1998). Complex language function depends more on higher-order semantic and syntactic knowledge, entailing integration across language domains and

having a significant working memory component. Thus it is possible that preterm birth results in complex language difficulties, by affecting the neural architecture supporting working memory and specifically its phonological component. There is increasing evidence that adverse cognitive outcome following preterm birth continues throughout school age and adolescence. General intelligence performance is on average significantly lower in preterm adults compared to controls (Hack *et al.*, 2002; Lefebvre *et al.*, 2005; Allin *et al.*, 2008); as is executive function, response inhibition and mental flexibility even after correcting for general intelligence (Nosarti *et al.*, 2007).

Preterm Brain Injury

With increasingly advanced imaging techniques, a spectrum of cerebral injuries and a global insult in brain development occurring between 26-40 weeks of gestation has been identified in preterm infants. The resulting pathological phenotype and clinical state has been termed the "*Encephalopathy of Prematurity*", which describes a complex amalgam of primary destructive disease and secondary maturational and trophic disturbances that may predict later developmental outcome in preterm infants (Allen, 2008; Volpe, 2009a, 2009b) (Figure 5).

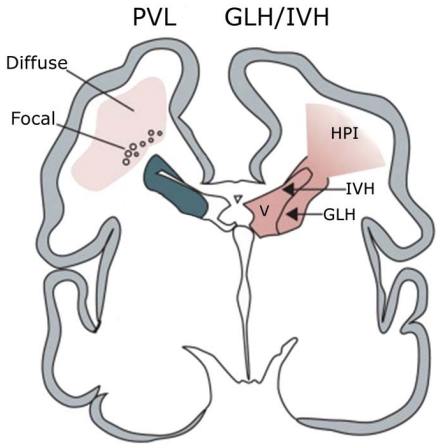

FIGURE 5 WHITE MATTER INJURY IN THE PRETERM NEONATE

Illustrated coronal section of common sites of white matter injury in a 28-week-old premature infant brain. White matter surrounding the lateral ventricles (V) is susceptible to ischaemic and haemorrhagic insult resulting in focal and diffuse periventricular leukomalacia (PVL; left) and/or germinal layer/intraventricular haemorrhage (GLH/IVH; right). In extreme cases of GLH/IVH, haemorrhagic parenchymal infarctions (HPI) can form. Figure reproduced and adapted from (Volpe, 2009a).

In the most severe cases of neuropathology, occurring in less than 5% of preterm infants (Larroque *et al.*, 2003; Dyet *et al.*, 2006) and termed cystic periventricular leukomalacia (PVL) (Volpe, 2008, 2009a), macroscopic periventricular white matter areas of necrosis result in the formation of multiple large cysts several weeks later (Banker and Larroche, 1962; Armstrong and Norman, 1974; Volpe, 2009a, 2009b) and severe neurodevelopmental outcome in childhood (Fazzi *et al.*, 1994; Cioni *et al.*, 1997; Resch *et al.*, 2000; Van Haastert *et al.*, 2008).

Another common form of neuropathology in preterm infants is diffuse-PVL (Volpe, 2008, 2009a). The associated diffuse white matter brain injury is accompanied by varying degrees of neuronal-axonal injury an tissue loss in the cortex, basal ganglia, thalamus and brainstem (Ment *et al.*, 2009; Volpe, 2009a). The highest incidence of PVL associated with preterm birth coincides with the timing of subplate development, indicating that around the 29th weeks of gestation development of the

subplate is specifically vulnerable to injury (Volpe, 2009a). Subplate neurons, that are critical for cortical and thalamic neural development and the establishment of functional neuronal connections, have been shown to be specifically affected by hypoxic-ischaemic injury and inflammation, and represent a likely area for primary insult in the preterm period accompanied by widespread secondary effects in both the white and grey matter (Volpe, 1996; McQuillen *et al.*, 2003; Kostović and Judaš, 2010), resulting in marked astrogliosis, microgliosis, and alterations in oligodendrocyte maturation (Armstrong *et al.*, 1995; Volpe, 2009a, 2009b; Volpe *et al.*, 2011).

Intraventricular haemorrhage (IVH) is another common injury affecting between 20-40% of extremely low birth weight infants (Larroque *et al.*, 2003; Kadri *et al.*, 2006; Volpe, 2008). It arises following germinal layer haemorrhage (GLH), which follows the rupture of the germinal matrix vasculature predominantly occurring within the first 48 hours of life (Hambleton and Wigglesworth, 1976; Vohr and Ment, 1996). IVH occurs once the bleeding is substantial enough to penetrate the ventricular wall, filling the cerebral ventricles, causing ventricular dilatation in around 5-10% of cases due to the alterations of cerebro-spinal fluid flow (de Vries *et al.*, 2001). Its pathogenesis is multi-factorial, including: a lack of cerebral autoregulation; frequent and sudden episodes of rapid cerebral blood flow change secondary to ventilatory support; an increased incidence of anaemia; and immature vascular integrity (Perlman *et al.*, 1983; Amato *et al.*, 1988; Bada *et al.*, 1990; Soul *et al.*, 2007; Volpe, 2008; Takashima *et al.*, 2009).

GLH and low-grade IVH may resolve by term without necessarily an increase in the risk of adverse outcome. However, moderate to severe IVH (grades III and IV, which result in ventricular dilatation and extension of the haemorrhage into the adjacent brain parenchyma respectively), is linked to high incidences of severe

neurodevelopmental disabilities in surviving infants (De Vries *et al.*, 1998; de Vries *et al.*, 2004; Sherlock *et al.*, 2005; Guzzetta *et al.*, 2007), with size and location of the haemorrhage modifying the nature and extent of this disability (De Vries *et al.*, 1999; Bassan *et al.*, 2007).

Quantitative imaging of the preterm brain

MRI quantification provides evidence of subtle alterations in the abnormal developing neonatal brain that are not visible with cranial ultrasonography. Furthermore, it provides the tools to perform objective and quantitative investigations of brain growth and development both at the macro- and microstructural level. From a clinical point of view, although the diagnosis of haemorrhagic infarction and cystic white-matter injury are already possible with cranial ultrasonography, the information derived from MRI techniques does not just allow better definition of lesion size and location but has added new knowledge to the pathophysiology underlying the aforementioned *"Encephalopathy of Prematurity"* (Volpe, 2009a).

Volumetric MRI studies

Although several studies have suggested that in preterm born neonates, cerebral volume is reduced compared to term-born peers (Hüppi, Warfield, *et al.*, 1998; Inder *et al.*, 2005; Thompson *et al.*, 2007), Boardman et al. has provided evidence that the global brain growth failure is not an inevitable consequence of preterm birth in the absence of cerebral injury, having shown that the total cerebral tissue volume is not significantly reduced in the majority of preterm infants (Boardman *et al.*, 2007). This result is consistent with other studies comparing term-born to preterm born neonates

without white-matter injury but suffered severe systemic illness. These studies showed a significant reduction in cortical volume and complexity in preterm infants that was associated with systemic illness severity in the neonatal period and neurodevelopmental outcome in childhood (Ajayi-Obe *et al.*, 2000; Inder *et al.*, 2005; Kapellou *et al.*, 2006; J. Dubois *et al.*, 2008; Kaukola *et al.*, 2009; Rathbone *et al.*, 2011).

Another volumetric phenotype associated with preterm birth is a reduction in subcortical grey matter growth even in the absence of cerebral injury. A series of studies employing manual and automated segmentation of brain structures in preterm infants, found distinct tissue loss in the subcortical grey matter encompassing the lentiform nucleus and thalamus when compared to term controls (Boardman *et al.*, 2006; Srinivasan *et al.*, 2007). This pattern of alteration is significantly worse in infants with white matter microstructural abnormalities (Boardman *et al.*, 2006).

Recent quantitative studies using voxel-based deformation morphometry have also highlighted a pattern of significant volume loss localised in the anterior temporal lobes and prefrontal areas, which is present as early as at term-equivalent age, (Ball *et al.*, 2012), and persists throughout in later childhood and adolescence (Peterson et al. 2000, Kesler et al. 2008, Nosarti et al. 2008, Nagy et al. 2009, Soria-Pastor 2009).

Diffusion MRI studies

Diffusion-weighted imaging provides a quantitative tool to study microstructural changes in the developing neonatal brain and measure sensitive biomarkers of white matter injury following preterm birth. Diffusion-weighted imaging metrics in the preterm infant brain are closely associated with age, and highlight non-uniform maturational patterns across the brain. Higher anisotropy and lower diffusivity can be measured from around 30 weeks gestational age along areas such as the posterior

limb of the internal capsule, where the cortico-spinal tracts starts myelinating. In contrast some association tracts remain poorly myelinated with high diffusivity up to term-equivalent age (Hüppi, Maier, *et al.*, 1998; Partridge *et al.*, 2004).

In the cortex, anisotropy peaks at 26 weeks gestational age and decreases with maturity, reaching zero by around 38 weeks, with initial values and rates of change higher in gyri compared to sulci (McKinstry *et al.*, 2002; Gupta *et al.*, 2005; Ball *et al.*, 2013). Changes in cortical anisotropy during this period occur first in the frontal and temporal poles followed by the perirolandic and medial occipital regions. Cortical diffusivity is higher in gyri than sulci and in frontal compared with occipital lobes, decreasing consistently with age (Ball *et al.*, 2013). Importantly, the degree of prematurity has a dose-dependent impact on cortical microstructural development with preterm infants at term-corrected age showing less mature cortex when compared to term-born infants. In addition the rate of cortical microstructural maturation has been shown to correlate locally with volumetric cortical growth, and to predict higher neurodevelopmental test scores at two years of age (Ball *et al.*, 2013).

By term equivalent age, clear differences are observed between the white-matter microstructure of a preterm and term-born neonate. Reduced anisotropy and/or higher diffusivity in preterm infants at term-equivalent age has been observed in the posterior limb of the internal capsule, corpus callosum, corona radiata, frontal white matter, the external capsule, the sagittal stratum and cerebral peduncle (Hüppi, Maier, *et al.*, 1998; Anjari *et al.*, 2007; Rose *et al.*, 2008). These differences appear to depend on the gestational age at birth (Skiöld *et al.*, 2010; Hasegawa *et al.*, 2011; Thompson *et al.*, 2011).

Other studies performing diffusion tractography of the cortico-spinal tracts, thalamic radiations and the corpus callosum in preterm infants at term-equivalent age have shown similar developmental changes in tract-specific measurements of anisotropy and diffusivity (Berman *et al.*, 2005; Partridge *et al.*, 2005; Aeby *et al.*, 2009; de Bruïne *et al.*, 2011; Hasegawa *et al.*, 2011).

Of interest these patterns of altered diffusivity and anisotropy at term-equivalent age have been shown to predict neurodevelopmental outcome in later childhood. Diffusivity in the centrum semiovale has been found to be associated with a general development quotient score assessed with the Griffiths Mental Development Scales (Huntley, 1996) at 2 years of age (Boardman *et al.*, 2010). In the absence of severe neurological disorders, a lower development quotient at 2 years of age was associated with higher mean diffusivity in the centrum semiovale at term (Krishnan *et al.*, 2007). Cognitive and motor outcome at 2 years was associated with fractional anisotropy in regions including the corpus callosum, fornix, the external capsule and posterior limb of the internal capsule (Counsell *et al.*, 2008; van Kooij *et al.*, 2012). More recently, cognitive scores at 2 years were correlated with structural connectivity (measured by mean diffusivity) between the thalamus and extensive cortical regions at term (Ball *et al.*, 2015).

In summary, diffusion-weighted imaging has shown that preterm brain injury is characterized by abnormalities throughout the white matter at term equivalent age (Counsell *et al.*, 2003; Anjari *et al.*, 2007; Ball *et al.*, 2010). These white matter abnormalities are observed in the presence of impaired cortical and thalamic growth by term (Ball *et al.*, 2012), and are associated with neurodevelopmental performance in early childhood (Boardman *et al.*, 2010). The microstructural correlates of preterm birth seem to be long-lasting and appear, at least in part, to contribute to the various cognitive deficits commonly seen in ex-preterm adolescents and adults (Nagy *et al.*,

2003, 2009; Skranes *et al.*, 2009; Eikenes *et al.*, 2011; Salvan *et al.*, 2014). This suggests that the impaired growth and development of connected cerebral regions in preterm infants has important functional consequences in later life.

Functional MRI studies

In recent years, functional brain imaging techniques have been used to examine brain function during infancy and in the preterm period. As in the adult brain, the characteristic topography of mature resting-state networks is present in preterm neonates at term equivalent age and is shaped during the critical preterm period of exuberant neural growth and axonal sprouting through the transient subcortical subplate (Doria *et al.*, 2010).

Although these networks qualitatively appear to be similar to those found in healthy term-born infants by term-equivalent age, a recent study has demonstrated that the pattern of functional connectivity between these networks is significantly altered in the preterm brain (Ball *et al.*, 2016). This result confirmed previous reports of altered functional connectivity between subcortical structures and higher-level association cortex following preterm birth (Smyser *et al.*, 2010, 2014).

Particular attention has been spent in the characterization of thalamocortical functional connectivity in preterm infants, as the thalamus appears to be particularly susceptible to injury following preterm birth. During the third trimester of human gestation a network of thalamo-cortical circuitry is established through the transient subplate, therefore representing a critical window of vulnerability in development of thalamocortical connectivity (Kostović and Jovanov-Milošević, 2006). In keeping with this, resting-state functional imaging in preterm infants has shown significant reductions in connection strength between high-order cortical regions and specific thalamic nuclei in comparison to term-born peers (Toulmin *et al.*, 2015).

Taken together these studies of the preterm brain function have shed new light on the systemic functional alteration of subcortical–cortical connections, mirroring previous findings of reduced structural connectivity in the developing preterm brain.

As past research has led to a greater understanding of the physiological processes describing normal and pathological human brain development, more has to be done to highlight the possible neural basis of treatments that can led to improvements in the long-term outcome of premature birth.

Chapter 3

The neurobiology of language

Language is uniquely human, and represents a fundamental feature of human cognition (Berwick *et al*., 2013). Its neural architecture is believed to be a distinct piece of the biological makeup of our brain (Pinker, 1995; Jackendoff and Pinker, 2005) and evidence regarding the neural correlates of human language has steadily accumulated (Friederici, 2011; Price, 2012). However, how this neural organization emerges in early life and supports the sophisticated process of learning natural language remains unclear (Kuhl, 2010; Dehaene-Lambertz and Spelke, 2015).

The basic design of language

Human language appears to be a recent evolutionary development. Suggested to arise within the past 100 000 years, there is wide evidence that the capacity for language has not evolved in any significant way since human ancestors left Africa, approximately 50 000–80 000 years ago (Tattersall, 2010). Although other species share similar characteristics of vocal sound production (Marler, 1970; Abe and Watanabe, 2011), the ability to combine symbolic representation in a rich and communicable systems of knowledge is uniquely human (Berwick *et al*., 2013).

Human language relies on a specific neurobiological basis, has independent and particular computational mechanisms, and yields to a possibly infinite number of

organised idioms (Chomsky, 1995). Each sentence is theoretically assigned to two separate systems or 'interfaces', units that are though to represent the computational architecture of the human language faculty. The first, a sensory-motor interface, connects the mental expressions formed by syntactic rules to the external world, via language production and perception. The second, a conceptual-intentional interface, connects these same mental expressions to semantic-pragmatic interpretation, reasoning, and planning.

The ontogenesis of language is further thought to arise from the joint interplay between three components (Hauser *et al*., 2002; Ramus and Fisher, 2009; Berwick *et al*., 2013; Monod, 2014): (a) a shared initial genetic endowment (possibly the result of a fixed language genotype); (b) environmental stimuli, such as the language spoken to children; and (c) general principles, such as the minimization of computational complexity, and external laws of growth and form. Factor (a) in turn has several components: (I) language- (and human-) specific components (often called 'universal grammar' (Chomsky, 1966)); (II) constraints imposed by the structure of the brain; and (III) other cognitive preconditions (e.g., a statistical analytical capacity) (Dehaene-Lambertz and Spelke, 2015). This core computational mechanism (referred as 'merge') must be able to combine already-constructed linguistic representation, yielding new, larger linguistic objects, and endows humans of the combinatorial-syntactic faculty (Berwick and Chomsky, 2011; Berwick *et al*., 2013).

Chomsky further argues that constraints imposed by the sensory-motor system's input-output channel dictate the word order patterns. The mapping from the internal linguistic representations to their ordered output versions is defined as externalization. Whilst this physical constraint seems to not alter how internal

syntactic and *conceptual*-intentional representations are constructed, process defined as internalization (Chomsky, 2007). It derives that communication is an auxiliary component of language, not its key function. Thus posing that language serves primarily as an internal 'instrument of thought' (Berwick and Chomsky, 2011).

The neuroanatomy of the language network in adulthood

In the last two decades, non-invasive in-vivo neuroimaging has helped us understand the neural basis of mature human language processing. As highlighted in recent literature reviews on the many hundreds of studies performed during this period, many findings have been replicated leading to some consistent and robust knowledge (Figure 6) (Vigneau *et al*., 2006; Price, 2012). In adulthood, language processing is supported by a complex brain network system composed of multiple computationally different areas (Figure 7).

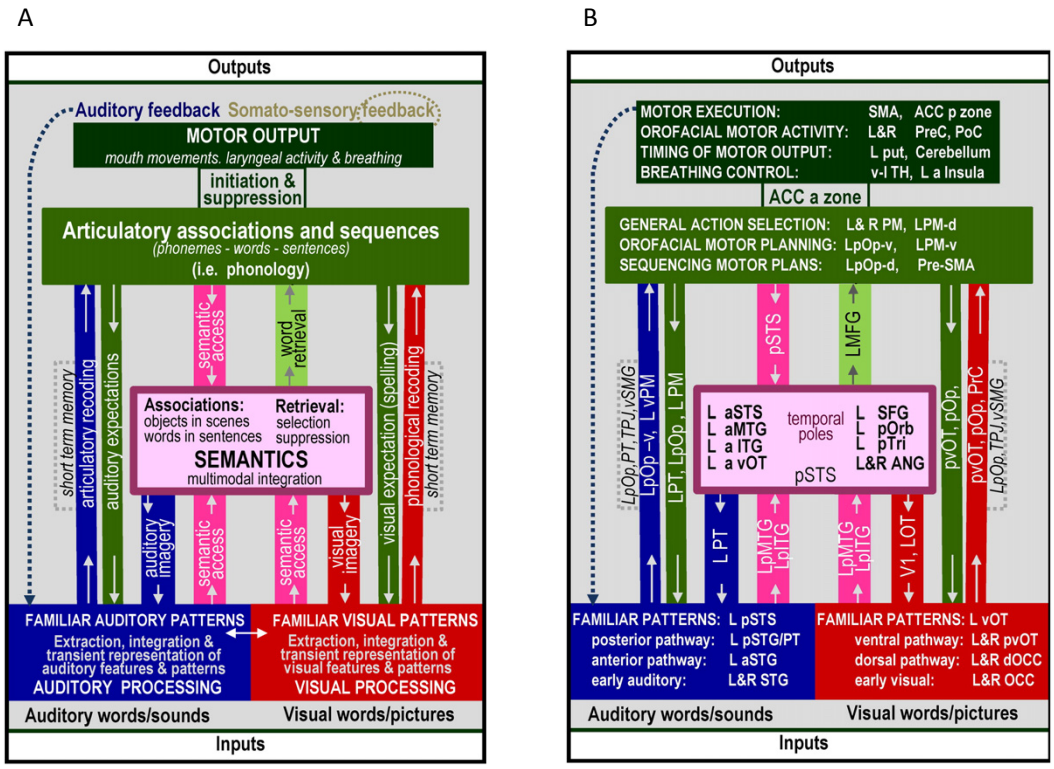

FIGURE 6 FUNCTIONAL (A) AND NEUROANATOMICAL (B) MODEL OF LANGUAGE PROCESSING STREAMS BASED ON NEUROIMAGING STUDIES

Figure reproduced and adapted from (Price, 2012).

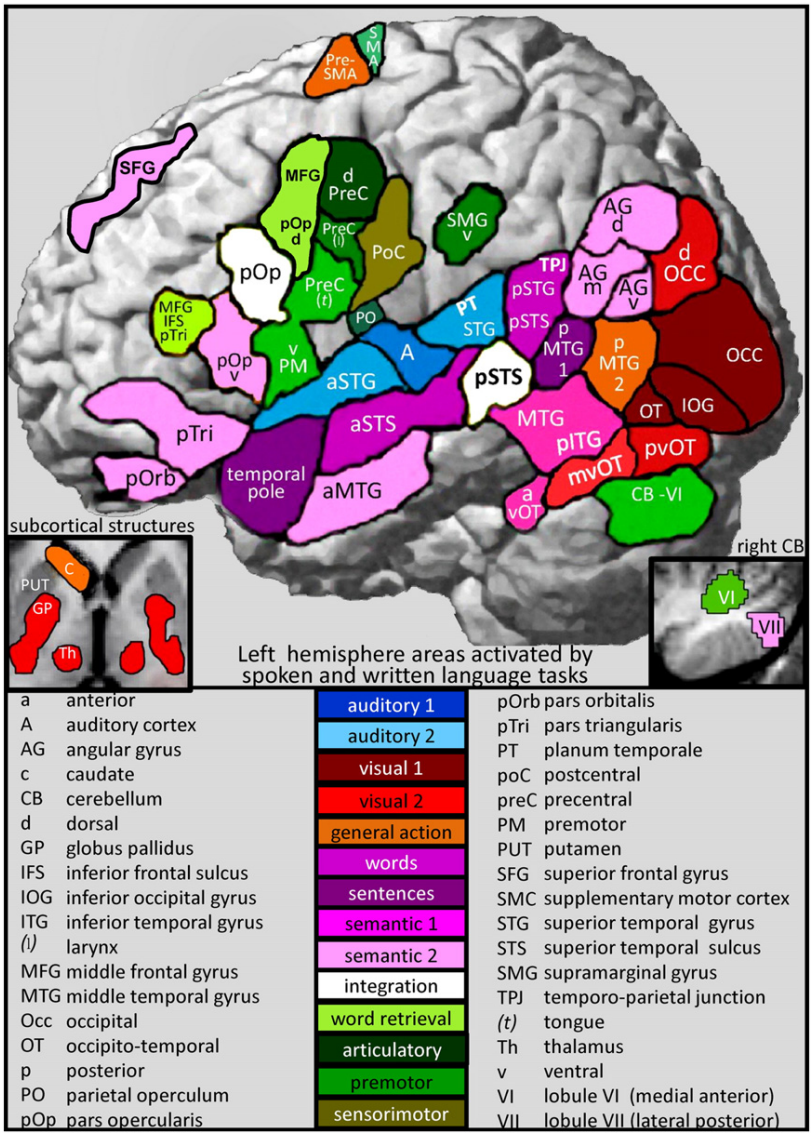

FIGURE 7 ADULT BRAIN MAP OF LANGUAGE PROCESSING AREAS. DIFFERENT COLOURS ARE ASSOCIATED WITH DIFFERENT TYPE OF LANGUAGE TASK

Blue = auditory stimuli (auditory 1 followed by auditory 2). Red/brown = visual stimuli (visual 1 then visual 2). Orange = general action selection (hand or speech). Pink/purple = different levels of semantic and syntactic processing depending on the task demands. Dark pink = semantic content of the stimuli; light pink = more activated for semantic than phonological decisions. Light purple = spoken and written sentences; dark purple = meaningful and grammatical sentences. Green = generating or rehearsing speech; light green = word retrieval; the dark green = silent phonological decisions; khaki green = mouth movements during speech. White areas (corresponding to Broca's and Wernicke's area) = both perception and production

tasks with familiar stimuli. It is suggested that these areas are the centre of the adult language network, receiving and sending information to all the other areas involved in perceiving and producing speech. Figure reproduced and adapted from (Price, 2012). Of interest, no functional or structural connection is shown in the image because the author argues it is not yet know how all the areas connect to one another.

Auditory speech

The neural basis for *auditory processing* (of speech and nonspeech sounds) have been repeatedly identified in the bilateral superior temporal gyri (STG) that include and surround Heschl's gyri (J Obleser *et al*., 2007; Jonas Obleser *et al*., 2007; Turkeltaub and Coslett, 2010; Dick *et al*., 2011) and have shown to be sensitive for frequency discriminations (Zaehle *et al*., 2008), spectral structure and temporal modulation (Britton *et al*., 2009; Leaver and Rauschecker, 2010).

Auditory imagery refers to hearing familiar sounds internally in the absence of external auditory stimuli and has been associated with left-lateralized activity in the planum temporale (PT) (Aleman *et al*., 2005; Bunzeck *et al*., 2005; Zatorre and Halpern, 2005; Xu *et al*., 2006; Pa and Hickok, 2008). This region has also shown to be involved in auditory working memory (Buchsbaum and D'Esposito, 2008; Koelsch *et al*., 2009; McGettigan *et al*., 2011) and in syntactic processing of auditory and written sentences (Friederici *et al*., 2009; Raettig *et al*., 2010; Richardson *et al*., 2010), suggesting the possibility that within the same temporoparietal region there are multiple overlapping functionally distinct circuits for perception and covert production (Hickok *et al*., 2009; Oberhuber *et al*., 2016), and that the left PT might be the receiver of top-down processing from higher-order language areas.

Speech sound processing or *phonological processing* refers to the ability of generating flexible sets of acoustic units (speech sounds), and its abstract knowledge is identified as phonological memory. Price's review (Price, 2012) shows that

phonological processing of speech sounds arises from the functional integration of acoustic processing (in temporal lobe regions) and articulatory processing (in premotor and frontoparietal regions). This is consistent with the growing number of studies showing that speech processing areas are activated also by non-speech stimuli (Zaehle *et al*., 2008; Schön *et al*., 2010) and that functional specialization arises in the network of regions (Hein and Knight, 2008; Londei *et al*., 2010).

Activation for speech was reported in the left posterior superior temporal cortex (consistently related to sound familiarity) (Wise *et al*., 2001; Hugdahl *et al*., 2003; Narain *et al*., 2003; Giraud *et al*., 2004; Benson *et al*., 2006; Rimol *et al*., 2006; Leech *et al*., 2009; Margulis *et al*., 2009; Liebenthal *et al*., 2010; Dick *et al*., 2011); the left anterior STG (consistently related to the acoustic complexity of speech) (Specht and Reul, 2003; Thierry *et al*., 2003; Thierry and Price, 2006; Leff *et al*., 2009; Obleser and Kotz, 2009; Rauschecker and Scott, 2009; Specht *et al*., 2009; Friederici *et al*., 2010; Leaver and Rauschecker, 2010; Agnew *et al*., 2011); the left inferior frontal and premotor areas (consistently related to articulatory re-coding that places top-down constraints on the disambiguation of speech sounds) (Homae *et al*., 2002; Booth *et al*., 2003; Burton *et al*., 2005; Husain *et al*., 2006); and the ventral supramarginal gyrus (vSMG, where there is accumulating evidence of a not-speech specific involvement) (Moser *et al*., 2009) or discriminating sounds on the basis of fine temporal features, typical of phonetic processing (Raizada and Poldrack, 2007; Zaehle *et al*., 2008; Myers *et al*., 2009; Turkeltaub and Coslett, 2010; Zevin *et al*., 2010).

Critically, responses that are more activated for speech than nonspeech sounds are not necessarily speech specific. The temporal cortex responds to nonspeech stimuli (i.e. pitch changes, melodies, familiarity or conceptual processes). Activation of the

left fronto-parietal cortex during speech may be related to general attention that provide top-down regulation of auditory functions (Davis *et al*., 2007; Zevin *et al*., 2010; Ravizza *et al*., 2011; Elmer *et al*., 2012). Therefore, the brain specialization for speech processing does not rely on restricted specific areas, but seems to be characterised by the involvement of a broader network of areas (Price and Friston, 2005).

Language comprehension requires short-term auditory memory and access to the semantic knowledge. Although these processes are quite clear from a computational point of view, their neuroanatomical correlates remain uncertain. Accessing semantics from auditory speech (or processing semantic associations) is observed in anterior temporal areas (such as anterior superior temporal sulcus (STS), lateral middle and inferior temporal gyrus (MTG & ITG) (Awad *et al*., 2007; Jobard *et al*., 2007; Binder *et al*., 2009; Binder and Desai, 2011). Whereas ventral inferior frontal areas are involved in selecting and retrieving task related semantic attributes when sentence meaning is ambiguous (Bilenko *et al*., 2009; Mashal *et al*., 2009; Obleser and Kotz, 2009; Szycik *et al*., 2009; Turner *et al*., 2009; Tyler *et al*., 2009; Willems *et al*., 2009; Liebenthal *et al*., 2010).

Language production

From a neuroanatomical perspective, language processing involved in speech production and speech comprehension overlap (Papathanassiou *et al*., 2000; Wise *et al*., 2001). They both involve access to the semantic system; or subarticulatory processing may be involved to perform auditory words discrimination; or vice versa auditory imagery may be involved in articulation (Price, 2012).

The most consistent result for *word retrieval* from semantics (when articulation and semantics are controlled) is the strong activation in the left middle frontal gyrus

(MFG) and posterior regions in the left MTG and ITG (Spalek and Thompson-Schill, 2008; Heim *et al*., 2009; Jeon *et al*., 2009; Whitney *et al*., 2009; Zubicaray and McMahon, 2009). Posterior middle and superior temporal lobe regions are active when word retrieval became more semantically demanding (Howard *et al*., 1992; Burton *et al*., 2001; Giraud and Price, 2001; Graves *et al*., 2007; Mechelli *et al*., 2007; Abel *et al*., 2009; Wilson *et al*., 2009; Ye *et al*., 2011; Peschke *et al*., 2012) or with lexical word form retrieval from the phonological store (Indefrey and Levelt, 2004); the temporo-parietal junction is more activated by speech production than speech perception (Wise *et al*., 2001); and activation in the anterior cingulate cortex (ACC) is associated with response suppression (Schulze *et al*., 2011). Word and sentence production have been shown to rely on the same cortical areas (Tremblay and Small, 2011).

Covert articulatory planning refers to the silent articulatory planning for the production of speech sounds (= *phonological output*). It refers to the premotor stages of speech production, evokes "inner speech", and occurs prior to overt articulation and independently from word retrieval. Speech-motor mapping has been linked with the activity in the ventral pars opercularis and the ventral premotor cortex (Papoutsi *et al*., 2009; Zheng *et al*., 2010). During silent articulation, the pre-supplementary motor area (pre-SMA) was associated with sequencing abstract motor plans while the SMA-proper was associated with the control of motor output (Alario *et al*., 2006). In contrast, mapping from motor movements to auditory imagery, involves areas that are common to speech and nonspeech sounds such as the PT and vSMG. Activation in the PT and inferior parietal lobe is higher during covert than overt production of sentences (Kleber *et al*., 2007; Andreatta *et al*., 2010), suggesting that activation in temporo-parietal regions might be related to the sensorimotor circuits that maintain sound representations for the production of speech (Koelsch *et al*.,

2009).

Auditory-motor feedback during speech production involves the computational control of the *mismatch* between auditory expectation and auditory feedback. In the context of linguistic development this aspect is of particular interest as, during language acquisition, auditory processing of self-produced speech is used to tune motor production so that the produced auditory output matches the intended auditory output. Thus auditory *feedback* is useful for monitoring and correcting speech errors.

Processing of self-produced vocalisations (auditory response to sounds produced by motor activity) was shown to be associated with BOLD activity in the bilateral STG (McGuire *et al*., 1996; Price and Moore, 1996; Hirano *et al*., 1997), whereas auditory imagery during articulation (auditory response that is anticipated from the motor activity) resulted in left lateralized posterior temporal activation (Shergill *et al*., 2001). Critically a *mismatch* between the expected and actual auditory feedback, has been found to increase the bilateral activity of the superior temporal cortex (Hashimoto and Sakai, 2003; Fu et al., 2006). It has been suggested that, during speech production, auditory imagery might have a pivotal role in forecasting the intended speech production, providing an internal model to which the auditory feedback should be matched to the anticipated auditory response (Heinks - Maldonado *et al*., 2005). Guenther (Guenther *et al*., 2006) proposed that neural processing in the posterior STG and PT becomes active when there is a mismatch between the expected speech and the actual sound of the speech, feeding back the error signal to the primary motor cortex in order to adjust the speech output so that it can be closer to that which was intended. It has been shown that STG activation increased when speech was distorted (quality of auditory feedback) (Christoffels and Formisano, 2007; Tourville *et al*., 2008; Zheng *et al*., 2010; Christoffels *et al*., 2011)

or when auditory feedback was delayed (Takaso *et al*., 2010). Subsequent studies have shown the left posterior PT, known to play a role in silent imagination, increases its activity when speech production is more error prone due to interference or speaking in a second language (Abel *et al*., 2009; Hocking *et al*., 2009; Simmonds *et al*., 2011; Parker Jones *et al*., 2014). As highlighted by Price, this is consistent with the mental imagery of the intended speech playing a role in monitoring speech production when it is error prone. It was also observed that during distorted feedback activation in the prefrontal cortex and rolandic cortical activity increased with bilateral superior temporal activation (Tourville *et al*., 2008), which suggested a role for these areas in modulating subsequent speech output, or in resolving interference.

Taken together, these findings describe a model of auditory monitoring of the spoken voice where 1) an internal model of the intended speech is generated (model prediction) in the core language areas (part opercularis and temporal regions); 2) this results in auditory imagery (auditory response that is anticipated from the motor activity) (in STG and PT); 3) this eventually result in a mismatch between expected vs. actual speech sound (auditory expectation vs. auditory feedback) and thus in a feedback that is sent to the primary motor cortex in order to adjust the speech output. As the predictions become more precise, activity in the auditory cortices (L&R STG) decreases (with more activation when predictions are less precise).

Dorsal and ventral pathways underlying language processing

The neural organisation for language processing can be further divided into the ventral and dorsal streams. Each of these pathways consists of specific brain regions linked via particular white matter bundles, that underlies diverse computational properties of language processing (Dick and Tremblay, 2012; Friederici, 2012; Berwick *et al*., 2013).

The dorsal pathway subserves two distinct language functions. A first white matter dorsal bundle connects the premotor cortex to the superior temporal cortex in order to support sensory-motor interface and repetition of speech (Saur *et al*., 2008); whilst the other dorsal connection wires the pars opercularis of the inferior frontal gyrus to the posterior superior temporal cortex to root core syntactic computations (Friederici *et al*., 2006). The latter dorsal stream is of particular interest as it serves as a functional/structural linkage to connect complex sentence structure building, taking place in the dorsal inferior frontal gyrus, with the integration of syntactic and semantic information, taking place in the posterior superior temporal cortex. This complex computational binding relies on the direct segment of the arcuate fasciculus, a dorsal bundle of white matter fibres that arches around the Sylvian fissure (Catani *et al*., 2005), and that enables humans to achieve sentence interpretation (Brauer *et al*., 2011; S. Wilson *et al*., 2011). Although the first dorsal connection subserving oral speech repetition has been shown to be present in infants, perhaps supporting auditory-/phonological-based language learning (Friederici *et al*., 2011; Mueller and Friederici, 2012), the full maturation of the arcuate fasciculus is currently believed to take place well after the perinatal period around the age of 7 years (Perani *et al*., 2011; Berwick *et al*., 2013; Skeide and Friederici, 2016).

The ventral pathway is involved in two distinct linguistic processes. The inferior fronto-occipital fasciculus connects the anterior temporal cortex with the inferior frontal cortex via, and is involved in semantic processing of lexical items (Lau *et al*., 2008; Binder *et al*., 2009). The uncinate fasciculus connects the anterior temporal cortex with the inferior frontal cortex and the frontal opercular cortex, in order to support processing of phrase structure information (Friederici and Gierhan, 2013). Indeed in the adult brain, the semantic variant subtype of primary progressive aphasia is related to abnormal microstructural integrity in the uncinate fasciculus

(Galantucci *et al*., 2011).

Development of language networks during childhood

Understanding the developmental trajectory of the typical language system is important for computational models of cognitive development and to further highlight the possible neural basis of atypical language development. However, age-related changes in the language brain network remain unclear.

A recent review of fMRI studies of language development from 1992–2014 (Weiss-Croft and Baldeweg, 2015), has investigate how the functional architecture of the language network develops during childhood. The first striking finding is the small number of studies (only 39) compared to the hundreds carried out in adulthood. Thus the authors investigated age-related changes in the neural organisation of macro-categories of language processing (expressive language, receptive language, and word-level decision-making). They aimed to identify the most reliable and well-replicated findings, whilst taking into account the effects of confounds such as sample size or task performance.

The most consistent finding, as suggested from the authors, was that typical development of the language system is characterised by progressive changes in lateral perisylvian cortex (functional activation increases with age in core semantic processing regions and in sensory and motor regions), as well as regressive changes in areas associated with the default mode network (activation decreases in frontal and medial control regions), hinting that with age language processing becomes more automatized. They also report that age effects previously found in frontal regions such as the Broca's area, appear strongly coupled to task performance, perhaps

suggesting the involvement of an underlying working memory component rather than maturational changes in the functional organisation of language.

Studies investigating the development of the *expressive language network* show that it is characterised by increasing activation in sensory and motor cortices (left premotor, bilateral primary motor, and left somatosensory cortex) and left supramarginal gyrus (Schlaggar *et al*., 2002; Brown *et al*., 2005; Fair *et al*., 2006; Krishnan *et al*., 2015). These studies also provide evidence for small increases in leftward lateralisation of activation in specific regions of the language network and temporal–parietal areas.

Studies that investigated the maturation of *receptive language network* suggest that activation in bilateral superior and middle temporal gyri increases during childhood and adolescence (Ahmad *et al*., 2003; Schofield *et al*., 2009; Berl *et al*., 2010, 2014; Richardson *et al*., 2010; Yeatman *et al*., 2010; Lidzba *et al*., 2011; Szaflarski *et al*., 2012; Monzalvo and Dehaene-Lambertz, 2013; Croft *et al*., 2014).

The widespread activation of the *semantic decision-making network* increases over regions including left pars triangularis of the inferior frontal gyrus, premotor cortex, medial frontal gyrus, and superior and middle temporal gyri, bilateral orbito-frontal cortex and visual association cortices, and right fusiform gyrus.

The *effect of verbal proficiency* on fMRI language activation was also investigated. Two results were replicated: activation in left orbito-frontal cortex was stronger in children with higher scores on standardized measures of verbal fluency (Wood *et al*., 2004)(Monzalvo and Dehaene-Lambertz, 2013); activation in the insula during sentence comprehension was stronger for children with slower processing speeds on tests of receptive grammar (Yeatman *et al*., 2010) and reading (Monzalvo and Dehaene-Lambertz, 2013). Regarding lateralisation of activation, studies suggest that

children and young adults between 6–24 years with a higher verbal intelligence quotient show more bilateral activation during sentence comprehension (Lidzba *et al*., 2011) and more left lateralised activation during phonological decision-making (Everts *et al*., 2009).

Weiss-Croft and Baldeweg (Weiss-Croft and Baldeweg, 2015) argue that the most robust and replicated findings of maturation in the functional-neuroanatomy supporting language are consistent with the 'Interactive Specialization' framework of cognitive development (Johnson, 2001, 2011). This posits that areas mediating a given function in adulthood become increasingly activated during childhood, reflecting specialisation of function within brain regions. Beside the increase in activation observed in sensory and motor regions during childhood and adolescence, children performing expressive language, receptive language, and semantic and phonological decision-making task fMRI studies also show a reduction in activation in higher-level fronto-parietal regions associated with top-down control. The authors of the review further suggested that as language skills become automatized during development, such performance can be mediated by low-level systems without the need for top-down control as the task becomes easier to perform. This observation is also consistent with the 'Skill Learning Hypothesis' formulated by Johnson (Johnson, 2001).

Of interest, the authors also observed that changes in language lateralisation are minimal after 5 years of age, reporting that studies which have investigated younger age ranges using Near-Infrared Spectroscopy show that language lateralisation may be established as early as three years of age (Paquette *et al*., 2015). It is also know that some degree of lateralization in response to passive speech listening can be seen as early as between 28–33 weeks of postmenstrual age in preterm infants

(Mahmoudzadeh *et al.*, 2013). Whether or not language lateralisation is crucially related to verbal proficiency remains an open question (Bishop, 2013). Everts et al. (Everts *et al*., 2009) reported that children with a higher verbal intelligence quotient show more left lateralised activation during phonological processing, whilst more bilateral activation was observed during semantic processing (Lidzba *et al*., 2011). The review authors concluded that language lateralisation may therefore be a complex phenomenon rather than a unitary trait, and appears to be modulated by linguistic demands rather than age.

This systematic review, although highlighting how neurolinguistic development remains poorly characterised, has shown that with maturation across childhood and adolescence, there is a progressive increase in activation in the core semantic system, a decrease in activation in the default mode network, and a shift in activation from high-level to lower-level cortices as language skills become automatized.

Acquisition of linguistic abilities during early postnatal life

Although during infancy language production lags behind language perception, the efficient acquisition of human linguistic abilities represents one of the key accomplishments of human development. During the first months of postnatal life, infants' abilities transition from the capacity to discriminate phonetic contrasts of all languages to become progressively more sensitive and specific to vowels and consonants combination of their native language, producing vocalization and babbling (Werker and Tees, 1984; Kuhl et al., 1992; Kuhl, 2004). The establishment of their own language phonetic repertoire during the first year of postnatal life will allow infants to progressively infer statistical patterns in speech inputs and the abstract structure of language (Bernard and Gervain, 2012; Shi, 2014). This rapid

process of development continues with the first production of words at 9-12 months of age, that culminates with the production of multiword utterances and grammar by 18-24 months of age (Dehaene-Lambertz and Spelke, 2015).

To understand the neurocognitive processes underlying the process of healthy language learning and impairment, it is therefore crucial to couple non-invasive in-vivo neuroimaging with the standardised assessments of these complex linguistic abilities. A diffuse and validated instrument for testing linguistic and cognitive abilities is the Bayley scales of infant and toddler development, third edition (Bayley, 2006), a standardized tool based on three latent factors determining the infant's cognitive abilities, linguistic abilities, and motor development. Omitting motor abilities, as these are not the focus of the work of this thesis, the measurement of the infant's cognitive and linguistic capacities relies on the actual abilities that she or he is able to demonstrate to the examiner during the testing session. Specifically, the receptive communication subscale aims to measure receptive language development, with items covering vocabulary and semantics (i.e. picture and object series identification; understanding of inhibitory words), and morphology and syntax (i.e. object categories identification; understanding of plurals; understanding of pronouns; understanding of past tense). Whilst the expressive communication subscale aims to test expressive language development, with its items measuring semantics (i.e. the use of one-word approximations; naming action picture series), morphology, and syntax (i.e. production of present progressive form; production of prepositions; explain how an object is used; production of multiple-word questions).

The cognitive scale aims to measure attention, problem solving, reasoning, memory, object novelty, two-step actions, size discrimination, number sequences repetition, and representational play. Particularly during this age period, it is important to

consider that linguistic abilities may not be independent of the general cognitive level, and therefore it is key to test general cognitive development when studying language learning. Furthermore, whether at this age human infants' cognition is better described by one single underlying factor or by multiple latent factors, is open to discussion. It is however critical to keep separate human infant's cognition from the instrument/s used to measure it, and the number of latent factors that better describe this instrument.

In the contest of healthy and impaired language learning, it is also important to highlight the concept of 'critical' period for language acquisition. As it would be explained in the following section, early brain development commits neural networks maturation to follow certain developmental trajectories. It is hypothesised that the tempo of these neural changes have a bidirectional coupling with the natural language input, thus reflecting and optimising the coding of specific developmental window for certain language patterns or domains (Kuhl, 2004; Werker and Hensch, 2015). It follows that: 1) a specific (neurocognitive) language learning trajectory builds on pattern previously learnt and 2) it further limits future learning (Peña et al., 2012); and that 3) impaired neurodevelopment, or improper environmental/linguistic stimulation, during specific time windows over this trajectory, do affect language learning within specific linguistic domains (Friedmann and Rusou, 2015).

Emergence of the neural basis for auditory speech and language perception during early infancy

Native language acquisition is one of the quintessential human traits and represents one of the greatest achievements of human learning (Kuhl, 2004, 2010; Dehaene-Lambertz and Spelke, 2015; Skeide and Friederici, 2016). Recent advances in non-

invasive in-vivo brain imaging have allowed the exploration of the neural correlates sub-serving this developmental process in newborn babies.

Mahmoudzadeh et al. investigated the preterm infant brain using NIRS, showing that mismatch responses to deviant phonemes are recorded in the bilateral posterior superior temporal cortex and in the inferior frontal cortex before term-equivalent age (Mahmoudzadeh *et al*., 2013). This suggested that the human brain during this period already present a sophisticated organization and that a neural basis for auditory speech processing might be already emerging as early as the third trimester.

By term age, full-term newborn babies show strong bilateral synchronization of haemodynamic activity in the posterior STG following passive listening to speech, but not such strong synchronization in the left inferior frontal gyrus (Perani *et al*., 2011). It is just from the age of 3 months onwards that infants passively listening to speech show activity bilaterally in the middle and posterior STG (during the first 3 seconds after stimulus onset), and in inferior frontal regions (between 7 and 9 seconds) (Dehaene-Lambertz *et al*., 2006). During the first year of age, infants also presents some neural correlates of music discordance and language prosody (Dehaene-Lambertz and Dehaene, 1994; Dehaene-Lambertz *et al*., 2006; Blasi *et al*., 2011; Baldoli *et al*., 2015).

Taken together, these findings indicate that more complex patterns in brain's language perception may be emerging during the first few months after birth, suggesting that the foundations of the neural architecture necessary for language perception may develop during this period (Figure 8).

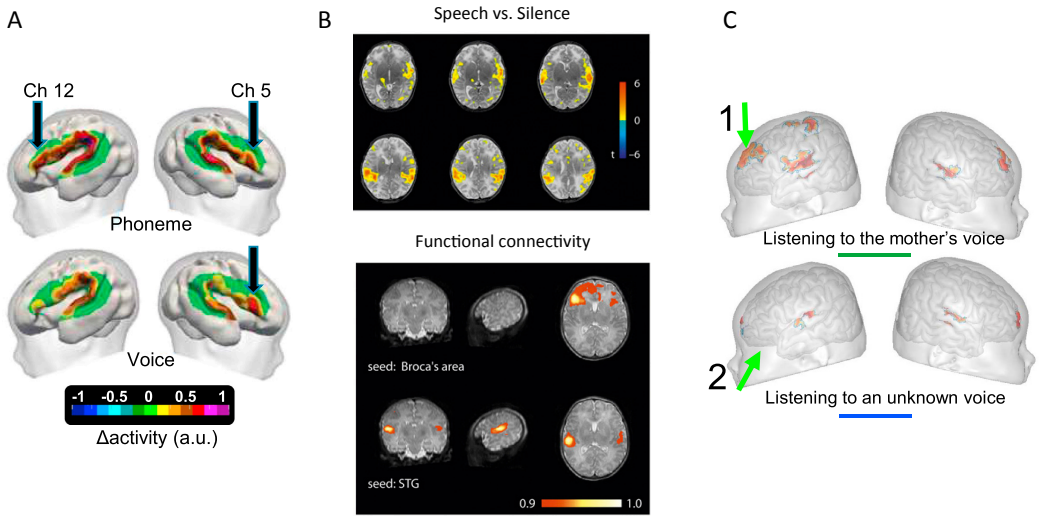

FIGURE 8 FUNCTIONAL NEURAL CORRELATES OF LANGUAGE PERCEPTION BEFORE, AROUND AND AFTER TERM-EQUIVALENT AGE

A) Oxyhemoglobin responses to a change of phoneme and a change of voice in 30 weeks GA preterm neonates, measured with NIRS. Figure reproduced and adapted from (Mahmoudzadeh *et al.*, 2013). B) Task-based and functional connectivity results of the fMRI contrast speech vs. silence in two-days old infants. Figure reproduced and adapted from (Perani *et al.*, 2011). C) fMRI responses to the baby's own mother's voice and to another mother's voice in two-month-old infants. Figure reproduced and adapted from (Dehaene-Lambertz *et al.*, 2010).

Development of the dorsal and ventral linguistic pathways during early infancy

The emergence of human linguistic abilities during infancy is mirrored by the early development of a dorsal and ventral white matter network. During the first six months of life, when the infants start to vocalise, the dorsal and ventral linguistic pathways seem to be organized in an adult-like manner. Indeed, these bundles are segregated in terms of microstructure and initial development (Dubois *et al.*, 2015). Although this findings might be partially influenced by the ability of disentangling crossing fibres configurations in low angular resolution diffusion-weighed acquisition protocols, during infancy there is an asynchronous maturation of these

pathways with the dorsal bundles being less mature than the ventral bundles, and with a closing of this gap as postnatal age increases (Dubois *et al*., 2015).

Asymmetries in fractional anisotropy maturation of white matter bundles represent another interesting factor that may influence language acquisition. During infancy the ventral pathway presents a bilateral adult-like pattern, with the dorsal tracts such as the arcuate fasciculus presenting some degree of leftward lateralization (Dubois *et al*., 2015). Although these observations are in agreement with mature brain models of language organization, in the adult brain more bilateral configurations of the arcuate fasciculus do relate to higher linguistic performance (Catani *et al*., 2007). Therefore suggesting that symmetry rather then asymmetry in arcuate fasciculus fractional anisotropy might be a marker for early language learning.

Genetic endowment for language and early environmental factors

The ontogeny of language is thought to arise from the joint influence of structural and functional brain maturation, genetic factors and environmental interaction. The relatively rapid acquisition of sophisticated natural language argues in favour of the early emergence of neural linguistic processing. However whether the brain's language architecture is genetically determined and present at birth or whether fast learning quickly specializes the human network remains unknown.

It has long been hypothesized that language acquisition is encoded in some way by a human genetic program (Chomsky 1959; Ramus and Fisher 2009). Early findings of a neural signature for auditory processing seem to support this. Primary speech-perception skills are likely to be driven by genetic factors that bias the auditory

processing system towards language-specific frequency spectra (Skeide and Friederici, 2016).

However, the genetic basis for language acquisition remains poorly understood and key questions remain including: is there a genetic basis for the brain language network? What is the role of early environmental exposure on language acquisition? Previous studies do not support the latter view. Preterm infants born as early as 28–33 weeks of postmenstrual age are able to detect deviant phoneme in a sequence of otherwise identical phonemes (Mahmoudzadeh *et al*., 2013). These early phonological skills are unlikely to be solely the result of minimal environmental exposure or of prenatal experience to sounds because frequencies above 300 Hz are strongly attenuated in utero. Furthermore, other studies have shown that although preterm infants experience an earlier and richer exposure to speech (no longer degraded by maternal tissue), speech perception skills in preterm infants are not more advanced than those of age-matched full-term infants (Peña *et al*., 2010, 2012).

Together, these findings are all consistent with the idea that early cortical development and neuronal network formation is largely experience-independent (Khazipov and Luhmann, 2006; Blankenship and Feller, 2010; Chen *et al*., 2013; Fjell *et al*., 2015). This advocates in favour of the prominent role of genetic factors in the emergence of the brain's language system. Nevertheless, active exposure to auditory stimuli is crucial for normal language acquisition and development (Werker and Tees, 2002; Kuhl, 2004; Benasich and Choudhury, 2014; Werker and Hensch, 2015).

Summary

The human brain's language network is characterized by multiple linked cortical

regions that represent different facets of language processing. Although increasing findings suggest the presence of neural correlates for auditory speech processing as early as third trimester, whether a brain's language network is already present around time of normal birth; whether it supports language learning and later computational abilities; and whether it is modulated by early environmental effects or driven by genetic factors, remains unknown.

Chapter 4

MRI Physics and Analysis

Diffusion-weighted MRI

The physical principal underlying diffusion-weighted imaging (DWI) is the stochastic movement of particles imparted by thermal energy described as Brownian motion. The formalization of this process in 1905 by A. Einstein, demonstrated that the mean displacement of a set of freely-diffusing particles is dependent on both the time taken to diffuse and the diffusion coefficient, or diffusivity, of the medium (Einstein, 1905):

$$\lambda = \sqrt{6Dt}$$

where λ is the root mean square displacement of a molecule in three dimensions over time t, and D is the diffusion coefficient of the medium. In the case of water at room temperature, D equals 2.3 x 10-3 mm2/s. This 'free' diffusion process can be described as a Gaussian function such that over a given time, the probability of a molecule arriving at a given point after a specific time is equal in all directions. Within a homogeneous medium (e.g. water), displacement due to diffusion can be described as isotropic. In contrast, the brain is clearly not a homogeneous medium and the presence of various cellular compartments creates barriers to diffusing water molecules, constraining their mean displacement over time (Beaulieu, 2002).

Of importance, the coherent organisation of long neuronal axons into tracts within the cerebral white matter preferentially favours diffusion along, rather than across, the length of the axons. This diffusional anisotropy of water molecules within the brain (or more specifically of water proton spins) was first demonstrated by Moseley et al. (Moseley *et al.*, 1990) (Figure 9).

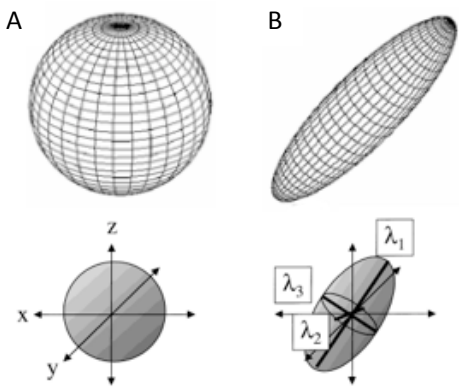

FIGURE 9 TENSOR FORMALISM FOR ISOTROPIC AND ANISOTROPIC DIFFUSION OF WATER MOLECULES

In a homogeneous brain medium, such as the cerebro-spinal fluid filled ventricles, water diffusion is equal in all directions, or isotropic (A); whilst, for instance along organised white-matter bundles, water diffusion is preferred along one direction (λ_1) over others (λ_2 and λ_3), or anisotropic.

A pulsed field gradient spin-echo sequence is commonly used to excite MR signal intensity to the magnitude of diffusion within the brain, induces diffusion weighting through two pulsed gradients applied either side of a 180˚RF pulse (Stejskal and Tanner, 1965). During the first diffusion gradient, spins accumulate a position-dependent phase shift, the RF pulse inverts the spins before the second diffusion gradient, equal in amplitude and duration to the first, rephases the spins to bring them into coherence and produce the MR signal. Spins that remain stationary between the application of the two gradients refocus completely; the two phase shifts cancelling

each other out with no loss of signal. Conversely, the random motion of spins induced by water diffusion results in the application of unequal phase shifts, intravoxel spin dephasing and a loss in signal amplitude. This is most evident in the fluid-filled structures of the brain such as the ventricles. The difference in measured signal between CSF and white-matter bundles is not due to differences in the self-diffusivity of water in each compartment (in both, this is around 2-3 x 10-3 mm2/s). Instead, the apparent difference in diffusivity is due to the effect of various cellular barriers restricting water displacement and, consequently, reducing signal attenuation.

The apparent diffusion coefficient (ADC) is commonly used in diffusion MRI to describe the estimated extent of water diffusivity accounting for impedance due to cellular barriers (Le Bihan *et al.*, 1986). Due to the coherent organisation of the cerebral white matter, ADC is dependent on the direction of the underlying alignment of axons relative to the applied diffusion gradients. ADC is therefore considered a rotationally variant measurement; it is maximally sensitive to diffusion occurring in the direction of the applied gradient. Through the application of several noncollinear diffusion-weighted gradients, it is possible to produce rotationally-invariant estimates of tissue diffusivity.

Diffusion Tensor Imaging

Diffusion Tensor Imaging (DTI) aims to model water diffusion fraction and describe the diffusion profile in a given voxel. Given the acquisition of (a minimum of six) linearly-independent diffusion gradients directions, a diffusion tensor will describe a voxel-specific ellipsoid iso-surface that represents the probability of diffusion from the origin. In the case of isotropic diffusion, this probability is equal in all directions and the diffusion tensor describes a sphere. In an anisotropic medium, e.g. cerebral

white matter, the orientation of the tensor ellipsoid is assumed to align with the underlying, dominant fibre orientation and can be expressed by three orthogonal eigenvectors and respective eigenvalues $\lambda 1$, $\lambda 2$ and $\lambda 3$ (Figure 9) (Basser *et al.*, 1994; Pierpaoli and Basser, 1996). The eigenvalues are rotationally-invariant, scalar metrics often used to summarise voxel-wise diffusion properties without a frame of reference. Mean diffusivity (MD) is calculated as the sum of the three eigenvalues, and represents the directionally- averaged tissue diffusivity. Fractional anisotropy (FA) describes the degree to which diffusion occurs along one axis preferentially over others (Pierpaoli and Basser, 1996). FA takes a value between 0 and 1, where 0 corresponds to a perfectly isotropic, spherical tensor ellipsoid and 1 corresponds to the limit of infinite anisotropy. Although lower than typical adult values, high FA (in the range of 0.35 – 0.50) in the neonatal brain is characteristic of well-developed white matter tracts (Dubois *et al.*, 2014).

Diffusion tensor imaging, and the pattern of voxel-wise diffusion direction that emerges from the underlying coherent diffusivity of the cerebral white matter bundles, can be also used in combination with tractography algorithms in order to reconstruct these cerebral tracts and study the whole-brain architecture or "connectome". This approach will be discussed in detail in "DWI analysis".

Multi-fibre modelling

A remarkable step forward in modelling water diffusion in the brain is multi-fibre modelling. A single fibre model is a good approximation for white matter voxels containing a single fibre population of axons. However, at the resolution scales currently available in the range of 1 – 3 mm^3, a single voxel can contain many thousands of axons forming coherent fibre bundles. One major limitation of DTI approaches is the inability to resolve the local diffusion profile of multiple crossing

fibre populations passing through a voxel with different orientations, misrepresenting the underlying tissue microstructure and hiding the directional information provided by the diffusion signal. Modelling diffusion within a complex fibre organisation as a Gaussian process under the assumption of a single dominant orientation is not always appropriate, creating a so called 'crossing-fibre problem'. Built upon high angular resolution diffusion imaging (HARDI), an acquisition scheme characterised by high b-values and high numbers of noncollinear gradient directions, a number of methods have been proposed to more accurately model multiple-fibre populations (Alexander, 2005), either by modelling the underlying diffusion profile to estimate distinct fibre orientations (Tuch *et al.*, 2002; Behrens, Woolrich, *et al.*, 2003; Assaf *et al.*, 2004; Chen *et al.*, 2004; Hosey *et al.*, 2005) or by inferring the diffusion profile directly with a model-free approach (Jansons and Alexander, 2003; Tournier *et al.*, 2004; Tuch, 2004; Wedeen *et al.*, 2005).

Of the model-based approaches, Behrens et al. demonstrated that a clinically feasible acquisition scheme (60 gradient directions with a *b*-value of 1000 s/mm2) is

adequate to detect 2 fibre populations in up to one third of white matter voxels using a 'ball and stick' compartment model (Behrens *et al.*, 2007). Here, the diffusion signal is modelled as a weighted combination of two compartments: anisotropic diffusion along the axis of each fibre population and isotropic diffusion of free water otherwise unattributed to axonal diffusion. Although a limitation of typical multi-tensor models is the need for prior information on the number of expected fibre populations per voxel, this technique allows the automatic estimation of the number of fibre populations supported by the data using Bayesian inference. This approach uses Automatic Relevance Determination (ARD) to fit a more complicated multiple fibre model at each voxel, but ensures (through use of shrinkage priors on all volume

fraction parameters above the first) that these variables are forced to zero where there is little evidence for them in the data (Behrens *et al.*, 2007).

A model-free approach for estimating the fibre orientation distribution directly from high angular resolution diffusion-weighted MRI data without the need for prior assumptions regarding the number of fibre populations is constrained spherical deconvolution (Tournier *et al.*, 2004, 2007). By assuming that all white matter fibre bundles in the brain share identical diffusion characteristics, any difference in diffusion anisotropy is implicitly assigned to partial volume effects. Thus the diffusion-weighted signal attenuation measured over the surface of a sphere can then be expressed as the convolution over the sphere of a response function (the diffusion-weighted attenuation profile for a typical fibre bundle) with the fibre orientation density function (ODF). The fibre ODF, which is the distribution of fibre orientations within the voxel, can therefore be obtained using spherical deconvolution. The advantage of this technique is that it can recover the fibre ODF in regions of multiple fibres crossing allowing superior performance independently of tractography algorithm used (Tournier *et al.*, 2012).

Diffusion-weighted MRI in neonates

Diffusion-weighted neuroimaging has provided a quantitative investigation of the developing human brain, highlighting how maturational changes in diffusivity and anisotropy are not uniform across the neonatal brain. From around 30 weeks gestational age structures such as the posterior limbs of the internal capsule experience early myelination, thus showing higher anisotropy and lower diffusivity. Whilst associative white-matter bundles (as the inter-hemispheric fibres) tend to

show relatively high diffusivity up to term-equivalent age (Hüppi, Maier, *et al.*, 1998; Partridge *et al.*, 2004). It follows that asynchronies between sensory-motor and associative cortical regions persist throughout the first year of postnatal life, mirroring the developmental tempo of the underlying white-matter maturation and myelination process (Deoni *et al.*, 2011; Dubois *et al.*, 2014). Indeed diffusion-weighted neuroimaging has shown that while white-matter diffusivity decrease and anisotropy increases, cortical anisotropy decreases with increasing gestational age, reaching zero by around 36 weeks (McKinstry *et al.*, 2002; Gupta *et al.*, 2005), and occurring first in the sensori-motor cortex followed by the occipital, temporal, and frontal regions (Gupta *et al.*, 2005; Ball *et al.*, 2013).

Anisotropy and diffusivity are therefore good markers to quantitatively describe the developing human brain and particularly the maturation of white matter bundles. The dense organisation of white matter fibres results in inherent anisotropy even in absence of myelin whilst the developmental process of myelination results in an increase of anisotropy mainly due to a decrease in extracellular distance between membranes (Beaulieu, 2002). However asynchronies in white-matter development appears striking in those local intersections between sensory and associative bundles. In crossing fibres regions the different developmental tempo of these bundles results in the initial increase in anisotropy (when the first bundle gets mature), followed by a subsequent decrease in anisotropy (when the second crossing bundle gets myelinated).

DWI analysis

In order to perform robust quantitative comparisons across subjects some pre-processing steps have to be carried out prior to DWI data analysis.

EPI requires specific MR scanner hardware that is capable of producing large, fast gradient oscillations. It is therefore susceptible to signal artefacts and geometric distortions due to eddy current effects and local field inhomogeneities caused by the rapidly switching gradients (Jezzard *et al.*, 1998).

Eddy currents create additional magnetic fields that are added to the spatial encoding gradients causing spins to experience different image gradients from that intended. This causes distortions in the reconstructed image, in the form of shears and stretches, primarily in the phase encoding direction which is encoded more gradually. Therefore susceptibility-induced distortion correction; eddy current induced distortion correction; and bias field correction, are usually applied in order to eliminate low frequency intensity inhomogeneities across the images (Tustison *et al.*, 2010; Andersson and Sotiropoulos, 2015).

Voxel-based

A method commonly used to analyse diffusion MRI data is voxel-based analysis. Scalar images such as the FA maps derived from diffusion tensor datasets, can be aligned with nonlinear registration to a common target space, smoothed and analysed with mass-univariate statistics. Although widely used several concerns about the interpretability of this style of analysis have been raised given the possible confounding effects of mis-registration, smoothing and partial voluming (Jones and Cercignani, 2010). Partial volume effects can prove problematic when transformed FA maps are analysed directly. In voxels that contain more than one type of tissue, a change in the ratio of tissue type can result in a change in intensity and interpretation as a microstructural change reflected by altered FA. Therefore, it can be difficult to separate changes in contrast due to altered FA from those caused by mis-registered or altered anatomical borders (i.e.: enlarged ventricles), a problem that is exacerbated

in clinical populations with known structural alterations (Simon et al. 2005, Smith et al. 2006).

In 2006 Smith et al. introduced tract-based spatial statistics (TBSS), an alternative method of voxel-wise DTI analysis that is not dependent on precise spatial alignment and does not require smoothing (Smith *et al.*, 2006). TBSS includes a skeletonization step that alleviates residual image misalignment and obviates the need for data smoothing. Precise spatial alignment is not required as a local search method identifies voxels of the highest intensity voxel nearby, or FA, which are assumed to represent the centre of each tract, or contiguous group of tracts, and creates a set of curved sheets, or tubes. The skeletonised dataset represents the centre of all white matter tracts common to the group and over which statistical analysis is performed. However, in recent years several studies have highlighted the potentially limited anatomical specificity of TBSS: only 10% of post-registration misalignment is corrected by the TBSS projection algorithm (Zalesky, 2011); the shape of the skeleton as well as the statistical results are rotationally variant (Edden and Jones, 2011); dependence of specificity and sensitivity of TBSS results on the registration target (Keihaninejad *et al.*, 2012); the projection search area for local FA maxima can partially cover the neighbouring fibre tracts causing mis-assignment (Bach *et al.*, 2014). Some studies have further questioned the underlying assumption of TBSS that the effect of interest occurs in voxels where the local FA is highest (Van Hecke *et al.*, 2009). The use of registration methods such as Diffusion Tensor Imaging ToolKit (DTI-TK) which use the full tensor information can notably reduce the merging of different white matter tracts (Wang *et al.*, 2011). Indeed the overall percentage of mis-assigned voxels can be reduced by a factor of about seven by replacing the TBSS registration procedure with the DTI-TK image registration approach (Bach *et al.*, 2014). Although TBSS is currently still the leading technique

for voxel-wise DTI analysis, the methodological considerations here reported and the interpretation problems concerning results in crossing-fibres regions have encouraged researchers to employ alternative approaches for DWI analysis.

Tractography

An alternative method for diffusion analysis is tractography. By exploiting directionally coherent diffusivity in the cerebral white matter it is possible to infer the path taken by specific white matter tracts through the brain (Mori *et al.*, 1999). This method can be used for in vivo dissection of white-matter tracts in order to extract tract-specific microstructural information (Wakana *et al.*, 2004); or to infer structural connectivity between remote cortical or subcortical (Behrens, Johansen-Berg, *et al.*, 2003) regions ; or to construct the whole-brain structural connectome (Bullmore *et al.*, 2009).

The first implementations of these algorithms, termed *deterministic tractography*, propagates streamlines from an initial seed region through the diffusion data with the direction of the principal eigenvector $\lambda 1$ at each point defining the direction of the next step (Conturo *et al.*, 1999; Mori *et al.*, 1999). This process continues until the streamline enters a region of low anisotropy, usually set as a hard threshold to ensure that streamlines remain in the white matter where directional diffusivity is well-defined, or makes a change in direction that exceeds a pre-set curvature limit, beyond which the pathway is deemed biologically implausible. Streamline techniques, constrained by anatomically informed Region-of-Interest (ROI), are able to delineate the major white matter fasciculi in a manner that is both reliable and consistent with known neuroanatomy (Catani *et al.*, 2002; Mori and van Zijl, 2002; Mori *et al.*, 2002; Wakana *et al.*, 2004, 2007; Ciccarelli *et al.*, 2008). However, deterministic tractography is reliant on the clear determination of the direction of maximal

diffusion in each voxel, a measurement that can be confounded by low spatial resolution; poor signal-to-noise ratio; and the presence of multiple fibre populations that cannot be modelled by the diffusion tensor. All these factors can introduce errors into the tract propagation (Mori and van Zijl, 2002; Le Bihan *et al.*, 2006; Ciccarelli *et al.*, 2008). Moreover the fact that it relies on relatively high anisotropy for accurate tracking further limits its application in neonatal populations, where cerebral white matter is characterised by generally lower anisotropy.

An alternative approach operates within a *probabilistic* framework, accounting for the uncertainty in voxel-wise diffusion estimates, and often utilising multi-fibre models of diffusion to allow tracking of more complex fibre configurations (Figure 10) (Behrens, Johansen-Berg, *et al.*, 2003; Behrens, Woolrich, *et al.*, 2003; Parker and Alexander, 2005; Behrens *et al.*, 2007; R. E. Smith *et al.*, 2012; Tournier *et al.*, 2012). This approach provides a distribution of the direction of maximal diffusion at each voxel (rather than a single point estimate), with a broad distribution reflecting increased uncertainty in the estimation. From each voxel in a given seed region multiple streamlines are propagated and the direction of each is drawn at random from the distribution of available directions, meaning that any given streamline need not follow the path of another. As each streamline steps through the diffusion data, a connectivity distribution of all possible pathways is built up, with the intensity at a given voxel representing the number of streamlines that have passed through it and reflecting the confidence of a connection existing between the voxel and seed region (Behrens, Woolrich, *et al.*, 2003).

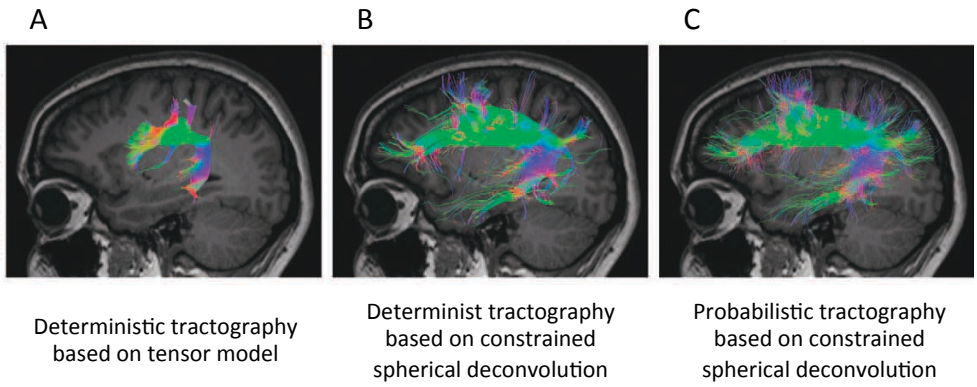

FIGURE 10 VISUAL COMPARISON BETWEEN DIFFERENT DIFFUSION MODELS AND TRACTOGRAPHY ALGORITHMS IN THE MATURE HUMAN BRAIN.

Tractography results of the superior longitudinal fasciculus, obtained using: A) deterministic tracking based on the tensor-model; B) constrained spherical deconvolution-based deterministic tracking; C) constrained spherical deconvolution-based probabilistic tracking. (An equal number of total streamlines were generated in all cases). Figure reproduced and adapted from (Tournier *et al.*, 2012).

Probabilistic tractography allows pathways to be traced in the presence of uncertainty, through multi-fibre populations and into regions of low anisotropy. Given these characteristics it has been proven to be particularly suitable for neonatal DWI analysis (Bassi *et al.*, 2008; Liu *et al.*, 2010; Ball *et al.*, 2015). Probabilistic tractography also provides a measure of connectivity in terms of pathway probability and has been used to reliably quantify connections between remote structures in both adult and paediatric populations (Behrens, Johansen-Berg, *et al.*, 2003; Johansen-Berg *et al.*, 2005; Counsell *et al.*, 2007; Traynor *et al.*, 2010).

Tractography can generally be used with a prior hypothesis related to the regions to be tested, or to investigate whole-brain connectivity in an exploratory manner (Sporns *et al.*, 2005; Hagmann *et al.*, 2008; Bullmore *et al.*, 2009; Bullmore and Sporns, 2012). These latter approach can be used to map structural connectivity

across the brain as complex networks, analysed with computational methods often drawn from graph theory, attributes of which appear to reflect normal development and are altered in disease states (Strogatz, 2001; Stam *et al.*, 2007; Bullmore *et al.*, 2009; Rubinov *et al.*, 2009).

Functional MRI

Over the last 20 years, Blood Oxygen Level Dependent (BOLD) contrast functional MRI (fMRI) has been widely applied to map human brain function. Largely owing to its non-invasive nature and high spatial resolution, fMRI has been a unique tool for characterising dynamic changes of human brain activity and to establish the foundation of non-invasive cognitive neuroscience (Ogawa and Lee, 1990; S Ogawa *et al.*, 1990; Seiji Ogawa *et al.*, 1990; Poldrack *et al.*, 2011). The physical principles underlying functional neuroimaging are T2* decay and BOLD contrast.

In gradient-echo experiments the measured signal does not decay exponentially as expected at the rate dictated by the tissue-specific T2 (Buxton, 2009). However the signal decreases more rapidly than predicted due to static sources of local magnetic field inhomogeneity (Buxton, 2009; Westbrook and Roth, 2011). This effect, named T2* decay or apparent transverse relaxation time, arises as static field inhomogeneity leads to a range of precessional frequencies, with the resultant loss of phase coherence "interfering" with and leading to a more rapid loss of net magnetisation (Buxton, 2009). T2* is always smaller because of fluctuations in B_0 field plus small-scale fluctuations due to the presence of paramagnetic and ferromagnetic agents such as deoxygenated blood in the brain vasculature.

The small-scale magnetic susceptibility due to the diamagnetic and paramagnetic properties of blood is the very underling concept of BOLD contrast fMRI. The

magnetic properties of Haemoglobin (Hb) are known to change depending on its oxygen binding state, with deoxygenated Hb (d-Hb) containing unpaired electrons which render it paramagnetic. The presence of paramagnetic d-Hb in the blood affects the resonance frequency of the vasculature and that of the surrounding tissue it supplies, resulting in measurable local resonance frequency modifications as the brain activity level changes (Figure 11) (Thulborn *et al.*, 1982; Ogawa and Lee, 1990; S Ogawa *et al.*, 1990; Seiji Ogawa *et al.*, 1990).

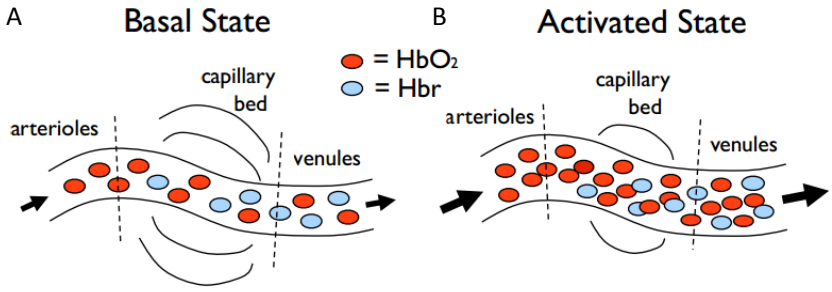

FIGURE 11 THE BLOOD OXYGEN LEVEL DEPENDENT (BOLD) SIGNAL.

A) Cerebral blood flow in a resting brain region. B) Due to increased neural activity the local cerebral flow increases more than the cerebral metabolic rate of oxygen, which results in more diamagnetic oxyhaemoglobin (HbO2), which is the basis of the BOLD signal. HbO2 = oxyhemoglobin; Hbr = deoxyhemoglobin. Figure reproduced and adapted from http://fsl.fmrib.ox.ac.uk.

Although the concept of paramagnetic d-Hb leading to more rapid proton spin dephasing and therefore a decrease in BOLD contrast is widely accepted, the biophysical factors underlying the relationship are not trivial (Buxton, 2009). As the vessels are larger in diameter and, due to passive dilatation have the largest increase in volume during acute increases in blood flow, the majority of shifts in oxygenation on the observed BOLD signal are thought to derive from the venous side of the

vasculature (Buxton *et al.*, 1998, 2004) or from the capillary system (Figure 12) (Attwell *et al.*, 2010; Hamilton *et al.*, 2010).

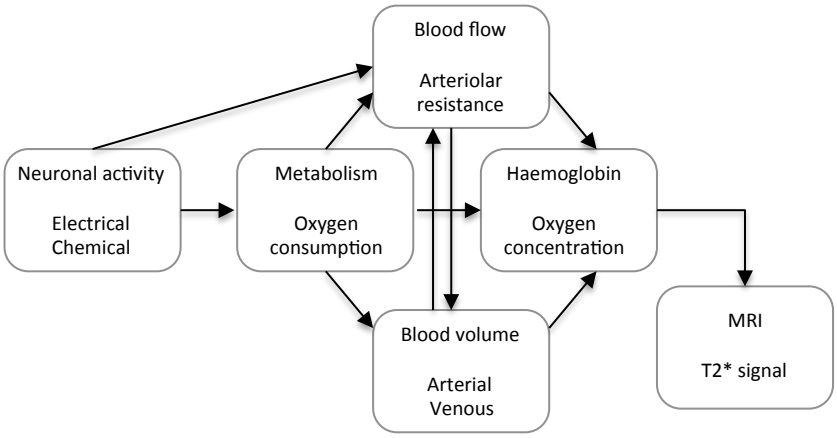

FIGURE 12 LOCALIZED INCREASES IN NEURAL ACTIVITY INCREASES METABOLIC DEMANDS THAT IS ACCOMPANIED BY INCREASES IN REGIONAL BLOOD FLOW.

The physiological basis of changes in BOLD signal fMRI measures is thought to be the vascular supply of glucose and oxygen required for neural activity, termed *neurovascular coupling* (Attwell and Iadecola, 2002; Logothetis and Pfeuffer, 2004; Mangia *et al.*, 2009; Cauli and Hamel, 2010; Jones and Rabiner, 2012; Kim and Ogawa, 2012). The energy required for changes in neurons' membrane electrical field potential, the basis of *neuronal activity* among local neuronal networks, is provided through the consumption of adenosine triphosphate (ATP). Its levels are maintained through the provision to the mitochondria of glucose and oxygen which is bound to haemoglobin. In the adult brain an increase in local blood flow to provide the required glucose and oxygen takes approximately 5 seconds (Buxton 2009). Neurovascular coupling is therefore considered an indirect measure of neuronal activity (Logothetis, 2008). While haemodynamic changes measured by fMRI take place over several seconds, activity dependent increases in BOLD contrast are considered representative of the average metabolic requirements for a population of

neurons, encompassing changes in both excitatory and inhibitory conductance, and both feed-forward and feedback processing (Smith *et al.*, 2001; Logothetis and Pfeuffer, 2004; Logothetis, 2008; Lee *et al.*, 2010).

Here, it is important to highlight how developmental changes in neurovascular coupling and neural energy consumption may obscure the interpretation of BOLD signal changes that result from a concomitant real development of neural signalling (Harris *et al.*, 2011). The relationship between neural activity and blood flow is indeed likely to be reshaped with development as the result of changes in 1) the synaptic architecture and signalling pathways that control blood flow; and in 2) the vascular system itself (Harris *et al.*, 2011). Therefore particular attention has to be used when analysing the developing brain, identifying and removing the effect of cardiac and blood vasculature system MRI artefacts. These BOLD fMRI signal components may hinder the biological significance of changes in neural function that result from development or from task-based, or the calculation of resting-state functional connectivity.

Resting-state functional-MRI

Since the first application of human fMRI (Bandettini *et al.*, 1992; Kwong *et al.*, 1992; Ogawa *et al.*, 1992) most of the studies have focused on changes in activity evoked by external stimuli, i.e.: the response demands of a task or a cognitive challenge. The use of 'activation' paradigms, in which the experimental manipulation results in the activation of cerebral circuits that are necessary for performing the task, has emphasized specific brain areas can be identified by increased activity relative to the baseline condition. In this context, spontaneous modulation of the BOLD signal which could not be attributed to the experimental paradigm or any other explicit input or output, had been interpreted as 'noise' in

task-response studies and was usually minimized through averaging (Deco *et al.*, 2011).

In recent years, researchers' attention has shifted to the investigation of slow (<0.1 Hz) spontaneous fluctuations of the BOLD fMRI signal in the resting brain. The (resting) human brain represents only 2% of total body mass but consumes 20% of the body's energy, most of which is used to support on-going neuronal signalling (Attwell and Laughlin, 2001). Indeed task-related increases in neuronal metabolism are usually small (<5%) when compared with this large resting energy consumption, suggesting perhaps that the brain 'at rest' is not in a resting condition (Ames, 2000; Attwell and Laughlin, 2001; Lennie, 2003; Shulman *et al.*, 2004; Raichle and Mintun, 2006).

Following the observations of Nyberg, L. et al., Shulman, G. L. et al., Raichle, M. E. et al., the idea of a default mode of brain function was proposed providing a framework for the study of intrinsic brain activity in the absence of an overt task (Nyberg *et al.*, 1996; Shulman *et al.*, 1997; Raichle *et al.*, 2001).

The initial observation of Biswal et al. of relatively consistent distributed patterns of activity during rest has led to the suggestion that it might be possible to characterize network dynamics without the need of an explicit task to drive brain activity (Biswal *et al.*, 1995). It has been demonstrated that brain regions that activate jointly seem to maintain a high correlation of BOLD signal fluctuations at rest, within a 'resting-state network' (RSN) of 'functionally connected' regions (Biswal *et al.*, 1995; Lowe *et al.*, 1998; Greicius *et al.*, 2003; Damoiseaux *et al.*, 2006; Rogers *et al.*, 2007). Further studies have also shown that in disorders in which cognition is disrupted, intrinsic activity dynamics also seem to be disrupted (Garrity *et al.*, 2007; Damoiseaux *et al.*, 2008; Greicius, 2008; Rombouts *et al.*, 2009).

In the last decade the study of slow spontaneous fluctuations in the BOLD fMRI signal have shown that the brain is very active even in the absence of explicit input or output; and is intrinsically organized into dynamic, anticorrelated functional networks (Figure 13) (Beckmann *et al.*, 2005; Fox *et al.*, 2005; Damoiseaux *et al.*, 2006; Raichle and Snyder, 2007). It has been further proposed that both task-driven neuronal responses and behaviour are reflections of this dynamic, on-going, functional organization of the brain.

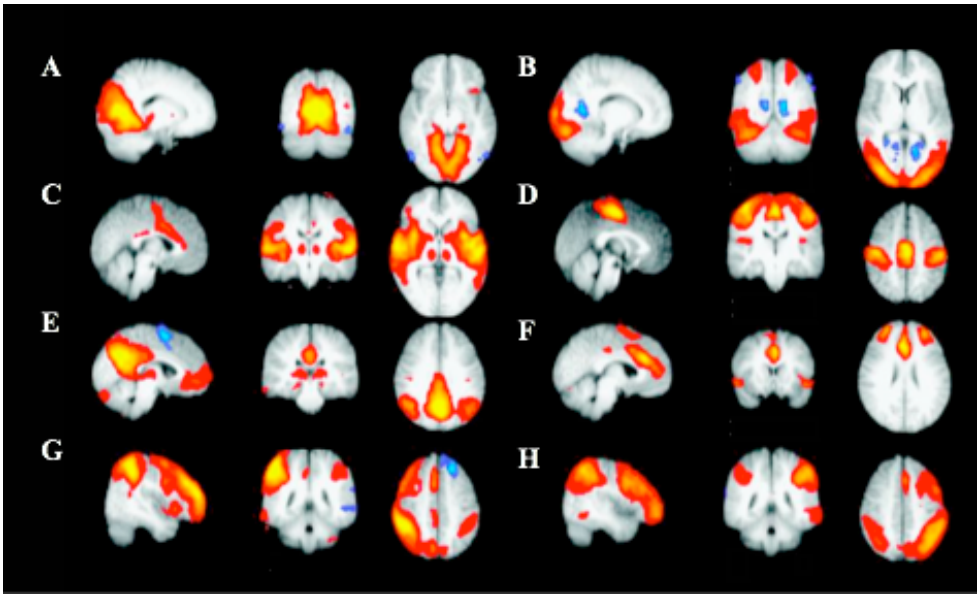

FIGURE 13 FUNCTIONAL RESTING-STATE NETWORKS IN THE MATURE HUMAN BRAIN

A) Medial visual; B) Lateral visual; C) Auditory; D) Sensory-motor; E) Default mode; F) Executive control; G) Right dorsal visual; H) Left dorsal visual networks. Figure reproduced and adapted from (Beckmann *et al.*, 2005).

The characterization of spatially coherent spontaneous slow fluctuations of the BOLD fMRI signal offers potential insights into large-scale brain organization at a systems level. Today we know not only that RSNs do reflect networks of brain function (Sadaghiani and Kleinschmidt, 2013) and that the extensive set of functional networks identified in the task fMRI literature can also be found in resting-state

fMRI data (Vincent *et al.*, 2007; Smith *et al.*, 2009), but also that these RSNs alter their dynamics to meet goal-directed activities or to satisfy task demands, enabling humans to perform and control complex cognitive functions necessary for everyday living (Cocchi *et al.*, 2013; Kim *et al.*, 2013; Deco *et al.*, 2015; Gu *et al.*, 2015).

However, the biological significance of such a rich and continuously present set of spontaneous, correlated activities in the resting brain is still unclear, but may allow the brain to be continuously engaged in undirected cognitive activities (both conscious thought processes and subconscious activity such as learning/unlearning) and respond to uncontrolled external stimuli (Smith, Vidaurre, *et al.*, 2013).

Resting-state fMRI in neonates

From 2007 a series of studies started investigating the ontogeny of RSNs, with the aim to clarify the role of this large-scale neural organization in early life. At the time of normal birth, previous studies have detected RSNs in the primary visual areas, somatosensory and motor cortices, temporal cortex, cerebellum, prefrontal cortex and an incomplete Default Mode Network (DMN) (Figure 14) (Fransson *et al.*, 2007, 2009, 2011; Smyser *et al.*, 2010).

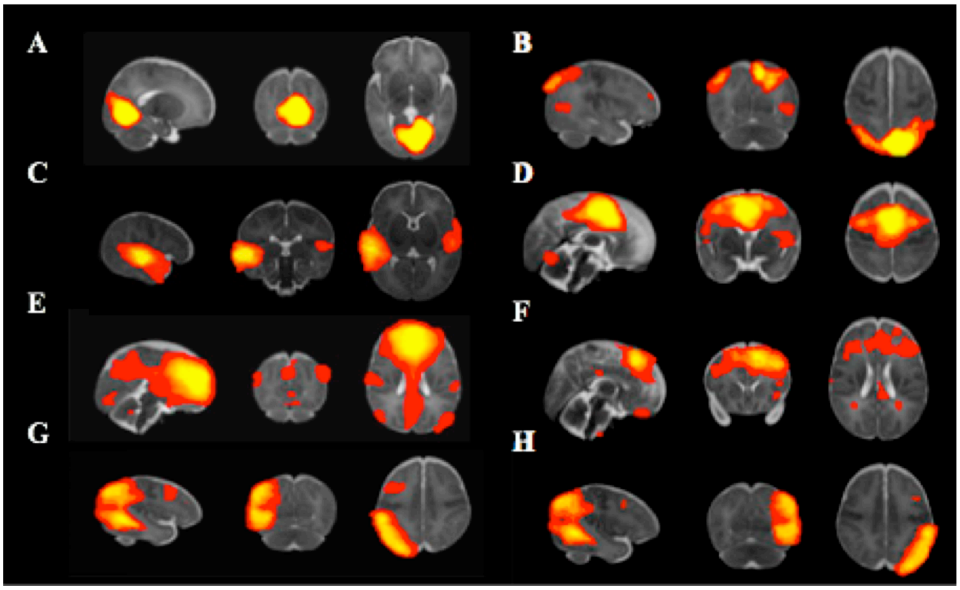

FIGURE 14 FUNCTIONAL RESTING-STATE NETWORKS IN THE NEONATAL HUMAN BRAIN

A) Medial visual; B) Lateral visual; C) Auditory; D) Sensory-motor; E) Default mode; F) Executive control; G) Right dorsal visual; H) Left dorsal visual networks. Figure reproduced and adapted from (Doria *et al.*, 2010).

However, the absence of the complete DMN, executive control network, and dorsal visual network suggested that the full RSN architecture may emerge during later childhood, in parallel with the development of corresponding cognitive functions. It was only in 2010 that a more comprehensive investigation of infant brain function showed how the full repertoire of resting-state networks emerges during the period of rapid neural growth before the normal time of birth at full term (Figure 15). This study showed how the visual, auditory, somatosensory, motor, default mode, frontoparietal, and executive control networks, although developing at different rates, were all present by term equivalent age (Doria *et al.*, 2010).

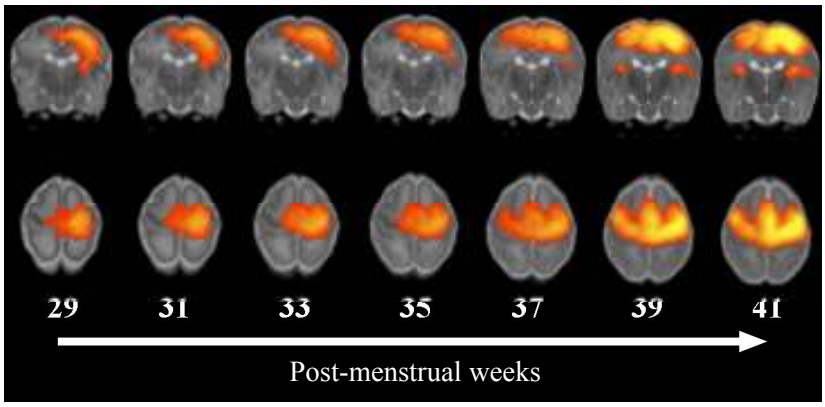

FIGURE 15 DEVELOPMENT OF THE MOTOR RSN DURING THE PRETERM PERIOD

The network can be clearly seen to progress from a unilateral representation at 29 weeks PMA, to a bilateral but spatially dispersed network at 35-37 weeks PMA, and finally to a well localised bilateral network with a clear pattern of connectivity between the left and right peri-rolandic cortices at 41 weeks PMA identical to that seen in the brains of adult subjects (numbers correspond to age expressed in PMA weeks). Figure reproduced and adapted from (Doria *et al.*, 2010).

Resting-state fMRI analysis

The fundamental premise of fMRI is that the acquired image intensity reflects the local blood flow and oxygenation changes which result from local neural activity (Ogawa *et al.*, 1992). However several confounds can hinder its study. Data pre-processing represents a first, essential step prior to the selective analyses, and aims to prepare the raw data for statistical analysis by reducing noise and removing clear sources of potential bias (Friston *et al.*, 1994; Smith *et al.*, 2001; Monti, 2011). Therefore a four-dimensional resting-state fMRI dataset requires extensive pre-processing before resting-state network analyses can be conducted.

Head-motion movement correction

Head motion has been shown to significantly confound resting-state fMRI studies leading to spurious patterns of connectivity (Power *et al.*, 2012; Satterthwaite *et al.*, 2012, 2013; Griffanti *et al.*, 2014; Pruim *et al.*, 2015). Therefore it represents a very important possible confound and source of potential bias which can lead to significant changes in local signal intensity and may be interpreted falsely as neural activity (Hajnal *et al.*, 1994; Smith *et al.*, 2001; Huettel *et al.*, 2004). This head-motion effect is particularly profound in areas with high-contrast boundaries such as is seen around the cortex on the surface of the brain, where even a small movement may lead to signal being derived from an entirely different source (such as CSF) during the course of time-series acquisition. For the purposes of motion correction, the head is considered to be a rigid body (i.e.: while there may be changes in position and orientation during the acquisition period, it is assumed there are no changes in shape) (Friston *et al.*, 1995, 1996; Smith *et al.*, 2001; Jenkinson *et al.*, 2002; Huettel *et al.*, 2004). Although this process of rigid-body realignment correction will produce fMRI data consisting of volumes which should be spatially identical to one another, significant (and more complex) residual effects still remain in the data (Friston *et al.*, 1996; Smith *et al.*, 2001; Muresan *et al.*, 2005). As the altered signal intensity may propagate into the subsequent acquired volumes (known as a "spin history effect"), regardless of whether any further displacement occurs in that period (Friston *et al.*, 1996; Muresan *et al.*, 2005), the relationship between movement and signal intensity is highly complex, with a single pattern of movement resulting in vastly different (and unpredictable) patterns of signal change across the brain (Friston *et al.*, 1996; Smith *et al.*, 2001; Beckmann and Smith, 2004).

The estimated displacement vectors derived from the rigid-body realignment can be used as covariates, based on the assumption that aberrant changes in image intensity will be linearly related to the measured head motion and therefore can be regressed

out (Smith *et al.*, 2001). However this method is limited in its effectiveness, as there are areas in the brain which move independently under normal conditions (such as areas with physiological pulsation) and therefore violate the rigid body assumption, and due to the profoundly non-linear relationship between head motion and BOLD contrast (Smith *et al.*, 2001; Beckmann and Smith, 2004).

An alternative method termed *scrubbing* has been suggested, and consists in the removal of those specific volumes corrupted by head-motion above a certain threshold measured on (Power *et al.*, 2014). This approach however presents several limitations in its effectiveness, such as the possibility that motion-related artefacts may propagate into the subsequent acquired volumes which may not necessarily be affected by aberrant motion; or the fact that by removing different number of volumes per subject it leads to subject-wise differences in the degrees of freedom, hindering functional connectivity estimation and inter-subject comparison.

An alternative and perhaps preferable method is to use a blind source separation technique such as Independent Component Analysis (ICA) to identify and filter out patterns of structured noise within the signal (such as in areas containing pulsating arteries, and changes related to patterns of head motion) (Beckmann and Smith, 2004).

Recently two automatic de-noising and artefact removal pipelines (FMRIB's FIX and AROMA) have been developed based on single-subject ICA identification of artefact and have proven superior results compared with several previous techniques (Griffanti *et al.*, 2014; Salimi-Khorshidi *et al.*, 2014; Pruim *et al.*, 2015).

EPI distortion correction

Another step in fMRI denoising is EPI distortion correction. Images acquired with an EPI sequence are particularly predisposed to particular forms of geometric distortion,

especially those due to magnetic field offset induced by differences in susceptibility in adjacent tissues (Buxton, 2009; Westbrook and Roth, 2011). EPI distortions usually result in geometric changes of position in the reconstructed image caused by changes in the signal phase along the phase-encoding direction. Because in the EPI phase encode direction there is a long time between phase encode lines, spins are acquiring phase due to off-resonance between acquisition lines in k-space. Given that we are using signal phase to encode spatial location, extra phase results in the wrong location during image reconstruction.

This inhomogeneity can be characterised and a B0 "field map" created by calculating the difference in signal phase between two images which have been acquired at different echo times (Jezzard and Balaban, 1995). This field map can then be used to "unwarp" the fMRI data by applying cost-function masking thereby ignoring areas of high signal loss (Jezzard and Balaban, 1995). Other approaches to prevent EPI distortion encompass the improvement of B_0 homogeneity or the reduction of time between phase-encoding lines: shimming; faster coverage of K-space along the Y direction, i.e. using parallel-imaging; blip-up blip-down acquisition (inversion in phase acquisition so that distortion change direction as well and signal can be recovered). Although these are very effective approaches, in a clinical setup they are extremely time-consuming and cannot always be implemented.

Signal Drop-out

Particular attention has to be spent in the identification of EPI signal drop-out. In contrast to EPI distortion, signal drop-out is a loss of signal caused by intravoxel dephasing due to large air-tissue inhomogeneity. Importantly, signal affected by drop-out is lost and can not be recovered. Possible remedies during fMRI acquisition are B_0 homogeneity improvement by shimming the coils; reduction in voxel-size;

and reduction in TE. In the adult brain, signal drop-out is common in the inferior frontal and temporal areas due to the presence of large air-filled sinuses adjacent to the brain (Jezzard and Clare, 1999; Buxton, 2009). In the preterm and term neonate, these areas of signal drop-out are not significant as the sphenoidal and frontal sinuses are not yet pneumatised.

Recently, multiband accelerated EPI sequences have been developed in order to allow faster acquisition of multiple slices simultaneously and reduce EPI distortions (Moeller *et al.*, 2010; Setsompop *et al.*, 2012). Not only do these sequences provide major improvements in spatial and/or temporal resolution, they can also improve overall statistical sensitivity and increase the information content of the data, in terms of reflecting the richness of the neural dynamics (Feinberg *et al.*, 2010; S. M. Smith *et al.*, 2012).

Temporal filtering

Temporal filtering can be done at both the high and low ends of the frequency spectrum of the BOLD signal time-series to remove unwanted time-series artefacts which are unquestionably not related to the experimental signal of interest (Friston *et al.*, 1994; Smith *et al.*, 2001; Huettel *et al.*, 2004).

High-pass filtering is used to remove low frequency drifts in the data, such as those caused by "scanner drift" (due to gradual changes in the scanner magnetic field during the acquisition), slow movements of the subject's head, and aliased physiological effects (such as subject breathing) (Friston *et al.*, 1994; Smith *et al.*, 2001). Low-pass filtering can also be used to remove high frequency noise (such as that caused by vascular pulsation), but has a potential downside in that the power of the later analysis may be reduced due to an effective "smoothing" of the time-series response (and in particular a dampening of high amplitude rapid responses) (Smith *et*

al., 2001). In resting-state fMRI analysis, high pass filtering is usually applied to data (in neonates for frequencies above 100-125 s ~ 0.01-0.008 Hz); but low pass filtering is not, so as not to reduce the strength of the signal of interest.

Spatial filtering

A low pass spatial filter is typically applied to fMRI data preferably after normalization to common target or template. Although counter-intuitive because of the induced blurring of the data, this step aims to increase the signal-to-noise ratio (SNR) of the data, to reduce the effect of misalignment, and eventually to reduce false positive rates due to the large number of data points generating multiple comparison statistical problems in the later analysis (Friston *et al.*, 1994; Smith *et al.*, 2001; Huettel *et al.*, 2004).

However, spatial smoothing may also generate a confounding effect due to differences in head-size when applied before normalization to standard template, or again might not achieve the same degree of uniform smoothing, which ensures that all subject images in a study have equal effective spatial resolution (Scheinost, Papademetris, *et al.*, 2014). Because differences in the intrinsic smoothness of images across a group are known to confound functional connectivity results, these smoothness differences can be eliminated via a uniform smoothing solution achieved using AFNI software. Given the small size of the infant brain, spatial smoothing has to be minimized to a small Gaussian kernel (i.e. of 3 mm full-width-half-maximum (FWHM)) to avoid undesirable mixing of signal across anatomically or functionally distinct areas whilst still enhancing signal-to-noise ratio and ameliorate the effects of functional misalignments across subjects (Smith, Vidaurre, *et al.*, 2013).

Resting State Network Identification

Resting-state fMRI measures spontaneous temporal fluctuations in brain activity (i.e., with the subject 'at rest') and is primarily used to estimate connectivity in the brain, under the assumption that functionally connected areas have temporally related spontaneous fluctuations in the measured BOLD time series.

As the brain is thought to be intrinsically organized into dynamic, distinct functional anatomical systems, the identification of RSNs becomes a key step in resting-state fMRI analysis and functional connectivity estimation (Beckmann *et al.*, 2005; Fox *et al.*, 2005; Damoiseaux *et al.*, 2006; Raichle and Snyder, 2007).

Although there was initially some concern that some patterns of spatially-extended spontaneous signals were of non-neural physiological origin, these concerns are increasingly being addressed (Murphy *et al.*, 2013). RSNs can be distinguished from each other because, although each has a relatively consistent time-course across its set of involved regions, the different networks have distinct time-courses (Beckmann *et al.*, 2005).

Early studies typically looked at functional connectivity via a small number of large-scale spatial maps (Beckmann *et al.*, 2005), or by computing seed-based correlation connectivity from a single seed voxel or region of interest, creating one or a few correlation-strength maps spanning the whole brain (Biswal *et al.*, 2010).

By contrast the nascent field of 'connectomics' (Sporns, 2013) generally attempts to study brain connectivity in a different way, first identifying a number of network nodes (functionally distinct brain regions) and then estimating the functional connections (network edges) between these nodes.

A very robust and replicated approach to generate nodes or parcellate the brain involves Independent Component Analysis (ICA) (Beckmann, 2012). ICA is a dimensionality reduction technique or, more precisely, a blind source separation

approach (Hyvärinen and Oja, 2000). The underlying assumption of ICA is that the measured data is generated from a mixture of the underlying independent signals of interest. ICA will therefore separate a multivariate mixed signal into additive subcomponents that are maximally independent. In contrast to other models such as Principal Component Analysis (PCA) or Factor Analysis, the prior distribution needed to estimate the probabilistic model is based on non-Gaussian priors of the latent variable (Figure 16).

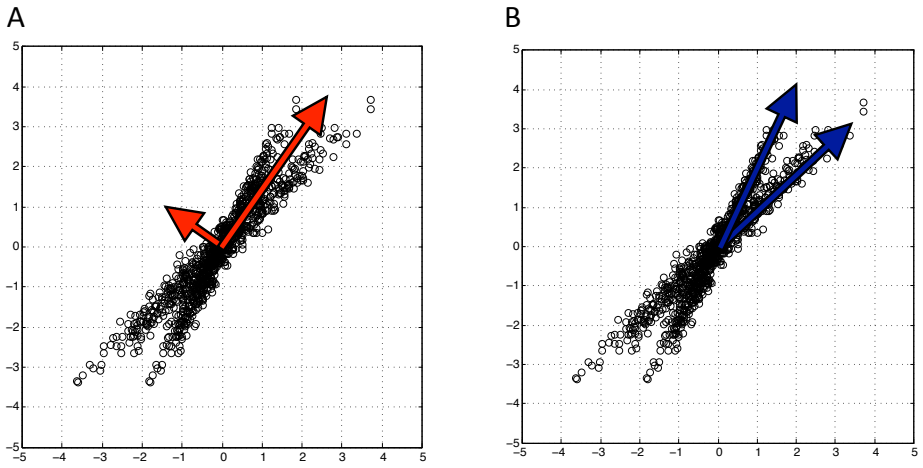

FIGURE 16 PCA VS. ICA ON NON-GAUSSIAN DATA

A) PCA finds projections of maximum amount of variance in Gaussian data (uses 2nd order statistics only); B) ICA finds projections of maximal independence in non-Gaussian data (using higher-order statistics).

When applying ICA to fMRI data, the resulting components would be characterised as pairs of spatial maps and related time-courses. The spatial map may represent a map of stimulus related functional activity, task-unrelated spontaneous intrinsic brain activity (or RSNs), or possible sources of artefact; whilst the time-courses (and relative spectra profile) would represent the component-specific time-course along the fMRI acquisition time (Beckmann and Smith, 2004; Beckmann, 2012). Crucially, the application of ICA decomposition of multiple subject fMRI data, allows that for

each ICA component it would be possible to extract the subject-specific representation and contribution, thus providing individual spatial-maps and time-courses.

In contrast to atlas-based parcellations, where atlas regions' boundaries may not take into account subject-specific differences in functional organization, an ICA parcellation approach generates a rich data-driven description of multiple networks in the brain but at the expense of no longer dictating in advance the regions with which the connectivity maps are related. Using ICA, each node of the network is described by a spatial map of varying weights; each map may overlap with other nodes' maps and may span more than one group of contiguously neighbouring points (Smith, Vidaurre, *et al.*, 2013; Smith, 2016).

In contrast to low-dimensional ICA parcellation, high-dimensional resting-state fMRI parcellation into many nodes (potentially hundreds) allows a richer analysis of the network connections. This approach is limited by the temporal resolution and the number of data points available, as ICA decomposition differentiates underlying blind sources based on time-spectra information. The risk of applying high-dimensionality ICA to non-high temporal resolution and short-acquisition resting-state fMRI data is to overfit noise.

However by shifting the emphasis from large-scale RSN maps into a network description of nodes and edges, new information and multiple features can be gained. In order to map the functional connectome, carry out connectivity modelling and compare connectomes across subjects, it is fundamental to achieve a common parcellation in each subject. This is why a group-level data-driven parcellation is preferable to random based parcels, which are known to mix signals belonging to functionally distinct areas (Glasser *et al.*, 2015; Yeo and Eickhoff, 2016).

Functional connectivity estimation

Based on the notion that the BOLD signal within functionally linked regions will co-fluctuate and that this represents synchronous spontaneous changes in brain processing states, the quantification of resting-state BOLD fMRI correlation-based connectivity is thought to reflect the connectivity pattern of RSNs (Deco *et al.*, 2011; Smith *et al.*, 2011; Smith, 2016).

Termed network edges, the connections between nodes are estimated by analysing the relationship between fMRI time series within the nodes (Figure 17) (Smith *et al.*, 2011). As a result, brain connectivity can be represented as a 'parcellated connectome', which can be visualized simply as an Nnodes × Nnodes network matrix or a graph (explicitly showing nodes and the strongest edges). Functional network connectivity analysis can therefore inform about functional specialisation (investigating the functional connectivity of each node separately) and functional integration (investigating how nodes interact with each other and form communities of functionally related clusters of nodes).

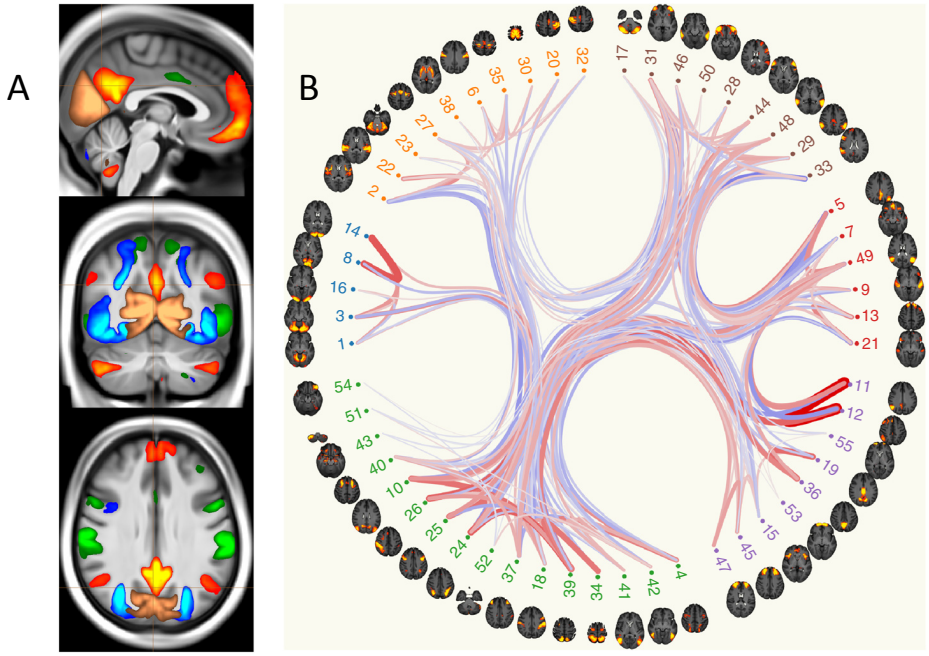

FIGURE 17 EXAMPLE OF RESTING-STATE FMRI NETWORKS AND FUNCTIONAL CONNECTIVITY IN THE HUMAN BRAIN NETWORK

A) Showing four group-average RSNs maps from a low-dimensional decomposition, including the default mode network (red-yellow), dorsal attention network (green), primary visual (copper) and higher level visual (dorsal and ventral streams, blue). B) Showing group-average connectome representation of 55 brain regions (network nodes) from a higher dimensional parcellation. Network nodes are represented by the external ring and are linked by the strongest individual functional connections are shown (positive in red, anticorrelations in blue). Figure reproduced and adapted from (Miller *et al.*, 2016).

Given a set of nodes' time series, correlation is one approach for inferring the network edges and assessing whether the regions are functionally connected. Many factors other than the direct anatomical node-to-node connection 'true strength' can affect correlation coefficients, including variations in signal amplitude and noise level (Friston, 2011).

Many different methods are being used in the literature to quantify resting-state functional connectivity. A recent work compared different connectivity estimation

approaches on rich, realistic simulated fMRI data for a wide range of underlying networks, experimental protocols and confounds (Smith *et al.*, 2011).

The results highlight that in general correlation-based approaches can be quite successful, methods based on higher-order statistics are less sensitive, whereas lag-based approaches perform very poorly. More specifically: there are several methods that can give high sensitivity to network connection detection on good quality fMRI data, in particular, partial correlation, regularised inverse covariance estimation and several Bayes net methods. With respect to the various confounds investigated in the study, the most striking result was that the use of functionally inaccurate ROIs (when defining the network nodes and extracting their associated time-series) is extremely damaging to network estimation; hence, results derived from inappropriate ROI definition (such as via structural atlases) should be regarded with great caution.

In general partial temporal correlation between nodes' time series aims to estimate direct connection strengths and tends to perform more accurately than full correlation (Smith *et al.*, 2011). Partial correlation refers to the normalised correlation between two time-series, after each has been adjusted by regressing out all other time-series in the data (all other network nodes). Although no directional information is given, this approach attempts to distinguish direct from indirect connections.

An efficient way to estimate partial correlations is via the inverse of the covariance matrix (Marrelec *et al.*, 2006). Under the constraint that this matrix is expected to be sparse, regularisation can be applied, for example, using the Lasso method (Banerjee *et al.*, 2006; Friedman *et al.*, 2008). This shrinks entries that are close to zero more than those that are not. The limit of the Lasso approach is that in high dimensional settings with inter-correlated time-series the regularization approach will chose to preserve randomly only one or few of these edges and shrink all the others to zero.

An alternative way to improve the stability of the estimates of partial correlation coefficients, is to use Tikhonov-regularized partial correlation, where no sparsity is enforced and a small amount of L2 regularization is applied (Smith, 2016). This has the effect of preserving the full range of inter-correlated network edges while enhancing robustness of partial correlation estimation.

Correlation-based connectivity, however, cannot reveal anything about causality or even whether connectivity is direct versus indirect (Marrelec *et al.*, 2006). The distinction between functional and effective connectivity is important for deciphering the underlying biological networks (Friston, 1994). Methods for effective connectivity modelling that have been applied to resting-state fMRI data are usually complex models with many parameters, each representing a biological or physical measure (such as average neuronal activity and (separately) the haemodynamic response to neural activity); these kind of models are ideally fit to data using probabilistic Bayesian methods such as dynamic causal modelling (Friston *et al.*, 2011; Woolrich and Stephan, 2013). This approach however is feasible only in the contest of task-based fMRI, where a specific network model with few nodes (and few pattern of effective connectivity) can be hypothesized as the result of an exogenous stimulation, as observational data such as resting-state fMRI is in general not a robust and safe tool for inferring causality (Pearl, 2009).

Another approach for network modelling comes from the domain of graph theory (Rubinov and Sporns, 2010; Fornito *et al.*, 2013; van den Heuvel and Sporns, 2013). This includes: the study of node clustering and hierarchies; the study of hubs (nodes, or clusters of nodes, that are particularly highly connected to other parts of the network); and deriving global network summary metrics such as small worldness (looking at how the communication and clustering acts over multiple scales) or measures of general network efficiency. As for correlation-based network

connectivity, these techniques are dependent on accurate network modelling at the lower level as in carefully constructed network matrices, regardless of how advanced or conceptually elegant a given graph-theoretical measure may be. One specific risk of this approach is the use of inappropriate node definition (Smith *et al.*, 2011; Craddock *et al.*, 2012), such as a gross structural atlas-based parcellation that poorly corresponds to functional boundaries and results in networks and graph-theory analyses whose neurobiological interpretability is limited. Another concern is that it is frequently the (thresholded) full correlation matrix that is input into graph-theoretical analyses rather than an estimate of direct network connections. Considering just part of the estimated network may therefore not be entirely correct. Another limitation is that graph theory can abstract the network matrix to a very high degree, summarising an entire study down to a single measure representing overall network efficiency, or small worldness, and any apparent change in this measure might not reflect a genuine change in the brain connectivity but rather any of a myriad of potential confounds (e.g., factors as basic as systematic group differences in head motion or heart rate) (Smith, Vidaurre, *et al.*, 2013).

Dynamic functional connectivity

In the last two decades fMRI has played a central role in characterizing the nontrivial spatial and topological structure of functional brain networks, but thus far has been limited in its capacity to study their temporal evolution having focused its study in a time-averaged sense.

Recent investigations of resting-state fMRI have emphasized the dynamic nature of functional networks (Deco *et al.*, 2009, 2011; Allen *et al.*, 2012; Calhoun *et al.*, 2014; Zalesky *et al.*, 2014; Hansen *et al.*, 2015; Zalesky and Breakspear, 2015). By empirically studying and modelling the property of nonstationarity (as temporal

variability in any given statistic or the signal variance changing over time), these studies aimed to shed new light on large-scale functional network dynamics. Studying correlation-based connectivity in a sliding-window fashion, these studies have shown that brain activity between pairs of neuroanatomical systems spontaneously fluctuates in and out of correlation over time in a globally coordinated manner, giving rise to sporadic intervals during which information can be efficiently exchanged between neuronal populations (Figure 18) (Zalesky *et al.*, 2014). These studies propose that dynamic fluctuations in the brain's organisational properties may minimise metabolic requirements while maintaining the brain in a responsive state. It has been proposed that the formation and dissolution of resting-state patterns reflects the exploration of possible functional network configurations around a stable anatomical skeleton, a property that may support effective information processing (Deco *et al.*, 2011).

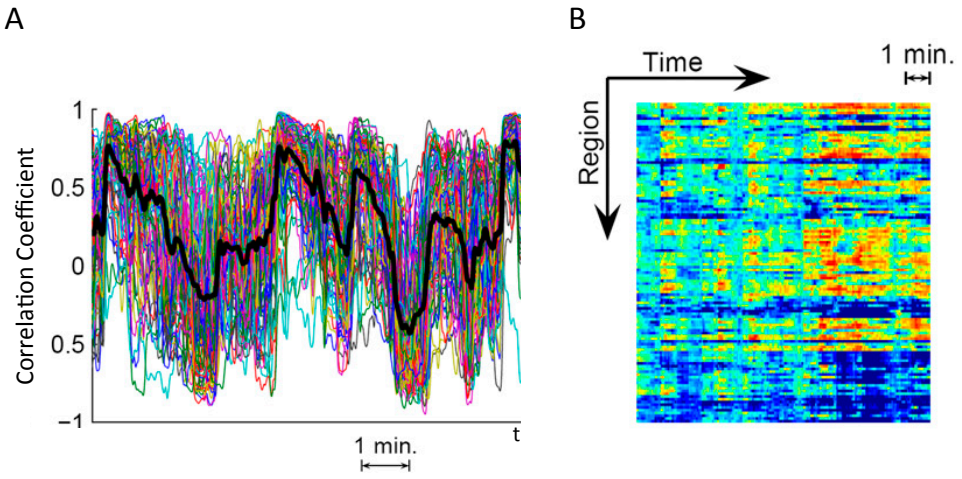

FIGURE 18 DYNAMIC FLUCTUATIONS OF RESTING-STATE NETWORKS FUNCTIONAL CONNECTIVITY IN THE MATURE HUMAN BRAIN

A) Time series of RSNs functional connectivity (Pearson's correlation coefficients) over time. Showing only top-100 most dynamic functional connections for one healthy, young adult. Synchronization between RSNs occurs at distinct moments in time, where multiple connections transition en masse between high and low levels of connectivity. B) Time-resolved

analysis of regional network efficiency. The figure shows that resting-state functional brain networks spontaneously reconfigure in such a way that multiple regions synchronously transition to high-efficiency states. Figures reproduced and adapted from (Zalesky *et al.*, 2014).

Recent studies using magnetoencephalography (MEG) and EEG (EEG), have shown evidence that functional connectivity within whole brain networks exhibit temporal variability on a time scale of seconds to tens of seconds (de Pasquale *et al.*, 2010; de Pasquale *et al.*, 2012; C. Chang *et al.*, 2013; Hutchison *et al.*, 2013; Brookes *et al.*, 2014). MEG scanners measure changes in the magnetic fields generated by electrical currents in the brain, which means that they can detect alterations in brain activity much more rapidly than fMRI.

Based on the assumption that to provide an effective substrate for cognitive processes functional networks should be able to rapidly reorganise and coordinate on a sub-second temporal scale (Bressler and Tognoli, 2006), Baker et al. used MEG to characterize whole-brain functional activity dynamics at high temporal resolution and to infer hidden dynamic states of brain network activity (Baker *et al.*, 2014). Importantly they studied MEG activity using a hidden Markov model, which infers a number of discrete brain states that recur at different points in time. The hidden Markov model (HMM) is a generative probabilistic model, in which the sequence in time of an observable variable is generated by a sequence of internal hidden states. These hidden states cannot be observed directly, and the transitions between hidden states are assumed to have the form of a Markov chain described by a transition probability matrix and an optimal states sequence (the Viterbi path). Each inferred state corresponds to a unique pattern of whole-brain spontaneous activity, which is modelled by a multivariate normal distribution and a state time-course indicating the points in time at which that state is active. These two characteristics allow the description of both the spatial and temporal characteristics of each inferred state.

They have shown that the HMM can independently identify fast transient brain states in MEG data that correspond to established RSNs. By assessing temporal changes in the occurrence of these states, this demonstrated that within-network functional connectivity is under-pinned by neuronal dynamics that fluctuate much more rapidly than has previously been shown (100-200 ms) (Figure 19). This work moves from the assumption that resting-state activity may be broken down into a set of distinct activity patterns that repeat over time and where only one functional state may be active at any one time. Although this might seem an oversimplification, it is in agreement with computational models of neuronal connectivity (Deco et al., 2011) and direct observations from both fMRI (Allen et al., 2012) and EEG (Britz et al., 2010; Musso et al., 2010; Yuan et al., 2012). The temporal organization of dynamic brain activity through these transient spatial patterns of coordination may therefore provide the flexibility required to adapt to the rapidly changing computational demands of cognitive processing (Bressler and Tognoli, 2006).

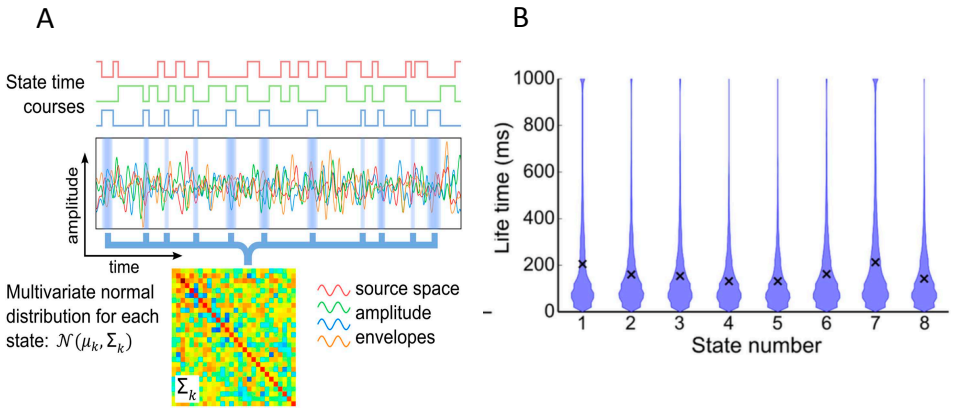

FIGURE 19 FAST TRANSIENT SEMI-STABLE STATES OF SPONTANEOUS ACTIVITY IN THE MATURE HUMAN BRAIN

A) Schematic cartoon of the HMM outputs. An HMM with K states is inferred from MEG or fMRI data. Each brain state is characterized by a multivariate normal distribution, and a state time-course (which is a binary sequence that indicates the points in time at which the state is active). B) Temporal characteristic (life time) of the brain states measured from MEG data.

Violin plot showing the distribution of life times values; the black crosses show the mean. Figures reproduced and adapted from (Baker *et al.*, 2014).

Methodological limitations of task-based neuroimaging approaches

The first two decades of human fMRI studies have relied on the application of task-based neuroimaging paradigms in order to study changes in neural activity evoked by external stimuli or tasks (Bandettini *et al.*, 1992; Kwong *et al.*, 1992; Ogawa *et al.*, 1992). This neuroimaging approach depends on the subtraction paradigm or on the event-related design.

The former, the subtraction paradigm, leans on several underlying assumptions that may not be always satisfied. For instance, it depends on the correct choice of a control task (the control task should remove all but the component of interest), therefore assuming a specific underlying neurocognitive model (even if a task does not explicitly involve a particular component, a subject may engage in it anyway). It relies on the assumption that a single component process can be inserted into a task without affecting other processes ("pure insertion"). The second, the event-related design, tries to overcome some limitations of the subtraction paradigm and is usually implemented together with modalities with high temporal resolution, such as NIRS and EEG. This approach presents several advantages, such as the opportunity to disentangle rapid changes in neural processing related to, for instance, rapid phonetic changes in linguistic stimuli; or the possibility of avoiding the modelling of slow BOLD responses in response to rapid stimulation. However, this approach has also several limitations. For instance, it is characterise by the low coverage across the whole-brain; by low signal to noise; by signal attenuation and reduced efficiency (requiring a longer acquisition time to achieve sufficient statistical power); and by poor or difficult source localization (with, in the case of NIRS, unexpected light

absorption and scattering that may take place along inconstant gyral surfaces such at the level of the Sylvian fissure). Thus this kind of approach allows the investigation of only those brain responses involving homogeneous brain surfaces at an extreme macro-scale.

Summary

With an increasing number of works using non-invasive in-vivo MRI in infancy, (both functional (Doria *et al.*, 2010; Smyser *et al.*, 2010, 2011, 2014; Kwon *et al.*, 2015; Ball *et al.*, 2016); and structural/diffusion (Counsell *et al.*, 2003; Dubois *et al.*, 2009, 2015, Ball *et al.*, 2012, 2014, 2015)), MRI has opened a new window into the functional and structural organization of the developing human brain.

Although the first two decades of human fMRI studies has mostly applied task-based neuroimaging paradigms (Bandettini *et al.*, 1992; Kwong *et al.*, 1992; Ogawa *et al.*, 1992), in recent years researchers' attention has shifted towards slow (<0.1 Hz) spontaneous fluctuations of the BOLD fMRI signal in the resting brain as an efficient tool to characterise human brain organisation (Raichle *et al.*, 2001; Fox and Raichle, 2007). Resting brain activity has a high-energy consumption (consumes 20% of the body's energy although accounting for only 2% of total body mass), and is supposed to support the on-going neuronal signalling (Attwell and Laughlin, 2001). Besides the interest concerning the biological mechanisms underlying resting-state spontaneous neural processes, this shift in research focus has also been fostered by possible criticisms regarding the reproducibility of task-based neuroimaging approaches.

Resting-state functional-MRI and diffusion weighted-MRI therefore represent a powerful, practical and ideal tool to investigate the human infant brain organization and to shed new light on the ontogeny of language in the human brain.

Rational of the analyses presented in the experimental chapters

As highlighted in the first chapter, the motivation underlying the work of this thesis is to better understand whether the human neonatal brain is biased toward language learning. By identifying structural and functional neural correlates that are linearly predictive of complex linguistic performance assessed at two years of age, in the following experimental chapters I aim to identify possible neural mechanisms underlying early language acquisition in the preterm human brain imaged at term equivalent age.

Although a control group is not present, thus hindering the capacity to generalise the presented results to the healthy-development population, it is important to note that I have nonetheless chosen a computational approach to model the effect of premature birth in the emergence of a language brain network. The effect of degree of prematurity (measured by gestational age at birth) is here modelled in a linear fashion as the modulation between brain and behaviour. Indeed testing for brain differences between preterm infants and controls may result in neural patterns that are not associated to degree of prematurity but driven by secondary clinical variables (i.e. mechanical ventilation). This approach further allows to disentangle the effect of premature birth from the effect of postnatal socioeconomic factors, providing specificity in the study of the brain-behaviour modulation due to prematurity.

The effect of number of days of ex-utero life was not considered of interest, as this variable is the linear subtraction of gestational weeks at birth from postmenstrual

weeks at scan. Instead, postmenstrual age at MRI was used previous to any association analyses to adjust for the maturational effect due the differences in age at scan. Indeed as shown in chapter 5, once the variance of postmenstrual age at scan is regressed out, the information carried by days of ex-utero life is collinear with gestational age at birth.

Although research question regarding both the direct effect of development (or grow) and degree of premature birth on brain structure and function are of primary interest, here they will result as off-topic, as the work of this thesis does focus on early predictors of language learning and on the modulation of degree of prematurity in this neurobehavioural link. Therefore I would point the reader interested in those topics to the other multiple works carried out within (but not exclusively) the Centre for the Developing Brain.

Standardised neurocognitive assessment of receptive, expressive linguistic abilities and cognitive capacities was carried out using the (previously described) Bayley Scales of Infant and Toddler Development, Third Edition (Bayley, 2006). The confounding effect of household's environment on linguistic and cognitive abilities (i.e. due to socioeconomic factors) was regressed using the Multiple Deprivation index. This index is currently the most widely used measure of socioeconomic deprivation for small areas (or neighbourhoods) in England (T. Smith et al., 2015). At a national level, the index of Multiple Deprivation was shown to be highly correlated with a primary school-level socio-economic indicator such as the proportion of pupils eligible for free school meals (Crawford and Greaves, 2013). Furthermore, in a previous study investigating a similar cohort of preterm born infants, the index of Multiple Deprivation was shown to be one of the most predictive measures of inter-subject differences in later neurodevelopment (Ball et

al., 2015). Although this measure is far from being perfect, as all measures, in the UK it represents a good, pragmatic socio-economic indicator.

From a methodological perspective the work of this thesis is also the result of an exploration of how neuroimaging measures may be helpful to predict i.e. behavioural measures from MRI data acquired years apart. This computational approach, allowing the estimation of a predictive (or mechanistic) models in brain-behaviour interaction, clearly differs in many ways from the most widely used regression approaches to brain imaging. Instead of using mass-univariate general linear testing of brain regions (or voxels, or white matter bundles) associated with a specific personality trait or developmental measure (i.e. a scalar measure of interest), brain measures are used as features in multiple regression approaches in order to maximise the prediction (and/or minimise the error) of the scalar measure of interest. This inversion of the problem, transforms the statistical approach in a problem of brain pattern identification (i.e. *"What is the brain pattern that better predict inter-subject differences in intelligence quotient?"*). Although the methodological implementation is not trivial, it allows to overcome some statistical limitations recently highlighted in the neuroscientific field. For instance, as sample size in neuroimaging studies is increasing (S. M. Smith *et al.*, 2015; Miller *et al.*, 2016), looking just at the statistical significance values will lead a higher chance of null hypothesis rejection; whilst, cross-validating a model and testing its prediction power on new data represents a more sound approach. It follows that this approach has the advantage of comparing multiple alternative models on the basis of the predictive power.

Chapter 5

Language ability in preterm children is associated with arcuate fasciculi microstructure at term

In this chapter I investigate the microstructural maturation of the arcuate fasciculus as a neuromarker for early language learning. The key motivations for this choice are the following: 1) the key role of arcuate fasciculus in the adult language system (Catani *et al.*, 2007; Berwick *et al.*, 2013); 2) comparison studies with primates show the organisation of this bundle as being human-specific (Rilling *et al*., 2008). (Indeed unpublished data presented by Marco Catani's lab at the Society for Neurobiology of language 2016 show the arcuate fasciculus as the only linguistic tract being present in humans but not in primates); 3) previous neuroimaging studies in infants using low-angular resolution DWI sequences and no adequate DWI processing, have led to the belief that the arcuate fasciculus during perinatal period does not reach the frontal terminations (Perani *et al.*, 2011). Jessica Dubois in 2015 indeed suggested that this finding might have been an artefact due to DWI characteristics rather then the true developmental pattern of infant brain development; 4) although ventral linguistic bundles are known to play a role in the language network during childhood development, these bundles are mainly known to support semantic processing of lexical items; thus one may hypotheses that these tracts become central in language learning at a later developmental stage. On the basis of the results presented in this chapter, further studies should explore the role of ventral linguistic bundles in human

language acquisition.

From a methodological perspective, in this chapter I have adapted DWI processing pipeline previously used in adult studies to human infant brain imaging data. For example, the combination of FSL Topup tool with the t2w image of the infant brain was here used to correct for EPI distortions. Future studies however should acquire b-zeros images with reversed phase-encode to correct DWI images more efficiently. In this chapter I have also explored multiple regression approaches in order to test the robustness of the results here presented against different regression methods, and in cross-validation settings.

This chapter, that is also part of a publication on the peer-reviewed journal Human Brain Mapping (see Appendix 2), discuss the specific role of the term-equivalent arcuate fasciculus in the later development of complex linguistic and cognitive abilities, and how this results support previous developmental models of auditory-verbal working memory.

Introduction

Comparative studies in humans and nonhuman primates have shown that the evolution of language has resulted from specific modifications of the cortical areas and pathways that mediate linguistic function (Rilling *et al.*, 2008). The arcuate fasciculus is a bilateral white-matter fibre tract linking the posterior superior temporal cortex (Wernicke's area) to Brodmann area 44 in the frontal cortex (Broca's area) via a dorsal projection that arches around the Sylvian fissure (Catani *et al.*, 2005; Rilling *et al.*, 2008). In the human brain, diffusion weighted imaging has shown that the organization and cortical terminations of this tract are strongly modified in comparison to primates and has demonstrated that the auditory regions

of the temporal cortex have a higher probability of connection via the dorsal pathway with the frontal cortices (Rilling *et al.*, 2008, 2011; De Schotten *et al.*, 2012). In contrast, axonal tracing studies in monkeys have shown that the arcuate fasciculus connects to more dorsally located regions, such as the extrastriate visual cortex (Petrides and Pandya, 1984; Schmahmann *et al.*, 2007). Taken together, these findings have generated the theory that the expanded direct dorsal pathway may be a key structure responsible for supporting the emergence of language in humans.

In human adults, the arcuate fasciculus has been proposed to play an important role in the core syntactic computation of complex sentences (Berwick *et al.*, 2013), in verbal short-term memory and in the perception of the phonetic structure of speech (Liberman and Mattingly, 1985). It is also hypothesized to play a distinctive role in speech production via the integration of auditory and motor representation. Predominantly at the syllable level, it is thought to map sensory targets in the auditory cortex to motor programs coded in Broca's area (Hickok and Poeppel, 2007; Hickok, 2012). Patients with injuries involving either the left or right arcuate fasciculus have impaired ability in phonological and word repetition tasks and in verbal short-term memory (Geschwind, 1965; Benson *et al.*, 1973; Damasio and Damasio, 1980; Alexander *et al.*, 1987). With regard to learning, the microstructural properties of the left direct segment of the arcuate fasciculus have been associated with the process of learning new words in adulthood (López-Barroso *et al.*, 2013), whilst improved performance in auditory verbal learning tasks are significantly associated with a less lateralized volumetric pattern of the direct pathways (Catani *et al.*, 2007). Children with Angelman Syndrome in whom neither the left nor right arcuate fasciculi can be identified on diffusion tractography have no oral language development, whereas when the left arcuate fasciculus cannot be identified language difficulties are always observed (B. J. Wilson *et al.*, 2011; Paldino *et al.*, 2016).

These observations confirm the crucial role of the arcuate fasciculus in speech acquisition (Hickok and Poeppel, 2007; Berwick *et al.*, 2013).

As infants have impoverished language production and their reception abilities were thought to be limited to the supra-segmental properties of speech, the role of the arcuate fasciculus has traditionally been considered to be secondary during the first stages of language acquisition. Although inferior frontal regions are activated in several fMRI studies in infants (Dehaene-Lambertz *et al.*, 2006; Perani *et al.*, 2011; Shultz *et al.*, 2014; Baldoli *et al.*, 2015), the ventral pathway, comprising the uncinate and the inferior fronto-occipital fasciculus, has been proposed to initially be the main functional linguistic pathway connecting temporal and frontal areas (Perani *et al.*, 2011; Brauer *et al.*, 2013; Dubois *et al.*, 2015). Recent advances in diffusion-weighted imaging have enabled the investigation of white-matter tracts thought to be involved in the acquisition of language and neurodevelopmental skills during the neonatal period (Perani *et al.*, 2011; Brauer *et al.*, 2013; Dubois *et al.*, 2015). These studies have suggested that, in contrast to the mature brain (where it terminates in Broca's area), the anterior direct segment of the arcuate fasciculus cannot be dissected after the premotor cortex (Dubois *et al.*, 2015). Whilst this finding may represent a genuine developmental difference in the extent of the arcuate fasciculus (Perani *et al.*, 2011; Brauer *et al.*, 2013; Dubois *et al.*, 2015), it could also reflect the low angular resolution used in the diffusion weighted sequences which may have limited delineation of the arcuate fasciculus in regions where the fibres cross with the cortico-spinal tracts and the corpus callosum in the corona radiata (Dubois *et al.*, 2015).

Premature birth is associated with verbal impairment, the severity of which increases with increasing prematurity at birth (Luu *et al.*, 2009, 2011; van Noort-van der Spek *et al.*, 2012). Previous studies of infant brain development have shown that white-

matter architecture is significantly altered following premature birth (Hüppi, Maier, *et al.*, 1998; Counsell *et al.*, 2003; Rose *et al.*, 2008; Ball *et al.*, 2014) and the degree of this alteration is directly related to performance in specific neurodevelopmental domains (Bassi *et al.*, 2008; Berman *et al.*, 2009; Groppo *et al.*, 2014). It is thus possible that premature delivery also affects the white-matter structures that sub-serve language function impacting on later linguistic behaviour.

To address the question of whether or not the arcuate fasciculus is a specific neurolinguistic precursor in early human infancy; and to assess whether the degree of prematurity affects arcuate fasciculus microstructure and drives the relationship with later linguistic behaviour, we used high *b* value HARDI in a cohort of 43 preterm born infants at term equivalent age and assessed their linguistic developmental performance at 2 years. We hypothesized that inter-subject differences in composite linguistic skills at 2 years would be associated with term equivalent FA of the left and right arcuate fasciculi. To act as a control, we tested whether any relationship between brain structure and language performance could also be associated with FA values of the cortico-spinal tracts.

Materials and methods

Infants

Preterm infants were recruited as part of the Eprime study, and were imaged at term equivalent age over a 3-year period (2010-2013) at Queen Charlotte's and Chelsea Hospital, London. The study was reviewed and approved by the National Research Ethics Service, and all infants were studied following written consent from their parents. A cohort of 43 preterm born infants (median age at birth of 30.14 GA weeks; range 24 - 32; 18 females) with no evidence of focal abnormality on MRI

were imaged using high-angular resolution diffusion-weighted neuroimaging at 42.14 PMA weeks (range 39 - 46) (Table 1), and followed up to around 22 months of age in order to assess their neurodevelopmental performance.

Characteristic	**Value**
Median (range) GA at birth (weeks)	30 (24 – 33)
Median (range) birth weight (grams)	1205 (645 – 1990)
Median (range) PMA at MRI (weeks)	42 (39 – 46)
Female, no (%)	18 (42%)
Chorioamnionitis, no (%)	1 (2%)
Intrauterine growth restriction, no (%)	7 (16%)
Median (range) mechanical ventilation (days)	0 (0 – 40)
Necrotizing enterocolitis requiring surgery, no (%)	1 (2%)
Mean (± SD) parental SES	17.4293 (±8.0772)

TABLE 1 INFANT CHARACTERISTICS

Acquisition of MRI imaging data at term equivalent age

All MRI studies were supervised by an experienced paediatrician or nurse trained in neonatal resuscitation. Pulse oximetry, temperature, and heart rate were monitored throughout the period of image acquisition; hearing protection in the form of silicone-based putty placed in the external ear (President Putty, Coltene; Whaledent)

and Mini-muffs (Natus Medical Inc.) was used for each infant. Sedation (25–50 mg/kg oral chloral hydrate) was administered to 33 infants. Imaging was acquired using an eight-channel phased array head coil on a 3-Tesla Philips Achieva MRI Scanner (Best, Netherlands) located on the Neonatal Intensive Care Unit. Whole-brain diffusion-weighted MRI data were acquired in 64 non-collinear directions with b value of 2500 s/mm^2 and 4 images without diffusion weighting (isotropic voxel size of 2 mm; TE= 62 ms; TR= 9000 ms). High-resolution anatomical images were acquired with pulse sequence parameters: T1 weighted 3D MPRAGE: TR = 17 ms, TE = 4.6 ms, flip angle 13°, slice thickness 0.8 mm, field-of-view 210 mm, matrix 256 × 256 (voxel size: 0.82 × 0.82 × 0.8 mm); and T2 weighted fast-spin echo: TR = 8670 ms, TE = 160 ms, flip angle 90°, slice thickness 2 mm with 1 mm overlap, field-of-view 220 mm, matrix 256 × 256 (effective voxel size: 0.86 × 0.86 × 1 mm).

Neurodevelopmental assessment

Standardized neurodevelopmental assessment at a median age of 22 months (range: 21 – 24 months; median of 20 months corrected for prematurity) was carried out by an experienced paediatrician or developmental psychologist with the Bayley Scales of Infant and Toddler Development, Third Edition (BSID-III) (Bayley, 2006).

MRI data pre-processing

T2-weighted brain volumes were bias corrected, brain extracted and tissue segmented into white matter, grey matter, deep grey matter structures, and cerebrospinal fluid using a neonatal specific segmentation tool (Makropoulos *et al.*, 2014). Diffusion MRI volumes were first visually inspected in order to detect and exclude data with motion artefact. All subjects included in the study had 5 or fewer volumes excluded due to head-motion. B0 field inhomogeneities, eddy currents, and

inter-volume motion were corrected using topup and eddy tools in FSL5 (Andersson *et al.*, 2003; Smith *et al.*, 2004; R. E. Smith *et al.*, 2015; Andersson and Sotiropoulos, 2016). B1 field inhomogeneity was corrected using Insight Segmentation and Registration Toolkit-N4 (ITK-N4) (Tustison et al., 2010). All rigid registrations in native subject space were estimated using FSL boundary-based registration optimized for neonatal tissue contrasts (Toulmin *et al.*, 2015); and nonlinear registrations to the T2-weighted template were estimated using ANTs (Avants *et al.*, 2008). All transformation pairs were calculated independently and combined into a single transform in order to reduce interpolation error.

Tractography of the arcuate fasciculi

Estimation of fibre orientation distribution was computed through constrained spherical deconvolution (CSD) (Tournier *et al.*, 2004, 2007), with a maximum spherical harmonic order of 8. We used the MRtrix3 package to perform anatomically constrained probabilistic tractography (http://www.mrtrix.org) (R. E. Smith *et al.*, 2012; Tournier *et al.*, 2012). Fibre tracking of the arcuate fasciculus was performed in each subject's native space independently for both hemispheres, using a two-region of interest approach. From the T2-weighted template, we back-projected two inclusion regions of interest and a seed-plane. To maximize the chances of virtually dissecting the arcuate fasciculus, the seed-plane was located in its direct dorsal pathway transverse to its antero-posterior direction, and random seed-streamlines were generated within it. The frontal region of interest was identified anterior to the central sulcus, in order to encompass the white matter of the posterior region of the inferior and middle frontal gyri. The temporal region of interest was defined in the white matter of the posterior part of the superior and middle temporal gyri (Figure 20) (Forkel *et al.*, 2014). The reconstructed tracts in both hemispheres were then thresholded at a minimum of ten streamlines per voxel, and the median FA

values in this masks (separately for the left and right hemisphere) were extracted as measures of white-matter microstructure (Beaulieu, 2002; López-Barroso *et al.*, 2013).

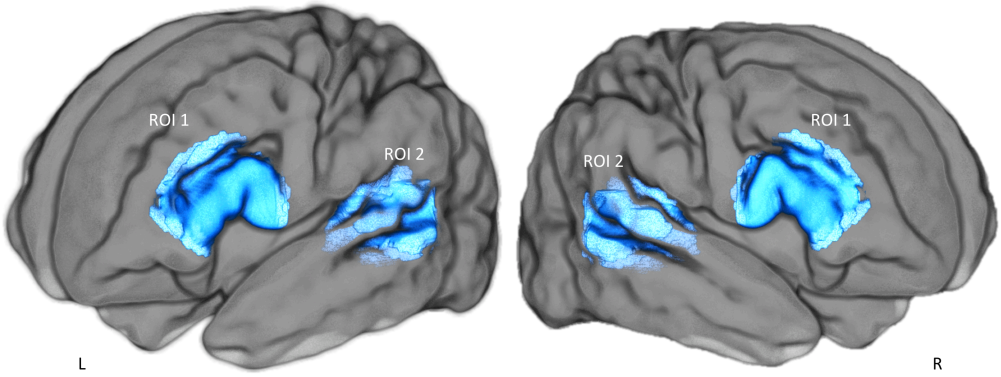

FIGURE 20 REGIONS OF INTEREST USED TO PERFORM ANATOMICALLY CONSTRAINED SPHERICAL DECONVOLUTION TRACTOGRAPHY OF THE DIRECT SEGMENT OF THE ARCUATE FASCICULUS

ROI 1: Broca's region (for the left and right hemisphere); ROI 2: Wernicke's region (for the left and right hemisphere). Fibre-tracking of the arcuate fasciculus was performed in each subject's native space independently for both hemispheres. Only streamlines crossing both regions of interest were considered.

Tractography of the cortico-spinal tracts

To act as control regions, the left and right cortico-spinal tracts were also delineated. From the T2-weighted template, we back-projected a seed-region (an axial delineation of the pons) and two inclusion regions (the posterior limbs of the internal capsule and two axial-planes at the level of the primary motor and somatosensory cortices). We then extracted the median FA value along the reconstructed tract in both hemispheres.

Statistical analysis

To address the microstructural effect of neonatal development and early environmental factors linked to premature delivery, we used a GLM to test the linear association between arcuate fasciculi FA, cortico-spinal tracts FA, and global white-matter median FA, with 1) PMA at scan (covaried for GA at birth); and 2) GA at birth (covaried for PMA at scan). The number of days of ex-utero life was highly correlated with PMA at scan and GA at birth (Pearson's correlation coefficient of postnatal age respectively with PMA and GA: $r = 0.79$; $p < 10^{-5}$; $r = -0.90$; $p < 10^{-5}$) and so we did not include this as a covariate in the model (Figure 21).

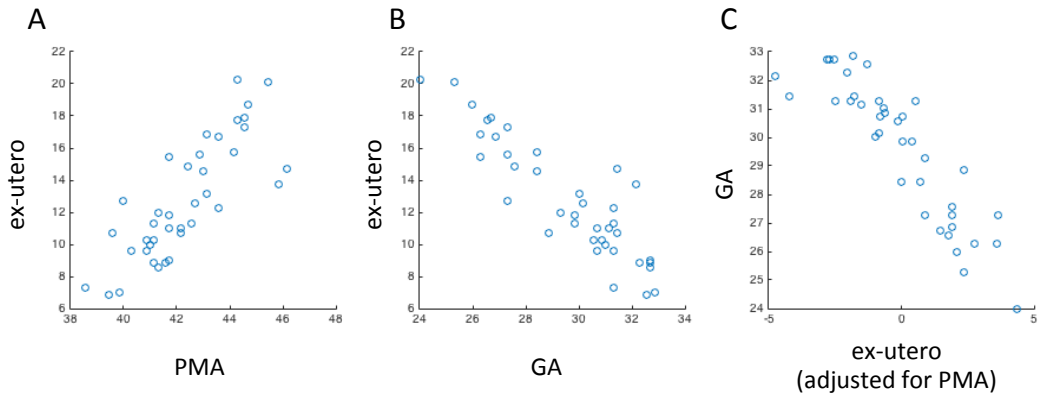

FIGURE 21 COLLINEARITY BETWEEN EX-UTERO LIFE AND PMA AT SCAN AND GA AT BIRTH

Showing A) scatter plot between PMA at scan and days of ex-utero life (Pearson's $r = 0.79$; $p < 10^{-5}$); B) scatter plot between GA at birth and days of ex-utero life (Pearson's $r = -0.90$; $p < 10^{-5}$); C) scatter plot between days of ex-utero life (after adjustment for PMA at scan) and GA at birth (Pearson's $r = -0.90$; $p < 10^{-5}$).

The primary goal of this study was to assess the role of the direct segments of the arcuate fasciculi in the early acquisition of linguistic function. To do this we tested whether inter-subject differences in composite linguistic skills at two years were associated with term equivalent fractional anisotropy (FA) of the left and right direct segments of the arcuate fasciculi.

We removed the effect of confound variables prior to the analysis; these were PMA (for the FA measures) and socioeconomic score (for linguistic skill measures). All features were standardized in the training sets to have zero mean and unit variance and the same transformation was then applied to the testing sets.

To test whether FA values of the left and right arcuate fasciculus was associated with composite linguistic skills at 2 years we first used cross-validated Ordinary Least Squares (OLS) regression. However, coefficient estimates for OLS rely on the independence of the model terms and in this case the measured FA in left and right arcuate fasciculus were highly correlated ($r = 0.58$; $p < 10^{-5}$). To overcome this, we used cross-validated Ridge regression (a linear least squares variant with L_2 regularization) and Partial Least Squares (PLS) regression. PLS is particularly suitable in cases where predictors are highly correlated or even collinear, i.e. where standard regression is not appropriate (Hotelling, 1936; Wegelin, 2000). The approach identifies linear combinations of the independent variables that optimally predict corresponding combinations of the dependent variables (Rosipal and Krämer, 2006). Here it was applied with mode A and deflation mode canonical (Wegelin, 2000).

We used leave-one-out cross-validated PLS to assess whether inter-subject differences in linguistic abilities at 2 years of age were associated with term equivalent FA of the left and right arcuate fasciculi. At each training iteration, the data for $n - 1$ subjects were used to train a PLS model; the learnt link was then used to generate the linguistic score for the left-out subject. Following all iterations, the correlation between PLS FA scores and PLS language scores was assessed. We then extracted the PLS relative loadings of involvement averaged across all cross-validation folds; the mean and SD of these parameters were extracted in order to assess model stability.

As a control, we also used the same cross-validated pipeline to test whether individual-differences in linguistic performance were associated with left and right cortico-spinal tracts FA.

To test whether early environmental influences associated with preterm birth or global white-matter volume (Northam *et al.*, 2012) were driving the identified brain-behaviour link in a dose-dependent fashion, we calculated the partial correlation between PLS FA scores and PLS language scores adjusting for GA at birth, global white matter volume, and sex.

Statistical significance was determined with non-parametric permutation testing (10 000 permutations) with correction for the FWE rate (Winkler *et al.*, 2014). All analysis were performed using MATLAB (R2015b, The MathWorks, Inc., Natick, MA, USA) and Scikit-learn (Pedregosa *et al.*, 2011).

Results

Neurodevelopmental assessment

At 2 years of age, the mean scores of the BSID-III composite language and cognitive abilities were respectively 90 (SD ± 16.20) and 92 (SD ± 11.85), with a correlation between the two of $r = 0.79$; $p = 10^{-5}$. No significant correlation was found between postmenstrual age at scan and composite language score. A trend toward significance was found between GA at birth and composite language score ($r = 0.21$; $p = 0.09$); a significant correlation was found between socioeconomic score (measured as the English Index of Multiple Deprivation) and composite language score ($r = -0.28$; $p = 0.03$).

Impact of prematurity on the arcuate fasciculus microstructure

During the term equivalent period, prominent development occurred in the left and right arcuate fasciculi microstructure (respectively FWE corrected p-values = 0.0002 and 0.0013) and in the cortico-spinal tracts (respectively left and right, FWE corrected p-values = 0. 0001 and 0.0016). Increased prematurity at birth was associated with significantly lower term equivalent FA of the left arcuate fasciculus (FWE corrected p-value = 0.0130) and a trend toward lower FA in right arcuate fasciculus (FWE corrected p-values = 0.0612) (Table 2).

	PMA (cov GA)	**GA (cov PMA)**
Left arcuate FA	0.0002	0.0130
Right arcuate FA	0.0013	0.0612
Left cortico-spinal FA	0.0001	0.3448
Right cortico-spinal FA	0.0016	0.8370
Global white-matter FA	0.0561	0.6732

TABLE 2 THE IMPACT OF DEGREE OF PREMATURITY ON WHITE MATTER MICROSTRUCTURE

We assessed the effect of age at scan and gestational age at birth on arcuate fasciculi, cortico-spinal tracts and global white-matter FA. Showing FWE corrected p-values from GLM testing (10 000 permutations). A) Between 39 – 46 postmenstrual weeks, significant development (measured by PMA at scan covaried GA at birth) occurs in the arcuate fasciculi and cortico-spinal tract microstructure, and shows a trend with global white-matter FA. B) Increased prematurity at birth (measured by GA at birth covaried PMA at scan) is significantly associated with lower term equivalent FA of left arcuate fasciculus and a non-significant trend is seen in the right arcuate fasciculus.

Term equivalent arcuate fasciculus microstructure is associated with inter-subject differences in linguistic skills

Although all cross-validated regression analyses identified statistically significant brain-behaviour associations, the PLS regression model achieved greater nonparametric statistical significance when compared to Ordinary Least Squares and Ridge regression (Table 3).

	Arcuate fasciculi FA		Cortico-spinal tracts FA	
	r	FWE-corrected p-value	r	FWE-corrected p-value
OLS	0.31	0.0275	-0.06	0.4839
Ridge	0.29	0.0305	-0.04	0.4556
PLS	0.36	0.0112	0.11	0.2785

TABLE 3 RELATIONSHIPS BETWEEN LINGUISTIC SKILLS AT 2 YEARS AND FA OF THE LEFT AND RIGHT ARCUATE FASCICULI AT TERM EQUIVALENT

Showing rho correlation coefficient between FA at term equivalent and language scores at two years across different regression models and respective FWE-corrected p-values (10 000 permutations). The cross-validated PLS regression demonstrated greater non-parametric statistical significance values. However, no statistically significant association was found when testing the link between linguistic scores and FA of the cortico-spinal tracts.

The cross-validated PLS analysis highlighted a statistically significant association between PLS FA scores and PLS language scores ($r = 0.36$; FWE–corrected p-value = 0.0110) (Figure 22). Across folds, the PLS mode accounted for 72% of variance in

the arcuate fasciculi FA. The mean of the identified PLS loadings (0.6650 for left and 0.7736 for right) was two orders of magnitude higher than their SD (0.0059 and 0.0099), highlighting strong model stability. The overall strong positive PLS loadings indicates that children who developed higher linguistic performance at two years were those with higher FA along both the left and right arcuate fasciculi at term equivalent age. The identified relationship was not driven by environmental factors associated with the environmental stresses of premature delivery, global white matter volume or sex (r = 0.32, FWE–corrected p-value = 0.0230).

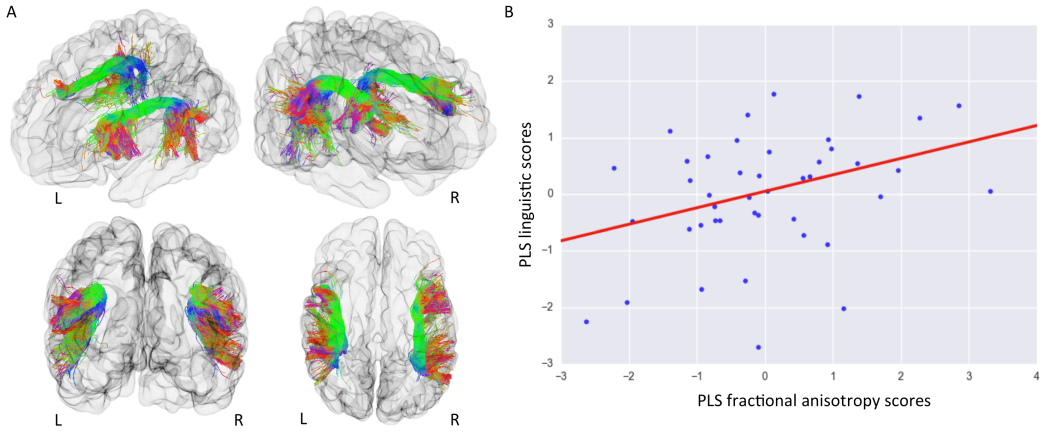

FIGURE 22 INTER-SUBJECT DIFFERENCES IN LINGUISTIC PERFORMANCE AT TWO YEARS WERE ASSOCIATED WITH TERM EQUIVALENT FA OF THE LEFT AND RIGHT ARCUATE FASCICULUS INDEPENDENTLY OF DEGREE OF PREMATURITY

A) Visualization of an infant brain and the reconstructed arcuate fasciculi from left-frontal; right-frontal; frontal and top view. B) Using cross-validated partial-least-square regression, one statistically significant mode of brain-behaviour co-variation between PLS FA scores and PLS language scores was identified (r = 0.36; FWE–corrected p-value = 0.0112). Term equivalent FA of the left and right arcuate fasciculi was associated with individual differences in composite linguistic skills in early childhood. This link was still present even when controlling

for degree of premature delivery measured by GA at birth (r = 0.32, FWE–corrected p-value = 0.0211).

To determine whether efficient linguistic abilities at 2 years were related to higher FA in both arcuate fasciculi, we tested the alternative hypothesis that lateralization in the arcuate fasciculi FA would be associated with later linguistic abilities. We found no significant association between the degree of asymmetry in the arcuate fasciculus microstructure ((Left FA−Right FA)/(Left+Right)) and composite linguistic skills at 2 years (GLM testing with 10000 permutations: positive contrast FWE_corrected_p=0.8918; negative contrast FWE_corrected_p=0.1129).

When cognitive scores at 2 years were added to the model as an additional response variable, inter-subject differences in linguistic and cognitive abilities remained associated with term-equivalent FA of left and right arcuate fasciculus (r = 0.37; FWE–corrected p-value = 0.0148). Higher linguistic and cognitive performance at two years of age were linked with higher FA along both the left and right arcuate fasciculi at term equivalent age. Across folds, the PLS mode accounted for 72% and 71% of variance respectively in X and Y space. High model stability in PLS loadings was highlighted also in this case (Figure 23, Table 4).

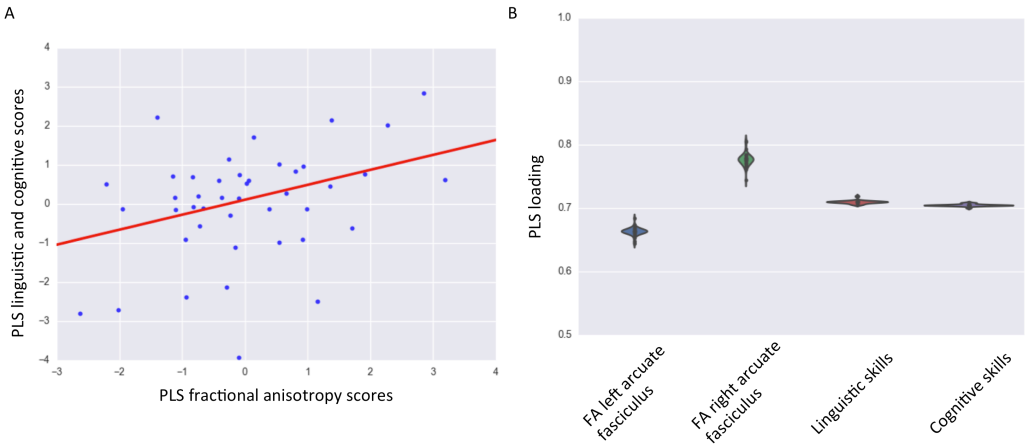

FIGURE 23 ASSOCIATION WITH INTER-SUBJECT DIFFERENCES IN LINGUISTIC AND COGNITIVE PERFORMANCE AT TWO YEARS OF AGE

A) A significant association was identified between PLS FA scores and PLS language and cognitive scores (r = 0.37; FWE–corrected p-value = 0.0148). B) PLS loadings of involvement with respect to the initial X space (left and right arcuate fasciculi) and Y space (composite linguistic and cognitive skills). Note the small dispersion around the means highlight strong model stability. Higher composite linguistic and cognitive skills in early childhood were linked to higher FA of the left and right arcuate fasciculi at term equivalent.

	PLS loadings of involvement
X space:	
FA of the left arcuate fasciculus	0.66 ± SD 0.006
FA of the right arcuate fasciculus	0.78 ± SD 0.009
Y space:	
Composite language abilities	0.71 ± SD 0.003
Composite cognitive abilities	0.71 ± SD 0.002

TABLE 4 PLS LOADINGS IN THE ASSOCIATION WITH INTER-SUBJECT DIFFERENCES IN LINGUISTIC AND COGNITIVE PERFORMANCE

Showing the PLS loadings of involvement in the identified link between the left and right arcuate fasciculus microstructure, and linguistic and cognitive performance. Mean PLS loadings of involvement ± SD averaged across folds. The PLS mode accounted for 72% and 71% of variance respectively in X and Y space. The small SDs of the estimated PLS loadings highlight strong model stability.

Of importance a link between arcuate fasciculus microstructure and language function was not present when using FA of the cortico-spinal tracts (r = 0.11, FWE–corrected p-value = 0.2785) *(*Figure 24*)*. Adding the cognitive scores to the model did not lead to a statistically significant association (r = 0.12, FWE–corrected p-value = 0.3339).

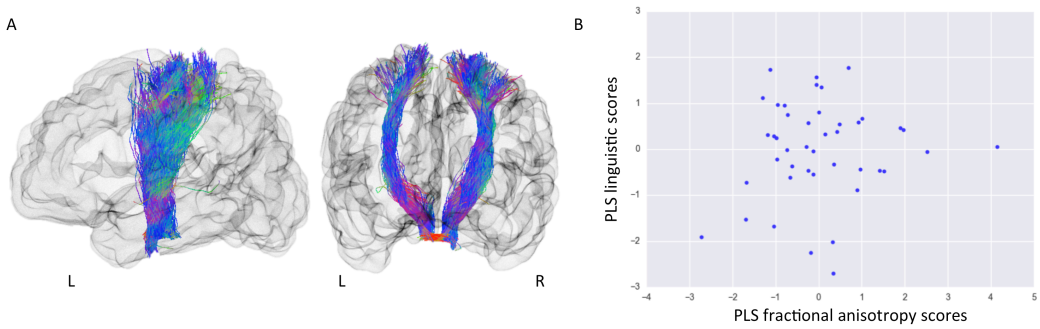

FIGURE 24 FA OF THE CORTICO-SPINAL TRACTS AT TERM EQUIVALENT AGE IS NOT ASSOCIATED WITH LINGUISTIC AND COGNITIVE ABILITIES AT TWO YEARS

A) Visualization of an infant brain and the reconstructed cortico-spinal tracts from left and frontal view. B) Scatter plot of PLS cortico-spinal tract FA scores vs. PLS linguistic scores. Term-equivalent FA of left and right cortico-spinal tracts was not associated with linguistic skills at two years (r = 0.11, FWE–corrected p-value = 0.2785), or with cognitive scores (r = 0.12, FWE–corrected p-value = 0.3339).

Discussion

Infants demonstrate linguistic abilities at birth, including discriminating close phonemes (Dehaene-Lambertz and Pena, 2001) and sentences from different languages (Mehler *et al.*, 2002). During the first year of postnatal life, rapid learning of the native language is evident and the discovery that the combinatorial properties of language can communicate information represent one of the most remarkable achievements of human learning. Although the underlying neural architecture of

language acquisition is believed to be a distinct piece of the biological makeup of the human brain (Pinker, 1995; Jackendoff and Pinker, 2005), the precise neural mechanisms that allow human infants to develop this high-order cognitive function remain unclear (Kuhl, 2010; Dehaene-Lambertz and Spelke, 2015; Skeide and Friederici, 2016). Preterm born children have impaired linguistic ability when compared to their term-born peers, even in the absence of major disabilities, which can persist as a long-lasting linguistic delay throughout childhood (van Noort-van der Spek *et al.*, 2012). Studying this population therefore provides an opportunity to test hypotheses concerning infant brain mechanisms linked to language acquisition and to assess the environmental effects of early life exposure.

Non-invasive brain imaging techniques provide an opportunity to assess the neuroanatomical basis of early language acquisition. Diffusion-weighted brain imaging allows the study of white-matter FA, a measure sensitive to the underlying tissue microstructure (Beaulieu, 2002). In adulthood, the brain architecture which sub-serves language function is relatively well-known (Hickok and Poeppel, 2007; Price, 2012; Berwick *et al.*, 2013), with the arcuate fasciculus (Catani *et al.*, 2005) representing a potential evolutionary marker of human linguistic capability.

This study shows that in preterm infants at the time of normal birth, well before the formal emergence of natural language, the microstructural properties of both the left and right arcuate fasciculi are associated with later linguistic abilities. Previous studies in adulthood and adolescence have linked its microstructural properties to word learning (López-Barroso *et al.*, 2013); the development of reading skills (Yeatman *et al.*, 2011, 2012); sentence comprehension performance (Skeide *et al.*, 2015), and it has been shown to support syntactic processing of language (den Ouden *et al.*, 2012). We found that symmetry in the left and right arcuate fasciculi FA, rather than asymmetry, was linked to later efficient linguistic abilities, which is in

accordance with the language deficiencies reported after both left and right hemispheric lesions in infants (Bates and Roe, 2001). Previous studies in post-term infants have shown a left hemispheric lateralization for speech processing in the posterior part of the superior temporal region (Dehaene-Lambertz *et al.*, 2002, 2006, 2010; Baldoli *et al.*, 2015), but not for inferior frontal regions (Dehaene-Lambertz *et al.*, 2006; Baldoli *et al.*, 2015). Indeed, left-lateralization in temporal areas increases during the first months of life (Perani *et al.*, 2011; Shultz *et al.*, 2014; Baldoli *et al.*, 2015). This bilateral linkage may also be due to the involvement of right frontal regions, which are also activated when infants listen to speech (Dehaene-Lambertz *et al.*, 2002, 2010), and are involved in attention, stimulus selection, and response to novelty. These are important processes for infants to comprehend social world requests, to communicate wants and needs, and to produce combinatorial-grammatical sentences by the age of two years.

We may speculate on the role of the arcuate fasciculi during the first stages of language acquisition. It provides a direct link between speech production and perception and an intracerebral mechanism for the ability at birth to imitate simple articulatory movements such as opening the mouth or protruding the lips is evident from birth (Meltzoff and Moore, 1977). Infants progressively converge toward recognizable patterns of verbal production (Kuhl and Meltzoff, 1996) and may benefit from the verbal buffer provided by the dorsal pathway to memorize and analyse speech segments (Dehaene-Lambertz *et al.*, 2006). The relationship between linguistic skills at 2 years and its microstructure confirm that the arcuate is a key element during the first stages of language learning.

Premature birth is associated with a long lasting signature on whole-brain architecture (Nosarti *et al.*, 2002; Counsell *et al.*, 2003; Ball *et al.*, 2012, 2014; Salvan *et al.*, 2014) and later neurodevelopment (Marlow *et al.*, 2005; Delobel-

Ayoub *et al.*, 2009; Johnson *et al.*, 2009; Northam *et al.*, 2012). While the absence of a direct comparison with term control infants limits our ability to assess the full impact of premature birth, we found that increasing prematurity at birth affects arcuate fasciculus microstructure but, in the absence of severe neonatal brain injury, only minimally modulates the identified link with later linguistic skill. Although previous behavioural studies have concluded that many of the language deficits in preterm-born children are more likely a result of general cognitive problems rather than a specific language impairment (Wolke and Meyer, 1999; Barre *et al.*, 2011), here we show that the linguistic impairment in preterm born children may result from the microstructural alteration of a fundamental brain language structure.

At the age of two years, however, measures of complex linguistic skills strongly correlate to domain-general cognitive performance. Therefore further investigations of specific cognitive domains are needed in our subjects at an older age in order to distinguish measures of formal intelligence quotient, working-memory and attention, from phonological, syntactic processing and semantics.

A potential limitation of this study is the use of FA as a measure of underlying white-matter microstructure. Although we used high angular resolution diffusion-MRI data and CSD based tractography to delineate the arcuate fasciculi, the observed relationship may be, at least in part, related to inter-subject differences in the configuration of crossing fibres.

Conclusion

In summary these results validate a neurolinguistic model in which arcuate fasciculus microstructure shortly after birth, plays a role in early language acquisition. We have shown that a brain-behaviour mode of co-variation links linguistic performance in

early childhood to a specific structure in the infant brain which is known to support complex language function in adulthood. The microstructure of the arcuate fasciculus at around the time of normal birth underpins linguistic development at 2 years of age independent of the extreme environmental influences caused by premature extrauterine life.

Chapter 6

Acquisition of expressive language is mediated by genetically linked auditory−motor brain activity at the time of normal birth

After having highlighted a structural neonatal brain network for language acquisition, here I study whether functional correlates of later linguistic development are also present and linked to genetic information. Indeed whether there is a genetic endowment in the ontogeny of a human language brain network remains currently unknown and is key to understand human language learning. In this chapter I plan to tackle this problem, and the work here presented (with the exception of the single-nucleotide polymorphism analysis) is my own. I investigate the association of inter-subject differences in expressive language performance at two years with term-equivalent maturation of auditory-motor brain function, a marker of expressive language development during childhood (Weiss-Croft and Baldeweg, 2015). The significant brain correlate was then tested (by another PhD-candidate, a colleague and friend of mine at the Centre for the Developing Brain) as an imaging phenotype for further genetic analyses, in order to test the association with a specific meta-analytic gene-set of interest. The work of this chapter extends our understanding of the joint relation between maturation of brain function, genetic factors and environmental influences.

Of interest, this work represents my first PhD project.

From a methodological perspective, in the following two chapters I investigate functional brain connectivity, a marker of brain function that indicates statistical co-dependencies between brain regions on the basis of co-fluctuation in the resting-state BOLD signal. To estimate resting state brain networks I have included a group of sixteen full-term newborns together with the preterm cohort of interest imaged at term equivalent age. The rational is to cover the gestational age range as a continuum, from prematurity to full term, in order to avoid any kind of bias in the estimation of these networks towards those specific (or exclusive) the premature population. In the same way in neuroimaging studies of the adult human population, resting state networks and functional connectivity are usually estimated in the healthy population and then used/applied to the pathological populations. This is not to bias the measures of interest to the specific study population thus limiting overfitting to the pathology of interest. Although the presence of some term born babies, no comparison between preterm born and term born infants is tested as the sample size of the latter, sixteen term babies, would not allow for reliable statistics representative of the whole population. Due to the same factor and the absence of neurodevelopmental assessment for the term-born infants group, no regression analyses are tested in a healthy development population.

Introduction

Although native language acquisition is one of the greatest human achievements of human learning, the emergence of the neural organization supporting its production in early life and its relationship with gene variation and environmental influences

remains poorly understood (Pinker, 1995; Kuhl, 2010; Dehaene-Lambertz and Spelke, 2015). In the last two decades, studies applying BOLD fMRI have provided profound new insights into the large-scale organization of the brain activity that subserve language both at rest and during specific tasks (Smith *et al.*, 2009; Price, 2012). This work has found that language function in the mature brain involves the close integration of activity in distinct areas responsible for both auditory and articulatory processing within the sensory and motor cortices (Papathanassiou *et al.*, 2000; Wise *et al.*, 2001; Hickok and Poeppel, 2007; Pulvermüller and Fadiga, 2010; Price, 2012). In addition, this neural network can be further parcellated into different processing streams which are thought to subserve specific facets of language processing (Hickok and Poeppel, 2007; Rauschecker and Scott, 2009), through distinct patterns of anatomical (Saur *et al.*, 2008) and functional connectivity (J Obleser *et al.*, 2007; Leff *et al.*, 2008; Eickhoff *et al.*, 2009; Londei *et al.*, 2010; Nath and Beauchamp, 2011; Osnes *et al.*, 2011).

Neuroimaging and behavioural studies suggest that the process of establishing the foundations of the neural organization responsible for language processing may have already begun before the time of normal birth, as specific neural responses during phonetic discrimination can be identified in preterm infants (Mahmoudzadeh *et al.*, 2013). By full term, newborn infants can readily discriminate phonetic contrasts in all languages (including those that they have never heard before) (Eimas *et al.*, 1971; Eimas, 1975; Lasky *et al.*, 1975; Werker and Lalonde, 1988) and specific responses can also be identified to more complex auditory stimuli including speech and sentence presentation, music discordance and language prosody (Dehaene-Lambertz and Dehaene, 1994; Dehaene-Lambertz *et al.*, 2006; Blasi *et al.*, 2011; Perani *et al.*, 2011; Baldoli *et al.*, 2015). During this critical juncture, the brain's large-scale functional architecture is rapidly established via an emerging dense framework of

long-range thalamo-cortical and cortico-cortical connections, resulting in the presence of a full repertoire of distinct RSNs by the time of normal birth and a specific "rich-club" organization of structural connectivity (Fransson *et al.*, 2007; Doria *et al.*, 2010; Ball *et al.*, 2014). Over the subsequent months, infants begin to recognize native-language sound combinations (Kuhl, 2004) and infer the abstract structure of language (Bernard and Gervain, 2012; Shi, 2014); and by two-three months of age, an adult-like cortical response to speech stimuli can be readily seen with left-lateralized activity in the planum temporale during discrimination of speech and music (Dehaene-Lambertz *et al.*, 2002). This process of rapid development culminates in the first production of words at 9-12 months of age, with grammar emerging by 18-24 months of age (Dehaene-Lambertz and Spelke, 2015).

A recent review of fMRI studies of human language development (Weiss-Croft and Baldeweg, 2015), has investigated age-related changes in the language brain organization. Throughout childhood a distinct expressive language network is recognizable and its development is characterised by increasing activation within the sensory and motor cortices (left premotor, bilateral primary motor, and left somatosensory cortex) and left supramarginal gyrus, with increasing leftward lateralization of activity in specific regions such as the temporal-parietal lobes (Schlaggar *et al.*, 2002; Brown *et al.*, 2005; Fair *et al.*, 2006; Krishnan *et al.*, 2015; Weiss-Croft and Baldeweg, 2015).

Whilst specific mutations in particular genes have been described to cause severe developmental disorders of speech and language (Enard *et al.*, 2002; Vargha-Khadem *et al.*, 2005); the genetic basis of normal language development as a whole is currently thought to be far more complex, involving common variations in multiple different genes (Berwick *et al.*, 2013). In contrast, it has been suggested that early life environmental factors are of critical importance for the neural systems

underlying language as emphasized by the observation that preterm born children have significantly lower linguistic performance when compared to their term-born peers, which persists throughout childhood (van Noort-van der Spek *et al.*, 2012). Studying this population therefore provides a unique opportunity to not only test specific hypotheses about the brain mechanisms linked to the earliest stages of language acquisition, but also crucially allows the study of how they may be specifically affected by early exposure to the ex-utero environment.

We used a combination of resting-state fMRI, whole genome sequencing, and developmental assessment in later childhood, to test the hypothesis that functional connectivity of the auditory-motor brain network would be present at the time of normal birth, well before the emergence of natural language later in childhood. We further hypothesized that if present, such connectivity would be fundamental for the acquisition of language during early infant development and would therefore be significantly associated with later expressive linguistic ability at 20 months of corrected age. To understand whether the establishment of such a relationship is driven by intrinsic or extrinsic factors, we then tested whether any identified brain-behaviour relationship was significantly associated with single nucleotide polymorphisms (SNPs) in genes previously linked to language function and/or impairment and if it was affected by key environmental factors such as the degree of prematurity at birth.

Materials and Methods

Subjects

Preterm infants were recruited as part of the ePrime (Evaluation of Magnetic Resonance Imaging to Predict Neurodevelopmental Impairment in Preterm Infants)

study and were imaged at term equivalent age over a 3 year period (2010-2013) at the Queen Charlotte and Chelsea Hospital, London. The ePrime study was reviewed and approved by the National Research Ethics Service, and all infants were studied following written consent from their parents. 150 preterm-born infants (80 males; median gestational age (GA) at birth 31 weeks; range 24 – 33 weeks) were scanned at term-equivalent age (median postmenstrual age (PMA) 43 weeks; range 38 – 45 weeks). 16 healthy term-born control infants were also examined (median gestational age at birth 40 weeks; range 37 – 42 weeks; median PMA at scan 43 weeks; range 40 – 46 weeks). 100 of the preterm born infants had follow-up neurodevelopmental assessment at 2 years of age. Infants with focal brain lesions (such as cystic periventricular leukomalacia or parenchymal haemorrhagic infarction) or diagnosed chromosomal abnormalities were excluded from the study group.

MRI acquisition

Imaging data was acquired using an eight-channel phased array head coil on a 3-Tesla Philips Achieva MRI Scanner (Best, Netherlands) located on the Neonatal Intensive Care Unit. Whole-brain resting state fMRI data was acquired using a T2*-weighted gradient echo (GRE) EPI sequence (parameters: TR = 1.5 s; TE = 45 ms; flip angle = 90°; 256 volumes; slice thickness = 3.25 mm; in- plane resolution = 2.5 mm x 2.5 mm; 22 slices; scan duration = 6.4 min). High-resolution T1- and T2-weighted MR imaging were acquired with parameters; MPRAGE T1-weighted MR imaging; TR = 17 ms, TE = 4.6 ms, flip angle 13°, slice thickness 0.8 mm, field-of-view 210 mm, matrix 256 × 256 (voxel size: 0.82mm × 0.82mm × 0.8mm), and T2 weighted fast-spin echo MR imaging; TR = 8670 ms, TE = 160 ms, flip angle 90°, slice thickness 1 mm, field-of-view 220 mm, matrix 256 × 256 (voxel size: 0.86mm × 0.86mm × 1mm). Sedation (25–50 mg/kg oral chloral hydrate) was administered to 125 of the preterm infants and to all of 16 term-born control infants.

Data selection and quality control

The T2-weighted MRI anatomical scans were reviewed in order to further exclude subjects with extensive brain abnormalities, major focal destructive parenchymal lesions, multiple punctate white matter lesions or white matter cysts. All MR-images were assessed for the presence of image artefacts (inferior-temporal signal dropout, aliasing, field inhomogeneity, etc.) and severe motion (for head-motion criteria see below). These exclusion criteria were designed so as not to bias the study of early language and brain development, whilst still preserving the full spectrum of clinical heterogeneity typical of a preterm born population.

Neurodevelopmental assessment

Neurodevelopmental assessment at a median age corrected for prematurity of 20 months (range 19-22 months) was carried out by an experienced paediatrician or developmental psychologist with the Bayley Scales of Infant and Toddler Development, Third Edition (Bayley, 2006). All tests were standardized according to full-term control children. Neurodevelopmental assessment data was present for 100 out of the total study population of 166 infants.

Resting-state fMRI pre-processing

Single-subject resting-state fMRI data was pre-processed using tools implemented in the FMRIB Software Library (FSL) (Jenkinson *et al.*, 2012) and consisted of removal of the first six functional volumes, correction for head motion (using rigid body realignment), and high-pass temporal filtering (cut-off 150s). As both the identification of resting state networks and the quantification of functional connectivity in resting-state fMRI may be seriously hindered by the presence of signal artefacts derived from other sources, the correct identification and removal of non-neural fluctuations in the sampled BOLD signal is crucial. Here we applied

single-subject ICA, followed by automatic component classification with FMRIB's ICA-based X-noiseifier (FIX) to identify statistically independent components which contained artefactual signal whilst preserving a conservative approach so as not to alter the underlying biological signal of interest (Salimi-Khorshidi *et al.*, 2014). FSL FIX was trained by supervised classification carried out by 3 independent observers on a sub-group representative of the overall study sample over different degrees of head motion. Denoising of individual resting-state fMRI datasets was performed by regressing out the full space of motion-related fluctuations (using 24 motion regressors generated from the initial head motion rigid body realignment) and only the unique variance of the identified artefactual ICA components (Griffanti *et al.*, 2014). The efficacy of this resting state fMRI denoising pipeline on our infant population has been previously published (Ball *et al.*, 2016). Individual subject resting-state data was then registered to a study-specific symmetrical T2-weighted template. All rigid registrations in native subject space were estimated using FSL boundary-based registration optimized for neonatal tissue contrasts (Toulmin et al., 2015); and nonlinear registrations to the T2-weighted template were estimated using Advanced Normalization Tools (ANTs) (Avants *et al.*, 2008; Klein *et al.*, 2009). All transformation pairs were calculated independently and combined into a single transform in order to reduce interpolation error. In order to avoid the confounding effects on functional connectivity estimation due to differences in spatial smoothing across subjects (Scheinost, Lacadie, *et al.*, 2014), a uniform smoothing solution was achieved iteratively using AFNI software. Given the smaller size of the infant brain, spatial smoothing was minimized to a Gaussian kernel of 3 mm FWHM to avoid undesirable mixing of signal across anatomically or functionally distinct areas whilst still enhancing signal-to-noise ratio and ameliorate the effects of functional misalignments across subjects (Smith, Vidaurre, *et al.*, 2013).

Resting State Network Identification

Large-scale RSNs were identified using group-level ICA decomposition (Smith *et al.*, 2009) performed on the group of *66 infants with no follow-up data*, comprising 50 preterm born infants and 16 term born infants. Functional datasets (each containing 250 volumes) were fed into a group-level-ICA carried out using FSL MELODIC (Multivariate Exploratory Linear Optimized Decomposition into Independent Components v3.0) implementing a temporal-concatenation approach and a fixed dimensionality of 25 components (individual datasets were temporally demeaned and had variance normalization applied) (Beckmann *et al.*, 2005, 2009; Smith, Beckmann, *et al.*, 2013; Toulmin *et al.*, 2015). Healthy term born infants were included in order to cover the full gestational age range from 25 to 42 gestational weeks and thus not bias the estimation of RSNs to those present only in prematurely born infants. All subsequent selective analyses were computed on a separate group consisting of the remaining *100 prematurely born infants* who were imaged at term-equivalent age and assessed for neurodevelopmental outcome at 20 months corrected age. Dual-regression (Beckmann *et al.*, 2009) was used to derive subject specific group-ICA time series (stage-1) and spatial maps (stage-2) for this group of 100 infants.

Auditory-motor brain network and functional connectivity

Sub-components of the auditory-motor network were derived from the larger-scale auditory and motor RSNs (estimated in the first group of 66 infants) following thresholding (using an alternative hypothesis test controlling for the local false discovery rate at p-values < 0.05) thus creating a hypothesis-driven region of interest (ROI). Group-level parcellation was then carried out within the ROI area by performing a temporally-concatenated group-level ICA on the second independent

group of 100 preterm-born infants. A fixed number of nine components were chosen in order to achieve a good balance between interpretability and robustness.

functional connectivity of edges within the auditory-motor brain network was quantified using FSLNets (v0.6) and MATLAB (R2015b, The MathWorks, Inc., Natick, MA, USA). Subject-specific z-transformed L1-regularized inverse covariance matrices were calculated in order to estimate the direct functional connections between components within the network of interest (Friedman *et al.*, 2008; Smith *et al.*, 2011; Smith, Vidaurre, *et al.*, 2013; Ball *et al.*, 2016).

Tests for head-motion confounds on auditory-motor functional connectivity

Head motion has been shown to significantly confound resting-state functional-MRI studies leading to spurious patterns of connectivity (Power *et al.*, 2012; Satterthwaite *et al.*, 2012, 2013; Griffanti *et al.*, 2014; Pruim *et al.*, 2015). We therefore implemented strict criteria for data selection, using FSL FIX (v1.061) for data denoising, and performed quantitative analyses in order to formally assess the effect of head-motion on RSNs functional connectivity. Head motion measures in our study-group were matched to those used in the studies of Pruim et al. (Pruim *et al.*, 2015) and Power et al. (Power *et al.*, 2012) (respectively average root mean square frame-wise displacement (RMS-FD) ± standard deviation (SD): 0.118 ± 0.090 mm and 0.146 ± 0.090 mm), in order to obtain a sensitive dataset using previously described denoising procedures (Ball *et al.*, 2016). The average RMS-FD for the whole sample was 0.0581 ± 0.0860 mm. No statistically significant correlation was found between subject head motion indices (mean and maximum RMS-FD) and postmenstrual age at scan or gestational age at birth. The influence of head-motion on auditory-motor brain network functional connectivity estimation was tested on the group of 100 infants (mean RMS-FD 0.0615 mm, SD 0.0236 mm). A general linear

model (GLM) was used to test for linear association between subject variability in head motion indices (mean and maximum RMS-FD) and functional connectivity variability for each auditory-motor network edge. A significant effect of head motion on auditory-motor brain network functional connectivity estimation was not found.

Brain-language association analysis

Functional connectivity of the auditory-motor brain network at term equivalent age was tested for an association with the expressive- and receptive-communicative scales of Bayley-III assessment at 20 months corrected age. Functional connectivity was linearly regressed against PMA at scan; and linguistic skills measures against socioeconomic score. Using a GLM, we tested for linear association between inter-subject differences in linguistic skills and functional connectivity strength for each of the 36 auditory-motor brain network edges, covarying for the fine-motor score of the Bayley-III. As general cognitive abilities were found to be highly correlated with language skills in our sample ($r = 0.69$; $p < 10^{-5}$), we did not control for this separately in the analysis.

We further tested whether early environmental influences linked with preterm birth were driving any identified brain-behaviour association, thus suggesting that the relationship would be an effect of premature delivery and not a pure developmental process. Using partial correlation between the identified brain phenotype and expressive linguistic abilities and adjusting for the subjects' GA at birth, we assessed whether the brain-behaviour relationship was still present. The number of days of ex-utero life was highly correlated with PMA at scan and GA at birth (Pearson's correlation coefficient of postnatal age respectively with PMA and GA: $r = 0.72$; $p < 10^{-5}$; $r = -0.89$; $p < 10^{-5}$) and so we did not include this as a covariate.

As left-lateralization is a characteristic feature of the mature expressive language functional network, we then tested whether lateralization of auditory-motor functional connectivity was present at term equivalent age; and if present, was linearly associated with receptive- and expressive-communication skills at 2 years of age. As the derived functional connectivity measures were already normalized across subjects, lateralization of functional connectivity was defined as the difference in functional connectivity strength between network edges linking the bilateral superior sensori-motor regions and the left and right superior temporal cortices.

All statistical testing was performed using a GLM and subject-wise permutation testing in order to derive nonparametric statistical significance on model fitting as implemented in FSL randomise (v2.9) (Winkler *et al.*, 2014). Statistical significance was defined as $p<0.05$ following correction for the Family-wise error (FWE) rate after 10,000 permutations per contrast (Winkler *et al.*, 2014). Regression residuals were also inspected in order to assess whether the residuals are consistent with stochastic error.

Genome-wide genotyping

Saliva samples from 58 unrelated preterm infants (from the second group of 100 infants) with both imaging and behavioural data were collected using Oragene DNA OG-250 kits (DNAGenotek Inc., Kanata, Canada) and genotyped on Illumina HumanOmniExpress-12 arrays (Illumina, San Diego, CA, USA). Filtering was carried out using PLINK (Chang *et al.*, 2014) (Software: https://www.cog-genomics.org/plink2). All individuals had a missing call frequency < 0.1. SNPs with Hardy-Weinberg equilibrium exact test p-values $\geq 1 \times 10^{-6}$, MAF ≥ 0.01 and genotyping rate > 0.99 were retained for analysis. After these filtering steps, 613,186 SNPs remained.

Brain imaging-language behaviour phenotype

An imaging brain-language phenotype was identified in the previous analysis by regressing the expressive-communicative component of the Bayley's score against the auditory-motor brain network. This was then used as a measure of the relationship between imaging and language traits and represented the quantitative phenotype in the genetic analysis.

Identifying genes independently associated with language impairment

142 putative genes previously independently associated with language impairment (Human Phenotype Ontology term HP:0002463: 'language impairment') in genome-wide association studies (GWAS) were selected in an unbiased fashion using the 'PrixFixe' strategy (Taşan *et al.*, 2015), that predicts causal genes based on a human cofunction network to identify functionally related genes within GWAS loci, as implemented in the GWASdb2 tool (http://jjwanglab.org/gwasdb) (Table 5). GWASdb2 combines curated collections of traits/diseases associated SNPs from published GWAS data up to a *p*-value of $<1^{-3}$, with their comprehensive functional annotations, as well as disease classifications.

Gene Symbol	**PrixFixe Score**
WT1	0.235343
LRP5	0.207502
BCL11A	0.177448
FOXE1	0.161854
SLC8A2	0.156343

GTF2F1	0.147854
ADD2	0.146895
PSPN	0.144778
XCL1	0.143825
PKN1	0.135914
TINF2	0.130381
COL4A3	0.12847
GPM6A	0.125978
KAT2B	0.115397
KPTN	0.107346
CD97	0.107124
CIDEB	0.106794
EID1	0.10373
THAP10	0.10334
ALK	0.101251
TPD52	0.100349
ADRA1D	0.100346

COL4A4	0.099279
HRSP12	0.096727
PPP2R5C	0.095283
MDGA1	0.095041
PTPRD	0.094848
C4orf19	0.091521
ACCN1	0.090981
GIMAP4	0.089454
TGM1	0.087311
PSME2	0.08706
RPS10	0.084276
NAPA	0.083692
LRRC49	0.082959
NEDD8	0.082622
BIN3	0.081702
LRRC16A	0.080914
TBXAS1	0.080111

LRRC1	0.079549
CNTN5	0.07794
ADCY4	0.077149
RPL30	0.07534
SPDEF	0.074838
LARP6	0.074159
XPA	0.073448
CCM2	0.07239
THRB	0.072089
FIGLA	0.071594
SUV420H1	0.071397
SGOL1	0.069797
CLDN14	0.069295
EIF3M	0.06814
EGR3	0.066987
KIF26A	0.066083
FAM46A	0.065241

TCF12	0.06514
LTB4R2	0.064635
GALNT10	0.064495
ZNF280D	0.06446
UBR3	0.062762
PLXNA1	0.061457
TRIM68	0.061041
LTB4R	0.060565
CEP152	0.060498
ZNF541	0.058816
DYSF	0.057829
ARHGEF7	0.05646
PURB	0.05574
GMPR2	0.055648
RABGGTA	0.055565
UACA	0.054438
NYNRIN	0.05407

OR51E2	0.053822
SEPW1	0.053648
CRB3	0.053375
DDX39A	0.053308
AGBL1	0.053083
ARHGAP22	0.050114
HK1	0.049594
RIPK3	0.048841
SHC4	0.048794
IPO4	0.048641
ESRRG	0.0484
CCDC141	0.047619
SH2D4B	0.046975
MYO3B	0.04639
NFATC4	0.045581
ACER2	0.044263
CHMP4A	0.043635

CGNL1	0.043457
GIMAP7	0.042721
METTL5	0.040768
GALNTL6	0.040016
TUSC3	0.039806
PDE10A	0.039451
C18orf1	0.039022
C14orf21	0.037721
TTC15	0.03753
MRPS28	0.037289
PCDH18	0.037267
TMEM132D	0.03681
SESTD1	0.036521
ASPG	0.034654
C13orf16	0.034013
C11orf24	0.0322
H2AFV	0.031987

TM9SF1	0.027956
WDFY4	0.027381
KHNYN	0.026959
DHRS1	0.026679
POP1	0.026241
BANF2	0.025905
KHSRP	0.024638
ACER1	0.023822
CHKA	0.02327
PLIN2	0.022514
XCL2	0.02193
EHD2	0.021067
MLIP	0.020997
SIM2	0.020851
WDR17	0.020111
GLTSCR2	0.019584
BTBD11	0.018613

MEIS3	0.017041
RBFOX3	0.016324
SLC9A9	0.016
TSSC1	0.015571
RRBP1	0.015416
GLTSCR1	0.015254
FAM135B	0.01461
DENND4C	0.014397
HKDC1	0.012768
C6orf118	0.012508
GIMAP8	0.012479
FAM158A	0.007927
SAP30L	0.007248
PDCD5	0.007121
TFAP2B	0.007054
C3orf58	0.00526
CHCHD6	0.00307

FAM21B	0.00161

TABLE 5 PUTATIVE GENES ASSOCIATED WITH LANGUAGE

Putative genes associated with language were selected using the Prixfixe method in the gwasdb2 tool (http://jjwanglab.org/gwasdb) (Li *et al.*, 2016). 142 putative genes previously independently associated with language impairment (Human Phenotype Ontology term HP:0002463: 'language impairment') in genome-wide association studies (GWAS) were used as input gene-set for association testing with the phenotype in the Joint Association of Genetic Variants (Lips *et al.*, 2015). Here are shown in descending order given magnitude score.

Gene-set association analysis

Two 'competitive control' methods (Wang *et al.*, 2010) were applied to test whether the imaging-language phenotype was more associated with language genes than any other set of randomly grouped genes. Competitive testing against random gene-sets was done as it allows robustness against population stratification.

Joint Association of Genetic Variants (JAG) (Lips *et al.*, 2015) was used, allowing comparison of the empirical p-values from 200 randomly generated gene-sets with the empirical p-value from the gene-set of interest. Significance was ascertained by 10,000 permutations of the phenotype, implicitly conditional on linkage disequilibrium, sample size, gene size, the number of SNPs per gene and the number of genes per group.

The association analysis using JAG was repeated gene-by-gene within the language gene-set to investigate which members of the gene-set might be predominantly contributing to the collective signal. This was done with 10,000 permutations plus adjustment for population structure using genomic control as implemented in PLINK (Purcell *et al.*, 2007). Genes linked to language impairment and significantly

associated with the imaging-language measure were annotated for biological function using the Webgestalt tool (*17*).

Results

Group ICA delineated a repertoire of 25 resting state networks in the first group of 66 infants with spatial representations similar to those described in the literature (Fransson *et al.*, 2007, 2009, 2011; Doria *et al.*, 2010; Smyser *et al.*, 2010). These RSNs included: medial visual; lateral visual; auditory; sensory-motor; default mode; and executive control network (Figure 25).

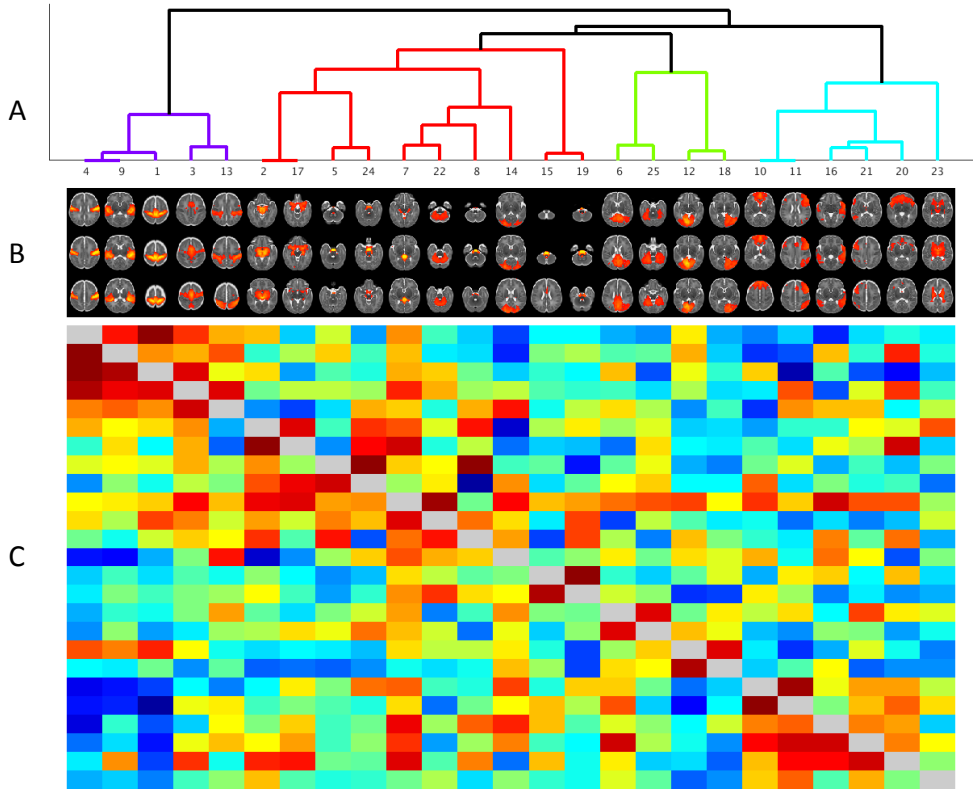

FIGURE 25 POPULATION-AVERAGE LARGE-SCALE RESTING STATE NETWORKS AT THE TIME OF NORMAL BIRTH

25 resting state networks were identified in a first group of 66 infants and are similar to those previously described in the literature. A) Hierarchical network clustering based on functional

connectivity, therefore bringing together groups of nodes with the strongest similarity between their resting-state time-series. B) Large-scale resting state networks. Each column represents three different axial views of a resting state network. The nodes are ordered according to the hierarchical clustering driven by the full correlation. C) The nodes X nodes population average full-correlation connectivity (below the diagonal); and the population average partial-correlation connectivity (above the diagonal).

The sensori-motor and auditory networks, which spatially encompassed the bilateral sensori-motor cortices, and superior temporal lobes (Figure 26.A), were then selected as regions of interest for the specific analysis of auditory-motor functional connectivity (Figure 26.B).

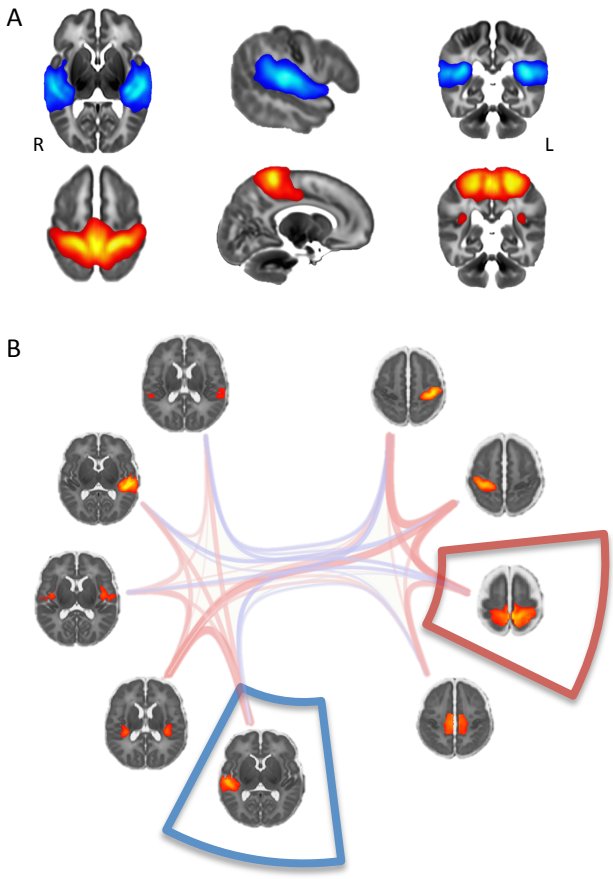

FIGURE 26 AUDITORY-MOTOR FUNCTIONAL BRAIN NETWORK AT THE TIME OF NORMAL BIRTH

(A) Large-scale auditory (blue) and primary sensory-motor (red) resting state network were estimated at the time of normal birth in the first group of infants. A group-level parcellation within these regions was then carried out in the second group of infants with neurodevelopmental assessment at 2 years. (B) Auditory-motor brain network functional connectivity was calculated using partial correlation (z-transformed L1-regularized inverse covariance). Line thickness is scaled by the pairwise correlation coefficient.

Neurodevelopmental assessment

The mean standardized score of composite language abilities for our study population was 90 ± standard deviation of 17 (range 53-132). No linear association was found between gestational age at birth and composite language abilities ($p = 0.3808$), whilst a trend toward significance was found between SES (measured as the English Index of Multiple Deprivation) and composite language score ($p = 0.11$). There was significant correlation between the receptive and expressive communication subscales of the Bayley assessment ($r = 0.59$; $p < 1\times10^{-5}$). A significant difference was found before and after de-confounding language scores for SES (paired t-test: $tstat = 6.8943$; $p = 5 \times10^{-10}$). No significant difference in linguistic performance was found between those infants who lived in predominately English speaking or bi-lingual households (two-sample t-test right-tail, before and after de-confounding, respectively: $tstat = 0.9014$; $p = 0.1848$; $tstat = 0.6158$; $p = 0.2697$).

Term equivalent auditory-motor functional connectivity is associated with inter-subject differences in expressive linguistic abilities

We tested the linear associations between linguistic skills and each of the 36 functional connectivity auditory-motor brain network edges. Prior to the analyses, the effects of postmenstrual age at scan were removed from the functional connectivity measures with linear regression, and the socioeconomic score was regressed from the linguistic skills measures. We found that there was a significant

negative association between *expressive*-communication skills and functional connectivity edge strength between the superior primary sensori-motor cortex (M1S1) and the right superior temporal cortex (STG and PT) (FWE–corrected p-value = 0.0017) (Figure 27). The identified functional connectivity edge explained 14% of the variance in the expressive-communicative abilities (Root Mean Squared Error = 0.932; F-statistic = 15.9). The association found indicates that children who developed higher expressive-communication skills at 2 years were those with negatively correlated BOLD fMRI auditory-motor activity at term equivalent age. The identified relationship was still present after controlling for GA at birth (correlation between functional connectivity and expressive-communication: $r = -0.37$; $p = 6\times10^{-5}$; partial correlation between functional connectivity and expressive-communication adjusted for GA at birth: $r = -0.37$; $p = 7\times10^{-5}$). The linear association between *receptive*-communication abilities and functional connectivity edge strength was not significant after correction for multiple comparisons.

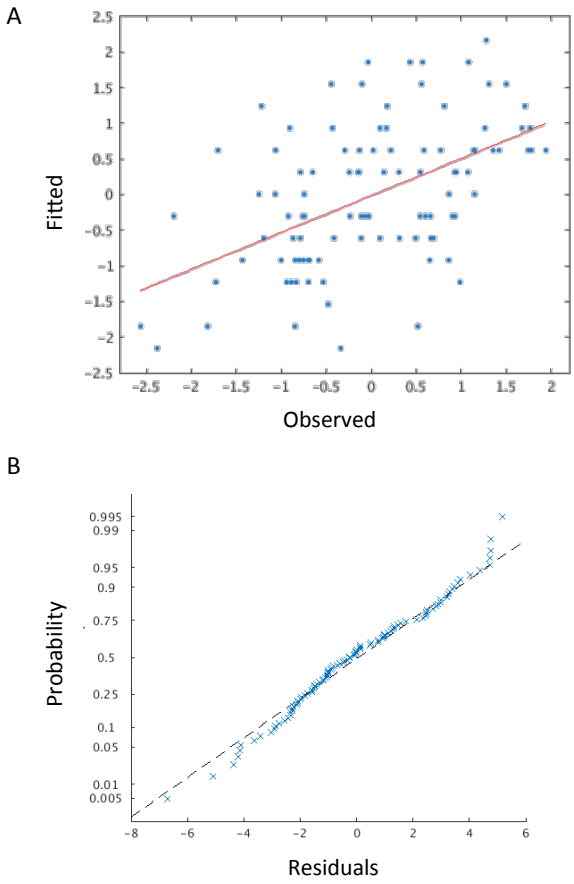

FIGURE 27 AUDITORY-MOTOR BRAIN NETWORK CONNECTIVITY IS ASSOCIATED WITH EXPRESSIVE LANGUAGE ABILITIES AT 2 YEARS OF AGE

A significant association was found between *expressive*-communication skills and functional connectivity edge strength between the superior primary sensori-motor cortex (red box) and the right superior temporal cortex (blue box). (A) Showing scatter plot of observed vs. fitted expressive language performance at 20 months corrected age. Auditory-motor functional connectivity explained 14% of the variance in the expressive-communicative abilities (FWE–corrected p-value = 0.0017), independent of GA at birth. B) Normal probability plot of regression residuals. The plot indicates that the residual in the association between auditory-motor brain network correlated activity and language performance follows a normal distribution.

The degree of leftward lateralization of functional connectivity between M1S1 and SGT/PT was significantly positively associated with *expressive*-communication abilities (FWE–corrected p-value = 0.0100); whilst there was a trend towards

significance with respect to the association with *receptive*-communication abilities (FWE–corrected p-value = 0.0546). The degree of left-lateralization of functional connectivity was associated to expressive-communication skills independent of the degree of prematurity (correlation between functional connectivity lateralization and expressive-communication: r = 0.37; p = 0.0207; partial correlation adjusted for GA at birth: r = 0.20; p = 0.0235).

No significant relationships were found between any of the functional connectivity edges and fine-motor subscale scores of the Bayley's assessment at 20 months corrected age (FWE–corrected p-value > 0.05 for all edges); and between any of the functional connectivity edges and head-motion RMS-FD (FWE–corrected p-value > 0.05 for all edges).

Language genes variation is associated with term equivalent expressive-language functional connectivity.

A self-contained test found a significant association of the imaging phenotype with the language gene-set (non-parametric $p \leq 0.006$), whilst a competitive test indicated that the imaging phenotype had a trend towards an association with the language gene-set in comparison to 200 random matched-control gene-sets (non-parametric $p \leq 0.06$).

The association analysis was repeated gene-by-gene within the language gene-set to investigate which members of the gene-set might be predominantly contributing to the collective signal. The gene-based test with 10,000 permutations and genomic control shortlisted a group of 9 genes with significant individual association ($p \leq 0.05$) with the imaging phenotype, of which 3 associations (GALNTL6, C11orf24 and SH2D4B) were below a stringent p-value of 0.01 (Table 6).

Gene	Adjusted p
GALNTL6	0.0033
SH2D4B	0.0143
C11orf24	0.0084
GLTSCR2	0.0236
SEPW1	0.0239
COL4A4	0.0305
FIGLA	0.0442
IPO4	0.0513
C3orf58	0.0525

TABLE 6 INDIVIDUAL GENES SIGNIFICANTLY ASSOCIATED WITH THE IMAGING PHENOTYPE

Results following association testing of each gene within the language gene-set, using the Joint Association of Genetic Variants (Lips *et al.*, 2015) self-contained method.

Discussion

Language is uniquely human and represents a fundamental feature of human cognition (Berwick *et al.*, 2013). Its neural architecture is believed to be a distinct piece of the biological makeup of our brain (Pinker, 1995; Jackendoff and Pinker, 2005); yet how this neural organization emerges in early life and supports the sophisticated process of learning language remains unclear (Kuhl, 2010; Dehaene-

Lambertz and Spelke, 2015). Although it has long been hypothesized that language acquisition is encoded in some way by our genetic program (Chomsky, 1959; Ramus and Fisher, 2009), the genetic basis of language acquisition remains poorly understood. The combination of non-invasive brain imaging with genotyping techniques therefore provides a unique opportunity to assess the neuroanatomical and genetic underpinnings of early language acquisition, while examining the effects of preterm birth allows a direct assessment of how early environmental exposure can influence these developmental processes.

A previous meta-analysis of the language task-based fMRI studies during childhood, have highlighted that the expressive-language brain network increases its activation in the sensory and motor cortices (left premotor, bilateral primary motor, and left somatosensory cortex) and left supramarginal gyrus, with increasing leftward lateralization (Schlaggar et al., 2002; Brown et al., 2005; Fair et al., 2006; Krishnan et al., 2015; Weiss-Croft and Baldeweg, 2015). The results here presented are in accordance with this model, and provide evidence that well before the formal emergence of natural language, activity within the STG/PT and M1S1 is significantly correlated, left-lateralized, and linked to expressive language performance at 2 years of age. Although the positive relation identified between leftward brain lateralization and later linguistic measures might be driven by the negative relation with the right STS/PG, these findings suggest that at the time of normal birth, the human brain already has at least some of the functional architecture required for the acquisition of expressive language.

Integration between the sensory and motor areas is central to the theory of a distinct "dorsal stream" of language processing which encompasses the premotor and posterior temporal cortices (Berwick *et al.*, 2013). This close relationship is also thought to represent a neural substrate for auditory feedback-based monitoring of

vocalization (E. F. Chang *et al.*, 2013); and for speech perception and language comprehension, with studies showing specific motor activation when processing speech sounds, word meanings and sentence structures (Pulvermüller, 2005; Londei *et al.*, 2010; Pulvermüller and Fadiga, 2010). It is also hypothesised that the auditory-motor feedback is likely to be particularly important during language acquisition (Price, 2012), as the auditory processing of self-produced speech is used to tune motor production to ensure that produced auditory output matches that intended (Christoffels and Formisano, 2007; Tourville *et al.*, 2008; Zheng *et al.*, 2010; Price, 2012). When auditory-motor feedback is distorted during speech production, there is increased activation in the prefrontal, rolandic, and bilateral superior temporal cortices (Tourville *et al.*, 2008), suggesting that it leads to modulation of subsequent speech output or may play a role in resolving interference. In the bilateral STG, response suppression during auditory processing is proportional to the quality of the feedback; and therefore when the processed speech is distorted or delayed superior temporal activation increases (Christoffels and Formisano, 2007; Tourville *et al.*, 2008; Takaso *et al.*, 2010; Zheng *et al.*, 2010). The results of this studies are therefore in accordance with the theory of an auditory-motor feedback in the process of language acquisition (Price, 2012).

Prematurity is known to have an adverse effect on both cognitive abilities and educational outcome, with lower intelligence quotient and mathematical scores non-linearly related to an increase in the degree of prematurity at birth for children born lower then 34 gestational weeks (Marlow *et al.*, 2005; Johnson *et al.*, 2009; Wolke *et al.*, 2015). Furthermore, in preterm-born children, delays in the acquisition of expressive language, receptive language processing, articulation, and deficits in phonological short-term memory are all relatively common, and together are likely to all contribute to impairments in the development of appropriate communication, joint

attention, and social interaction skills (Caravale *et al.*, 2005; Ortiz-Mantilla *et al.*, 2008; Luu *et al.*, 2009, 2011; Foster-Cohen *et al.*, 2010; Van Noort - Van Der Spek *et al.*, 2010; Barre *et al.*, 2011; Vohr, 2014). Although a number of studies have shown that prematurity is associated with widespread and persistent alterations of the brain's structural and functional architecture (Counsell *et al.*, 2003; Ball *et al.*, 2012, 2014; Salvan *et al.*, 2014), we found in our population that increasing prematurity at birth minimally modulated the identified link between brain function and behaviour and functional lateralization. These findings are in accordance with other studies of infants, children and adults, which have shown that both lateralization of language brain areas and altered functional brain connectivity are not related to the degree of prematurity (Gozzo *et al.*, 2009; Schafer *et al.*, 2009; Myers *et al.*, 2010; Scheinost, Lacadie, *et al.*, 2014; Kwon *et al.*, 2015). It has further been shown that earlier exposure to speech in preterm infants does not lead to an accelerated developmental language trajectory, suggesting that in preterm infants early environmental exposure does not influence the phonetic repertoire in the first weeks following birth (Peña *et al.*, 2012; Cusack *et al.*, 2016). Our findings are therefore consistent with the idea that cortical development and neuronal network formation is largely experience-independent in the language system and is likely to be predominately shaped by genetic and intrinsically-generated influences (Khazipov and Luhmann, 2006; Blankenship and Feller, 2010; Chen *et al.*, 2013; Fjell *et al.*, 2015).

We identified significant associations between a language-specific brain endophenotype and a set of genes linked to language in previous studies. Two of the three most significant genes (GALNTL6 and SH2D4B) have previously been associated not only with language impairment (Nudel *et al.*, 2014) but also with temporal lobe volume (Kohannim *et al.*, 2012). They are thought to have roles primarily related to fundamental cellular functions (such as intracellular location and

Golgi membrane function). The third gene: C11orf24, has been implicated in Golgi vesicle trafficking at dendrites (Fraisier *et al.*, 2013; Valenzuela and Perez, 2015) and is located in a recombination hotspot around the low-density lipoprotein-receptor-related protein 5 (LRP5) gene (Twells *et al.*, 2001). Ramus and Fisher have hypothesized that the genetic ontogeny of language is most significantly associated with genes which are involved in aspects of brain development and related to specific language brain areas (Chomsky, 1959; Ramus and Fisher, 2009). With this in mind, two of the identified genes are of particular interest: GALNTL6 which is involved in the post-translational modification of proteins and is highly expressed in embryonic neurodevelopment (Bennett *et al.*, 2012; Nakayama *et al.*, 2014), and SH2D4B which has been identified as a possible transeQTL and "master regulator" of an autism-related network controlling SEMA5A gene expression (Cheng *et al.*, 2013).

In this study we specifically studied a large population of preterm born infants, which allowed us to explore whether environmental influences linked to preterm delivery altered the link between early patterns of functional brain connectivity and linguistic development. Whilst we found that, in the absence of overt patterns of brain injury, the degree of prematurity at birth does not modulate the identified brain-behaviour linkage, a further direct comparison to a large population of healthy term born infants with standardized neurodevelopmental assessment is needed to be certain that our findings can be generalized to normal human development. In addition, further work could benefit from investigating the relationship between brain architecture around the time of normal birth and more specific measures of phonological abilities at an older age, such as syntactic processing and semantics, as well as assess how environmental factors in multi-lingual environments may modulate the neural basis of language acquisition.

Conclusion

To conclude, the findings of this study support the notion of a functionally organized human brain that is already prepared for complex language learning at the time of normal birth, well before the emergence of natural language behaviour. Our results stimulate further consideration about the molecular biology underlying human language development, and emphasize the joint influence of neural, genetic factors and environmental stimuli in its emergence.

Chapter 7

Time-resolved functional connectivity in the neonatal brain supports efficient later development of linguistic and cognitive abilities through dynamic network integration

In the previous chapter I have tested a hypothesis-based association between auditory-motor neonatal brain function and later expressive language development. However a wider dynamic brain network may be involved in supporting efficient language acquisition. In this chapter I present a holistic, data-driven, computational approach aimed to link term-equivalent time-resolved brain functional connectivity with complex cognitive and linguistic performances at two years, in order to identify a brain model supporting later neurocognitive development.

Current neuroscientific literature is characterising the human brain as a dynamic organ (Baker *et al.*, 2014; Braun *et al.*, 2015; James M Shine *et al.*, 2016). Here I investigate dynamic neonatal brain function as a neuromarker for later neurodevelopment. Functional brain connectivity is usually studied as the grand-average over the full fMRI acquisition time, quantified as the statistical Pearson's correlation coefficient, not taking into account that this value may fluctuate over time. Recent studies have used time-resolved measures of functional connectivity to measure volatility or fluctuation in brain function, in order to better characterise

aberrant brain mechanisms between healthy and pathological populations (Demirtaş *et al.*, 2016). Standard measures of fluctuation such as standard deviation and variance are also used in the recent literature to characterise global metastability of a system (Hellyer *et al.*, 2015; Váša *et al.*, 2015), hinting the possibility that the brain system moves between locally synchronized but globally de-synchronized states (Deco *et al.*, 2015; Gu *et al.*, 2015; Bassett and Sporns, 2017).

Adapting a sliding-window approach commonly used in adult fMRI research (Hutchison *et al.*, 2013; Liu and Duyn, 2013), here I study fluctuations of functional brain connectivity across fMRI acquisition time. For each separate window, I quantify the correlation coefficient within each time window. This results, for each pair of resting state networks, in an array of values over time. The mean and variance of these arrays are then computed in order to assess how strong and variable functional connectivity is between resting state networks.

These features of functional brain connectivity are then used to test the relation with cognitive and linguistic abilities at two years. In doing so, I adapt multivariate approach based on canonical correlation analysis that was recently used in adults neuroimaging studies in order to investigate brain-behaviour links (S. M. Smith *et al.*, 2015; Miller *et al.*, 2016). A latent factor (or linear combination) within time-resolved measures of neonatal brain function is identified, such that it is maximally correlated with a latent factor (or linear combination) within the neurodevelopmental measures at two years of age. Therefore cognitive and linguistic abilities, and motor development, are interpreted as multiple measures or facets of a unique underlying behavioural factor: a common approach in cognitive sciences. The correlation between brain and behavioural latent factors is then tested in a cross-validation setting and permutations are run to assess statistical significance. The underlying identified factors, or brain and behaviour models, are then characterised.

For the identified brain latent factor, network graph analyses are chosen in order to better characterise the large parameter- (or feature-) space. Indeed graph theoretical notions have recently been applied to the neurosciences shedding new light in the complex functional and structural organisation of the human brain network (Bullmore *et al.*, 2009). Here, brain network graph statistics are quantified for the identified parameters of the brain latent factor (or brain model), and further tested against behavioural scores in order to understand whether a computational characteristic of this estimated network is associated to efficient neurodevelopment.

The combination of advance measures of neonatal dynamic brain function with multivariate regression approaches and graph theory, although of not trivial implementation, represents a novel, powerful tool to study possible brain mechanisms supporting efficient neurocognitive development, in a period when complex cognitive behaviour is not yet fully present.

Introduction

Exploring how cognition and behaviour relates to brain function may shed new light into the mechanistic brain basis of human environmental interaction (Smith, 2016). Recent work linking whole-brain connectivity to cognition has shown distinct mechanisms of human brain processing. One of these is a general mode of population covariation that links a fronto-parietal network to demographic factors and behaviour, modulates many cognitive processes, and is associated to a general intelligence factor (S. M. Smith *et al*., 2015). A second, a global network integration mechanism, relates effective cognitive performance to time-resolved integrated states

of brain activity, and may be related to fluctuations in arousal (James M Shine *et al*., 2016; James M. Shine *et al*., 2016).

Spontaneous, synchronous fluctuations in the BOLD fMRI signal are thought to reflect RSNs (Smith, 2016). These neural systems, present during both task and at rest (Vincent *et al*., 2007; Smith *et al*., 2009), are shown to alter their dynamics to meet goal-directed activities or to satisfy task demands, enabling humans to perform the complex cognitive functions necessary for everyday living (Cocchi *et al*., 2013; Kim *et al*., 2013; Braun *et al*., 2015; Deco *et al*., 2015; Gu *et al*., 2015; James M. Shine *et al*., 2016). However, whether this dynamic coupling of brain networks is relevant to language and cognitive development is unknown.

Understanding developmental trajectories of the human brain's cognitive networks is important for computational models of real-life behaviour and cognitive development, and ultimately to highlight how they are altered in disease. Preterm children are at increased risk for cognitive, language, and behavioural impairment (Bhutta *et al.*, 2002; Wolke *et al.*, 2015). Studying preterm born infants at the time of normal birth therefore represents a unique opportunity to test hypotheses regarding the ontogeny of cognitive brain networks, and to shed new light on how premature environmental exposure may affect the emergence of human neurocognitive systems. Key questions are thus: do inter-individual differences in cognitive function in childhood depend upon dynamic brain function as a neonate; how is this brain-behaviour linkage influenced by early environmental exposure.

In this work, we hypothesized that dynamic neonatal brain networks interactions represent a marker for the later development of efficient cognitive and linguistic abilities. We combined time-resolved neonatal resting-state fMRI functional connectivity and developmental assessment in later childhood to study a neonatal

model supporting neurocognitive development and assess how key environmental factors such as the degree of prematurity at birth may influence it. As part of the ePrime cross-sectional study we acquired resting-state fMRI data in a large cohort of 100 prematurely born infants at term equivalent age (38-44 PMA weeks). At 20 months corrected age we followed up these children assessing their level of motor, language and cognitive development (Johnson *et al*., 2004; Bayley, 2006). By employing a sliding window analysis over fMRI acquisition time (Hutchison *et al*., 2013; Liu and Duyn, 2013) we investigated dynamic interactions of resting-state brain networks (James M. Shine *et al*., 2016). We quantified the mean and the variance of functional connectivity over time in order to estimate respectively strength and fluctuation (or variability) of time-resolved functional connectivity (Figure 28.A) (Demirtaş *et al*., 2016). We used canonical correlation analysis (CCA) to identify a brain-behaviour model of population co-variation (S. M. Smith *et al*., 2015; Miller *et al*., 2016) linking differences in dynamic interactions of resting-state brain networks at the time of normal birth to inter-individual differences in neurodevelopmental scores at two years (Figure 28.B). In order to describe the identified brain model, we assessed how functional brain connectivity strength and fluctuations were involved (Figure 28.C), and depicted these characteristics at the network's nodal level (Figure 28.D). Finally, as in the adult brain efficient cognitive functions rely upon the ability to dynamically integrate information across specialized brain regions (James M. Shine *et al*., 2016), we hypothesized that network integration in the identified brain network model was related to efficient cognitive development (Figure 28.E).

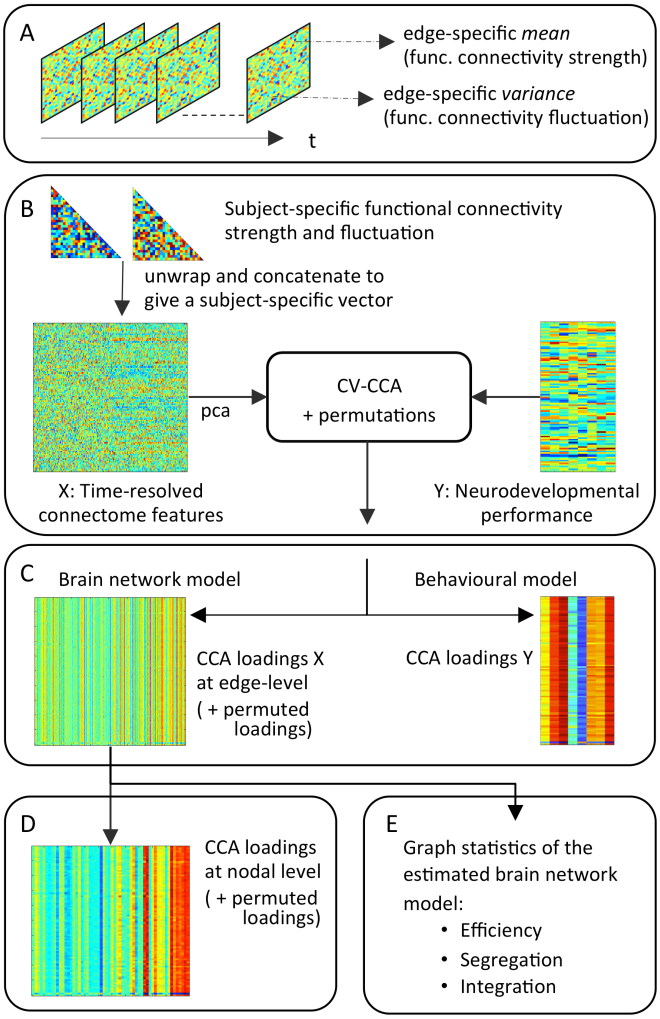

FIGURE 28 LINKING DYNAMIC BRAIN NETWORK INTERACTION TO COGNITIVE DEVELOPMENT

We hypothesized that dynamic neonatal brain networks interactions represent a marker for later cognitive and linguistic development. A) In resting-state fMRI data of 100 prematurely born infants at the time of normal birth, we employed a sliding window analysis and, for each window, calculated functional connectivity between RSNs. We estimated features of *functional connectivity strength* and *fluctuation* as edge-specific functional connectivity *mean* and *variance* across time-windows. As these matrices are symmetric, we only kept the values below the diagonal and unwrapped and concatenated all rows to give a single vector per subject. B) Using cross-validated canonical correlation analysis (CV-CCA), we identified cognitive-image pairs linking time-resolved functional connectivity metrics at the time of normal birth to neurodevelopmental scores in early childhood. C) Across all folds, we extracted the CCA loading vectors to characterise the pattern of neonatal brain network

connectivity (brain network model) linked to the set of cognitive abilities at two years (behavioural model). D) Separately for functional connectivity strength and fluctuation, we characterised the extracted CCA loading vectors at the brain network's nodal-level. E) Based on edge-level CCA loading vectors, we studied the graph theoretical measures of efficiency, segregation, and integration, and tested whether as in adulthood, network integration in the identified brain network model was related to efficient cognitive development.

Materials and Methods

For the work of this chapter the same infants, neuroimaging data, and pre-processing pipeline implemented in the previous chapter has been used. Notably novel post-processing analyses are here implemented.

Neurodevelopmental assessment

At 20 months corrected age we followed up these children assessing their level of motor, language and cognitive development using the BSID-III scales of infant and toddler development and the Parent Report of Children's Abilities Revised (PARCAR) (14, 15). Neurodevelopmental assessment data was present for 100 out of the total study population of 166 infants.

Group-level ICA-parcellation and (individual subject) nodes time-series

Large-scale RSNs were identified using group-level ICA decomposition (Smith *et al*., 2009) performed on the group of *66 infants with no follow-up data*, comprising 50 preterm born infants and 16 term born infants. Functional datasets (each containing 250 volumes) were fed into a group-level-ICA carried out using FSL MELODIC v3.0 implementing a temporal-concatenation approach and a fixed dimensionality of 60 components (individual datasets were temporally demeaned and had variance normalization applied) (Beckmann *et al*., 2005, 2009; Smith,

Beckmann, *et al*., 2013; Toulmin *et al*., 2015). Healthy term born infants were included in order to cover the full gestational age range from 25 to 42 gestational weeks and thus not bias the estimation of RSNs to those present only in prematurely born infants. All subsequent selective analyses were computed on a separate group consisting of the remaining *100 prematurely born infants* who were imaged at term-equivalent age and assessed for neurodevelopmental outcome at 20 months corrected age. Dual-regression (Beckmann *et al*., 2009) was used to derive subject specific group-ICA time-series (stage-1) and spatial maps (stage-2) for this group of 100 infants.

Group-level developmental RSNs where identified using FSL Linked ICA (Groves *et al*., 2012). Linked ICA is a data-driven, unsupervised approach for multimodal data fusion that aims to identify structured patterns of variance across multiple imaging modalities. Here we applied this approach to resting-state fMRI data, treating each RSN as it was a different modality. Under the assumption that during term equivalent period (38-44 postmenstrual weeks) a maturational process will occur for the RSNs but not for noise-components, we used FSL's Linked ICA (FLICA) (implemented in Matlab (R2015a)) (Groves *et al*., 2011, 2012) on subject-specific group-ICA spatial maps seeking for a linked mode of variation across RSNs that was best described by increasing postmenstrual age at scan. FLICA was run on the full dataset (100 subjects × 60 RSNs candidates) for 1000 iterations with an upper limit of 10 components specified.

Time-resolved functional connectivity of the neonatal brain

Time-resolved whole-brain functional connectivity, was quantified between the 29 RSNs linked by perinatal development in a sliding-window fashion using Tikhonov-

regularized partial correlation with FSLNets (S. M. Smith *et al*., 2015) and MATLAB (R2015b, The MathWorks, Inc., Natick, MA, USA).

Instead of considering the grand average functional connectivity collapsed over time, the whole acquisition time-course was split into smaller time windows with length of 30 seconds (= 20 volumes; TR of 1.5 seconds) and no gap between windows. This allows that functional connectivity could be calculated reliably for each time window avoiding spurious fluctuations (Allen *et al*., 2012; Zalesky *et al*., 2014; Deco *et al*., 2015; Leonardi and Van De Ville, 2015). Indeed in a recent paper from Van De Ville and colleagues (Leonardi and Van De Ville, 2015), the authors further demonstrate the optimality of a 30 seconds time window for quantifying dynamic reconfiguration of networks. Our choice of window size is therefore align with state of the art methods for uncovering dynamic fluctuations in functional connectivity neuroimaging BOLD data (Braun *et al*., 2015). This procedure yielded a subject-specific vector of weighted adjacency matrices describing the functional connectome in each time window.

For each pair of RSNs, we calculated *mean* and *variance* of functional connectivity along sliding-window vector (therefore across fMRI acquisition time). This provided subject's measures of time-resolved functional connectivity: one symmetric 29 × 29 *functional connectivity-strength* matrix and one symmetric 29 × 29 *functional connectivity-fluctuation* matrix. As these matrices are symmetric, we only kept values on one side of the diagonal, resulting in 406 + 406 unique features per subject (for each of the two matrices, 29 × 28 / 2). Combining across subjects resulted in a 100 × 812 matrix (subject × connectome features).

Assessment of head-motion confound on time-resolved time-resolved functional brain connectivity

Head motion has been shown to significantly confound resting-state functional-MRI studies leading to spurious patterns of connectivity (Power *et al*., 2012; Satterthwaite *et al*., 2012, 2013; Griffanti *et al*., 2014; Pruim *et al*., 2015). We therefore implemented strict criteria for data selection, using FSL FIX (v1.061) for data denoising, and performed quantitative analyses in order to formally assess the effect of head-motion on RSNs functional connectivity. Head motion measures in our study-group were matched to those used in the studies of Pruim et al. (Pruim *et al*., 2015) and Power et al. (Power *et al*., 2012) (RMS-FD ± SD: 0.118 ± 0.090 mm and 0.146 ± 0.090 mm), in order to obtain a sensitive dataset using previously described denoising procedures (Ball *et al*., 2016). The average RMS-FD for the whole sample was 0.0581 ± 0.0860 mm.

Brain-behaviour model of population co-variation

To identify a brain-behaviour model of population co-variation that predicted the link between dynamic brain connectome at the time of normal birth and inter-individual differences in cognitive and motor behaviour at 2 years, we carried out a train-test validation analysis based on CCA (Avants *et al*., 2014; S. M. Smith *et al*., 2015; Miller *et al*., 2016). CCA is a cross decomposition method used to model covariance structures in multidimensional spaces (Hotelling, 1936; Wegelin, 2000). The approach identifies the linear direction in the first space X that explains the maximum variance direction in the second space Y. The result is a canonical correlation between two canonical variates, U and V, that represent linear transformations of variable sets X and Y such that: U=a' X and V=b' Y, where a and b are the canonical vectors or weights sought by the model. Once a pair of canonical variates is found, a successive pair is sought subject to the constraint that they are uncorrelated with the first pair, and so on.

Prior to leave-one-out cross-validated CCA, we removed the effect of confound variables: connectome features were first regressed for PMA at scan; neurodevelopmental measures for socioeconomic score. All features were standardized in the training sets to have zero mean and unit variance and the same transformation was then applied to the testing sets. For each training dataset, standardization and dimensionality reduction of connectome features was performed using PCA (two separate PCAs for functional connectivity strength and fluctuation with equal number of components).

The reduced set of connectome features and the set of neurodevelopmental scores were then passed to a CCA. The trained CCA transformations were then applied into the left-out test data set of connectome features and neurodevelopmental scores, in order to estimate subject vectors U_1 and V_1 for the test data set. As in Smith et al., we correlated canonical pairs U_1 and V_1 (S. M. Smith *et al.*, 2015) and calculated the mean-squared-error (MSE). The statistical significance of the correlation and MSE between canonical pairs were assessed sequentially with a permutation test, swapping the rows of second feature matrix (neurodevelopmental scores) with respect to the first 10 000 times and recording the maximum correlation between pairs and MSE. To test whether the identified brain-behaviour relationship was driven by degree of prematurity (measured by GA at birth) or in-scanner head motion (RMS-FD), we used linear partial correlation between the canonical pairs U_1 and V_1 while controlling for GA at birth or RMS-FD. Correction for the FWE rate was applied across estimated modes. All analysis were performed using MATLAB (R2015b, The MathWorks, Inc., Natick, MA, USA) and Scikit-learn (Pedregosa *et al.*, 2011).

Behavioural canonical variate pair

To characterize the identified mode of covariation, we extracted the *CCA loading vectors* across all estimated folds for connectome features and neurodevelopmental variables. To investigate differential contributions in CCA loading vectors with no assumptions on whether or not these features were normally distributed, non-parametric statistical tests were preferred although generally less powerful than the parametric counterparts in the rejection of the null hypothesis (Gibbons and Chakraborti, 2011).

The extracted *Y block of CCA loading vectors* matched the initial neurodevelopmental sub-scales, and was grouped in accordance to the cognitive domains affiliation. The "cognitive abilities" group contained the general cognitive sub-scales of BSID-III and PARCAR; the "language abilities" was formed by the receptive- and expressive-linguistic sub-scales of BSID-III, and the vocabulary and word-use sub-scales of PARCAR; "motor abilities" group comprised the gross- and fine-motor sub-scales of BSID-III).

Brain imaging canonical variate pair

For each fold, we multiplied the extracted *X block of CCA loading vectors* by the estimated PCAs eigenvectors, so to spatially map the CCA modulation loadings back to the original set of connectome features and characterise CCA loadings of time-resolved functional connectivity. In order to assess statistical significance of connectome CCA loadings, we performed the same procedure on the CCA permuted models and calculated FWE-corrected p-values of each brain network-edge (separately for functional connectivity strength and fluctuation; considering equal or greater values if the feature-specific CCA loading average across folds was positive; equal or smaller values if negative). FSLNets was then used to create connectome images of statistically significant edges, visualizing median *connectome CCA*

loading across folds (separately for brain connectome strength and fluctuation). By linking brain regions (nodes) through their interactions (functional connectivity edge strength and dynamics), we analysed the estimated brain network at the individual node-level characterizing *nodal-level* CCA loadings. We converted subject-specific edge-level CCA loadings (square nodes × nodes matrix) to nodal-level CCA loadings, by summing up across edges involving each node (vector of nodal values) (S. M. Smith *et al.*, 2015). We then repeated the same procedure for CCA permuted models so to assess statistical significance of *nodal* CCA loading non-parametrically (separately for brain functional connectivity strength and fluctuation).

Graph theoretical statistics of the identified brain network model

As it has recently been shown that integrated states of brain network configuration relate to cognitive performance (James M. Shine *et al*., 2016), here we investigated the neonatal brain model of cognitive development using graph theoretical measures of efficiency, segregation and integration (Bullmore *et al*., 2009). We considered the estimated CCA loadings across all folds (therefore subject-specific) as the representation of a cognitive brain network at the time of normal birth. In order to not bias the analysis to only those edges significantly more involved then in the permuted models, all network edges were included. We calculated subject-specific graph theoretical measures separately for connectome strength and fluctuation in order to disentangle the contribution of these two factors at the global network level. As a first check we compared *graph density* between the two networks to ensure these were comparable (James M. Shine *et al*., 2016). Networks were matched for density and did not differ in network sparsity (Wilcoxon Signed-rank test: p-value = 1). At the systemic-level, we then calculated network *global efficiency* as a proxy for functional integration (Rubinov and Sporns, 2010). Because global efficiency can

only be computed from weighted networks with positive weights (or binary networks) (Barch *et al*., 2013), CCA connectome strength and dynamics were first thresholded to include only positive edge weights before calculating global efficiency (James M. Shine *et al*., 2016).

In order to quantify network segregation and integration, we first identified brain network modules: groups of densely interconnected network nodes, which often are the basis for specialized subunits of cognitive processing (Betzel and Bassett, 2016; Sporns and Betzel, 2016). By performing multi-scale community detection across a range of structural resolution parameter γ (Porter *et al*., 2009; Onnela *et al*., 2012; Gu *et al*., 2015). To make this analysis comparable with other studies in the literature, we used the group-average functional connectivity matrix estimated using FSLNets from the whole fMRI time-series acquisition. By maximizing the modularity quality function (Newman, 2006) using a Louvain-like (Blondel *et al*., 2008) locally greedy algorithm (Jutla *et al*., 2011) (with 100 optimizations) for multiple values of γ, we quantitatively estimate consensus between partitions calculating partitions similarity as z-score of the Rand coefficient (Traud *et al*., 2011). Maximum mean partition similarity was achieved for $\gamma = 1.5$, hinting at the presence of especially well-defined modules. At that parameter value we uncovered a partition of the brain into 3 bilaterally symmetric modules. We then estimated brain network *segregation* as within-module connectivity (WT), calculating module-degree Z score, and network *integration* as between-module connectivity (BT), calculating participation coefficient (Bullmore and Sporns, 2012; James M Shine *et al*., 2016).

Results

Resting state Networks identification

Group-level RSNs were first estimated by performing ICA in an initial set of 66 infants. All subsequent selective analyses were then computed on a separate group consisting of the 100 prematurely born infants who were imaged at term-equivalent age and assessed for neurodevelopmental outcome at 20 months corrected age.

Developmental RSNs were identified using FSL Linked ICA (Groves *et al.*, 2012) seeking a linked mode of variation across RSNs across subjects around time of normal birth. The main mode of maturation consisted of 29 RSNs representing those RSNs previously shown in the literature (Smith *et al.*, 2009; Doria *et al.*, 2010) (Figure 29). This mode accounted for 33% of RSNs variance; correlated strongly with postmenstrual age (corrected p-value < 1 × 10-5); was not associated with in scanner head motion (measured by average RMS-FD); GA at birth, or with neurodevelopmental measures at 2 years. During the six-week period around the time of normal birth, a prominent, linked mode of maturation drives RSNs development.

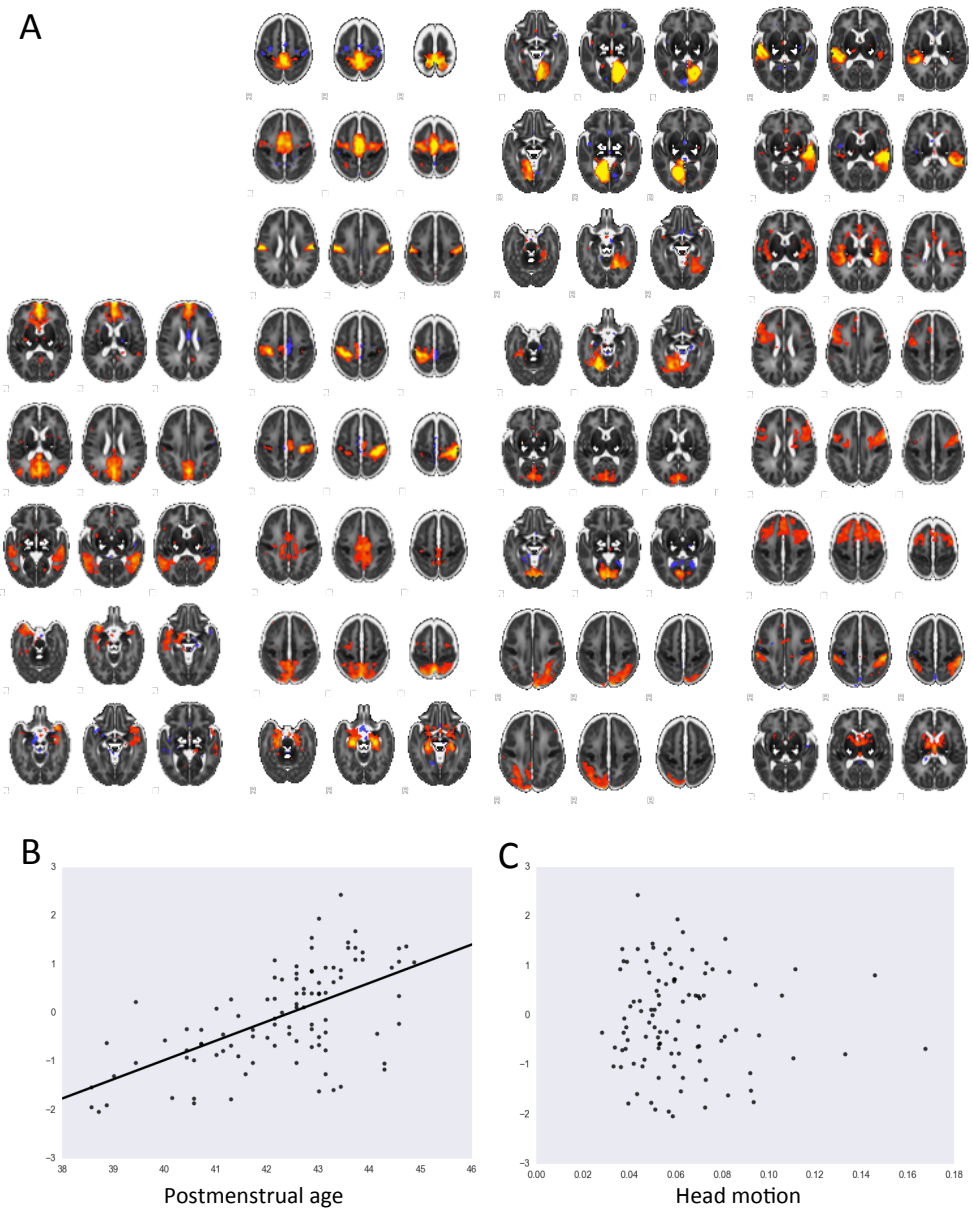

FIGURE 29 DEVELOPMENTAL RESTING STATE NETWORKS

A linked mode of variation across resting state networks (RSNs) across subjects was identified in the 6 weeks around time of normal birth. A) Spatial correlation of the identified mode of variation on RSNs maps. B) This mode was significantly correlated with postmenstrual age at scan (corrected p-value = 6.8×10^{-11}), accounted for 33% of variance, and C) was not associated with in-scanner head motion. These findings suggest that around neonatal age, RSNs are driven by a linked prominent mode of development.

Neurodevelopmental assessment

At 20 months corrected age we followed up these children assessing their level of motor, language and cognitive development using the BSID-III and the PARCAR (Johnson *et al*., 2004; Bayley, 2006). BSID's "*general cognitive abilities"* sub-scale was the only variable significantly correlated with gestational age at birth (Pearson's $r = 0.21$; $p = 0.0338$ not corrected for multiple comparison; for all other sub-scales of interest: $p > 0.3307$); and significantly correlated with SES, measured as the English Index of Multiple Deprivation (Pearson's $r = -0.23$; $p = 0.0244$ not corrected for multiple comparison; for all other sub-scales of interest: $p > 0.1369$). No significant difference in linguistic performance was found between those infants who lived in predominately English speaking or bi-lingual households (two-sample t-test right-tail, before and after de-confounding for SES, respectively: tstat = 0.9014; $p = 0.1848$; tstat = 0.6158; $p = 0.2697$).

Time-resolved neonatal brain network model linked to efficient cognitive development

We investigated brain network dynamics using sliding time windows of whole-brain resting-state fMRI data and Tikhonov-regularized partial correlation (Braun *et al*., 2015; S. M. Smith *et al*., 2015). Across each vector of weighted adjacency matrices (therefore across fMRI acquisition time), we calculated *mean* and *variance* of the functional connectivity between each pair of RSNs to yield subject-specific features of *connectome strength* and *fluctuation* (Figure 28.A). There was no significant association between these metrics and in-scanner head motion (univariate general linear model testing: for all connectome features FWE-corrected p-value > 0.12).

In order to identify time-resolved metrics of resting state brain functional connectivity at the time of normal birth linked to cognitive-image pairs, we used CCA (S. M. Smith *et al*., 2015; Miller *et al*., 2016) (Figure 28.B). In a train-test

validation analysis, CCA was only run on a training-subset of the data, and the estimated transformation was then applied onto the left-out test data set of connectome features and neurodevelopmental scores in order to estimate predicted subject vectors U_1 and V_1 for the test data set (Pedregosa *et al*., 2011). Finally, correlation and MSE between predicted canonical pairs U_1 and V_1 was assessed. Nested cross-validation was used to assess the number of PCA components fed to the CCA models leading to lower mean squared error and higher canonical correlation (Figure 30).

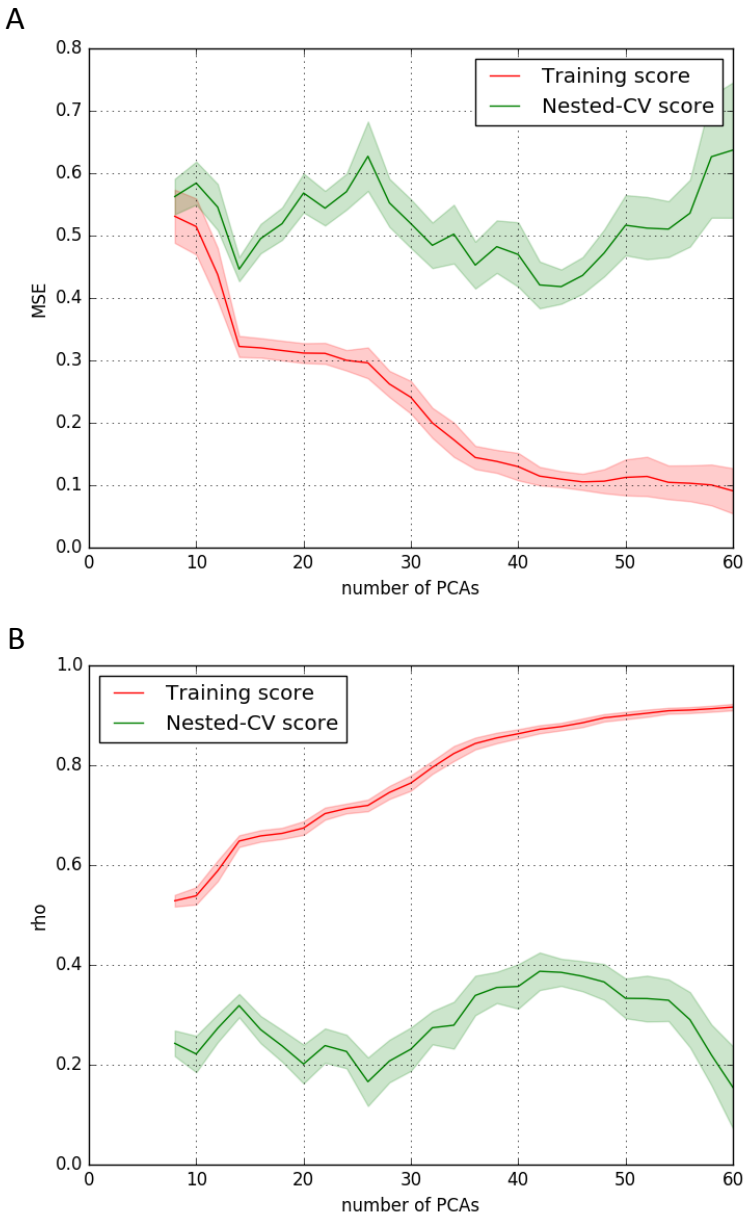

FIGURE 30 NESTED CROSS-VALIDATION RESULTS

Nested cross-validation was used to assess the number of PCA components fed to the CCA models leading to lower mean squared error and higher canonical correlation. The set of 44 PCAs (22 PCAs for functional connectivity strength and 22 PCAs for functional connectivity dynamics) had on average A) the lower Mean Squared Error (average MSE = 0.4182) and B) the higher canonical correlation (average rho = 0.39).

We identified a single statistically significant mode of co-variation (r = 0.4236; FWE-corrected p-value = 0.0043; MSE = 0.3860; FWE-corrected p-value = 0.0145,

corrected for multiple comparisons across all modes estimated). This mode represented a pair of canonical variates along which patterns of time-resolved neonatal brain connectome metrics and sets of neurodevelopmental scores at two years co-varied in a similar way across subjects (Figure 31.A).

To understand whether the establishment of such a relationship was driven by extrinsic influences, we used partial correlation between U_1 and V_1 to test whether the identified mode of covariation was affected by key environmental factors such as the degree of prematurity at birth. Adjusting for this factor did not change the nature of the identified mode of co-variation ($r = 0.41$; FWE-corrected p-value = 0.0063), suggesting that early environmental exposure has a minimal effect on this relationship.

To summarize, we identified one significant mode of population covariation for which individual subjects' strength of involvement was highly similar for both the time-resolved neonatal brain connectome and a subset of neurodevelopmental abilities.

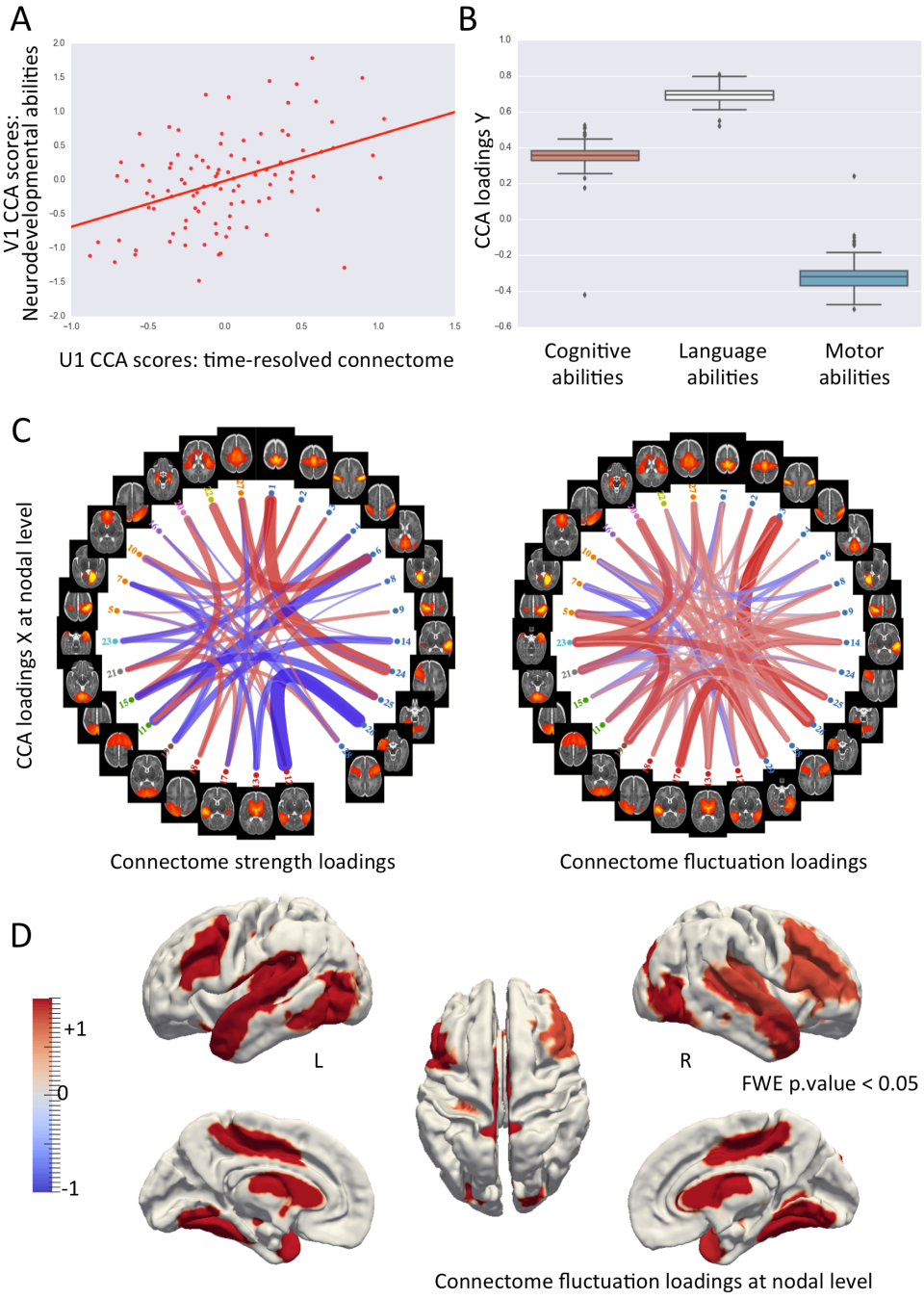

FIGURE 31 TIME-RESOLVED BRAIN NETWORK FUNCTIONAL CONNECTIVITY IS LINKED TO EFFICIENT DEVELOPMENT OF LATER COGNITIVE AND LINGUISTIC FUNCTIONS

A) Scatter plot of significant CCA mode, with one point per subject (r = 0.4236; FWE-corrected p-value = 0.0043), for which individual subjects' strength of involvement with this mode was highly similar for both a specific pattern of time-resolved neonatal brain functional connectivity and a subset of developmental scores in cognitive and linguistic abilities at two years. B) Showing Y block CCA loadings grouped by cognitive domain. Linguistic and

cognitive functions were significantly more involved then motor development (effect size r = 0.61). C) Significant X block CCA loadings at edge-level (compared against CCA permuted models). In the identified co-variance mode, there was significantly higher involvement of connectome fluctuation. D) Significant X block CCA loadings at nodal-level (compared against those estimated in CCA permuted models). Neonates with highly dynamic RSNs brain connectivity in the prefrontal, temporal and striatal regions, show greater linguistic and cognitive abilities later in childhood.

Linguistic-cognitive factor in childhood linked with neonatal brain network

In order to characterize the identified cognitive factor and the brain network significantly involved in the identified brain-behaviour relation, for each estimated fold we extracted the *CCA loading vectors*.

We found *language* and *cognitive* abilities had significantly higher influence on the identified mode of co-variation with respect to *motor* development (Bonferroni-corrected p-values $< 1 \times 10^{-4}$). These results provide evidence of how cognitive and linguistic functions modulate the identified brain-behaviour link. High-scoring subjects in this covariance mode (Figure 31.A, data points located in the upper right of the scatter plot) have high relative performances in linguistic and cognitive functions and low relative scores in motor abilities (and vice versa for low scoring subjects).

Anatomy of neonatal brain network linked with linguistic-cognitive abilities at two years

To uncover the neuroanatomical systems predictive of later linguistic and cognitive development, we extracted the brain connectome *CCA loading vectors* across all folds. These were mapped to the original brain connectome features at the network edge-level, and then summarized at the network nodal-level.

We calculated edge-specific statistical significance of *connectome* CCA loadings by comparing these values to those estimated in the permuted CCA models (Figure 31.C). Only 52 brain network-edges were highlighted as statistically significant from connectome strength features (FWE-corrected p-values < 0.05); compared to 119 edges from connectome fluctuations. This over-representation of dynamics network interactions was also corroborated by the significantly higher mean value of CCA loadings involved in the CCA mode (compared to functional connectivity strength; Wilcoxon rank sum test: $Z = -30.7$; p-value $< 1 \times 10^{-5}$; effect size $r = 0.82$). These results underline the importance of fluctuations in time-resolved resting-state fMRI functional connectivity in the link between neonatal brain function and neurocognitive development.

We then summarised connectome CCA loading vectors at the nodal level (Figure 28.D). Four network nodes or RSNs had statistically significant functional connectivity strength (compared to permuted CCA models; FWE-corrected p-values < 0.05). Whilst ten RSNs had statistically significant functional connectivity fluctuation, including bilaterally the middle frontal gyrus, the anterior and posterior superior temporal cortices, the striatal region, posterior cingulate cortex, and the posterior fusiform areas (Figure 31.D). Average CCA loadings of RSNs fluctuation had significantly higher involvement compared those of RSNs strength (Wilcoxon rank sum test: $Z = -28.7$; p-value $< 1 \times 10^{-5}$; effect size $r = 0.77$), suggesting that neonates with highly dynamic RSNs connectivity in the prefrontal, temporal and striatal regions, show greater linguistic and cognitive performance later in childhood. This result is aligned with the observation that in the mature brain, functionally connected prefrontal and temporal regions changes their activity to support auditory-verbal working-memory (Buchsbaum *et al.*, 2005).

Computational integration in the neonatal brain network supports efficient cognitive development

As the ability to dynamically integrate information across specialized brain regions is key for an efficient adult cognitive brain system (James M. Shine *et al.*, 2016), we further hypothesized that, in the identified neonatal brain network, network integration emerged from fluctuations in functional connectivity, and that was associated to efficient cognitive development.

Based on edge-level CCA loadings values of connectome strength and fluctuation we constructed two separate networks. We calculated the graph-theoretic measure of *global efficiency* (Rubinov and Sporns, 2010) and found that connectome fluctuation resulted in greater global efficiency than connectome strength (Figure 32.A) (comparing global efficiency Z values normalized by CCA permuted models; median of efficiency strength and efficiency fluctuation were = 1.3 and 2.2, respectively; Wilcoxon Signed-rank test: $Z = -8.6766$; p-value $< 1 \times 10^{-5}$; effect size $r = 0.61$). Furthermore global efficiency of connectome fluctuation was significantly higher than chance (compared to global efficiency computed on CCA permuted models; p-value = 0.0005). However, global efficiency was not directly associated with greater linguistic and cognitive skills ($r = 0.04$; $p = 0.6833$). Although dynamic fluctuations of neonatal RSNs enhance the global ability to rapidly combine specialized information (Bullmore *et al.*, 2009; Bullmore and Sporns, 2012), these results suggests that efficient neurocognitive abilities in childhood do not result from global network integration but rather they may develop from the dynamic network integration of specialised regions.

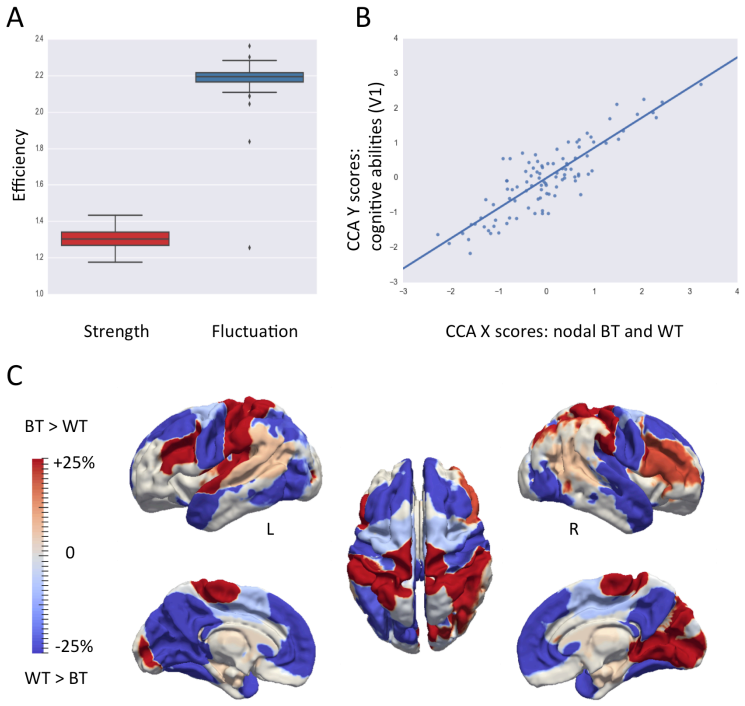

FIGURE 32 FLEXIBLE GLOBAL NETWORK INTEGRATION AS A NEONATAL BRAIN MECHANISM FOR EFFICIENT DEVELOPMENT OF LATER COGNITIVE FUNCTIONS

We characterise the identified neonatal brain network model using graph theoretical measures. A) Connectome fluctuation of the identified cognitive network leads to significantly greater global efficiency (effect size: r = 0.61). B) At the nodal-level, network integration and segregation of connectome fluctuation are linked to efficient cognitive development (V1) (r = 0.87; FWE-corrected p-values = 0.0018). C) Greater linguistic and cognitive scores at two years were linked to a typical left-lateralized network of dynamic connector hubs in linguistic regions with high integration and low segregation (hot colours), and with the default mode network having the opposite pattern (cold colours), demonstrating the key role of dynamic network integration for the later development of complex, adaptive linguistic and cognitive abilities.

As in the adult brain it is indeed known that greater cognitive skills are linked to greater integration and reduced segregation between dynamic, specialized brain areas (James M. Shine *et al.*, 2016), we tested this alternative hypothesis. We quantified network integration as network participation coefficient (between-module

connectivity; BT); and network segregation as network module-degree Z score (within-module connectivity; WT) (James M. Shine *et al.*, 2016). We found a significant linear association (tested using CCA: r = 0.87; p-value = 0.0018) linking dynamic *nodal* integration and segregation with the previously identified cognitive/linguistic phenotype (V_1) (Figure 32.B). Greater linguistic and cognitive scores at two years were positively linked to a typical left-lateralized linguistic network of connector hubs (regions with high integration and low segregation (Rubinov and Sporns, 2010)), and negatively linked with the default mode network (having the opposite pattern) (Figure 32.C). Together these findings show that dynamic interactions between neonatal brain RSNs results in flexible connector hubs with high integration and low segregation that may support efficient development of linguistic and cognitive functions in childhood.

Testing of head motion effect in the relationships between functional connectivity and behaviour

Head motion is known to lead to spurious pattern of brain functional connectivity (Power *et al.*, 2012; Satterthwaite *et al.*, 2012, 2013; Griffanti *et al.*, 2014; Pruim *et al.*, 2015), and to be a likely source of systematic bias in the measurement of functional connectivity-behaviour relationships (Siegel *et al.*, 2016). We therefore tested whether the identified relationship between time-resolved functional connectivity and cognitive and linguistic skills was driven by in-scanner head motion. Adjusting for Root mean squared frame-wise displacement (RMS-FD) did not change the mode of co-variation (adjusting for RMS-FD: r = 0.42; FWE-corrected p-value = 0.0053;), demonstrating no significant effect of this confound in the identified brain-behaviour relationship. Although head motion has been shown to

significantly confound resting-state fMRI studies leading to spurious patterns of connectivity (Power *et al.*, 2012; Satterthwaite *et al.*, 2012, 2013; Griffanti *et al.*, 2014; Pruim *et al.*, 2015), our findings demonstrate how the strict criteria and the motion-denoising approach here applied allowed us to minimize the contamination of this important confound.

In a similar way no CCA loading vector was significantly associated with in-scanner head motion (univariate general linear model testing the linear association between RMS-FD values and edge- /nodal-level CCA loading; FWE-corrected p-values > 0.12 for all tests). Likewise, no significant association was found between graph theoretical measures and RMS-FD or gestational age at birth (linear association tested using CCA between graph measures with, respectively, RMS-FD: p-value = 0.86; and with GA at birth: p-value = 0.30).

Discussion

We studied the dynamic interactions of resting-state brain networks in preterm infants at the time of normal birth, by quantifying the mean and variance of functional connectivity over sliding windows (Figure 28.A). By linking these features of strength and fluctuation (or variability) in time-resolved functional brain connectivity with later developmental scores at two years of age, we revealed a neonatal brain network model supporting later neurocognitive development: greater cognitive and linguistic performances at two years were significantly associated with neonatal brain connectome strength and fluctuation, independent of key environmental factors such as the degree of prematurity at birth. Specifically, it was showed that efficient cognitive development in childhood is mainly supported by fluctuations in functional connectivity in the neonatal brain. Suggesting that greater

dynamic interactions in a bilateral network of middle frontal, striatal, temporal, posterior cingulate, and posterior fusiform regions, are an important features of the neonatal brain organisation supporting efficient, later development of cognitive functions.

It has indeed been suggested that fluctuations in resting state brain organization are an essential emergent feature of a complex brain network systems and are important in the brain–behaviour relationship (Baker *et al.*, 2014). Initial findings of these fluctuations have been shown in studies using electrophysiology (VanRullen *et al.*, 2011) and computational modelling approaches (Zalesky *et al.*, 2014; Breakspear, 2017). Recent fMRI experiments have confirmed these results and provided evidence of time-sensitive changes of brain network activity over multiple temporal-scales, from fast-transient activity (Baker *et al.*, 2014) to dynamic patterns over longer periods of time, with transition between states of high and low connectivity strength (Zalesky *et al.*, 2014), or between topologically different temporal metastates (James M Shine *et al.*, 2016). Thus, our results extend previous studies on the temporal organization of the human brain network demonstrating the importance of fluctuations in functional connectivity for efficient neonatal brain development and later linguistic and cognitive abilities.

We were also able to show that in the identified brain network linked to later cognitive development, fluctuations of time-resolved functional connectivity resulted in significantly greater network efficiency, perhaps indicating a facilitation of the overall capacity for parallel information transfer and integrated processing (Bullmore and Sporns, 2012; Deco *et al.*, 2015). This finding is indeed aligned with recent work showing that time-varying resting activity in the mature human brain connectome spends most of the time in topological integrated patterns of high global efficiency, and that during tasks it is able to increase connectivity between area in order to

enable fast effective cognitive control and performance (James M Shine *et al.*, 2016; James M. Shine *et al.*, 2016).

Finally, we established that later, efficient development of cognitive and linguistic abilities resulted from the key role of flexible connector hubs in typical left-lateralized linguistic regions (with high integration and low segregation), and in the default mode network (with the opposite pattern), suggesting neonatal network integration as a mechanistic process supporting cognitive development in childhood. The fact that complex brain processes, such as executive functions or the acquisition of cognitive and linguistic abilities, would benefit from high global efficiency of information transfer across the network, has been previously hypothesised (Bullmore and Sporns, 2012). Connector hubs, known to mediate most inter-modular connections (Rubinov and Sporns, 2010), have a central role in generating globally efficient information flow, yielding to an increase in efficiency and in turn benefits adaptive effective behaviour (Bullmore and Sporns, 2012; Heuvel *et al.*, 2016). Together, our results posit that dynamic integration of the neonatal brain connectome represents a neural mechanism supporting effective development of language and general cognitive abilities in childhood. Recent fMRI studies have provided evidence of the importance of network dynamics for effective behavioural performance, showing that in adulthood higher brain function relies upon the ability to flexibly integrate information across networks of brain regions in order to support learning (Bassett *et al.*, 2011), complex cognitive abilities (Cole *et al.*, 2014; Bassett *et al.*, 2015) and working memory (Braun *et al.*, 2015; James M. Shine *et al.*, 2016). Here, we extend these studies to human brain development and language learning by showing how dynamic integration in the neonatal brain network is linked to effective development of linguistic and cognitive functions in childhood.

Around the time of normal birth, in a period of prominent maturation and dramatic topological changes when no complex high-order cognitive behaviour is present (Dehaene-Lambertz and Spelke, 2015), dynamic neonatal brain activity is already central, supporting later development of cognitive functions, with this link minimally affected by early environmental influences related to the degree of premature delivery. Although a number of studies have shown that prematurity is associated with widespread and persistent alterations of the brain's structural and functional architecture (Counsell *et al.*, 2003; Ball *et al.*, 2012, 2014; Salvan *et al.*, 2014), it has also been shown that earlier exposure to speech in preterm infants does not lead to an accelerated development of phonological skills, suggesting that during the first year of age brain maturation is a main constraint in the shaping of the phonetic repertoire (Peña *et al.*, 2012; Cusack *et al.*, 2016). Our results are therefore consistent with the idea that early cortical development and neuronal network formation is largely experience-independent and is likely to be predominately shaped by genetic and intrinsically-generated influences (Khazipov and Luhmann, 2006; Blankenship and Feller, 2010; Chen *et al.*, 2013; Fjell *et al.*, 2015).

Our findings show that dynamic neonatal brain function predicts the ability at 2 years to communicate wants and needs, to understand and use names, to product combinatorial-grammatical sentences, and the ability to efficiently perform attention, memory and problem solving tasks (Johnson *et al.*, 2004; Bayley, 2006); all of which depend on the emergence and manipulation of symbolic representations and effective speed of processing, fundamental milestones of early development which rely on early working memory (Kuhl, 2010; Dehaene-Lambertz and Spelke, 2015). It is indeed thought that the refinement of basic auditory skills, together with increases in working memory resources, convey the emergence of higher-order language function and top-down processing (Skeide and Friederici, 2016). Here, we have shown that

efficient developmental scores of linguistic and cognitive abilities at two years are related to the dynamic integration of a left-lateralized neonatal brain network of prefrontal, temporal and motor areas that, in the mature brain, are typically associated with verbal working memory (Buchsbaum and D'Esposito, 2008; Koelsch *et al.*, 2009; McGettigan *et al.*, 2011; Price, 2012; Weiss-Croft and Baldeweg, 2015). These regions have been shown to chance their activity during complex auditory-verbal working memory tasks (Buchsbaum *et al.*, 2005; Buchsbaum and D'Esposito, 2008) and have been suggested as a brain basis not just for on-line phonological rehearsal but also to master new words and unfamiliar phonemes combinations (Baddeley, 2003). Although there are probably computational differences between these regions, together this dynamic network of connector hubs may represent a brain basis for the emergence and development of verbal working memory, easing temporary information integration and sustaining the processing of new internal representations, thus allowing the emergence of adaptive behaviours. In current models of working memory, it is indeed predicted that during the maintenance of verbal material the prefrontal cortex performs top-down control on language specific areas in order to select and enhance relevant verbal representation (Curtis and D'Esposito, 2003). The identified dynamic neonatal brain network therefore resembles that neurocognitive basis predicted to ease the acquisition of auditory-verbal working memory and to drive language learning (Baddeley *et al.*, 1998).

A limitation of our work is the use of a statistical model to identify a brain network precursor for later neurocognitive development, at a time when formal high-order cognitive behaviour is minimal. However, it is not known whether indirect precursors of cognitive functions present around neonatal age (i.e. eyes gaze cueing attention) may be able to explain as much variance in later neurocognitive development. Another limitation is the fact that our investigations of dynamic brain

activity do not take into account the underlying neural mechanism driving global fluctuations (synaptic excitation and inhibition and its balance); further studies should address how computational models of brain network coupling changes during early human development (Deco *et al.*, 2015; Breakspear, 2017).

Conclusion

Together, our results demonstrate that dynamic neonatal brain integration is closely related to the development of linguistic and cognitive functions in childhood. By enhancing information transfer between specialist regions, high integration and low segregation in a flexible network of connector regions mediates the later development of efficient language and cognitive abilities, potentially providing the flexible neural resources for the acquisition and development of auditory-verbal working memory (Baddeley et al., 1998). As in the mature brain, higher brain functions rely upon the ability to dynamically integrate information across specialized brain regions. Brain network integration, eased by dynamic RSNs interactions, therefore represents a brain mechanism for efficient cognitive development.

Chapter 8

Summary

In this thesis I aimed to examine whether the human brain is predisposed for language learning from the time of normal birth, and to assess how early environmental and linguistic experience may affect early neurolinguistic development.

Preterm birth represents both a neurodevelopmental risk factor and a unique chance to study the joint influence of premature linguistic exposure and brain maturation in the early emergence of the human language brain. Understanding typical and atypical neurodevelopmental trajectories of language brain development can help us understand this fundamental evolutionary achievement of human cognition, and further provide early quantitative biomarkers to assess the efficacy of potential neurobehavioral treatments at an early age.

The primary hypothesis of this thesis was that at the time of normal birth, organized resting-state functional and structural connectivity between regions resembling an adult-like brain language network, would be present and related to complex language abilities in early childhood. Thus challenging the assumption that the early acquisition of language abilities merely relies on the bilateral organization of the temporal cortices allowing only bottom-up cognitive processing. Here I tested this hypothesis through the combination of computational neuroimaging, high-resolution term-equivalent resting-state fMRI and diffusion-weighted MRI data, and

neurodevelopmental assessments during a period of dramatic development in linguistic and cognitive capacities.

In chapter 5, evidence is provided of organised structural bilateral connectivity between the temporal cortices and the prefrontal regions, present at the time of normal birth and related to later complex linguistic abilities. Specifically, the bilateral arcuate fasciculus, a fundamental structure of the mature brain language network known to mediate verbal working memory and word learning, is significantly associated with later composite linguistic and cognitive abilities, independent of premature environmental exposure. These findings suggest that differences in arcuate fasciculi microstructure at the time of normal birth have a significant impact on language development and modulate the first stages of language learning. In Appendix 2 I also show the study of another cortico-cortical white matter bundle of interest, the superior longitudinal fasciculus (analysis that for timing reasons was not included in the thesis submission). This structure, which in the adult brain mediates spatial working memory, in the neonatal brain is not associated with linguistic performance during early childhood. This result further strengthens the specificity of the arcuate fasciculus as a key structure in the human language brain network.

In chapter 6, it is reported that auditory-motor spontaneous synchronised correlated brain activity is present at term-equivalent, leftward lateralised and significantly associated with later expressive-linguistic abilities independent of degree of prematurity at birth. Besides resembling a functional mechanism specific of the developing expressive-language network, this language brain phenotype is linked to a meta-analytic linguistic gene-set independently associated to language function and/or impairment. These results support the notion of a functionally organized human brain that is already organised for complex language learning at the time of

normal birth, and further emphasize the joint influence of neural, genetic factors and environmental stimuli in the early emergence of the human language brain network.

In chapter 7, it is shown that fluctuations of time-resolved functional connectivity in a bilateral network of prefrontal, striatal, and temporal regions, support efficient development of language and cognitive functions in childhood. This network of flexible connector hubs that in the mature brain is typically associated with verbal working memory, is shown to ease network efficiency and information integration. These findings support the notion that flexible neural resources at the time of normal birth may represent a computational brain mechanism for the acquisition and development of auditory-verbal working memory.

Together, the work of this thesis advances previous knowledge of the early emergence of the neurobiology of language. It further confutes the previous belief that the organization of intra-hemispheric connectivity in the language network is yet to be established during the term-equivalent period and only develops with prolonged language exposure. The results of this thesis provide evidence of a distributed and flexible neural architecture that is already organised for language learning as early as at the time of normal birth, despite the fact that minimal behavioural correlates of high-order brain functions are present. This neural architecture may support the emergence of top-down as well as of bottom-up language processing, easing the later, efficient development of auditory-verbal working memory.

Further considerations

Whether language acquisition and its neural correlates are independent from general cognitive processes has not a trivial answer. Although language brain regions are

active from early in postnatal life (Mahmoudzadeh *et al.*, 2013), during early childhood the additional involvement of the prefrontal cortex in language learning has been highlighted (Nuñez et al., 2011; Skeide et al., 2014) and suggested as a mechanism to cope with effortful, not fully automatized, learning (Jeon and Friederici, 2015). Therefore, the involvement of prefrontal regions in brain language acquisition may suggest an early interaction between not-yet-fully specialised linguistic regions, and domain-general cognitive processing, possibly easing the development of efficient verbal working memory.

Furthermore whether the neonatal brain mechanisms here shown are specific to linguistic acquisition in preterm infants or resemble global neurodevelopment can be seen as a modelling issue. Hypothesising a common brain substrate (or latent factor) underlying multiple cognitive functions, (as it was applied in chapter 7 and in the adult human brain (S. M. Smith *et al.*, 2015)), provided a parsimonious model with good explanatory power. The advantage of the work of this thesis is that a competitive model with i.e. a contrasting theory can be tested in future studies and the predictive power can be compared. The data-driven approach here applied (specifically in chapter 7) suggests that in preterm infants the functional brain basis supporting later neurocognitive development is strongly biased towards high involvement of language specific factors, with a minor contribution of general cognitive factors, as it would be inevitable given the strong dependency between these cognitive domains.

Another issue worth considering is whether one of the functional or structural brain mechanisms here highlighted is more important than the others. The fact that multiple brain predictors of linguistic (and cognitive) abilities have been here highlighted corroborates the presence of an underlying neonatal brain bias towards language acquisition. Therefore these multiple brain predictors have to be considered

in a holistic perspective as multiple facets of the same neurocognitive developmental process. However, how these functional and structural measures do relate to each other is not trivial question and indeed represents one of the cutting-edge frontiers of the neurosciences. A recent review (Breakspear, 2017) has indeed highlighted what has been in the last years a step forward from previous studies considering trivial relations between measures of diffusion and functional connectivity. The current status of the most advance research highlights how complex biophysical models of large-scale dynamic activity can simulate dynamic neural activity in the adult human brain. How these mechanistic processes linking brain structure and function may differ in the developing brain (i.e. GABA switch) or have a role in the process of language learning is topic of future studies.

There is however another possible modelling approach linking dynamic brain activity, the underlying structural connectome, and cognitive functions or development. (This approach was indeed one of the topics of my PhD studies although unfortunately it was not included in this thesis due to timing issue). As resting state fMRI activity can be interpreted and spatially decomposed in underlying clusters called resting state networks; the dynamic fluctuations of these networks' BOLD signal can be used to model multiple, semi-stable brain states (or dynamic modes) of activity that are recurrent over time of fMRI acquisition (Baker *et al.*, 2014; Vidaurre *et al.*, 2016). It follows that if the human brain cycles through these multiple states of activity, it can be hypothesises that a linear dynamical system is emerging from the underlying structural brain network. Therefore a way to model brain states transition within a linear dynamical system assumption is by assessing brain network's controllability properties (Pasqualetti *et al.*, 2013). Structural controllability of the human brain network can be identified as one possible mechanistic principle governing brain state transition (Gu *et al.*, 2015; Bassett and

Sporns, 2017). Whiting this framework, it is possible to estimate a network node's capacity to steer (or drive) the functional activity of the entire brain system between any of these states. Therefore certain regions would be more likely to be central in governing brain system dynamic transition i.e. between a rest and a language task condition. By applying this framework to the human developing brain, it is possible to link this structural/functional characteristic of the neonatal human brain with linguistic and cognitive development in childhood. This would allow a better understanding of whether inter-subject differences in a mechanistic process of brain system dynamic activity can predict later neurocognitive development and shed new light into the brain basis of human language acquisition.

Limitations

Although in all the studies here reported degree of prematurity at birth minimally modulated the identified relationships between language brain architecture and later linguistic abilities, it is not known to which extent these findings can be generalized to normal brain development. The replication and further comparison to a large population of healthy term born infants with standardized neurodevelopmental assessment is therefore needed. However, as discussed in previous chapters, during the first year of life language acquisition is constrained by brain development and not accelerated by premature linguistic exposure. Furthermore, the identified language infant brain phenotypes resemble those of an adult-like language system. Therefore the language brain mechanisms reported here are likely to represent genuine structures of the healthy human language brain architecture and not specific traits of the preterm population.

A limitation of these studies is the lack of longitudinal imaging and a single linguistic assessment. As mentioned in chapter 5, at the age of two years measures of complex linguistic skills strongly correlate to domain-general cognitive performance. Thus more specific and sensitive measures such as phonological skills, syntactic processing or semantics assessed at an older age, would benefit further work and help to understand how environmental factors in multi-lingual environments may modulate the neural basis of language acquisition.

The use of sedation, in order to minimise head movements during MRI acquisition, may confound fMRI data analysis of brain function. Avoiding sedation, however, increases the chances of discarding subjects, thus possibly biasing the dataset towards those neurological phenotypes that do not move. In-scanner head-motion has a widespread and general impact, hindering all kinds of neuroimaging acquisition and often forcing the researcher to discard large amounts of valuable data. Thus a trade-off between light-sedation and a strong statistical power deriving from a large cohort of subject was the rationale behind the work of this thesis. Furthermore the effect of sedation on neonatal brain functional connectivity can not be inferred from fMRI studies in adulthood as the chemical compounds used in human adults (or primates) are different; provide a much stronger sedation; and may therefore provide a different neural signature. Further computational studies highlighting the effect of sedation on infant brain function are needed.

Future directions

Below are summarised some possible directions for future study to extend upon the work presented in this thesis.

First of all, future work should exploit more sensitive and specific neurocognitive testing at different time-points, in order to assess subject-specific trajectories of neurolinguistic development. This would allow us to understand (in absence of overt patterns of brain injury or brain abnormalities) the major neural and environmental factors that cause preterm born children to develop normal rather then delayed linguistic capacities, or that lead to specific language impairment (SLI), or to general neurodevelopmental impairment.

A natural extension of the work of this thesis is the investigation of the whole-brain white-matter architecture and how it relates inter-subject difference in language development. In the adult brain several white-matter bundles such as the uncinate or the inferior-longitudinal fasciculus have been associated with language processing. However it cannot be ruled out the contribution of a more extended brain system that links those regions involved in auditory-verbal working memory or in the brain-wide semantic system. Combining high-angular resolution diffusion-weighted MRI at term-equivalent age with advance computational neuroimaging may shed new light on the brain-wide human architecture supporting the early acquisition of complex linguistic abilities.

Future research should also take into account the fact that language, although being special in its underlying fixed neural organisation, is only one facet of the complex human cognitive system. Therefore it shares the intrinsic property of the human brain being a dynamic and flexible organ. As noted in chapter 7, the dynamic properties of human brain functional connectivity are a key computational feature of both the mature and the infant human brain. In adulthood, integrated and segregated states of brain activity have been shown both at rest and during task. Whether these brain states of dynamic functional activity are already present around the time of normal birth or develop in parallel with the emergence of cognitive behaviour is

incompletely unknown. Future work should investigate how the emergence of this basic property of the human cognitive system may represent a neural basis for language and cognitive development.

Conclusions

The foremost goal of this thesis was to characterise the emergence of the language network in the neonatal human brain. To do so, I linked state-of-the-art methods of brain imaging with computational modelling. In addition to providing new mechanistic understanding of the neurophysiological processes mediating neurocognitive development, this approach can shed new light on the pathophysiology underlying neurodevelopmental difficulties in ex-preterm infants. Identifying early computational models of brain development and impairment may help the translation of research into clinical practice, identifying new targets for developing therapies and key windows for early intervention.

References

Aarnoudse-Moens CSH, Weisglas-Kuperus N, van Goudoever JB, Oosterlaan J. Meta-analysis of neurobehavioral outcomes in very preterm and/or very low birth weight children. Pediatrics 2009; 124: 717–728.

Abe K, Watanabe D. Songbirds possess the spontaneous ability to discriminate syntactic rules. 2011; 14: 1067–1074.

Abel S, Dressel K, Bitzer R, Kümmerer D, Mader I. The separation of processing stages in a lexical interference fMRI-paradigm. Neuroimage 2009

Aeby A, Liu Y, De Tiege X, Denolin V, David P, Balériaux D, et al. Maturation of thalamic radiations between 34 and 41 weeks' gestation: a combined voxel-based study and probabilistic tractography with diffusion tensor imaging. Am. J. Neuroradiol. 2009; 30: 1780–1786.

Agnew Z, McGettigan C, Scott S. Discriminating between auditory and motor cortical responses to speech and nonspeech mouth sounds. J. Cogn. Neurosci. 2011

Ahmad Z, Balsamo L, Sachs B, Xu B, Gaillard W. Auditory comprehension of language in young children Neural networks identified with fMRI. Neurology 2003

Ajayi-Obe M, Saeed N, Cowan FM, Rutherford MA, Edwards AD. Reduced development of cerebral cortex in extremely preterm infants. Lancet 2000; 356: 1162–1163.

Alario F, Chainay H, Lehericy S, Cohen L. The role of the supplementary motor area (SMA) in word production. Brain Res. 2006

Aleman A, Formisano E, Koppenhagen H. The functional neuroanatomy of metrical stress evaluation of perceived and imagined spoken words. Cerebral 2005

Alexander DC. Multiple‐Fiber Reconstruction Algorithms for Diffusion MRI. Ann. N. Y. Acad. Sci. 2005; 1064: 113–133.

Alexander MP, Naeser MA, Palumbo CL. Correlations of subcortical lesions sites and aphasia profiles. Brain 1987; 110: 961–988.

Allen E a., Damaraju E, Plis SM, Erhardt EB, Eichele T, Calhoun VD. Tracking whole-brain connectivity dynamics in the resting state. Cereb. cortex 2012; 24: bhs352.

Allen MC. Neurodevelopmental outcomes of preterm infants. Curr. Opin. Neurol. 2008; 21: 123–128.

Allendoerfer KL, Shatz CJ. The subplate, a transient neocortical structure: its role in the development of connections between thalamus and cortex. Annu. Rev. Neurosci. 1994; 17: 185–218.

Allin M, Walshe M, Fern A, Nosarti C, Cuddy M, Rifkin L, et al. Cognitive maturation in preterm and term born adolescents. J. Neurol. Neurosurg. Psychiatry 2008; 79: 381–386.

Amato M, Fauchere JC, Hermann Jr U. Coagulation Abnormalities in Low Birth Weight Infants with Peri-lntraventricular Hemorrhage. Neuropediatrics 1988; 19: 154–157.

Ames A. CNS energy metabolism as related to function. Brain Res. Rev. 2000; 34: 42–68.

Ananth C V, Misra DP, Demissie K, Smulian JC. Rates of preterm delivery among Black women and White women in the United States over two decades: an age-

period-cohort analysis. Am. J. Epidemiol. 2001; 154: 657–665.

Anderson PJ, Doyle LW. Executive functioning in school-aged children who were born very preterm or with extremely low birth weight in the 1990s. Pediatrics 2004; 114: 50–57.

Andersson JLR, Skare S, Ashburner J. How to correct susceptibility distortions in spin-echo echo-planar images: application to diffusion tensor imaging. Neuroimage 2003; 20: 870–888.

Andersson JLR, Sotiropoulos SN. Non-parametric representation and prediction of single-and multi-shell diffusion-weighted MRI data using Gaussian processes. Neuroimage 2015; 122: 166–176.

Andersson JLR, Sotiropoulos SN. An integrated approach to correction for off-resonance effects and subject movement in diffusion MR imaging. Neuroimage 2016; 125: 1063–1078.

Andreatta R, Stemple J, Joshi A, Jiang Y. Task-related differences in temporo-parietal cortical activation during human phonatory behaviors. Neurosci. Lett. 2010

Anjari M, Srinivasan L, Allsop JM, Hajnal J V., Rutherford MA, Edwards AD, et al. Diffusion tensor imaging with tract-based spatial statistics reveals local white matter abnormalities in preterm infants. Neuroimage 2007; 35: 1021–1027.

Armstrong D, Norman MG. Periventricular leucomalacia in neonates complications and sequelae. Arch. Dis. Child. 1974; 49: 367–375.

Armstrong E, Schleicher A, Omran H, Curtis M, Zilles K. The ontogeny of human gyrification. Cereb. cortex 1995; 5: 56–63.

Assaf Y, Freidlin RZ, Rohde GK, Basser PJ. New modeling and experimental framework to characterize hindered and restricted water diffusion in brain white

matter. Magn. Reson. Med. 2004; 52: 965–978.

Attwell D, Buchan AM, Charpak S, Lauritzen M, MacVicar BA, Newman EA. Glial and neuronal control of brain blood flow. Nature 2010; 468: 232–243.

Attwell D, Iadecola C. The neural basis of functional brain imaging signals. Trends Neurosci. 2002; 25: 621–625.

Attwell D, Laughlin SB. An energy budget for signaling in the grey matter of the brain. J. Cereb. Blood Flow Metab. 2001; 21: 1133–1145.

Avants B, Libon D, Rascovsky K, Boller A. Sparse canonical correlation analysis relates network-level atrophy to multivariate cognitive measures in a neurodegenerative population. Neuroimage 2014

Avants BB, Epstein CL, Grossman M, Gee JC. Symmetric diffeomorphic image registration with cross-correlation: evaluating automated labeling of elderly and neurodegenerative brain. Med. Image Anal. 2008; 12: 26–41.

Awad M, Warren JE, Scott SK, Turkheimer FE, Wise RJS. A common system for the comprehension and production of narrative speech. J. Neurosci. 2007; 27: 11455–11464.

Bach M, Laun FB, Leemans A, Tax CMWW, Biessels GJ, Stieltjes B, et al. Methodological considerations on tract-based spatial statistics (TBSS). Neuroimage 2014; 100: 358–369.

Bada HS, Korones SB, Perry EH, Arheart KL, Ray JD, Pourcyrous M, et al. Mean arterial blood pressure changes in premature infants and those at risk for intraventricular hemorrhage. J. Pediatr. 1990; 117: 607–614.

Baddeley A. Working memory: looking back and looking forward. Nat. Rev. Neurosci. 2003; 4: 829–839.

Baddeley A, Gathercole S, Papagno C. The Phonological Loop as a Language Learning Device. Psychol. Rev. 1998; 105: 158–173.

Baker AP, Brookes MJ, Rezek IA, Smith SM, Behrens T, Smith PJP, et al. Fast transient networks in spontaneous human brain activity. Elife 2014; 3: e01867.

Baldoli C, Scola E, Della Rosa PA, Pontesilli S, Longaretti R, Poloniato A, et al. Maturation of preterm newborn brains: a fMRI-DTI study of auditory processing of linguistic stimuli and white matter development. Brain Struct. Funct. 2015; 220: 3733–51.

Ball G, Aljabar P, Arichi T, Tusor N, Cox D, Merchant N, et al. Machine-learning to characterise neonatal functional connectivity in the preterm brain. Neuroimage 2016; 124: 267–275.

Ball G, Aljabar P, Zebari S, Tusor N, Arichi T, Merchant N, et al. Rich-club organization of the newborn human brain. Proc. Natl. Acad. Sci. U. S. A. 2014; 111: 7456–61.

Ball G, Boardman JP, Rueckert D, Aljabar P, Arichi T, Merchant N, et al. The effect of preterm birth on thalamic and cortical development. Cereb. Cortex 2012; 22: 1016–1024.

Ball G, Counsell SJ, Anjari M, Merchant N, Arichi T, Doria V, et al. An optimised tract-based spatial statistics protocol for neonates: applications to prematurity and chronic lung disease. Neuroimage 2010; 53: 94–102.

Ball G, Pazderova L, Chew A, Tusor N, Merchant N, Arichi T, et al. Thalamocortical Connectivity Predicts Cognition in Children Born Preterm. Cereb. Cortex 2015: 1–9.

Ball G, Srinivasan L, Aljabar P, Counsell SJ, Durighel G, Hajnal J V, et al.

Development of cortical microstructure in the preterm human brain. Proc. Natl. Acad. Sci. U. S. A. 2013; 110: 9541–6.

Bandettini PA, Wong EC, Hinks RS, Tikofsky RS, Hyde JS. Time course EPI of human brain function during task activation. Magn. Reson. Med. 1992; 25: 390–397.

Banerjee O, Ghaoui L El, d'Aspremont A, Natsoulis G. Convex optimization techniques for fitting sparse Gaussian graphical models. In: Proceedings of the 23rd international conference on Machine learning - ICML '06. New York, New York, USA: ACM Press; 2006. p. 89–96.

Banker BQ, Larroche J-C. Periventricular leukomalacia of infancy: a form of neonatal anoxic encephalopathy. Arch. Neurol. 1962; 7: 386–410.

Barch DM, Burgess GC, Harms MP, Petersen SE, Schlaggar BL, Corbetta M, et al. Function in the human connectome: task-fMRI and individual differences in behavior. Neuroimage 2013; 80: 169–89.

Barre N, Morgan A, Doyle LW, Anderson PJ. Language abilities in children who were very preterm and/or very low birth weight: a meta-analysis. J. Pediatr. 2011; 158: 766–774.

Bassan H, Limperopoulos C, Visconti K, Mayer DL, Feldman HA, Avery L, et al. Neurodevelopmental outcome in survivors of periventricular hemorrhagic infarction. Pediatrics 2007; 120: 785–792.

Basser PJ, Mattiello J, LeBihan D. MR diffusion tensor spectroscopy and imaging. Biophys. J. 1994; 66: 259.

Bassett D, Wymbs N, Porter M. Dynamic reconfiguration of human brain networks during learning. Proc. 2011

Bassett D, Yang M, Wymbs N, Grafton S. Learning-induced autonomy of

sensorimotor systems. Nat. Neurosci. 2015

Bassett DS, Sporns O. Network neuroscience. Nat. Neurosci. 2017; 20: 353–364.

Bassi L, Ricci D, Volzone A, Allsop JM, Srinivasan L, Pai A, et al. Probabilistic diffusion tractography of the optic radiations and visual function in preterm infants at term equivalent age. Brain 2008; 131: 573–582.

Bates E, Roe K. A vJ Language Development in Children with Unilateral Brain Injury. Handb. Dev. Cogn. Neurosci. 2001: 281.

Battin M, Rutherford MA. Magnetic resonance imaging of the brain in preterm infants: 24 weeks' gestation to term. MRI neonatal brain. Saunders, London 2002: 25–49.

Bax MCO. Terminology and classification of cerebral palsy. Dev. Med. Child Neurol. 1964; 6: 295–297.

Bayley N. Bayley scales of infant and toddler development. 2006.

Beaulieu C. The basis of anisotropic water diffusion in the nervous system–a technical review. NMR Biomed. 2002; 15: 435–455.

Beck S, Wojdyla D, Say L, Betran AP, Merialdi M, Requejo JH, et al. The worldwide incidence of preterm birth: a systematic review of maternal mortality and morbidity. Bull. World Health Organ. 2010; 88: 31–38.

Beckmann CF. Modelling with independent components. Neuroimage 2012; 62: 891–901.

Beckmann CF, DeLuca M, Devlin JT, Smith SM. Investigations into resting-state connectivity using independent component analysis. Philos. Trans. R. Soc. London B Biol. Sci. 2005; 360: 1001–1013.

Beckmann CF, Smith SM. Probabilistic Independent Component Analysis for

Functional Magnetic Resonance Imaging. IEEE Trans. Med. Imaging 2004; 23: 137–152.

Beckmann, Mackay, Filippini, Smith. Group comparison of resting-state FMRI data using multi-subject ICA and dual regression. Neuroimage 2009; 47: S148.

Behrens TEJ, Berg HJ, Jbabdi S, Rushworth MFS, Woolrich MW. Probabilistic diffusion tractography with multiple fibre orientations: What can we gain? Neuroimage 2007; 34: 144–155.

Behrens TEJ, Johansen-Berg H, Woolrich MW, Smith SM, Wheeler-Kingshott CAM, Boulby PA, et al. Non-invasive mapping of connections between human thalamus and cortex using diffusion imaging. Nat. Neurosci. 2003; 6: 750–757.

Behrens TEJ, Woolrich MW, Jenkinson M, Johansen-Berg H, Nunes RG, Clare S, et al. Characterization and propagation of uncertainty in diffusion-weighted MR imaging. Magn. Reson. Med. 2003; 50: 1077–1088.

Benasich A, Choudhury N. Plasticity in developing brain: Active auditory exposure impacts prelinguistic acoustic mapping. J. 2014

Benes FM. Myelination of cortical-hippocampal relays during late adolescence. Schizophr. Bull. 1989; 15: 585.

Bennett EP, Mandel U, Clausen H, Gerken TA, Fritz TA, Tabak LA. Control of mucin-type O-glycosylation: a classification of the polypeptide GalNAc-transferase gene family. Glycobiology 2012; 22: 736–756.

Benson DF, Sheremata WA, Bouchard R, Segarra JM, Price D, Geschwind N. Conduction aphasia: a clinicopathological study. Arch. Neurol. 1973; 28: 339.

Benson R, Richardson M, Whalen D, Lai S. Phonetic processing areas revealed by sinewave speech and acoustically similar non-speech. Neuroimage 2006

Berl M, Duke E, Mayo J, Rosenberger L. Functional anatomy of listening and reading comprehension during development. Brain Lang. 2010

Berl MMM, Mayo J, Parks EEN, Rosenberger LR, Vanmeter J, Ratner NB, et al. Regional differences in the developmental trajectory of lateralization of the language network. Hum. Brain Mapp. 2014; 35: 270–284.

Berman JI, Glass HC, Miller SP, Mukherjee P, Ferriero DM, Barkovich AJ, et al. Quantitative fiber tracking analysis of the optic radiation correlated with visual performance in premature newborns. Am. J. Neuroradiol. 2009; 30: 120–124.

Berman JI, Mukherjee P, Partridge SC, Miller SP, Ferriero DM, Barkovich AJ, et al. Quantitative diffusion tensor MRI fiber tractography of sensorimotor white matter development in premature infants. Neuroimage 2005; 27: 862–871.

Bernard C, Gervain J. Prosodic cues to word order: what level of representation? 2012

Berwick RC, Chomsky N. The biolinguistic program: The current state of its development. biolinguistic Enterp. New Perspect. Evol. Nat. Hum. Lang. Fac. 2011: 19–41.

Berwick RC, Friederici AD, Chomsky N, Bolhuis JJ. Evolution, brain, and the nature of language. Trends Cogn. Sci. 2013; 17: 89–98.

Betzel RF, Bassett DS. Multi-scale brain networks. Neuroimage 2016; 7: 446–451.

Bhutta AT, Cleves MA, Casey PH, Cradock MM, Anand KJS. Cognitive and behavioral outcomes of school-aged children who were born preterm: a meta-analysis. Jama 2002; 288: 728–737.

Le Bihan D, Breton E, Lallemand D, Grenier P, Cabanis E, Laval-Jeantet M. MR imaging of intravoxel incoherent motions: application to diffusion and perfusion in

neurologic disorders. Radiology 1986; 161: 401–407.

Le Bihan D, Poupon C, Amadon A, Lethimonnier F. Artifacts and pitfalls in diffusion MRI. J. Magn. Reson. Imaging 2006; 24: 478–488.

Bilenko N, Grindrod C, Myers E. Neural correlates of semantic competition during processing of ambiguous words. J. Cogn. 2009

Binder JR, Desai RH. The Neurobiology of Semantic Memory Jeffrey. Trends Cogn. Sci. 2011; 15: 527–536.

Binder JR, Desai RH, Graves WW, Conant LL. Where is the semantic system? A critical review and meta-analysis of 120 functional neuroimaging studies. Cereb. Cortex 2009; 19: 2767–96.

Bishop DVM. Cerebral Asymmetry and Language Cerebral Asymmetry and Language. 2013; 340

Biswal B, Zerrin Yetkin F, Haughton VM, Hyde JS. Functional connectivity in the motor cortex of resting human brain using echo-planar mri. Magn. Reson. Med. 1995; 34: 537–541.

Biswal BB, Mennes M, Zuo X-N, Gohel S, Kelly C, Smith SM, et al. Toward discovery science of human brain function. Proc. Natl. Acad. Sci. U. S. A. 2010; 107: 4734–4739.

Blankenship AG, Feller MB. Mechanisms underlying spontaneous patterned activity in developing neural circuits. Nat. Rev. Neurosci. 2010; 11: 18–29.

Blasi A, Mercure E, Lloyd-Fox S, Thomson A, Brammer M, Sauter D, et al. Early specialization for voice and emotion processing in the infant brain. Curr. Biol. 2011; 21: 1220–1224.

Bloch F. Nuclear induction. Phys. Rev. 1946; 70: 460.

Blondel B, Kaminski M. Trends in the occurrence, determinants, and consequences of multiple births. In: Seminars in perinatology. Elsevier; 2002. p. 239–249.

Blondel VD, Guillaume J-L, Lambiotte R, Lefebvre E. Fast unfolding of communities in large networks. J. Stat. Mech. Theory Exp. 2008; 10008: 6.

Boardman JP, Counsell SJ, Rueckert D, Hajnal J V, Bhatia KK, Srinivasan L, et al. Early growth in brain volume is preserved in the majority of preterm infants. Ann. Neurol. 2007; 62: 185–192.

Boardman JP, Counsell SJ, Rueckert D, Kapellou O, Bhatia KK, Aljabar P, et al. Abnormal deep grey matter development following preterm birth detected using deformation-based morphometry. Neuroimage 2006; 32: 70–78.

Boardman JP, Craven C, Valappil S, Counsell SJ, Dyet LE, Rueckert D, et al. A common neonatal image phenotype predicts adverse neurodevelopmental outcome in children born preterm. Neuroimage 2010; 52: 409–414.

Booth J, Burman D, Meyer J. Relation between brain activation and lexical performance. Hum. brain 2003

Botting N, Powls A, Cooke RWI, Marlow N. Attention deficit hyperactivity disorders and other psychiatric outcomes in very low birthweight children at 12 years. J. Child Psychol. Psychiatry 1997; 38: 931–941.

Bracewell M, Marlow N. Patterns of motor disability in very preterm children. Ment. Retard. Dev. Disabil. Res. Rev. 2002; 8: 241–248.

Brauer J, Anwander A, Friederici AD. Neuroanatomical prerequisites for language functions in the maturing brain. Cereb. Cortex 2011; 21: 459–466.

Brauer J, Anwander A, Perani D, Friederici AD. Dorsal and ventral pathways in language development. Brain Lang. 2013; 127: 289–295.

Braun U, Schäfer A, Walter H, Erk S, Romanczuk-Seiferth N, Haddad L, et al. Dynamic reconfiguration of frontal brain networks during executive cognition in humans. Proc. Natl. Acad. Sci. 2015; 112: 11678–11683.

Breakspear M. Dynamic models of large-scale brain activity. Nat. Neurosci. 2017; 20: 340–352.

Breslau N, Chilcoat H, DelDotto J, Andreski P, Brown G. Low birth weight and neurocognitive status at six years of age. Biol. Psychiatry 1996; 40: 389–397.

Breslau N, DelDotto JE, Brown GG, Kumar S, Ezhuthachan S, Hufnagle KG, et al. A gradient relationship between low birth weight and IQ at age 6 years. Arch. Pediatr. Adolesc. Med. 1994; 148: 377–383.

Bressler SL, Tognoli E. Operational principles of neurocognitive networks. Int. J. Psychophysiol. 2006; 60: 139–148.

Briscoe J, Gathercole SE, Marlow N. Short-term memory and language outcomes after extreme prematurity at birth. J. Speech, Lang. Hear. Res. 1998; 41: 654–666.

Britton B, Blumstein S, Myers E, Grindrod C. The role of spectral and durational properties on hemispheric asymmetries in vowel perception. Neuropsychologia 2009

Brookes MJ, O'Neill GC, Hall EL, Woolrich MW, Baker A, Palazzo Corner S, et al. Measuring temporal, spectral and spatial changes in electrophysiological brain network connectivity. Neuroimage 2014; 91: 282–299.

Brown TT, Lugar HM, Coalson RS, Miezin FM, Petersen SE, Schlaggar BL. Developmental changes in human cerebral functional organization for word generation. Cereb. Cortex 2005; 15: 275–90.

de Bruïne FT, van Wezel-Meijler G, Leijser LM, van den Berg-Huysmans AA, van Steenis A, van Buchem MA, et al. Tractography of developing white matter of the

internal capsule and corpus callosum in very preterm infants. Eur. Radiol. 2011; 21: 538–547.

Buchsbaum BR, D'Esposito M. The search for the phonological store: from loop to convolution. Cogn. Neurosci. J. 2008; 20: 762–778.

Buchsbaum BR, Olsen RKR, Koch P, Berman KKF. Human dorsal and ventral auditory streams subserve rehearsal-based and echoic processes during verbal working memory. Neuron 2005; 48: 687–697.

Bullmore E, Bullmore E, Sporns O, Sporns O. Complex brain networks: graph theoretical analysis of structural and functional systems. Nat Rev Neurosci 2009; 10: 186–198.

Bullmore E, Sporns O. The economy of brain network organization. Nat. Rev. Neurosci. 2012; 13: 336–349.

Bunzeck N, Wuestenberg T, Lutz K, Heinze H. Scanning silence: mental imagery of complex sounds. Neuroimage 2005

Burke C, Morrison JJ. Perinatal factors and preterm delivery in an Irish obstetric population. J. Perinat. Med. 2000; 28: 49–53.

Burton M, LoCasto P, Krebs-Noble D, Gullapalli R. A systematic investigation of the functional neuroanatomy of auditory and visual phonological processing. Neuroimage 2005

Burton M, Noll D, Small S. The anatomy of auditory word processing: individual variability. Brain Lang. 2001

Buxton RB. Introduction to functional magnetic resonance imaging: principles and techniques. Cambridge university press; 2009.

Buxton RB, Uludağ K, Dubowitz DJ, Liu TT. Modeling the hemodynamic response

to brain activation. Neuroimage 2004; 23: S220–S233.

Buxton RB, Wong EC, Frank LR. Dynamics of blood flow and oxygenation changes during brain activation: The balloon model. Magn. Reson. Med. 1998; 39: 855–864.

Bystron I, Blakemore C, Rakic P. Development of the human cerebral cortex: Boulder Committee revisited. Nat. Rev. Neurosci. 2008; 9: 110–122.

Calhoun VD, Miller R, Pearlson G, Adalı T. The Chronnectome: Time-Varying Connectivity Networks as the Next Frontier in fMRI Data Discovery. Neuron 2014; 84: 262–274.

Caravale B, Tozzi C, Albino G, Vicari S. Cognitive development in low risk preterm infants at 3–4 years of life. Arch. Dis. Childhood-Fetal Neonatal Ed. 2005; 90: F474–F479.

Catani M, Allin MPG, Husain M, Pugliese L, Mesulam MM, Murray RM, et al. Symmetries in human brain language pathways correlate with verbal recall. Proc. Natl. Acad. Sci. 2007; 104: 17163–17168.

Catani M, Howard RJ, Pajevic S, Jones DK. Virtual in Vivo Interactive Dissection of White Matter Fasciculi in the Human Brain. Neuroimage 2002; 17: 77–94.

Catani M, Jones DK, Ffytche DH. Perisylvian language networks of the human brain. Ann. Neurol. 2005; 57: 8–16.

Cauli B, Hamel E. Revisiting the role of neurons in neurovascular coupling. Front. Neuroenergetics 2010; 2

Chang C, Liu Z, Chen MC, Liu X, Duyn JH. EEG correlates of time-varying BOLD functional connectivity. Neuroimage 2013; 72: 227–236.

Chang CC, Chow CC, Tellier LCAM, Vattikuti S, Purcell SM, Lee JJ. Second-generation PLINK: rising to the challenge of larger and richer datasets. ArXiv e-

prints 2014

Chang EF, Niziolek CA, Knight RT, Nagarajan SS, Houde JF. Human cortical sensorimotor network underlying feedback control of vocal pitch. Proc. Natl. Acad. Sci. 2013; 110: 2653–2658.

Chen C-H, Fiecas M, Gutierrez ED, Panizzon MS, Eyler LT, Vuoksimaa E, et al. Genetic topography of brain morphology. Proc. Natl. Acad. Sci. 2013; 110: 17089–17094.

Chen Y, Guo W, Zeng Q, He G, Vemuri B, Liu Y. Recovery of intra-voxel structure from HARD DWI. In: Biomedical Imaging: Nano to Macro, 2004. IEEE International Symposium on. IEEE; 2004. p. 1028–1031.

Cheng Y, Quinn JF, Weiss LA. An eQTL mapping approach reveals that rare variants in the SEMA5A regulatory network impact autism risk. Hum. Mol. Genet. 2013; 22: 2960–2972.

Chi JG, Dooling EC, Gilles FH. Gyral development of the human brain. Ann. Neurol. 1977; 1: 86–93.

Chomsky N. A review of BF Skinner's Verbal Behavior. Language (Baltim). 1959; 35: 26–58.

Chomsky N. Cartesian Linguistics: A Chaper in the History of Rationalist Thought. Royal Blind Society of New South Wales.; 1966.

Chomsky N. The minimalist program. Cambridge Univ Press; 1995.

Chomsky N. Approaching UG from below. Interfaces+ recursion= Lang. 2007; 89: 1–30.

Christoffels I, Formisano E. Neural correlates of verbal feedback processing: an fMRI study employing overt speech. Hum. brain 2007

Christoffels I, Ven V van de, Waldorp L. The sensory consequences of speaking: parametric neural cancellation during speech in auditory cortex. PLoS 2011

Ciccarelli O, Catani M, Johansen-Berg H, Clark C, Thompson A. Diffusion-based tractography in neurological disorders: concepts, applications, and future developments. Lancet Neurol. 2008; 7: 715–727.

Cioni G, Fazzi B, Coluccini M, Bartalena L, Boldrini A, van Hof-van Duin J. Cerebral visual impairment in preterm infants with periventricular leukomalacia. Pediatr. Neurol. 1997; 17: 331–338.

Cocchi L, Zalesky A, Fornito A, Mattingley JB. Dynamic cooperation and competition between brain systems during cognitive control. Trends Cogn. Sci. 2013; 17: 493–501.

Cole M, Bassett D, Power J, Braver T. Intrinsic and task-evoked network architectures of the human brain. Neuron 2014

Conturo TE, Lori NF, Cull TS, Akbudak E, Snyder AZ, Shimony JS, et al. Tracking neuronal fiber pathways in the living human brain. Proc. Natl. Acad. Sci. 1999; 96: 10422–10427.

Counsell SJ, Allsop JM, Harrison MC, Larkman DJ, Kennea NL, Kapellou O, et al. Diffusion-weighted imaging of the brain in preterm infants with focal and diffuse white matter abnormality. Pediatrics 2003; 112: 1–7.

Counsell SJ, Dyet LE, Larkman DJ, Nunes RG, Boardman JP, Allsop JM, et al. Thalamo-cortical connectivity in children born preterm mapped using probabilistic magnetic resonance tractography. Neuroimage 2007; 34: 896–904.

Counsell SJ, Edwards AD, Chew ATM, Anjari M, Dyet LE, Srinivasan L, et al. Specific relations between neurodevelopmental abilities and white matter

microstructure in children born preterm. Brain 2008; 131: 3201–3208.

Craddock RC, James GA, Holtzheimer PE, Hu XP, Mayberg HS. A whole brain fMRI atlas generated via spatially constrained spectral clustering. Hum. Brain Mapp. 2012; 33: 1914–1928.

Crawford C, Greaves E. A comparison of commonly used socioeconomic indicators: their relationship to educational disadvantage and relevance to Teach First. IFS Reports, Institute for Fiscal Studies; 2013.

Croft L, Baldeweg T, Sepeta L, Zimmaro L, Berl M. Vulnerability of the ventral language network in children with focal epilepsy. Brain 2014

Curtis C, D'Esposito M. Persistent activity in the prefrontal cortex during working memory. Trends Cogn. Sci. 2003

Cusack R, Ball G, Smyser C. A neural window on the emergence of cognition. Ann. New 2016

Damasio H, Damasio AR. The anatomical basis of conduction aphasia. Brain 1980; 103: 337–350.

Damoiseaux JS, Beckmann CF, Arigita EJS, Barkhof F, Scheltens P, Stam CJ, et al. Reduced resting-state brain activity in the 'default network' in normal aging. Cereb. cortex 2008; 18: 1856–1864.

Damoiseaux JS, Rombouts S, Barkhof F, Scheltens P, Stam CJ, Smith SM, et al. Consistent resting-state networks across healthy subjects. Proc. Natl. Acad. Sci. 2006; 103: 13848–13853.

Davis M, Coleman M, Absalom A. Dissociating speech perception and comprehension at reduced levels of awareness. Proc. 2007

de Pasquale F, Della Penna S, Snyder AZ, Marzetti L, Pizzella V, Romani GL, et al.

A Cortical Core for Dynamic Integration of Functional Networks in the Resting Human Brain. Neuron 2012; 74: 753–764.

Deco G, Jirsa V, McIntosh AR, Sporns O, Kötter R, Kotter R. Key role of coupling, delay, and noise in resting brain fluctuations. Proc. Natl. Acad. Sci. 2009; 106: 10302–10307.

Deco G, Jirsa VK, McIntosh AR. Emerging concepts for the dynamical organization of resting-state activity in the brain. Nat. Rev. Neurosci. 2011; 12: 43–56.

Deco G, Tononi G, Boly M, Kringelbach ML. Rethinking segregation and integration: contributions of whole-brain modelling. Nat. Rev. Neurosci. 2015; 16: 430–439.

Dehaene-Lambertz G, Dehaene S. Speed and cerebral correlates of syllable discrimination in infants. Nature 1994; 370: 292–295.

Dehaene-Lambertz G, Dehaene S, Hertz-Pannier L. Functional neuroimaging of speech perception in infants. Science 2002; 298: 2013–2015.

Dehaene-Lambertz G, Hertz-Pannier L, Dubois J, Mériaux S, Roche A, Sigman M, et al. Functional organization of perisylvian activation during presentation of sentences in preverbal infants. Proc. Natl. Acad. Sci. 2006; 103: 14240–14245.

Dehaene-Lambertz G, Montavont A, Jobert A, Allirol L, Dubois J, Hertz-Pannier L, et al. Language or music, mother or Mozart? Structural and environmental influences on infants' language networks. Brain Lang. 2010; 114: 53–65.

Dehaene-Lambertz G, Pena M. Electrophysiological evidence for automatic phonetic processing in neonates. Neuroreport 2001; 12: 3155–3158.

Dehaene-Lambertz G, Spelke ES. The Infancy of the Human Brain. Neuron 2015; 88: 93–109.

Delobel-Ayoub M, Arnaud C, White-Koning M, Casper C, Pierrat V, Garel M, et al. Behavioral problems and cognitive performance at 5 years of age after very preterm birth: the EPIPAGE Study. Pediatrics 2009; 123: 1485–1492.

Demirtaş M, Tornador C, Falcón C. Dynamic functional connectivity reveals altered variability in functional connectivity among patients with major depressive disorder. Hum. brain 2016

Deoni SCL, Mercure E, Blasi A, Gasston D, Thomson A, Johnson M, et al. Mapping infant brain myelination with magnetic resonance imaging. J. Neurosci. 2011; 31: 784–791.

Dhavan R, Tsai L-H. A decade of CDK5. Nat. Rev. Mol. cell Biol. 2001; 2: 749–759.

Dick AS, Tremblay P. Beyond the arcuate fasciculus: Consensus and controversy in the connectional anatomy of language. Brain 2012: aws222.

Dick F, Lee H, Nusbaum H, Price C. Auditory-motor expertise alters 'speech selectivity' in professional musicians and actors. Cereb. Cortex 2011

Doria V, Beckmann CF, Arichi T, Merchant N, Groppo M, Turkheimer FE, et al. Emergence of resting state networks in the preterm human brain. Proc. Natl. Acad. Sci. U. S. A. 2010; 107: 20015–20020.

Dubois J, Benders M, Borradori-Tolsa C, Cachia a., Lazeyras F, Ha-Vinh Leuchter R, et al. Primary cortical folding in the human newborn: An early marker of later functional development. Brain 2008; 131: 2028–2041.

Dubois J, Benders M, Cachia A, Lazeyras F, Ha-Vinh Leuchter R, Sizonenko S V., et al. Mapping the Early Cortical Folding Process in the Preterm Newborn Brain. Cereb. Cortex 2008; 18: 1444–1454.

Dubois J, Dehaene-Lambertz G, Kulikova S, Poupon C, Hüppi PS, Hertz-Pannier L. The early development of brain white matter: A review of imaging studies in fetuses, newborns and infants. Neurosci. (v Tisk. 2014; dostupné z: 1–24.

Dubois J, Hertz-Pannier L, Cachia a., Mangin JF, Le Bihan D, Dehaene-Lambertz G. Structural asymmetries in the infant language and sensori-motor networks. Cereb. Cortex 2009; 19: 414–423.

Dubois J, Poupon C, Thirion B, Simonnet H, Kulikova S, Leroy F, et al. Exploring the early organization and maturation of linguistic pathways in the human infant brain. Cereb. Cortex 2015: bhv082.

Dudink J, Buijs J, Govaert P, van Zwol AL, Conneman N, van Goudoever JB, et al. Diffusion tensor imaging of the cortical plate and subplate in very-low-birth-weight infants. Pediatr. Radiol. 2010; 40: 1397–1404.

Dyet LE, Kennea N, Counsell SJ, Maalouf EF, Ajayi-Obe M, Duggan PJ, et al. Natural history of brain lesions in extremely preterm infants studied with serial magnetic resonance imaging from birth and neurodevelopmental assessment. Pediatrics 2006; 118: 536–548.

Edden RA, Jones DK. Spatial and orientational heterogeneity in the statistical sensitivity of skeleton-based analyses of diffusion tensor MR imaging data. J. Neurosci. Methods 2011; 201: 213–219.

Eickhoff S, Heim S, Zilles K. A systems perspective on the effective connectivity of overt speech production. A Math. … 2009

Eikenes L, Løhaugen GC, Brubakk A-M, Skranes J, Håberg AK. Young adults born preterm with very low birth weight demonstrate widespread white matter alterations on brain DTI. Neuroimage 2011; 54: 1774–1785.

Eimas P. Auditory and phonetic coding of the cues for speech: Discrimination of the distinction by young infants. Percept. Psychophys. 1975

Eimas P, Siqueland E, Jusczyk P, Vigorito J. Speech perception in infants. Science 1971

Einstein A. Un the movement of small particles suspended in statiunary liquids required by the molecular-kinetic theory 0f heat. Ann. Phys 1905; 17: 549–560.

Elmer S, Meyer M, Jäncke L. Neurofunctional and behavioral correlates of phonetic and temporal categorization in musically trained and untrained subjects. Cereb. Cortex 2012

Enard W, Przeworski M, Fisher SE, Lai CSL, Wiebe V, Kitano T, et al. Molecular evolution of FOXP2, a gene involved in speech and language. Nature 2002; 418: 869–872.

Everts R, Lidzba K, Wilke M, Kiefer C. Strengthening of laterality of verbal and visuospatial functions during childhood and adolescence. Hum. brain 2009

Fair D, Brown T, Petersen S. A comparison of analysis of variance and correlation methods for investigating cognitive development with functional magnetic resonance imaging. Developmental 2006

Fazzi E, Orcesi S, Caffi L, Ometto A, Rondini G, Telesca C, et al. Neurodevelopmental outcome at 5-7 years in preterm infants with periventricular leukomalacia. Neuropediatrics 1994; 25: 134–139.

Feinberg DA, Moeller S, Smith SM, Auerbach E, Ramanna S, Glasser MF, et al. Multiplexed Echo Planar Imaging for Sub-Second Whole Brain FMRI and Fast Diffusion Imaging. PLoS One 2010; 5: e15710.

Fjell AM, Grydeland H, Krogsrud SK, Amlien I, Rohani DA, Ferschmann L, et al.

Development and aging of cortical thickness correspond to genetic organization patterns. Proc. Natl. Acad. Sci. 2015; 112: 15462–15467.

Forkel SJ, De Schotten MT, Dell'Acqua F, Kalra L, Murphy DGM, Williams SCR, et al. Anatomical predictors of aphasia recovery: A tractography study of bilateral perisylvian language networks. Brain 2014; 137: 2027–2039.

Fornito A, Zalesky A, Breakspear M. Graph analysis of the human connectome: promise, progress, and pitfalls. Neuroimage 2013; 80: 426–444.

Foster-Cohen SH, Friesen MD, Champion PR, Woodward LJ. High prevalence/low severity language delay in preschool children born very preterm. J. Dev. Behav. Pediatr. 2010; 31: 658–667.

Foulder-Hughes LA, Cooke RWI. Motor, cognitive, and behavioural disorders in children born very preterm. Dev. Med. Child Neurol. 2003; 45: 97–103.

Fox MD, Raichle ME. Spontaneous fluctuations in brain activity observed with functional magnetic resonance imaging. Nat. Rev. Neurosci. 2007; 8: 700–711.

Fox MD, Snyder AZ, Vincent JL, Corbetta M, Van Essen DC, Raichle ME. The human brain is intrinsically organized into dynamic, anticorrelated functional networks. Proc. Natl. Acad. Sci. U. S. A. 2005; 102: 9673–9678.

Fraisier V, Kasri A, Miserey-Lenkei S, Sibarita J-B, Nair D, Mayeux A, et al. C11ORF24 Is a Novel Type I Membrane Protein That Cycles between the Golgi Apparatus and the Plasma Membrane in Rab6-Positive Vesicles. PLoS One 2013; 8: e82223.

Fransson P, Åden U, Blennow M, Lagercrantz H. The functional architecture of the infant brain as revealed by resting-state fMRI. Cereb. Cortex 2011; 21: 145–154.

Fransson P, Skiöld B, Engström M, Hallberg B, Mosskin M, Åden U, et al.

Spontaneous Brain Activity in the Newborn Brain During Natural Sleep—An fMRI Study in Infants Born at Full Term. Pediatr. Res. 2009; 66: 301–305.

Fransson P, Skiold B, Horsch S, Nordell A, Blennow M, Lagercrantz H, et al. Resting-state networks in the infant brain. Proc. Natl. Acad. Sci. 2007; 104: 15531–15536.

Friederici A. The brain basis of language processing: from structure to function. Physiol. Rev. 2011

Friederici A, Bahlmann J, Heim S. The brain differentiates human and non-human grammars: functional localization and structural connectivity. Proc. 2006

Friederici A, Kotz S, Scott S. Disentangling syntax and intelligibility in auditory language comprehension. Hum. brain 2010

Friederici A, Makuuchi M, Bahlmann J. The role of the posterior superior temporal cortex in sentence comprehension. Neuroreport 2009

Friederici AD. The cortical language circuit: From auditory perception to sentence comprehension. Trends Cogn. Sci. 2012; 16: 262–268.

Friederici AD, Gierhan SM. The language network. Curr. Opin. Neurobiol. 2013; 23: 250–254.

Friederici AD, Mueller JL, Oberecker R. Precursors to natural grammar learning: preliminary evidence from 4-month-old infants. PLoS One 2011; 6: e17920–e17920.

Friedman J, Hastie T, Tibshirani R. Sparse inverse covariance estimation with the graphical lasso. Biostatistics 2008; 9: 432–441.

Friedmann N, Rusou D. Critical period for first language: the crucial role of language input during the first year of life. Curr. Opin. Neurobiol. 2015; 35: 27–34.

Friston KJ. Functional and effective connectivity in neuroimaging: a synthesis. Hum.

Brain Mapp. 1994; 2: 56–78.

Friston KJ. Functional and effective connectivity: a review. Brain Connect. 2011; 1: 13–36.

Friston KJ, Ashburner J, Frith CD, Poline J-B, Heather JD, Frackowiak RSJ. Spatial registration and normalization of images. Hum. Brain Mapp. 1995; 3: 165–189.

Friston KJ, Jezzard P, Turner R. Analysis of functional MRI time-series. Hum. Brain Mapp. 1994; 1: 153–171.

Friston KJ, Li B, Daunizeau J, Stephan KE. Network discovery with DCM. Neuroimage 2011; 56: 1202–1221.

Friston KJ, Williams S, Howard R, Frackowiak RSJ, Turner R. Movement-Related effects in fMRI time-series. Magn. Reson. Med. 1996; 35: 346–355.

Galantucci S, Tartaglia M, Wilson S, Henry M. White matter damage in primary progressive aphasias: a diffusion tensor tractography study. Brain 2011

Gardner MO, Goldenberg RL, Cliver SP, Tucker JM, Nelson KG, Copper RL. The origin and outcome of preterm twin pregnancies. Obstet. Gynecol. 1995; 85: 553–557.

Garrity AG, Pearlson GD, McKiernan K, Lloyd D, Kiehl KA, Calhoun VD. Aberrant 'default mode' functional connectivity in schizophrenia. Am. J. Psychiatry 2007; 164: 450–457.

Gervain J, Macagno F, Cogoi S. The neonate brain detects speech structure. Proc. 2008

Geschwind N. Disconnexion syndromes in animals and man. Brain 1965; 88: 585.

Gibbons JD, Chakraborti S. Nonparametric Statistical Inference. In: International Encyclopedia of Statistical Science. Berlin, Heidelberg: Springer Berlin Heidelberg;

2011. p. 977–979.

Gilles FH, Leviton A, Dooling EC. The developing human brain: growth and epidemiologic neuropathology. Butterworth-Heinemann; 2013.

Giraud A, Kell C, Thierfelder C, Sterzer P. Contributions of sensory input, auditory search and verbal comprehension to cortical activity during speech processing. Cerebral 2004

Giraud A, Price C. The constraints functional neuroimaging places on classical models of auditory word processing. J. Cogn. Neurosci. 2001

Glasser MF, Coalson T, Robinson E, Hacker C, Harwell J, Yacoub E, et al. A Multi-modal parcellation of human cerebral cortex. Nature 2015

Goldenberg RL, Culhane JF, Iams JD, Romero R. Epidemiology and causes of preterm birth. Lancet 2008; 371: 75–84.

Goldenberg RL, Rouse DJ. Prevention of premature birth. N. Engl. J. Med. 1998; 339: 313–320.

Gómez DM, Berent I, Benavides-Varela S, Bion RAH, Cattarossi L, Nespor M, et al. Language universals at birth. Proc. Natl. Acad. Sci. U. S. A. 2014; 111: 5837–41.

Goyen T-A, Lui K. Developmental coordination disorder in 'apparently normal' schoolchildren born extremely preterm. Arch. Dis. Child. 2009; 94: 298–302.

Goyen T, Lui K, Woods R. Visual‐motor, visual‐perceptual, and fine motor outcomes in very‐low‐birthweight children at 5 years. Dev. Med. Child Neurol. 1998; 40: 76–81.

Gozzo Y, Vohr B, Lacadie C, Hampson M, Katz KH, Maller-Kesselman J, et al. Alterations in neural connectivity in preterm children at school age. Neuroimage 2009; 48: 458–463.

de Graaf-Peters VB, Hadders-Algra M. Ontogeny of the human central nervous system: what is happening when? Early Hum. Dev. 2006; 82: 257–266.

Graves W, Grabowski T, Mehta S. A neural signature of phonological access: distinguishing the effects of word frequency from familiarity and length in overt picture naming. J. Cogn. 2007

Greicius M. Resting-state functional connectivity in neuropsychiatric disorders. Curr. Opin. Neurol. 2008; 21: 424–430.

Greicius MD, Krasnow B, Reiss AL, Menon V. Functional connectivity in the resting brain: a network analysis of the default mode hypothesis. Proc. Natl. Acad. Sci. 2003; 100: 253–258.

Griffanti L, Salimi-Khorshidi G, Beckmann CF, Auerbach EJ, Douaud G, Sexton CE, et al. ICA-based artefact removal and accelerated fMRI acquisition for improved resting state network imaging. Neuroimage 2014; 95: 232–247.

Groppo M, Ricci D, Bassi L, Merchant N, Doria V, Arichi T, et al. Development of the optic radiations and visual function after premature birth. Cortex 2014; 56: 30–37.

Groves AR, Smith SM, Fjell AM, Tamnes CK, Walhovd KB, Douaud G, et al. Benefits of multi-modal fusion analysis on a large-scale dataset: life-span patterns of inter-subject variability in cortical morphometry and white matter microstructure. Neuroimage 2012; 63: 365–380.

Groves AR, Westlye LT, Smith SM, Woolrich MW. Linked ICA of multiple WM & GM measures reveals multimodal components with distinct age profiles Multimodal MRI group studies. Brain 2011; 9: 177404.

Gu S, Pasqualetti F, Cieslak M, Telesford QKQ, Alfred BY, Kahn AE, et al.

Controllability of structural brain networks. Nat. Commun. 2015; 6

Guenther F, Ghosh S, Tourville J. Neural modeling and imaging of the cortical interactions underlying syllable production. Brain Lang. 2006

Gupta RK, Hasan KM, Trivedi R, Pradhan M, Das V, Parikh NA, et al. Diffusion tensor imaging of the developing human cerebrum. J. Neurosci. Res. 2005; 81: 172–178.

Guzzetta A, Staudt M, Petacchi E, Ehlers J, Erb M, Wilke M, et al. Brain representation of active and passive hand movements in children. Pediatr. Res. 2007; 61: 485–490.

de Haan M, Bauer PJ, Georgieff MK, Nelson CA. Explicit memory in low-risk infants aged 19 months born between 27 and 42 weeks of gestation. Dev. Med. Child Neurol. 2000; 42: 304–312.

Van Haastert IC, De Vries LS, Eijsermans MJC, Jongmans MJ, Helders PJM, Gorter JW. Gross motor functional abilities in preterm‐born children with cerebral palsy due to periventricular leukomalacia. Dev. Med. Child Neurol. 2008; 50: 684–689.

Habas PA, Scott JA, Roosta A, Rajagopalan V, Kim K, Rousseau F, et al. Early folding patterns and asymmetries of the normal human brain detected from in utero MRI. Cereb. cortex 2011: bhr053.

Hack M, Flannery DJ, Schluchter M, Cartar L, Borawski E, Klein N. Outcomes in young adulthood for very-low-birth-weight infants. N. Engl. J. Med. 2002; 346: 149–157.

Hagberg B, Hagberg G, Olow I, Wendt L V. The changing panorama of cerebral palsy in Sweden. VII. Prevalence and origin in the birth year period 1987‐90. Acta Paediatr. 1996; 85: 954–960.

Hagmann P, Cammoun L, Gigandet X, Meuli R, Honey CJ, Wedeen VJ, et al. Mapping the Structural Core of Human Cerebral Cortex. PLoS Biol. 2008; 6: e159.

Hajnal J V, Myers R, Oatridge A, Schwieso JE, Young IR, Bydder GM. Artifacts due to stimulus correlated motion in functional imaging of the brain. Magn. Reson. Med. 1994; 31: 283–291.

Hambleton G, Wigglesworth JS. Origin of intraventricular haemorrhage in the preterm infant. Arch. Dis. Child. 1976; 51: 651–659.

Hamilton NB, Attwell D, Hall CN. Pericyte-mediated regulation of capillary diameter: a component of neurovascular coupling in health and disease. Front. Neuroenergetics 2010; 2: 5.

Hansen EC a., Battaglia D, Spiegler A, Deco G, Jirsa VK. Functional connectivity dynamics: Modeling the switching behavior of the resting state. Neuroimage 2015; 105: 525–535.

Harris JJ, Reynell C, Attwell D. The physiology of developmental changes in BOLD functional imaging signals. Dev. Cogn. Neurosci. 2011; 1: 199–216.

Harvey JM, O'Callaghan MJ, Mohay H. Executive function of children with extremely low birthweight: a case control study. Dev. Med. Child Neurol. 1999; 41: 292–297.

Hasegawa T, Yamada K, Morimoto M, Morioka S, Tozawa T, Isoda K, et al. Development of corpus callosum in preterm infants is affected by the prematurity: in vivo assessment of diffusion tensor imaging at term-equivalent age. Pediatr. Res. 2011; 69: 249–254.

Hatten ME. Central nervous system neuronal migration. Annu. Rev. Neurosci. 1999; 22: 511–539.

Hauser M, Chomsky N, Fitch W. The faculty of language: what is it, who has it, and how did it evolve? Science 2002

Van Hecke W, Leemans A, De Backer S, Jeurissen B, Parizel PM, Sijbers J. Comparing isotropic and anisotropic smoothing for voxel-based DTI analyses: A simulation study. Hum. Brain Mapp. 2009; 31: NA-NA.

Heim S, Eickhoff S, Amunts K. Different roles of cytoarchitectonic BA 44 and BA 45 in phonological and semantic verbal fluency as revealed by dynamic causal modelling. Neuroimage 2009

Hein G, Knight R. Superior temporal sulcus—it's my area: or is it? J. Cogn. Neurosci. 2008

Heinks‐Maldonado T, Mathalon D, Gray M. Fine‐tuning of auditory cortex during speech production. 2005

Hellyer P, Scott G, Shanahan M. Cognitive flexibility through metastable neural dynamics is disrupted by damage to the structural connectome. J. 2015

Herrmann K, Antonini A, Shatz CJ. Ultrastructural evidence for synaptic interactions between thalamocortical axons and subplate neurons. Eur. J. Neurosci. 1994; 6: 1729–1742.

Heuvel M van den, Bullmore E, Sporns O. Comparative connectomics. Trends Cogn. Sci. 2016

van den Heuvel MP, Sporns O. Network hubs in the human brain. Trends Cogn. Sci. 2013; 17: 683–696.

Hickok G. Computational neuroanatomy of speech production. Nat. Rev. Neurosci. 2012; 13: 135–145.

Hickok G, Okada K, Serences JT. Area Spt in the human planum temporale supports

sensory-motor integration for speech processing. J. Neurophysiol. 2009; 101: 2725–2732.

Hickok G, Poeppel D. The cortical organization of speech processing. Nat. Rev. Neurosci. 2007; 8: 393–402.

Hille ETM, Weisglas-Kuperus N, Van Goudoever JB, Jacobusse GW, Ens-Dokkum MH, de Groot L, et al. Functional outcomes and participation in young adulthood for very preterm and very low birth weight infants: the Dutch Project on Preterm and Small for Gestational Age Infants at 19 years of age. Pediatrics 2007; 120: e587–e595.

Hirano S, Kojima H, Naito Y, Honjo I, Kamoto Y. Cortical processing mechanism for vocalization with auditory verbal feedback. 1997

Hocking J, McMahon K, Zubicaray G de. Semantic context and visual feature effects in object naming: an fMRI study using arterial spin labeling. J. Cogn. 2009

Homae F, Hashimoto R, Nakajima K, Miyashita Y. From perception to sentence comprehension: the convergence of auditory and visual information of language in the left inferior frontal cortex. Neuroimage 2002

Horbar JD, Badger GJ, Carpenter JH, Fanaroff AA, Kilpatrick S, LaCorte M, et al. Trends in mortality and morbidity for very low birth weight infants, 1991–1999. Pediatrics 2002; 110: 143–151.

Hosey T, Williams G, Ansorge R. Inference of multiple fiber orientations in high angular resolution diffusion imaging. Magn. Reson. Med. 2005; 54: 1480–1489.

Hotelling H. Relations between two sets of variates. Biometrika 1936; 28: 321–377.

Howard D, Patterson K, Wise R, Brown W, Friston K. The cortical localization of the lexicons. Brain 1992

Huddy CLJ, Johnson A, Hope PL. Educational and behavioural problems in babies of 32–35 weeks gestation. Arch. Dis. Childhood-Fetal Neonatal Ed. 2001; 85: F23–F28.

Huettel SA, Song AW, McCarthy G. Functional magnetic resonance imaging. Sinauer Associates Sunderland; 2004.

Hugdahl K, Thomsen T, Ersland L, Rimol L, Niemi J. The effects of attention on speech perception: an fMRI study. Brain Lang. 2003

Huntley M. The Griffiths mental development scales: from birth to 2 years. Assoc. Res. Infant Child Dev. 1996

Hüppi PS, Maier SE, Peled S, Zientara GP, Barnes PD, Jolesz FA, et al. Microstructural development of human newborn cerebral white matter assessed in vivo by diffusion tensor magnetic resonance imaging. Pediatr. Res. 1998; 44: 584–590.

Hüppi PS, Warfield S, Kikinis R, Barnes PD, Zientara GP, Jolesz FA, et al. Quantitative magnetic resonance imaging of brain development in premature and mature newborns. Ann. Neurol. 1998; 43: 224–235.

Husain F, Fromm S, Pursley R. Neural bases of categorization of simple speech and nonspeech sounds. Hum. brain 2006

Hutchison RM, Womelsdorf T, Allen EA, Bandettini PA, Calhoun VD, Corbetta M, et al. Dynamic functional connectivity: Promise, issues, and interpretations. Neuroimage 2013; 80: 360–378.

Huttenlocher PR, Dabholkar AS. Regional differences in synaptogenesis in human cerebral cortex. J. Comp. Neurol. 1997; 387: 167–178.

Hyvärinen a., Oja E. Independent component analysis: Algorithms and applications.

Neural Networks 2000; 13: 411–430.

Iannucci TA, Tomich PG, Gianopoulos JG. Etiology and outcome of extremely low-birth-weight infants. Am. J. Obstet. Gynecol. 1996; 174: 1896–1902.

Indefrey P, Levelt W. The spatial and temporal signatures of word production components. Cognition 2004

Inder TE, Warfield SK, Wang H, Huppi PS, Volpe JJ. Abnormal cerebral structure is present at term in premature infants. Pediatrics 2005; 115: 286–294.

Jackendoff R, Pinker S. The nature of the language faculty and its implications for evolution of language (Reply to Fitch, Hauser, and Chomsky). Cognition 2005; 97: 211–225.

Jaekel J, Baumann N, Wolke D. Effects of gestational age at birth on cognitive performance: a function of cognitive workload demands. PLoS One 2013; 8: e65219.

Jansons KM, Alexander DC. Persistent angular structure: new insights from diffusion magnetic resonance imaging data. Inverse Probl. 2003; 19: 1031.

Jenkinson M, Bannister P, Brady M, Smith S. Improved Optimization for the Robust and Accurate Linear Registration and Motion Correction of Brain Images. Neuroimage 2002; 17: 825–841.

Jenkinson M, Beckmann CF, Behrens TEJ, Woolrich MW, Smith SM. Fsl. Neuroimage 2012; 62: 782–790.

Jeon HA, Friederici AD. Degree of automaticity and the prefrontal cortex. Trends Cogn. Sci. 2015; 19: 244–250.

Jeon H, Lee K, Kim Y, Cho Z. Neural substrates of semantic relationships: common and distinct left-frontal activities for generation of synonyms vs. antonyms. Neuroimage 2009

Jezzard P, Balaban RS. Correction for geometric distortion in echo planar images from B0 field variations. Magn. Reson. Med. 1995; 34: 65–73.

Jezzard P, Barnett AS, Pierpaoli C. Characterization of and correction for eddy current artifacts in echo planar diffusion imaging. Magn. Reson. Med. 1998; 39: 801–812.

Jezzard P, Clare S. Sources of Distortions in Functional MRI Data. Hum. Brain Mapp. 1999; 8: 80–85.

Jobard G, Vigneau M, Mazoyer B, Tzourio-Mazoyer N. Impact of modality and linguistic complexity during reading and listening tasks. Neuroimage 2007

Johansen-Berg H, Behrens TEJ, Sillery E, Ciccarelli O, Thompson AJ, Smith SM, et al. Functional-anatomical validation and individual variation of diffusion tractography-based segmentation of the human thalamus. Cereb. Cortex 2005; 15: 31–9.

Johnson MH. Functional brain development in humans. Nat. Rev. Neurosci. 2001; 2: 475–483.

Johnson MH. Interactive specialization: a domain-general framework for human functional brain development? Dev. Cogn. Neurosci. 2011; 1: 7–21.

Johnson MH, De Haan M. Developmental cognitive neuroscience: An introduction. John Wiley & Sons; 2015.

Johnson S, Fawke J, Hennessy E, Rowell V, Thomas S, Wolke D, et al. Neurodevelopmental disability through 11 years of age in children born before 26 weeks of gestation. Pediatrics 2009; 124: e249–e257.

Johnson S, Hollis C, Kochhar P, Hennessy E, Wolke D, Marlow N. Psychiatric disorders in extremely preterm children: longitudinal finding at age 11 years in the

EPICure study. J. Am. Acad. Child Adolesc. Psychiatry 2010; 49: 453–463.

Johnson S, Marlow N, Wolke D, Davidson L, Marston L, O'Hare A, et al. Validation of a parent report measure of cognitive development in very preterm infants. Dev. Med. Child Neurol. 2004; 46: 389–397.

Jones DK, Cercignani M. Twenty‐five pitfalls in the analysis of diffusion MRI data. NMR Biomed. 2010; 23: 803–820.

Jones T, Rabiner EA. The development, past achievements, and future directions of brain PET. J. Cereb. Blood Flow Metab. 2012; 32: 1426–1454.

Jutla IS, Jeub LGS, Mucha PJ. A generalized Louvain method for community detection implemented in MATLAB. URL http//netwiki. amath. unc. edu/GenLouvain 2011

Kadri H, Mawla AA, Kazah J. The incidence, timing, and predisposing factors of germinal matrix and intraventricular hemorrhage (GMH/IVH) in preterm neonates. Child's Nerv. Syst. 2006; 22: 1086–1090.

Kanold P, Luhmann H. The subplate and early cortical circuits. Annu. Rev. Neurosci. 2010

Kapellou O, Counsell SJ, Kennea N, Dyet L, Saeed N, Stark J, et al. Abnormal cortical development after premature birth shown by altered allometric scaling of brain growth. PLoS Med. 2006; 3: 1382–1390.

Kaukola T, Kapellou O, Laroche S, Counsell SJ, Dyet LE, Allsop JM, et al. Severity of perinatal illness and cerebral cortical growth in preterm infants. Acta Paediatr. 2009; 98: 990–995.

Keihaninejad S, Ryan NS, Malone IB, Modat M, Cash D, Ridgway GR, et al. The Importance of Group-Wise Registration in Tract Based Spatial Statistics Study of

Neurodegeneration: A Simulation Study in Alzheimer's Disease. PLoS One 2012; 7: e45996.

Khazipov R, Luhmann HJ. Early patterns of electrical activity in the developing cerebral cortex of humans and rodents. Trends Neurosci. 2006; 29: 414–418.

Kim DJ, Park B, Park HJ. Functional connectivity-based identification of subdivisions of the basal ganglia and thalamus using multilevel independent component analysis of resting state fMRI. Hum. Brain Mapp. 2013; 34: 1371–1385.

Kim S-G, Ogawa S. Biophysical and physiological origins of blood oxygenation level-dependent fMRI signals. J. Cereb. Blood Flow Metab. 2012; 32: 1188–1206.

Kinney HC, Ann brody B, Kloman AS, Gilles FH. Sequence of Central Nervous System Myelination in Human Infancy. II. Patterns of Myelination in Autopsied Infants. J. Neuropathol. Exp. Neurol. 1988; 47: 217–234.

Kleber B, Birbaumer N, Veit R, Trevorrow T, Lotze M. Overt and imagined singing of an Italian aria. Neuroimage 2007

Klein A, Andersson J, Ardekani B a., Ashburner J, Avants B, Chiang MC, et al. Evaluation of 14 nonlinear deformation algorithms applied to human brain MRI registration. Neuroimage 2009; 46: 786–802.

Van der Knaap MS, van Wezel-Meijler G, Barth PG, Barkhof F, Adèr HJ, Valk J. Normal gyration and sulcation in preterm and term neonates: appearance on MR images. Radiology 1996; 200: 389–396.

Koelsch S, Schulze K, Sammler D, Fritz T. Functional architecture of verbal and tonal working memory: an FMRI study. Hum. brain 2009

Kohannim O, Hibar DP, Stein JL, Jahanshad N, Hua X, Rajagopalan P, et al. Discovery and replication of gene influences on brain structure using LASSO

regression. Front. Neurosci. 2012; 6

van Kooij BJM, de Vries LS, Ball G, van Haastert IC, Benders MJNL, Groenendaal F, et al. Neonatal tract-based spatial statistics findings and outcome in preterm infants. Am. J. Neuroradiol. 2012; 33: 188–194.

Kostović I, Jovanov-Milošević N. The development of cerebral connections during the first 20–45 weeks' gestation. In: Seminars in Fetal and Neonatal Medicine. Elsevier; 2006. p. 415–422.

Kostović I, Judaš M. Correlation between the sequential ingrowth of afferents and transient patterns of cortical lamination in preterm infants. Anat. Rec. 2002; 267: 1–6.

Kostović I, Judaš M. The development of the subplate and thalamocortical connections in the human foetal brain. Acta Paediatr. 2010; 99: 1119–1127.

Kostovic I, Rakic P. Developmental history of the transient subplate zone in the visual and somatosensory cortex of the macaque monkey and human brain. J. Comp. Neurol. 1990; 297: 441–470.

Krishnan ML, Dyet LE, Boardman JP, Kapellou O, Allsop JM, Cowan F, et al. Relationship between white matter apparent diffusion coefficients in preterm infants at term-equivalent age and developmental outcome at 2 years. Pediatrics 2007; 120: e604–e609.

Krishnan S, Leech R, Mercure E, Lloyd-Fox S. Convergent and divergent fMRI responses in children and adults to increasing language production demands. Cerebral 2015

Kuhl PK. Early language acquisition: cracking the speech code. Nat. Rev. Neurosci. 2004; 5: 831–843.

Kuhl PK. Brain Mechanisms in Early Language Acquisition. Neuron 2010; 67: 713–727.

Kuhl PK, Meltzoff AN. Infant vocalizations in response to speech: vocal imitation and developmental change. J. Acoust. Soc. Am. 1996; 100: 2425–38.

Kuhl PK, Williams KA, Lacerda F, Stevens KN, Lindblom B. Linguistic experience alters phonetic perception in infants by 6 months of age. Science 1992; 255: 606–608.

Kwon SH, Scheinost D, Lacadie C, Sze G, Schneider KC, Dai F, et al. Adaptive mechanisms of developing brain: Cerebral lateralization in the prematurely-born. Neuroimage 2015; 108: 144–150.

Kwong KK, Belliveau JW, Chesler DA, Goldberg IE, Weisskoff RM, Poncelet BP, et al. Dynamic magnetic resonance imaging of human brain activity during primary sensory stimulation. Proc. Natl. Acad. Sci. 1992; 89: 5675–5679.

Landry SH, Smith KE, Swank PR. Environmental effects on language development in normal and high-risk child populations. In: Seminars in pediatric neurology. Elsevier; 2002. p. 192–200.

Larroque B, Marret S, Ancel P-Y, Arnaud C, Marpeau L, Supernant K, et al. White matter damage and intraventricular hemorrhage in very preterm infants: the EPIPAGE study. J. Pediatr. 2003; 143: 477–483.

Lasky R, Syrdal-Lasky A, Klein R. VOT discrimination by four to six and a half month old infants from Spanish environments. J. Exp. Child 1975

Lau E, Phillips C, Poeppel D. A cortical network for semantics:(de) constructing the N400. Nat. Rev. Neurosci. 2008

Lauterbur PC. Image formation by induced local interactions: examples employing

nuclear magnetic resonance. 1973

Leaver A, Rauschecker J. Cortical representation of natural complex sounds: effects of acoustic features and auditory object category. J. Neurosci. 2010

Lee JH, Durand R, Gradinaru V, Zhang F, Goshen I, Kim D-S, et al. Global and local fMRI signals driven by neurons defined optogenetically by type and wiring. Nature 2010; 465: 788–792.

Leech R, Holt LL, Devlin JT, Dick F. Expertise with artificial nonspeech sounds recruits speech-sensitive cortical regions. J. Neurosci. 2009; 29: 5234–5239.

Lefebvre F, Mazurier É, Tessier R. Cognitive and educational outcomes in early adulthood for infants weighing 1000 grams or less at birth. Acta Paediatr. 2005; 94: 733–740.

Leff A, Iverson P, Schofield T, Kilner J, Crinion J. Vowel-specific mismatch responses in the anterior superior temporal gyrus: an fMRI study. Cortex 2009

Leff AP, Schofield TM, Stephan KE, Crinion JT, Friston KJ, Price CJ. The cortical dynamics of intelligible speech. J. Neurosci. 2008; 28: 13209–13215.

Lennie P. The cost of cortical computation. Curr. Biol. 2003; 13: 493–497.

Leonardi N, Van De Ville D. On spurious and real fluctuations of dynamic functional connectivity during rest. Neuroimage 2015; 104: 430–436.

Li MJ, Liu Z, Wang P, Wong MP, Nelson MR, Kocher J-PA, et al. GWASdb v2: an update database for human genetic variants identified by genome-wide association studies. Nucleic Acids Res. 2016; 44: D869–D876.

Liberman AM, Mattingly IG. The motor theory of speech perception revised. Cognition 1985; 21: 1–36.

Lidzba K, Schwilling E, Grodd W, Krägeloh-Mann I. Language comprehension vs.

language production: age effects on fMRI activation. Brain Lang. 2011

Liebenthal E, Desai R, Ellingson M. Specialization along the left superior temporal sulcus for auditory categorization. Cerebral 2010

Lips ES, Kooyman M, de Leeuw C, Posthuma D. JAG: A Computational Tool to Evaluate the Role of Gene-Sets in Complex Traits. Genes (Basel). 2015; 6: 238–251.

Liu X, Duyn JH. Time-varying functional network information extracted from brief instances of spontaneous brain activity. Proc. Natl. Acad. Sci. U. S. A. 2013; 110: 4392–7.

Liu Y, Balériaux D, Kavec M, Metens T, Absil J, Denolin V, et al. Structural asymmetries in motor and language networks in a population of healthy preterm neonates at term equivalent age: A diffusion tensor imaging and probabilistic tractography study. Neuroimage 2010; 51: 783–788.

Lockwood CJ, Toti P, Arcuri F, Paidas M, Buchwalder L, Krikun G, et al. Mechanisms of abruption-induced premature rupture of the fetal membranes: thrombin-enhanced interleukin-8 expression in term decidua. Am. J. Pathol. 2005; 167: 1443–1449.

Logothetis NK. What we can do and what we cannot do with fMRI. Nature 2008; 453: 869–878.

Logothetis NK, Pfeuffer J. On the nature of the BOLD fMRI contrast mechanism. Magn. Reson. Imaging 2004; 22: 1517–1531.

Londei A, D'Ausilio A, Basso D, Sestieri C. Sensory-motor brain network connectivity for speech comprehension. Hum. brain 2010

López-Barroso D, Catani M, Ripollés P, Dell'Acqua F, Rodríguez-Fornells A, de Diego-Balaguer R. Word learning is mediated by the left arcuate fasciculus. Proc.

Natl. Acad. Sci. U. S. A. 2013; 110: 13168–73.

Lowe MJ, Mock BJ, Sorenson JA. Functional connectivity in single and multislice echoplanar imaging using resting-state fluctuations. Neuroimage 1998; 7: 119–132.

Luoma L. Speech and language development of children born at 32 weeks' gestation: a 5‐year prospective follow‐up study. Dev. Med. Child Neurol. 1998; 40: 380–387.

Luu TM, Vohr BR, Allan W, Schneider KC, Ment LR. Evidence for catch-up in cognition and receptive vocabulary among adolescents born very preterm. Pediatrics 2011; 128: 313–322.

Luu TM, Vohr BR, Schneider KC, Katz KH, Tucker R, Allan WC, et al. Trajectories of receptive language development from 3 to 12 years of age for very preterm children. Pediatrics 2009; 124: 333–341.

Maas LC, Mukherjee P, Carballido-Gamio J, Veeraraghavan S, Miller SP, Partridge SC, et al. Early laminar organization of the human cerebrum demonstrated with diffusion tensor imaging in extremely premature infants. Neuroimage 2004; 22: 1134–1140.

Mahmoudzadeh M, Dehaene-Lambertz G, Fournier M, Kongolo G, Goudjil S, Dubois J, et al. Syllabic discrimination in premature human infants prior to complete formation of cortical layers. Proc. Natl. Acad. Sci. U. S. A. 2013; 110: 4846–51.

Makropoulos A, Gousias IS, Ledig C, Aljabar P, Serag A, Hajnal J V, et al. Automatic whole brain MRI segmentation of the developing neonatal brain. Med. Imaging, IEEE Trans. 2014; 33: 1818–1831.

Mangia S, Giove F, Tkáč I, Logothetis NK, Henry P-G, Olman CA, et al. Metabolic and hemodynamic events after changes in neuronal activity: current hypotheses, theoretical predictions and in vivo NMR experimental findings. J. Cereb. Blood Flow

Metab. 2009; 29: 441–463.

Mansfield P. Multi-planar image formation using NMR spin echoes. J. Phys. C Solid State Phys. 1977; 10: L55.

Mansfield P, Grannell PK. NMR'diffraction'in solids? J. Phys. C solid state Phys. 1973; 6: L422.

Margulis E, Mlsna L, Uppunda A. Selective neurophysiologic responses to music in instrumentalists with different listening biographies. Hum. brain 2009

Marler P. A comparative approach to vocal learning: Song development in white-crowned sparrows. J. Comp. Physiol. Psychol. 1970; 71: 1–25.

Marlow N, Hennessy EM, Bracewell MA, Wolke D. Motor and executive function at 6 years of age after extremely preterm birth. Pediatrics 2007; 120: 793–804.

Marlow N, Wolke D, Bracewell MA, Samara M. Neurologic and developmental disability at six years of age after extremely preterm birth. N. Engl. J. Med. 2005; 352: 9–19.

Marrelec G, Krainik A, Duffau H, Pélégrini-Issac M, Lehéricy S, Doyon J, et al. Partial correlation for functional brain interactivity investigation in functional MRI. Neuroimage 2006; 32: 228–237.

Mashal N, Faust M, Hendler T, Jung-Beeman M. An fMRI study of processing novel metaphoric sentences. Laterality 2009

Mattison DR, Damus K, Fiore E, Petrini J, Alter C. Preterm delivery: a public health perspective. Paediatr. Perinat. Epidemiol. 2001; 15: 7–16.

McCarton CM, Brooks-Gunn J, Wallace IF, Bauer CR, Bennett FC, Bernbaum JC, et al. Results at age 8 years of early intervention for low-birth-weight premature infants: The Infant Health and Development Program. Jama 1997; 277: 126–132.

McGettigan C, Warren J, Eisner F. Neural correlates of sublexical processing in phonological working memory. J. Cogn. 2011

McGuire P, Silbersweig D, Murray R. Functional anatomy of inner speech and auditory verbal imagery. Psychological 1996

McKinstry RC, Mathur A, Miller JH, Ozcan A, Snyder AZ, Schefft GL, et al. Radial organization of developing preterm human cerebral cortex revealed by non-invasive water diffusion anisotropy MRI. Cereb. Cortex 2002; 12: 1237–1243.

McQuillen PS, Sheldon RA, Shatz CJ, Ferriero DM. Selective vulnerability of subplate neurons after early neonatal hypoxia-ischemia. J. Neurosci. 2003; 23: 3308–3315.

McRobbie DW, Moore EA, Graves MJ, Prince MR. MRI from Picture to Proton. Cambridge university press; 2007.

Mechelli A, Josephs O, Ralph L, Matthew A. Dissociating stimulus‐driven semantic and phonological effect during reading and naming. Hum. brain 2007

Mehler J, Jusczyk P, Lambertz G, Halsted N, Bertoncini J, Amiel-Tison C. A precursor of language acquisition in young infants. Psycholinguist. Crit. concepts Psychol. 2002; 4: 25.

Meltzoff AN, Moore MK. Imitation of facial and manual gestures by human neonates. Science 1977; 198: 75–78.

Ment LR, Hirtz D, Hüppi PS. Imaging biomarkers of outcome in the developing preterm brain. Lancet Neurol. 2009; 8: 1042–1055.

Miller K, Alfaro-Almagro F, Bangerter N. Multimodal population brain imaging in the UK Biobank prospective epidemiological study. Nature 2016

Moeller S, Yacoub E, Olman CA, Auerbach E, Strupp J, Harel N, et al. Multiband

multislice GE-EPI at 7 tesla, with 16-fold acceleration using partial parallel imaging with application to high spatial and temporal whole-brain fMRI. Magn. Reson. Med. 2010; 63: 1144–1153.

Monod J. Le hasard et la nécessité. Essai sur la philosophie naturelle de la biologie moderne. Seuil; 2014.

Monti MM. Statistical analysis of fMRI time-series: a critical review of the GLM approach. Front. Hum. Neurosci. 2011; 5

Monzalvo K, Dehaene-Lambertz G. How reading acquisition changes children's spoken language network. Brain Lang. 2013

Moore T, Hennessy EM, Myles J, Johnson SJ, Draper ES, Costeloe KL, et al. Neurological and developmental outcome in extremely preterm children born in England in 1995 and 2006: the EPICure studies. Bmj 2012; 345: e7961.

Mori S, Crain BJ, Chacko VP, Van Zijl PCM. Three-dimensional tracking of axonal projections in the brain by magnetic resonance imaging. Ann. Neurol. 1999; 45: 265–269.

Mori S, Kaufmann WE, Davatzikos C, Stieltjes B, Amodei L, Fredericksen K, et al. Imaging cortical association tracts in the human brain using diffusion-tensor-based axonal tracking. Magn. Reson. Med. 2002; 47: 215–223.

Mori S, van Zijl PCM. Fiber tracking: principles and strategies - a technical review. NMR Biomed. 2002; 15: 468–480.

Moseley ME, Cohen Y, Kucharczyk J, Mintorovitch J, Asgari HS, Wendland MF, et al. Diffusion-weighted MR imaging of anisotropic water diffusion in cat central nervous system. Radiology 1990; 176: 439–445.

Moser D, Baker J, Sanchez C. Temporal order processing of syllables in the left

parietal lobe. J. 2009

Mrzljak L, Uylings H, Kostovic I, van Eden CG. Prenatal development of neurons in the human prefrontal cortex. II. A quantitative Golgi study. J. Comp. Neurol. 1992; 316: 485–496.

Mueller J, Friederici A. Auditory perception at the root of language learning. Proc. 2012

Muresan L, Renken R, Roerdink JBTM, Duifhuis H. Automated correction of spin-history related motion artefacts in fMRI: simulated and phantom data. IEEE Trans. Biomed. Eng. 2005; 52: 1450–1460.

Murphy K, Birn RM, Bandettini PA. Resting-state fMRI confounds and cleanup. Neuroimage 2013; 80: 349–359.

Myers E, Blumstein S, Walsh E. Inferior frontal regions underlie the perception of phonetic category invariance. Psychological 2009

Myers EH, Hampson M, Vohr B, Lacadie C, Frost SJ, Pugh KR, et al. Functional connectivity to a right hemisphere language center in prematurely born adolescents. Neuroimage 2010; 51: 1445–1452.

Nagy Z, Ashburner J, Andersson J, Jbabdi S, Draganski B, Skare S, et al. Structural correlates of preterm birth in the adolescent brain. Pediatrics 2009; 124: e964–e972.

Nagy Z, Westerberg H, Skare S, Andersson JL, Lilja A, Flodmark O, et al. Preterm children have disturbances of white matter at 11 years of age as shown by diffusion tensor imaging. Pediatr. Res. 2003; 54: 672–679.

Nakayama Y, Nakamura N, Kawai T, Kaneda E, Takahashi Y, Miyake A, et al. Identification and expression analysis of zebrafish polypeptide α-N-acetylgalactosaminyltransferase Y-subfamily genes during embryonic development.

Gene Expr. Patterns 2014; 16: 1–7.

Narain C, Scott S, Wise R, Rosen S, Leff A. Defining a left-lateralized response specific to intelligible speech using fMRI. Cerebral 2003

Nath AR, Beauchamp MS. Dynamic changes in superior temporal sulcus connectivity during perception of noisy audiovisual speech. J. Neurosci. 2011; 31: 1704–1714.

Newman M. Modularity and community structure in networks. Proc. Natl. Acad. 2006

van Noort-van der Spek IL, Franken M-CJP, Weisglas-Kuperus N. Language Functions in Preterm-Born Children: A Systematic Review and Meta-analysis. Pediatrics 2012; 129: 745–754.

Van Noort‐Van Der Spek IL, Franken MJP, Wieringa MH, WEISGLAS‐KUPERUS N. Phonological development in very‐low‐birthweight children: an exploratory study. Dev. Med. Child Neurol. 2010; 52: 541–546.

Northam GB, Liégeois F, Tournier J-D, Croft LJ, Johns PN, Chong WK, et al. Interhemispheric temporal lobe connectivity predicts language impairment in adolescents born preterm. Brain 2012; 135: 3781–3798.

Nosarti C, Al‐Asady MHS, Frangou S, Stewart AL, Rifkin L, Murray RM. Adolescents who were born very preterm have decreased brain volumes. Brain 2002; 125: 1616–1623.

Nosarti C, Giouroukou E, Micali N, Rifkin L, Morris RG, Murray RM. Impaired executive functioning in young adults born very preterm. J. Int. Neuropsychol. Soc. 2007; 13: 571–581.

Nudel R, Simpson NH, Baird G, O'Hare A, Conti‐Ramsden G, Bolton PF, et al.

Genome‐wide association analyses of child genotype effects and parent‐of‐origin effects in specific language impairment. Genes, Brain Behav. 2014; 13: 418–429.

Nuñez C, Dapretto M, Katzir T, Starr A, Bramen J, Kan E, et al. fMRI of syntactic processing in typically developing children: Structural correlates in the inferior frontal gyrus. Dev. Cogn. Neurosci. 2011; 1: 313–323.

Nyberg L, McIntosh AR, Cabeza R, Nilsson L-G, Houle S, Habib R, et al. Network analysis of positron emission tomography regional cerebral blood flow data: ensemble inhibition during episodic memory retrieval. J. Neurosci. 1996; 16: 3753–3759.

Oberhuber M, Hope TMH, Seghier ML, Parker Jones O, Prejawa S, Green DW, et al. Four Functionally Distinct Regions in the Left Supramarginal Gyrus Support Word Processing. Cereb. Cortex 2016

Obleser J, Kotz S. Expectancy constraints in degraded speech modulate the language comprehension network. Cereb. Cortex 2009

Obleser J, Wise R, Dresner M. Functional integration across brain regions improves speech perception under adverse listening conditions. J. 2007

Obleser J, Zimmermann J, Van Meter J, Rauschecker JP. Multiple stages of auditory speech perception reflected in event-related FMRI. Cereb. Cortex 2007; 17: 2251–2257.

Offidani C, Pomini F, Caruso A, Ferrazzani S, Chiarotti M, Fiori A. Cocaine during pregnancy: a critical review of the literature. Minerva Ginecol. 1995; 47: 381–390.

Ogawa S, Lee T-M. Magnetic resonance imaging of blood vessels at high fields:In vivo andin vitro measurements and image simulation. Magn. Reson. Med. 1990; 16: 9–18.

Ogawa S, Lee T-M, Nayak AS, Glynn P. Oxygenation-sensitive contrast in magnetic resonance image of rodent brain at high magnetic fields. Magn. Reson. Med. 1990; 14: 68–78.

Ogawa S, Lee TM, Kay AR, Tank DW. Brain magnetic resonance imaging with contrast dependent on blood oxygenation. Proc. Natl. Acad. Sci. U. S. A. 1990; 87: 9868–72.

Ogawa S, Tank DW, Menon R, Ellermann JM, Kim SG, Merkle H, et al. Intrinsic signal changes accompanying sensory stimulation: functional brain mapping with magnetic resonance imaging. Proc. Natl. Acad. Sci. 1992; 89: 5951–5955.

Olsén P, Läärä E, Rantakallio P, Järvelin M-R, Sarpola A, Hartikainen A-L. Epidemiology of preterm delivery in two birth cohorts with an interval of 20 years. Am. J. Epidemiol. 1995; 142: 1184–1193.

Onnela J, Fenn D, Reid S, Porter M, Mucha P. Taxonomies of networks from community structure. Phys. Rev. E 2012

Ordidge RJ, Mansfield P, Coupland RE. Rapid biomedical imaging by NMR. Br. J. Radiol. 1981; 54: 850–855.

Ortiz-Mantilla S, Choudhury N, Leevers H, Benasich AA. Understanding language and cognitive deficits in very low birth weight children. Dev. Psychobiol. 2008; 50: 107–126.

Osnes B, Hugdahl K, Specht K. Effective connectivity analysis demonstrates involvement of premotor cortex during speech perception. Neuroimage 2011

den Ouden D-B, Saur D, Mader W, Schelter B, Lukic S, Wali E, et al. Network modulation during complex syntactic processing. Neuroimage 2012; 59: 815–823.

Pa J, Hickok G. A parietal–temporal sensory–motor integration area for the human

vocal tract: Evidence from an fMRI study of skilled musicians. Neuropsychologia 2008

Paldino MJ, Hedges K, Golriz F. The arcuate fasciculus and language development in a cohort of pediatric patients with malformations of cortical development. Am. J. Neuroradiol. 2016; 37: 169–175.

Papathanassiou D, Etard O, Mellet E, Zago L, Mazoyer B, Tzourio-Mazoyer N. A Common Language Network for Comprehension and Production: A Contribution to the Definition of Language Epicenters with PET. 2000.

Papoutsi M, Zwart J de, Jansma J. From phonemes to articulatory codes: an fMRI study of the role of Broca's area in speech production. Cerebral 2009

Paquette N, Lassonde M, Vannasing P, Tremblay J. Developmental patterns of expressive language hemispheric lateralization in children, adolescents and adults using functional near-infrared spectroscopy. Neuropsychologia 2015

Parker GJM, Alexander DC. Probabilistic anatomical connectivity derived from the microscopic persistent angular structure of cerebral tissue. Philos. Trans. R. Soc. Lond. B. Biol. Sci. 2005; 360: 893–902.

Parker Jones 'Ōiwi, Prejawa S, Hope TMH, Oberhuber M, Seghier ML, Leff AP, et al. Sensory-to-motor integration during auditory repetition: a combined fMRI and lesion study. Front. Hum. Neurosci. 2014; 8: 24.

Partanen E, Kujala T, Näätänen R, Liitola A, Sambeth A, Huotilainen M. Learning-induced neural plasticity of speech processing before birth. Proc. Natl. Acad. Sci. U. S. A. 2013; 110: 15145–50.

Partridge SC, Mukherjee P, Berman JI, Henry RG, Miller SP, Lu Y, et al. Tractography‐based quantitation of diffusion tensor imaging parameters in white

matter tracts of preterm newborns. J. Magn. Reson. Imaging 2005; 22: 467–474.

Partridge SC, Mukherjee P, Henry RG, Miller SP, Berman JI, Jin H, et al. Diffusion tensor imaging: serial quantitation of white matter tract maturity in premature newborns. Neuroimage 2004; 22: 1302–1314.

de Pasquale F, Della Penna S, Snyder AZ, Lewis C, Mantini D, Marzetti L, et al. Temporal dynamics of spontaneous MEG activity in brain networks. Proc. Natl. Acad. Sci. U. S. A. 2010; 107: 6040–6045.

Pasqualetti F, Zampieri S, Bullo F. Controllability Metrics and Algorithms for Complex Networks. arXiv Prepr. arXiv1308.1201 2013; 1: 3287–3292.

Pearl J. Causal inference in statistics: An overview. Statistics Surveys 3 96–146. 2009

Pedregosa F, Varoquaux G, Gramfort A, Michel V, Thirion B, Grisel O, et al. Scikit-learn: Machine learning in Python. J. Mach. Learn. Res. 2011; 12: 2825–2830.

Peña M, Pittaluga E, Mehler J. Language acquisition in premature and full-term infants. Proc. Natl. 2010

Peña M, Werker JF, Dehaene-Lambertz G, Pena M. Earlier Speech Exposure Does Not Accelerate Speech Acquisition. J. Neurosci. 2012; 32: 11159–11163.

Perani D, Saccuman MC, Scifo P, Anwander A, Spada D, Baldoli C, et al. Neural language networks at birth. Proc. Natl. Acad. Sci. 2011; 108: 16056–16061.

Perkins L, Hughes E, Srinivasan L, Allsop J, Glover A, Kumar S, et al. Exploring cortical subplate evolution using magnetic resonance imaging of the fetal brain. Dev. Neurosci. 2007; 30: 211–220.

Perlman JM, McMenamin JB, Volpe JJ. Fluctuating cerebral blood-flow velocity in respiratory-distress syndrome: relation to the development of intraventricular

hemorrhage. N. Engl. J. Med. 1983; 309: 204–209.

Peschke C, Ziegler W, Eisenberger J, Baumgaertner A. Phonological manipulation between speech perception and production activates a parieto-frontal circuit. Neuroimage 2012

Petrides M, Pandya DN. Projections to the frontal cortex from the posterior parietal region in the rhesus monkey. J. Comp. Neurol. 1984; 228: 105–116.

Pierpaoli C, Basser PJ. Toward a quantitative assessment of diffusion anisotropy. Magn. Reson. Med. 1996; 36: 893–906.

Pinker S. The language instinct: The new science of language and mind. Penguin UK; 1995.

Platt MJ, Cans C, Johnson A, Surman G, Topp M, Torrioli MG, et al. Trends in cerebral palsy among infants of very low birthweight (< 1500 g) or born prematurely (< 32 weeks) in 16 European centres: a database study. Lancet 2007; 369: 43–50.

Poldrack RA, Mumford JA, Nichols TE. Handbook of functional MRI data analysis. Cambridge University Press; 2011.

Porter M, Onnela J, Mucha P. Communities in networks. Not. AMS 2009

Power JD, Barnes K a., Snyder AZ, Schlaggar BL, Petersen SE. Spurious but systematic correlations in functional connectivity MRI networks arise from subject motion. Neuroimage 2012; 59: 2142–2154.

Power JD, Mitra A, Laumann TO, Snyder AZ, Schlaggar BL, Petersen SE. Methods to detect, characterize, and remove motion artifact in resting state fMRI. Neuroimage 2014; 84: 320–341.

Price C, Friston K. Functional ontologies for cognition: The systematic definition of structure and function. Cogn. Neuropsychol. 2005

Price C, Moore C. The neural regions sustaining object recognition and naming. R. … 1996

Price CJ. A review and synthesis of the first 20years of PET and fMRI studies of heard speech, spoken language and reading. Neuroimage 2012; 62: 816–847.

Pruim RHR, Mennes M, Buitelaar JK, Beckmann CF. Evaluation of ICA-AROMA and alternative strategies for motion artifact removal in resting state fMRI. Neuroimage 2015; 112: 278–287.

Pulvermüller F. Opinion: Brain mechanisms linking language and action. Nat. Rev. Neurosci. 2005; 6: 576–582.

Pulvermüller F, Fadiga L. Active perception: sensorimotor circuits as a cortical basis for language. Nat. Rev. Neurosci. 2010; 11: 351–360.

Purcell EM, Torrey HC, Pound R V. Resonance absorption by nuclear magnetic moments in a solid. Phys. Rev. 1946; 69: 37.

Purcell S, Neale B, Todd-Brown K, Thomas L, Ferreira MAR, Bender D, et al. PLINK: A Tool Set for Whole-Genome Association and Population-Based Linkage Analyses. Am. J. Hum. Genet. 2007; 81: 559–575.

Rabi II, Zacharias JR, Millman S, Kusch P. A New Method of Measuring Nuclear Magnetic Moment. Phys. Rev. 1938; 53: 318–318.

Raettig T, Frisch S, Friederici A, Kotz S. Neural correlates of morphosyntactic and verb-argument structure processing: an EfMRI study. Cortex 2010

Raichle ME, MacLeod AM, Snyder AZ, Powers WJ, Gusnard DA, Shulman GL. A default mode of brain function. Proc. Natl. Acad. Sci. 2001; 98: 676–682.

Raichle ME, Mintun MA. Brain work and brain imaging. Annu. Rev. Neurosci. 2006; 29: 449–476.

Raichle ME, Snyder AZ. A default mode of brain function: a brief history of an evolving idea. Neuroimage 2007; 37: 1083–1090.

Raizada R, Poldrack R. Selective amplification of stimulus differences during categorical processing of speech. Neuron 2007

Rakic P. Principles of neural cell migration. Experientia 1990; 46: 882–891.

Rakic P. Evolution of the neocortex: a perspective from developmental biology. Nat. Rev. Neurosci. 2009; 10: 724–735.

Rakic P, Cameron RS, Komuro H. Recognition, adhesion, transmembrane signaling and cell motility in guided neuronal migration. Curr. Opin. Neurobiol. 1994; 4: 63–69.

Ramus F, Fisher SE. Genetics of language. In: The cognitive neurosciences, 4th ed. MIT Press; 2009. p. 855–871.

Rathbone R, Counsell SJ, Kapellou O, Dyet L, Kennea N, Hajnal J, et al. Perinatal cortical growth and childhood neurocognitive abilities. Neurology 2011; 77: 1510–1517.

Rauschecker JP, Scott SK. Maps and streams in the auditory cortex: nonhuman primates illuminate human speech processing. Nat. Neurosci. 2009; 12: 718–724.

Ravizza S, Hazeltine E, Ruiz S, Zhu D. Left TPJ activity in verbal working memory: implications for storage-and sensory-specific models of short term memory. Neuroimage 2011

Resch B, Vollaard E, Maurer U, Haas J, Rosegger H, Müller W. Risk factors and determinants of neurodevelopmental outcome in cystic periventricular leucomalacia. Eur. J. Pediatr. 2000; 159: 663–670.

Richardson FM, Thomas MSC, Price CJ. Neuronal Activation for Semantically

Reversible Sentences. J. Cogn. Neurosci. 2010; 22: 1283–1298.

Rilling JK, Glasser MF, Jbabdi S, Andersson J, Preuss TM. Continuity, divergence, and the evolution of brain language pathways. Front Evol Neurosci 2011; 3

Rilling JK, Glasser MF, Preuss TM, Ma X, Zhao T, Hu X, et al. The evolution of the arcuate fasciculus revealed with comparative DTI. Nat. Neurosci. 2008; 11: 426–428.

Rimol L, Specht K, Hugdahl K. Controlling for individual differences in fMRI brain activation to tones, syllables, and words. Neuroimage 2006

Rogers BP, Morgan VL, Newton AT, Gore JC. Assessing functional connectivity in the human brain by fMRI. Magn. Reson. Imaging 2007; 25: 1347–1357.

Roizen JD, Asada M, Tong M, Tai H-H, Muglia LJ. Preterm birth without progesterone withdrawal in 15-hydroxyprostaglandin dehydrogenase hypomorphic mice. Mol. Endocrinol. 2008; 22: 105–112.

Rombouts SARB, Damoiseaux JS, Goekoop R, Barkhof F, Scheltens P, Smith SM, et al. Model-free group analysis shows altered BOLD FMRI networks in dementia. Hum. Brain Mapp. 2009; 30: 256–266.

Romero R, Gómez R, Chaiworapongsa T, Conoscenti G, Cheol Kim J, Mee Kim Y. The role of infection in preterm labour and delivery. Paediatr. Perinat. Epidemiol. 2001; 15: 41–56.

Rose SA, Feldman JF. Memory and processing speed in preterm children at eleven years: a comparison with full-terms. Child Dev. 1996: 2005–2021.

Rose SE, Hatzigeorgiou X, Strudwick MW, Durbridge G, Davies PSW, Colditz PB. Altered white matter diffusion anisotropy in normal and preterm infants at term-equivalent age. Magn. Reson. Med. 2008; 60: 761–767.

Rosipal R, Krämer N. Overview and recent advances in partial least squares. In: Subspace, latent structure and feature selection. Springer; 2006. p. 34–51.

Rubinov M, Knock SA, Stam CJ, Micheloyannis S, Harris AWF, Williams LM, et al. Small-world properties of nonlinear brain activity in schizophrenia. Hum. Brain Mapp. 2009; 30: 403–416.

Rubinov M, Sporns O. Complex network measures of brain connectivity: uses and interpretations. Neuroimage 2010; 52: 1059–1069.

Rushe TM, Rifkin L, Stewart AL, Townsend JP, Roth SC, Wyatt JS, et al. Neuropsychological outcome at adolescence of very preterm birth and its relation to brain structure. Dev. Med. Child Neurol. 2001; 43: 226–233.

Sadaghiani S, Kleinschmidt A. Functional interactions between intrinsic brain activity and behavior. Neuroimage 2013; 80: 379–386.

Saigal S, Hoult LA, Streiner DL, Stoskopf BL, Rosenbaum PL. School difficulties at adolescence in a regional cohort of children who were extremely low birth weight. Pediatrics 2000; 105: 325–331.

Saigal S, den Ouden L, Wolke D, Hoult L, Paneth N, Streiner DL, et al. School-age outcomes in children who were extremely low birth weight from four international population-based cohorts. Pediatrics 2003; 112: 943–950.

Salimi-Khorshidi G, Douaud G, Beckmann CF, Glasser MF, Griffanti L, Smith SM. Automatic denoising of functional MRI data: Combining independent component analysis and hierarchical fusion of classifiers. Neuroimage 2014; 90: 449–468.

Salvan P, Froudist Walsh S, Allin MPG, Walshe M, Murray RM, Bhattacharyya S, et al. Road work on memory lane—Functional and structural alterations to the learning and memory circuit in adults born very preterm. Neuroimage 2014; 102: 152–161.

Satterthwaite TD, Elliott M a., Gerraty RT, Ruparel K, Loughead J, Calkins ME, et al. An improved framework for confound regression and filtering for control of motion artifact in the preprocessing of resting-state functional connectivity data. Neuroimage 2013; 64: 240–256.

Satterthwaite TD, Wolf DH, Loughead J, Ruparel K, Elliott M a., Hakonarson H, et al. Impact of in-scanner head motion on multiple measures of functional connectivity: Relevance for studies of neurodevelopment in youth. Neuroimage 2012; 60: 623–632.

Saur D, Kreher BW, Schnell S, Kümmerer D, Kellmeyer P, Vry M-S, et al. Ventral and dorsal pathways for language. Proc. Natl. Acad. Sci. 2008; 105: 18035–18040.

Schafer RJ, Lacadie C, Vohr B, Kesler SR, Katz KH, Schneider KC, et al. Alterations in functional connectivity for language in prematurely born adolescents. Brain 2009; 132: 661–670.

Scheinost D, Lacadie C, Vohr BR, Schneider KC, Papademetris X, Constable RT, et al. Cerebral Lateralization is Protective in the Very Prematurely Born. Cereb. Cortex 2014: 1–9.

Scheinost D, Papademetris X, Constable RT. The impact of image smoothness on intrinsic functional connectivity and head motion confounds. Neuroimage 2014; 95: 13–21.

Schlaggar BL, Brown TT, Lugar HM, Visscher KM, Miezin FM, Petersen SE. Functional neuroanatomical differences between adults and school-age children in the processing of single words. Science 2002; 296: 1476–1479.

Schmahmann JD, Pandya DN, Wang R, Dai G, D'Arceuil HE, de Crespigny AJ, et al. Association fibre pathways of the brain: parallel observations from diffusion

spectrum imaging and autoradiography. Brain 2007; 130: 630–653.

Schofield T, Iverson P, Kiebel S. Changing meaning causes coupling changes within higher levels of the cortical hierarchy. Proc. 2009

Schön D, Gordon R, Campagne A, Magne C. Similar cerebral networks in language, music and song perception. Neuroimage 2010

De Schotten MT, Dell'Acqua F, Valabregue R, Catani M. Monkey to human comparative anatomy of the frontal lobe association tracts. Cortex 2012; 48: 82–96.

Schulze K, Zysset S, Mueller K. Neuroarchitecture of verbal and tonal working memory in nonmusicians and musicians. Hum. brain 2011

Setsompop K, Gagoski BA, Polimeni JR, Witzel T, Wedeen VJ, Wald LL. Blipped-controlled aliasing in parallel imaging for simultaneous multislice echo planar imaging with reduced g-factor penalty. Magn. Reson. Med. 2012; 67: 1210–1224.

Shergill S, Bullmore E, Brammer M. A functional study of auditory verbal imagery. Psychological 2001

Sherlock RL, Anderson PJ, Doyle LW, Group VICS. Neurodevelopmental sequelae of intraventricular haemorrhage at 8 years of age in a regional cohort of ELBW/very preterm infants. Early Hum. Dev. 2005; 81: 909–916.

Shi R. Functional morphemes and early language acquisition. Child Dev. Perspect. 2014; 8: 6–11.

Shine JM, Bissett PG, Bell PT, Koyejo O, Balsters JH, Gorgolewski KJ, et al. The Dynamics of Functional Brain Networks: Integrated Network States during Cognitive Task Performance. Neuron 2016; 92: 544–554.

Shine JM, Koyejo O, Poldrack RA. Temporal metastates are associated with differential patterns of time-resolved connectivity, network topology, and attention.

Proc. Natl. Acad. Sci. U. S. A. 2016; 113: 9888–91.

Shulman GL, Fiez JA, Corbetta M, Buckner RL, Miezin FM, Raichle ME, et al. Common blood flow changes across visual tasks: II. Decreases in cerebral cortex. J. Cogn. Neurosci. 1997; 9: 648–663.

Shulman RG, Rothman DL, Behar KL, Hyder F. Energetic basis of brain activity: implications for neuroimaging. Trends Neurosci. 2004; 27: 489–495.

Shultz S, Vouloumanos A, Bennett RH, Pelphrey K. Neural specialization for speech in the first months of life. Dev. Sci. 2014; 17: 766–774.

Siegel JS, Mitra A, Laumann TO, Seitzman BA, Raichle M, Corbetta M, et al. Data Quality Influences Observed Links Between Functional Connectivity and Behavior. Cereb. Cortex 2016

Simmonds A, Wise R, Dhanjal N. A comparison of sensory-motor activity during speech in first and second languages. J. 2011

Skeide M a., Brauer J, Friederici AD. Brain functional and structural predictors of language performance. Cereb. Cortex 2015: bhv042.

Skeide MA, Brauer J, Friederici AD. Syntax gradually segregates from semantics in the developing brain. Neuroimage 2014; 100: 106–111.

Skeide M, Friederici A. The ontogeny of the cortical language network. Nat. Rev. Neurosci. 2016

Skiöld B, Horsch S, Hallberg B, Engström M, Nagy Z, Mosskin M, et al. White matter changes in extremely preterm infants, a population‐based diffusion tensor imaging study. Acta Paediatr. 2010; 99: 842–849.

Skranes J, Lohaugen GC, Martinussen M, Indredavik MS, Dale AM, Haraldseth O, et al. White matter abnormalities and executive function in children with very low

birth weight. Neuroreport 2009; 20: 263–266.

Slattery MM, Morrison JJ. Preterm delivery. Lancet 2002; 360: 1489–1497.

Smith RE, Tournier J-D, Calamante F, Connelly A. Anatomically-constrained tractography: improved diffusion MRI streamlines tractography through effective use of anatomical information. Neuroimage 2012; 62: 1924–1938.

Smith RE, Tournier J-D, Calamante F, Connelly A. SIFT2: Enabling dense quantitative assessment of brain white matter connectivity using streamlines tractography. Neuroimage 2015; 119: 338–351.

Smith S. Linking cognition to brain connectivity. Nat. Neurosci. 2016; 19: 7–9.

Smith SM, Beckmann CF, Andersson J, Auerbach EJ, Bijsterbosch J, Douaud G, et al. Resting-state fMRI in the Human Connectome Project. Neuroimage 2013; 80: 144–168.

Smith SM, Fox PTM, Miller KL, Glahn DC, Fox PTM, Mackay CE, et al. Correspondence of the brain's functional architecture during activation and rest. Proc. Natl. Acad. Sci. 2009; 106: 13040–13045.

Smith SM, Jenkinson M, Johansen-Berg H, Rueckert D, Nichols TE, Mackay CE, et al. Tract-based spatial statistics: voxelwise analysis of multi-subject diffusion data. Neuroimage 2006; 31: 1487–1505.

Smith SM, Jenkinson M, Woolrich MW, Beckmann CF, Behrens TEJ, Johansen-Berg H, et al. Advances in functional and structural MR image analysis and implementation as FSL. Neuroimage 2004; 23: S208–S219.

Smith SM, Matthews PM, Jezzard P. Functional MRI: an introduction to methods. Oxford university press; 2001.

Smith SM, Miller KL, Moeller S, Xu J, Auerbach EJ, Woolrich MW, et al.

Temporally-independent functional modes of spontaneous brain activity. Proc. Natl. Acad. Sci. 2012; 109: 3131–3136.

Smith SM, Miller KL, Salimi-Khorshidi G, Webster M, Beckmann CF, Nichols TE, et al. Network modelling methods for FMRI. Neuroimage 2011; 54: 875–891.

Smith SM, Nichols TE, Vidaurre D, Winkler AM, Behrens TEJ, Glasser MF, et al. A positive-negative mode of population covariation links brain connectivity, demographics and behavior. Nat. Neurosci. 2015; 18: 1565–1567.

Smith SM, Vidaurre D, Beckmann CF, Glasser MF, Jenkinson M, Miller KL, et al. Functional connectomics from resting-state fMRI. Trends Cogn. Sci. 2013; 17: 666–682.

Smith T, Noble M, Noble S, Wright G, McLennan D, Plunkett E. The English Indices of Deprivation 2015. London Dep. Communities Local Gov. 2015

Smyser CD, Inder TE, Shimony JS, Hill JE, Degnan AJ, Snyder AZ, et al. Longitudinal analysis of neural network development in preterm infants. Cereb. Cortex 2010; 20: 2852–2862.

Smyser CD, Snyder a. Z, Shimony JS, Mitra a., Inder TE, Neil JJ. Resting-State Network Complexity and Magnitude Are Reduced in Prematurely Born Infants. Cereb. Cortex 2014: 1–12.

Smyser CD, Snyder AZ, Neil JJ. Functional connectivity MRI in infants: Exploration of the functional organization of the developing brain. Neuroimage 2011; 56: 1437–1452.

Soul JS, Hammer PE, Tsuji M, Saul JP, Bassan H, Limperopoulos C, et al. Fluctuating pressure-passivity is common in the cerebral circulation of sick premature infants. Pediatr. Res. 2007; 61: 467–473.

Spalek K, Thompson-Schill S. Task-dependent semantic interference in language production: an fMRI study. Brain Lang. 2008

Specht K, Osnes B, Hugdahl K. Detection of differential speech-specific processes in the temporal lobe using fMRI and a dynamic 'sound morphing' technique. Hum. Brain Mapp. 2009

Specht K, Reul J. Functional segregation of the temporal lobes into highly differentiated subsystems for auditory perception: an auditory rapid event-related fMRI-task. Neuroimage 2003

Sporns O. The human connectome: origins and challenges. Neuroimage 2013; 80: 53–61.

Sporns O, Betzel RF. Modular brain networks. Annu. Rev. Psychol. 2016; 67: 613–640.

Sporns O, Tononi G, Kötter R. The Human Connectome: A Structural Description of the Human Brain. PLoS Comput. Biol. 2005; 1: e42.

Srinivasan L, Dutta R, Counsell SJ, Allsop JM, Boardman JP, Rutherford MA, et al. Quantification of deep gray matter in preterm infants at term-equivalent age using manual volumetry of 3-tesla magnetic resonance images. Pediatrics 2007; 119: 759–765.

Stam CJ, Jones BF, Nolte G, Breakspear M, Scheltens P. Small-world networks and functional connectivity in Alzheimer's disease. Cereb. Cortex 2007; 17: 92–9.

Steer P. The epidemiology of preterm labour. BJOG An Int. J. Obstet. Gynaecol. 2005; 112: 1–3.

Stehling MJ, Howseman AM, Ordidge RJ, Chapman B, Turner R, Coxon R, et al. Whole-body echo-planar MR imaging at 0.5 T. Radiology 1989; 170: 257–263.

Stejskal EO, Tanner JE. Spin diffusion measurements: spin echoes in the presence of a time‐dependent field gradient. J. Chem. Phys. 1965; 42: 288–292.

Stephens BE, Vohr BR. Neurodevelopmental outcome of the premature infant. Pediatr. Clin. North Am. 2009; 56: 631–646.

Stiles J, Jernigan T. The basics of brain development. Neuropsychol. Rev. 2010

Strogatz SH. Exploring complex networks. Nature 2001; 410: 268–276.

Szaflarski JP, Rajagopal A, Altaye M, Byars AW, Jacola L, Schmithorst VJ, et al. Left-handedness and language lateralization in children. Brain Res. 2012; 1433: 85–97.

Szycik G, Jansma H, Münte T. Audiovisual integration during speech comprehension: An fMRI study comparing ROI‐based and whole brain analyses. Hum. Brain Mapp. 2009

Takashima S, Itoh M, Oka A. A history of our understanding of cerebral vascular development and pathogenesis of perinatal brain damage over the past 30 years. In: Seminars in pediatric neurology. Elsevier; 2009. p. 226–236.

Takaso H, Eisner F, Wise R, Scott S. The effect of delayed auditory feedback on activity in the temporal lobe while speaking: a positron emission tomography study. J. Speech, Lang. 2010

Taşan M, Musso G, Hao T, Vidal M, MacRae CA, Roth FP. Selecting causal genes from genome-wide association studies via functionally coherent subnetworks. Nat. Methods 2015; 12: 154–159.

Tattersall I. Human evolution and cognition. Theory Biosci. 2010; 129: 193–201.

Taylor HG, Klein N, Minich NM, Hack M. Middle‐school‐age outcomes in children with very low birthweight. Child Dev. 2000; 71: 1495–1511.

Thierry G, Giraud A, Price C. Hemispheric dissociation in access to the human semantic system. Neuron 2003

Thierry G, Price C. Dissociating verbal and nonverbal conceptual processing in the human brain. J. Cogn. Neurosci. 2006

Thompson DK, Inder TE, Faggian N, Johnston L, Warfield SK, Anderson PJ, et al. Characterization of the corpus callosum in very preterm and full-term infants utilizing MRI. Neuroimage 2011; 55: 479–490.

Thompson DK, Warfield SK, Carlin JB, Pavlovic M, Wang HX, Bear M, et al. Perinatal risk factors altering regional brain structure in the preterm infant. Brain 2007; 130: 667–677.

Thulborn KR, Waterton JC, Matthews PM, Radda GK. Oxygenation dependence of the transverse relaxation time of water protons in whole blood at high field. Biochim. Biophys. Acta - Gen. Subj. 1982; 714: 265–270.

Tobi EW, Heijmans BT, Kremer D, Putter H, Delemarre-van de Waal HA, Finken MJJ, et al. DNA methylation of IGF2, GNASAS, INSIGF and LEP and being born small for gestational age. Epigenetics 2011; 6: 171–176.

Toulmin H, Beckmann CF, O'Muircheartaigh J, Ball G, Nongena P, Makropoulos A, et al. Specialization and integration of functional thalamocortical connectivity in the human infant. Proc. Natl. Acad. Sci. 2015: 201422638.

Tournier J-D, Calamante F, Connelly A. Robust determination of the fibre orientation distribution in diffusion MRI: non-negativity constrained super-resolved spherical deconvolution. Neuroimage 2007; 35: 1459–1472.

Tournier J-D, Calamante F, Gadian DG, Connelly A. Direct estimation of the fiber orientation density function from diffusion-weighted MRI data using spherical

deconvolution. Neuroimage 2004; 23: 1176–1185.

Tournier JD, Calamante F, Connelly A. MRtrix: Diffusion tractography in crossing fiber regions. Int. J. Imaging Syst. Technol. 2012; 22: 53–66.

Tourville J, Reilly K, Guenther F. Neural mechanisms underlying auditory feedback control of speech. Neuroimage 2008

Traud A, Kelsic E, Mucha P, Porter M. Comparing community structure to characteristics in online collegiate social networks. SIAM Rev. 2011

Traynor C, Heckemann RA, Hammers A, O'Muircheartaigh J, Crum WR, Barker GJ, et al. Reproducibility of thalamic segmentation based on probabilistic tractography. Neuroimage 2010; 52: 69–85.

Tremblay P, Small S. Motor response selection in overt sentence production: a functional MRI study. Front. Psychol. 2011

Tuch DS. Q-ball imaging. Magn. Reson. Med. 2004; 52: 1358–1372.

Tuch DS, Reese TG, Wiegell MR, Makris N, Belliveau JW, Wedeen VJ. High angular resolution diffusion imaging reveals intravoxel white matter fiber heterogeneity. Magn. Reson. Med. 2002; 48: 577–582.

Turkeltaub P, Coslett H. Localization of sublexical speech perception components. Brain Lang. 2010

Turner T, Fridriksson J, Baker J, Jr DE. Obligatory Broca's area modulation associated with passive speech perception. 2009

Tustison NJ, Avants BB, Cook PA, Zheng Y, Egan A, Yushkevich PA, et al. N4ITK: improved N3 bias correction. IEEE Trans. Med. Imaging 2010; 29: 1310–1320.

Twells RCJ, Metzker ML, Brown SD, Cox R, Garey C, Hammond H, et al. The sequence and gene characterization of a 400-kb candidate region for IDDM4 on

chromosome 11q13. Genomics 2001; 72: 231–242.

Tyler L, Shafto M, Randall B, Wright P. Preserving syntactic processing across the adult life span: the modulation of the frontotemporal language system in the context of age-related atrophy. Cerebral 2009

Valenzuela JI, Perez F. Diversifying the secretory routes in neurons. Front. Neurosci. 2015; 9: 358.

VanRullen R, Busch N, Drewes J. Ongoing EEG phase as a trial-by-trial predictor of perceptual and attentional variability. Front. 2011

Vargha-Khadem F, Gadian DG, Copp A, Mishkin M. FOXP2 and the neuroanatomy of speech and language. Nat. Rev. Neurosci. 2005; 6: 131–138.

Váša F, Shanahan M, Hellyer P, Scott G, Cabral J. Effects of lesions on synchrony and metastability in cortical networks. Neuroimage 2015

Vidaurre D, Quinn AJ, Baker AP, Dupret D, Tejero-Cantero A, Woolrich MW. Spectrally resolved fast transient brain states in electrophysiological data. Neuroimage 2016; 126: 81–95.

Vigneau M, Beaucousin V, Hervé PY, Duffau H, Crivello F, Houdé O, et al. Meta-analyzing left hemisphere language areas: Phonology, semantics, and sentence processing. Neuroimage 2006; 30: 1414–1432.

Vincent JL, Patel GH, Fox MD, Snyder AZ, Baker JT, Van Essen DC, et al. Intrinsic functional architecture in the anaesthetized monkey brain. Nature 2007; 447: 83–86.

Vohr B. Speech and language outcomes of very preterm infants. In: Seminars in Fetal and Neonatal Medicine. Elsevier; 2014. p. 78–83.

Vohr B, Ment LR. Intraventricular hemorrhage in the preterm infant. Early Hum. Dev. 1996; 44: 1–16.

Vohr BR, Wright LL, Poole WK, McDonald SA. Neurodevelopmental outcomes of extremely low birth weight infants< 32 weeks' gestation between 1993 and 1998. Pediatrics 2005; 116: 635–643.

Volpe JJ. Subplate neurons-missing link in brain injury of the premature infant? Pediatrics 1996; 97: 112–113.

Volpe JJ. Neurology of the newborn. 5th. Philadelphia: Saunders Elsevier 2008

Volpe JJ. Brain injury in premature infants: a complex amalgam of destructive and developmental disturbances. Lancet Neurol. 2009a; 8: 110–124.

Volpe JJ. The encephalopathy of prematurity—brain injury and impaired brain development inextricably intertwined. In: Seminars in pediatric neurology. Elsevier; 2009. b. p. 167–178.

Volpe JJ, Kinney HC, Jensen FE, Rosenberg PA. The developing oligodendrocyte: key cellular target in brain injury in the premature infant. Int. J. Dev. Neurosci. 2011; 29: 565–582.

De Vries LS, Groenendaal F, Van Haastert IC, Eken P, Rademaker KJ, Meiners LC. Asymmetrical myelination of the posterior limb of the internal capsule in infants with periventricular haemorrhagic infarction: an early predictor of hemiplegia. Neuropediatrics 1999; 30: 314–319.

de Vries LS, van Haastert I-LC, Rademaker KJ, Koopman C, Groenendaal F. Ultrasound abnormalities preceding cerebral palsy in high-risk preterm infants. J. Pediatr. 2004; 144: 815–820.

De Vries LS, Rademaker KJ, Groenendaal F, Eken P, Van Haastert IC, Vandertop WP, et al. Correlation between neonatal cranial ultrasound, MRI in infancy and neurodevelopmental outcome in infants with a large intraventricular haemorrhage

with or without unilateral parenchymal involvement. Neuropediatrics 1998; 29: 180–188.

de Vries LS, Roelants-van Rijn AM, Rademaker KJ, van Haastert IC, Beek FJA, Groenendaal F. Unilateral parenchymal haemorrhagic infarction in the preterm infant. Eur. J. Paediatr. Neurol. 2001; 5: 139–149.

Vuadens F, Benay C, Crettaz D, Gallot D, Sapin V, Schneider P, et al. Identification of biologic markers of the premature rupture of fetal membranes: proteomic approach. Proteomics 2003; 3: 1521–1525.

Wakana S, Caprihan A, Panzenboeck MM, Fallon JH, Perry M, Gollub RL, et al. Reproducibility of quantitative tractography methods applied to cerebral white matter. Neuroimage 2007; 36: 630–644.

Wakana S, Jiang H, Nagae-Poetscher LM, van Zijl PCM, Mori S. Fiber Tract–based Atlas of Human White Matter Anatomy1. Radiology 2004; 230: 77–87.

Wang K, Li M, Hakonarson H. Analysing biological pathways in genome-wide association studies. Nat. Rev. Genet. 2010; 11: 843–854.

Wang Y, Gupta A, Liu Z, Zhang H, Escolar ML, Gilmore JH, et al. DTI registration in atlas based fiber analysis of infantile Krabbe disease. Neuroimage 2011; 55: 1577–1586.

Wedeen VJ, Hagmann P, Tseng WI, Reese TG, Weisskoff RM. Mapping complex tissue architecture with diffusion spectrum magnetic resonance imaging. Magn. Reson. Med. 2005; 54: 1377–1386.

Wegelin JA. A Survey of Partial Least Squares (PLS) Methods, with Emphasis on the Two-Block Case. 2000

Weiss-Croft LJL, Baldeweg T. Maturation of language networks in children: A

systematic review of 22years of functional MRI. Neuroimage 2015; 123: 269–281.

Werker J, Hensch T. Critical periods in speech perception: new directions. Psychology 2015

Werker J, Lalonde C. Cross-language speech perception: Initial capabilities and developmental change. Dev. Psychol. 1988

Werker J, Tees R. Cross-language speech perception: Evidence for perceptual reorganization during the first year of life. Infant Behav. Dev. 2002

Werker JF, Tees RC. Cross-language speech perception: Evidence for perceptual reorganization during the first year of life. Infant Behav. Dev. 1984; 7: 49–63.

Westbrook C, Roth CK. MRI in Practice. John Wiley & Sons; 2011.

Whitney C, Weis S, Krings T, Huber W. Task-dependent modulations of prefrontal and hippocampal activity during intrinsic word production. J. Cogn. 2009

Willems R, Özyürek A, Hagoort P. Differential roles for left inferior frontal and superior temporal cortex in multimodal integration of action and language. Neuroimage 2009

Wilson-Costello D, Friedman H, Minich N, Siner B, Taylor G, Schluchter M, et al. Improved neurodevelopmental outcomes for extremely low birth weight infants in 2000–2002. Pediatrics 2007; 119: 37–45.

Wilson BJ, Sundaram SK, Huq AHM, Jeong JW, Halverson SR, Behen ME, et al. Abnormal language pathway in children with Angelman syndrome. Pediatr. Neurol. 2011; 44: 350–356.

Wilson S, Galantucci S, Tartaglia M, Rising K. Syntactic processing depends on dorsal language tracts. Neuron 2011

Wilson S, Isenberg A, Hickok G. Neural correlates of word production stages

delineated by parametric modulation of psycholinguistic variables. Hum. Brain Mapp. 2009

Winkler AMA, Ridgway GRG, Webster MA, Smith SSM, Nichols TE. Permutation inference for the general linear model. Neuroimage 2014; 92: 381–397.

Wise R, Scott S, Blank S, Mummery C, Murphy K. Separate neural subsystems withinWernicke's area'. Brain 2001

Wolke D, Meyer R. Cognitive status, language attainment, and prereading skills of 6-year-old very preterm children and their peers: the Bavarian Longitudinal Study. Dev. Med. Child Neurol. 1999; 41: 94–109.

Wolke D, Strauss VY-C, Johnson S, Gilmore C, Marlow N, Jaekel J. Universal gestational age effects on cognitive and basic mathematic processing: 2 cohorts in 2 countries. J. Pediatr. 2015; 166: 1410–1416.

Wood a G, Harvey a S, Wellard RM, Abbott DF, Anderson V, Kean M, et al. Language cortex activation in normal children. Neurology 2004; 63: 1035–1044.

Wood NS, Marlow N, Costeloe K, Gibson AT, Wilkinson AR. Neurologic and developmental disability after extremely preterm birth. N. Engl. J. Med. 2000; 343: 378–384.

Woolrich MW, Stephan KE. Biophysical network models and the human connectome. Neuroimage 2013; 80: 330–338.

Xu Y, Gandour J, Talavage T, Wong D. Activation of the left planum temporale in pitch processing is shaped by language experience. Hum. brain 2006

Yakovlev PI, Lecours AR. The myelogenetic cycles of regional maturation of the brain. Reg. Dev. brain early life 1967: 3–70.

Ye Z, Habets B, Jansma B, Münte T. Neural basis of linearization in speech

production. J. Cogn. 2011

Yeatman J, Ben-Shachar M, Glover G. Individual differences in auditory sentence comprehension in children: An exploratory event-related functional magnetic resonance imaging investigation. Brain Lang. 2010

Yeatman JD, Dougherty RF, Ben-Shachar M, Wandell BA. Development of white matter and reading skills. Proc. Natl. Acad. Sci. 2012; 109: E3045–E3053.

Yeatman JD, Dougherty RF, Rykhlevskaia E, Sherbondy AJ, Deutsch GK, Wandell B a., et al. Anatomical properties of the arcuate fasciculus predict phonological and reading skills in children. J. Cogn. Neurosci. 2011; 23: 3304–3317.

Yeo BTT, Eickhoff SB. Systems neuroscience: A modern map of the human cerebral cortex. Nature 2016

Zaehle T, Geiser E, Alter K, Jancke L, Meyer M. Segmental processing in the human auditory dorsal stream. Brain Res. 2008

Zalesky A. Moderating registration misalignment in voxelwise comparisons of DTI data: a performance evaluation of skeleton projection. Magn. Reson. Imaging 2011; 29: 111–125.

Zalesky a., Fornito a., Cocchi L, Gollo LL, Breakspear M. Time-resolved resting-state brain networks. Proc. Natl. Acad. Sci. 2014; 111: 10341–10346.

Zalesky A, Breakspear M. Towards a statistical test for functional connectivity dynamics. Neuroimage 2015; 114: 466–470.

Zatorre R, Halpern A. Mental concerts: musical imagery and auditory cortex. Neuron 2005

Zevin J, Yang J, Skipper J. Domain general change detection accounts for 'dishabituation' effects in temporal–parietal regions in functional magnetic

resonance imaging studies of speech. J. 2010

Zheng Z, Munhall K, Johnsrude I. Functional overlap between regions involved in speech perception and in monitoring one's own voice during speech production. J. Cogn. Neurosci. 2010

Zubicaray G de, McMahon K. Auditory context effects in picture naming investigated with event-related fMRI. Cogn. Affect. Behav. 2009

Appendix A: MRI Physics and Analysis

Magnetic Resonance Imaging

The foundations of MRI are the physical principles of nuclear magnetic resonance (NMR), which provides the measured signal (Rabi *et al.*, 1938; Bloch, 1946; Purcell *et al.*, 1946), and the localization of this NMR signal in space (Lauterbur, 1973; Mansfield and Grannell, 1973).

NMR signal

NMR measurements are based on the quantum mechanical spin properties of atomic nuclei within a magnetic field. Elementary particles, in particular protons, exhibit a property called spin, an intrinsic angular momentum. Charged particles that have spin appear to rotate about their axis, producing a magnetic moment on the nuclei. This property is most notable in the hydrogen protons (^{1}H) that exist abundantly in water, and by far the most abundant atom in the human body (McRobbie *et al.*, 2007; Westbrook and Roth, 2011).

In the presence of a strong external magnetic field (B_0), the magnetic moment interacts with that field inducing a rotation about the axis of B_0, termed precession (Figure 33). The magnetic moment of the particle will precess around the field with angular frequency ω_0 determined by the equation:

$$\omega_0 = \gamma B_0$$

where ω_0 is the Larmor frequency (or resonant frequency) and γ is the gyromagnetic ratio – a constant for specific nuclei in a magnetic field (γ = 42.57 MHz/T for 1H).

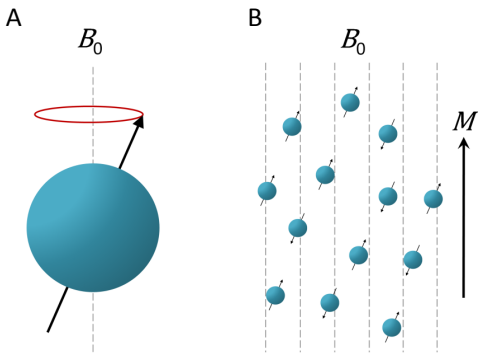

FIGURE 33 SPIN PRECESSION IN A MAGNETIC FIELD

Protons possess spin, a quantum property that induces a molecular moment (A; black arrow) along the axis of rotation. When an external magnetic field is applied, spins precess about the field with frequency ω (A) and align parallel to it (B), producing a net magnetisation vector M.

Given a specific body of atomic nuclei in the presence of a magnetic field, some will have spins aligned with the B_0 field and some anti-aligned with it. If the number of aligned and anti-aligned spins is equal, from the principles of thermodynamics, the net contribution of the nuclei is equal and there is a state of equilibrium with respect to B_0. If this is the case then it is not possible to distinguish any signal from them.

To measure a signal, the net equilibrium magnetization M_0 must be perturbed or excited, such that a component of magnetisation lies in the plane orthogonal to the B_0 field. To do so, an external B_1 field is applied. B_1 is a transverse radiofrequency (RF) electromagnetic field with a frequency set to the Larmor frequency ω_0 and a magnitude order of μT (in contrast to B_0 field that is static with magnitude generally in the order of Tesla). By applying the B_1 field to the system, with ^{1}H-specific resonant frequency, hydrogen protons are excited into the higher energy state –

reducing longitudinal (parallel to B_0) magnetisation – and inducing phase coherence in the precessing spins – increasing transverse (parallel to B_1) magnetisation (Figure 34). The degree to which net magnetisation rotates away from the longitudinal axis is termed the *flip angle*. As the magnetisation vector rotates in the transverse plane it induces a current in a receiver coil placed perpendicular to B_0, which is recorded as an oscillating MR signal.

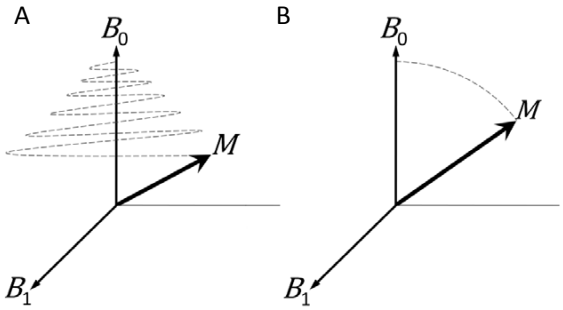

FIGURE 34 RF-EXCITATION OF PRECESSING SPINS

The application of an RF-excitation field $B1$ causes the net magnetisation vector to spiral towards the transverse plane at the angular frequency ω (A). In a rotating frame of reference (B) this can be represented as a rotation of the vector towards the xy-plane.

The cessation of the transverse RF pulse causes the spins to gradually revert to their original state. This process is characterized by two *relaxation* times: $T1$ (or spin-lattice relaxation), is the time taken for longitudinal magnetisation to recover to 63% of its equilibrium as spins return to a low energy state; and *T2* (or spin-spin relaxation), which is the time taken for 63% of the received MRI signal to decay due to a loss of coherence in the precessing spins and a decrease in transverse magnetisation. In practice, signal decay due to dephasing occurs faster than is suggested by $T2$ due to local inhomogeneity of $B0$: this time is referred to as $T2*$.

Importantly, $T1$ and $T2$ are not constant and differ according to the medium in which they are measured. This provides the contrast mechanism necessary to image the different tissues of the brain.

Localization of NMR signal

To perform imaging, the NMR signals must be spatially localised. This is achieved by using spatially-varying magnetic gradients, another set of magnetic fields to modify the spatial distribution of the main magnetic field B0 and therefore encode space (Lauterbur, 1973). These are configured such that a series of linear gradients are present in B0 in each orthogonal direction.

With these gradients present, the angular frequency of precession at each spatial location is given by:

$$\omega x = (B0 + Gx)$$

where G is an additional magnetic gradient applied over an axis (x) and exerts a position dependent shift in the precessional frequency (ω) of spins in the magnetic field. It is then possible to find the location of a signal from the angular frequency of the magnetisation that produces that signal. This is known as frequency encoding.

In addition, a gradient applied along the y axis (Gy) can be used to alter the phase of the precessing spins, inducing position-dependent phase shifts. By using phase-encoding gradients of different magnitudes, precessing spins along the y-axis acquire a specific, and position-dependent, rate of change of phase (or frequency) in the y-axis. The spatial position is therefore encoded in a two-dimensional plane according to both the phase and frequency of the received signal.

These data are stored in *k*-space, a two-dimensional matrix in the spatial frequency domain, where one row is filled after each phase-encoding step and from which the MR image can be calculated by two-dimensional Fourier transform.

To encode the third-dimensional direction a third additional gradient is used by applying a slice-select gradient (*Gz*) perpendicularly to both *Gx* and *Gy*. By altering the RF pulse frequency, consecutive 'slices' of *z* can be excited prior to two-dimensional phase- and frequency-encoding in the *xy* plane.

T_1 and T_2-weighting

Although a discussion of different RF pulse sequences is not the purpose of this thesis, it has to be highlighted that the timing of each magnetic gradient and RF pulse is critical for MR acquisition and image contrast. The received MR signal is governed by two tissue-dependent properties (*T*1 and *T*2) and by altering the time between consecutive RF excitations pulses (repetition time; TR) and between the RF excitation pulse and signal readout (echo time; TE), it is possible to achieve different *T*1- and *T*2-weighting (Figure 35).

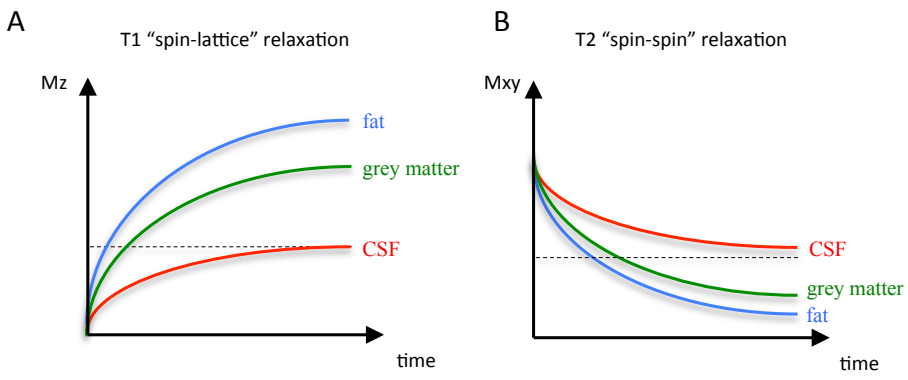

FIGURE 35 T1- AND T2-WEIGHETD IMAGE CONTRAST DEPENDS ON TIME CONSTANTS T1 AND T2 BEING DIFFERENT ACROSS BRAIN TISSUES.

A) T1 is defined as the time taken for the longitudinal magnetisation (Mz) to recover to 63% of its equilibrium value, and is considerably longer for fluid (such as cerebro-spinal fluid, CSF) in comparison to fat (such as myelinated white-matter regions). B) T2 is defined as the time taken for 63% of the transverse magnetisation (Mxy) to decay due to spin dephasing, and is shorter when protons are bound to macromolecules such as fat.

*T*1-weighted images are typically acquired with variants of a gradient-echo sequence, a rapid sequence that allows for smaller flip angles and shorter TR and TE times. A shorter TR does not allow for full recovery of longitudinal magnetisation before the next RF pulse. Thus, in tissues with long *T*1 (such as cerebro-spinal fluid, CSF), magnetisation does not recover fully before RF excitation, resulting in lower transverse magnetisation and less contribution to the MR signal after excitation. *T*2-weighted images are typically acquired using spin-echo sequences with longer TR (greater than *T*1) to allow full recovery of longitudinal magnetisation and a larger flip angle to maximise transverse magnetisation after RF excitation. The TE is usually selected in order to maximise the difference in signal T2 decay or relaxation time between tissue types.

During a spin-echo sequence, signal attenuation due loss of phase coherence is counteracted by the application of a 180° RF pulse at time *t* which flips the magnetization in the *xy* plane, causing the spins to rephase at time *2t*. As the spins continue to de-phase according to the local field this leads to a recovery of alignment and partial recovery of signal, producing a phase-coherent MR signal. This sequence can be extended to include multiple rephasing RF pulses (an echo train) continually flipping magnetisation and providing multiple signal readouts from an initial single

90˚RF excitation pulse. As each echo fills a row of *k*-space, fast spin echo sequences greatly decrease scanning time.

To achieve even faster acquisitions, echo-planar imaging (EPI) has been developed (Mansfield, 1977; Ordidge *et al.*, 1981). In contrast to sequences that fill *k*-space one row at a time, this technique can fill *k*- space with a single acquisition, allowing whole-brain images in under 100 ms through the rapid switching of gradients. The basic EPI sequence requires rapid oscillation of the frequency-encoding gradient to produce a train of gradient echoes, each one of which is phase encoded differently (Stehling *et al.*, 1989).

EPI requires specific MR scanner hardware that is capable of producing large, fast gradient oscillations and is susceptible to signal artefacts and geometric distortions due to eddy current effects and local field inhomogeneities caused by the rapidly switching gradients (Jezzard *et al.*, 1998). Also, single-shot EPI is commonly of poorer contrast and lower resolution than other forms of MRI, but it allows the capture of rapidly changing dynamic processes, most notably changes in blood oxygenation in functional MRI and the diffusion of water molecules in diffusion MRI, that have led to wide application as a clinical and research tool.

Appendix B: Paper accepted for publication

Language ability in preterm children is associated with arcuate fasciculi microstructure at term

P Salvan, JD Tournier, D Batalle, S Falconer, A Chew, N Kennea, P Aljabar, G Dehaene-Lambertz, T Arichi, AD Edwards, SJ Counsell,

Human Brain Mapping 2017

Language Ability in Preterm Children Is Associated with Arcuate Fasciculi Microstructure at Term

Piergiorgio Salvan,[1] J. Donald Tournier,[1] Dafnis Batalle,[1] Shona Falconer,[1] Andrew Chew,[1] Nigel Kennea,[2] Paul Aljabar,[1] Ghislaine Dehaene-Lambertz,[3] Tomoki Arichi,[1,4] A. David Edwards,[1,4]* and Serena J. Counsell[1]

[1]*Centre for the Developing Brain, Division of Imaging Sciences & Biomedical Engineering, King's College London, United Kingdom*
[2]*Neonatal unit, St. George's University Hospital NHS, London, United Kingdom*
[3]*INSERM-CEA, Neurospin Center, Cognitive Neuroimaging Unit, Gif-Sur-Yvette, France*
[4]*Department of Bioengineering, Imperial College London, United Kingdom*

Abstract: In the mature human brain, the arcuate fasciculus mediates verbal working memory, word learning, and sublexical speech repetition. However, its contribution to early language acquisition remains unclear. In this work, we aimed to evaluate the role of the direct segments of the arcuate fasciculi in the early acquisition of linguistic function. We imaged a cohort of 43 preterm born infants (median age at birth of 30 gestational weeks; median age at scan of 42 postmenstrual weeks) using high *b* value high-angular resolution diffusion-weighted neuroimaging and assessed their linguistic performance at 2 years of age. Using constrained spherical deconvolution tractography, we virtually dissected the arcuate fasciculi and measured fractional anisotropy (FA) as a metric of white matter development. We found that term equivalent FA of the left and right arcuate fasciculi was significantly associated with individual differences in linguistic and cognitive abilities in early childhood, independent of the degree of prematurity. These findings suggest that differences in arcuate fasciculi microstructure at the time of normal birth have a significant impact on language development and modulate the first stages of language learning. *Hum Brain Mapp 00:000–000, 2017*.

Key words: diffusion magnetic resonance imaging; infant; language development; brain; preterm birth

Contract grant sponsor: National Institute for Health Research (NIHR) under its Programme Grants for Applied Research Programme; Contract grant number: RP-PG-0707-10154; Contract grant sponsor: Academic Clinical Lectureship; Contract grant sponsor: Medical Research Council (UK); Contract grant number: MR/K006355/1 and MR/L011530/1; Contract grant sponsor: PhD studentship.

*Correspondence to: Professor A.D. Edwards, Centre for the Developing Brain, Department of Perinatal Imaging and Health, Division of Imaging Sciences and Biomedical Engineering, King's College London, First Floor South Wing, St Thomas' Hospital, London SE1 7EH, UK. E-mail: ad.edwards@kcl.ac.uk

Received for publication 6 December 2016; Revised 31 March 2017; Accepted 17 April 2017.

DOI: 10.1002/hbm.23632
Published online 00 Month 2017 in Wiley Online Library (wileyonlinelibrary.com).

INTRODUCTION

Comparative studies in humans and nonhuman primates have shown that the evolution of language has resulted from specific modifications of the cortical areas and pathways that mediate linguistic function [Rilling et al., 2008]. The arcuate fasciculus is a bilateral white-matter fiber tract linking the posterior superior temporal cortex (Wernicke's area) to Brodmann area 44 in the frontal cortex (Broca's area) via a dorsal projection that arches around the Sylvian fissure [Catani et al., 2005; Rilling et al., 2008]. In the human brain, diffusion weighted imaging has shown that the organization and cortical terminations of this tract are strongly modified in comparison to primates and has demonstrated that the auditory regions of the temporal cortex have a higher probability of connection via the dorsal pathway with the frontal cortices [Rilling et al., 2008, 2011; de Schotten et al., 2012]. In contrast, axonal tracing studies in monkeys have shown that the arcuate fasciculus connects to more dorsally located regions, such as the extrastriate visual cortex [Petrides and Pandya, 1984; Schmahmann et al., 2007]. Taken together, these findings have generated the theory that the expanded direct dorsal pathway may be a key structure responsible for supporting the emergence of language in humans.

In human adults, the arcuate fasciculus has been proposed to play an important role in the core syntactic computation of complex sentences [Berwick et al., 2013], in verbal short-term memory and in the perception of the phonetic structure of speech [Liberman and Mattingly, 1985]. It is also hypothesized to play a distinctive role in speech production via the integration of auditory and motor representation. Predominantly at the syllable level, it is thought to map sensory targets in the auditory cortex to motor programs coded in Broca's area [Hickok, 2012; Hickok and Poeppel, 2007]. Patients with injuries involving either the left or right arcuate fasciculus have impaired ability in phonological and word repetition tasks and in verbal short-term memory [Alexander et al., 1987; Benson et al., 1973; Damasio and Damasio, 1980; Geschwind, 1965]. With regard to learning, the microstructural properties of the left direct segment of the arcuate fasciculus have been associated with the process of learning new words in adulthood [López-Barroso et al., 2013], whilst improved performance in auditory verbal learning tasks are significantly associated with a less lateralized volumetric pattern of the direct pathways [Catani et al., 2007]. Children with Angelman Syndrome in whom neither the left nor right arcuate fasciculi can be identified on diffusion tractography have no oral language development, whereas when the left arcuate fasciculus cannot be identified language difficulties are always observed [Paldino et al., 2016; Wilson et al., 2011]. These observations confirm the crucial role of the arcuate fasciculus in speech acquisition [Berwick et al., 2013; Hickok and Poeppel, 2007].

As infants have impoverished language production and their reception abilities were thought to be limited to the supra-segmental properties of speech, the role of the arcuate fasciculus has traditionally been considered to be secondary during the first stages of language acquisition. Although inferior frontal regions are activated in several fMRI studies in infants [Baldoli et al., 2015; Dehaene-Lambertz et al., 2006; Perani et al., 2011; Shultz et al., 2014], the ventral pathway, comprising the uncinate and the inferior fronto-occipital fasciculus, has been proposed to initially be the main functional linguistic pathway connecting temporal and frontal areas [Brauer et al., 2013; Dubois et al., 2015; Perani et al., 2011]. Recent advances in diffusion-weighted imaging have enabled the investigation of white-matter tracts thought to be involved in the acquisition of language and neurodevelopmental skills during the neonatal period [Brauer et al., 2013; Dubois et al., 2015; Perani et al., 2011]. These studies have suggested that, in contrast to the mature brain (where it terminates in Broca's area), the anterior direct segment of the arcuate fasciculus cannot be dissected after the premotor cortex [Dubois et al., 2015]. Whilst this finding may represent a genuine developmental difference in the extent of the arcuate fasciculus [Brauer et al., 2013; Dubois et al., 2015; Perani et al., 2011], it could also reflect the low angular resolution used in the diffusion weighted sequences, which may have limited delineation of the arcuate fasciculus in regions where the fibers cross with the cortico-spinal tracts and the corpus callosum in the corona radiata [Dubois et al., 2015].

Premature birth is associated with verbal impairment, the severity of which increases with increasing prematurity at birth [Luu et al., 2009, 2011; van Noort-van der Spek et al., 2012]. Previous studies of infant brain development have shown that white-matter architecture is significantly altered following premature birth [Ball et al., 2014; Counsell et al., 2003; Hüppi et al., 1998; Rose et al., 2008] and the degree of this alteration is directly related to performance in specific neurodevelopmental domains [Bassi et al., 2008; Berman et al., 2009; Groppo et al., 2014]. It is thus possible that premature delivery also affects the white-matter structures that subserve language function impacting on later linguistic behavior.

To address the question of whether or not the arcuate fasciculus is a specific neurolinguistic precursor in early human infancy; and to assess whether the degree of prematurity affects arcuate fasciculus microstructure and drives the relationship with later linguistic behavior, we used high b value high-angular resolution diffusion-weighted imaging (HARDI) in a cohort of 43 preterm born infants at term equivalent age and assessed their linguistic developmental performance at 2 years. We hypothesized that intersubject differences in composite linguistic skills at 2 years would be associated with term equivalent fractional anisotropy (FA) of the left and right arcuate fasciculi. To act as a control, we tested whether any relationship

between brain structure and language performance could also be associated with FA values of the cortico-spinal tracts and the superior longitudinal fasciculi.

MATERIALS AND METHODS

Infants

Preterm infants were recruited as part of the Evaluation of Preterm Imaging study (Eprime), and were imaged at term equivalent age over a 3 year period (2010–2013) at Queen Charlotte's and Chelsea Hospital, London. The study was reviewed and approved by the National Research Ethics Service, and all infants were studied following written consent from their parents. A cohort of 43 preterm born infants [median age at birth of 30.14 gestational (GA) weeks; range 24–32; 18 females] with no evidence of focal abnormality on MRI were imaged using high-angular resolution diffusion-weighted neuroimaging at 42.14 postmenstrual (PMA) weeks (range 39–46) (Table I), and followed up to around 22 months of age to assess their neurodevelopmental performance.

TABLE I. Infant characteristics

Characteristic	Value
Median (range) GA at birth (weeks)	30 (24 – 33)
Median (range) birth weight (grams)	1205 (645 – 1990)
Median (range) PMA at MRI (weeks)	42 (39 – 46)
Female, no (%)	18 (42%)
Chorioamnionitis, no (%)	1 (2%)
Intrauterine growth restriction, no (%)	7 (16%)
Median (range) mechanical ventilation (days)	0 (0 – 40)
Necrotizing enterocolitis requiring surgery, no (%)	1 (2%)
Mean (± SD) parental SES	17.4293 (±8.0772)

Acquisition of MRI Imaging Data at Term Equivalent Age

All MRI studies were supervised by an experienced pediatrician or nurse trained in neonatal resuscitation. Pulse oximetry, temperature, and heart rate were monitored throughout the period of image acquisition; hearing protection in the form of silicone-based putty placed in the external ear (President Putty, Coltene; Whaledent) and Mini-muffs (Natus Medical) was used for each infant. Sedation (25–50 mg/kg oral chloral hydrate) was administered to 33 infants. Imaging was acquired using an eight-channel phased array head coil on a 3-Tesla Philips Achieva MRI Scanner (Best, The Netherlands) located on the Neonatal Intensive Care Unit. Whole-brain diffusion-weighted MRI data were acquired in 64 noncollinear directions with b value of 2500 s/mm^2 and 4 images without diffusion weighting (isotropic voxel size of 2 mm; TE = 62 ms; TR = 9000 ms). High-resolution anatomical images were acquired with pulse sequence parameters: T1 weighted 3D MPRAGE: TR = 17 ms, TE = 4.6 ms, flip angle 13°, slice thickness 0.8 mm, field-of-view 210 mm, matrix 256 × 256 (voxel size: 0.82 × 0.82 × 0.8 mm); and T2 weighted fast-spin echo: TR = 8670 ms, TE = 160 ms, flip angle 90°, slice thickness 2 mm with 1 mm overlap, field-of-view 220 mm, matrix 256 × 256 (effective voxel size: 0.86 × 0.86 × 1 mm).

Neurodevelopmental Assessment at 22 Months

Standardized neurodevelopmental assessment at a median age of 22 months (range: 21–24 months; median of 20 months corrected for prematurity) was carried out by an experienced pediatrician or developmental psychologist with the Bayley Scales of Infant and Toddler Development, Third Edition (BSID-III) [Bayley, 2006].

MRI Data Preprocessing

T2-weighted brain volumes were bias corrected, brain extracted and tissue segmented into white matter, gray matter, deep gray matter structures, and cerebrospinal fluid using a neonatal specific segmentation tool [Makropoulos et al., 2014]. Diffusion MRI volumes were first visually inspected to detect and exclude data with motion artifact. All subjects included in the study had 5 or fewer volumes excluded due to head-motion. B0 field inhomogeneities, eddy currents, and intervolume motion were corrected using topup and eddy tools in FSL5 [Andersson and Sotiropoulos, 2016; Andersson et al., 2003; Smith et al., 2004, 2015]. B1 field inhomogeneity was corrected using ITK-N4 [Tustison et al., 2010]. All rigid registrations in native subject space were estimated using FSL boundary-based registration optimized for neonatal tissue contrasts [Toulmin et al., 2015]; and nonlinear registrations to the T2-weighted template were estimated using Advanced Normalization Tools [Avants et al., 2008]. All transformation pairs were calculated independently and combined into a single transform to reduce interpolation error.

Tractography of the Arcuate Fasciculi

Estimation of fiber orientation distribution was computed through constrained spherical deconvolution [Tournier et al., 2004, 2007], with maximum spherical harmonic order of 8. We used the MRtrix3 package to perform anatomically constrained probabilistic tractography (http://www.mrtrix.org) [Smith et al., 2012; Tournier et al., 2012]. Fiber-tracking of the arcuate fasciculus was performed in each subject's native space independently for both hemispheres, using a two-region of interest approach. From the T2-weighted template, we back-projected two inclusion regions of interest and a seed-plane. To maximize the chances of virtually dissecting the arcuate fasciculus, the

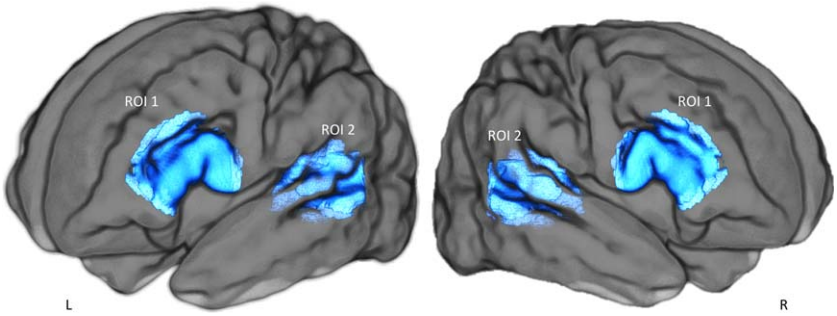

Figure 1.
Regions of interest used to perform anatomically constrained spherical deconvolution tractography of the direct segment of the arcuate fasciculus. ROI 1: Broca's region (for the left and right hemisphere); ROI 2: Wernicke's region (for the left and right hemisphere). Fiber-tracking of the arcuate fasciculus was performed in each subject's native space independently for both hemispheres. Only streamlines crossing both regions of interest were considered.

seed-plane was located in its direct dorsal pathway transverse to its antero-posterior direction, and random seed-streamlines were generated within it. The frontal region of interest was identified anterior to the central sulcus, to encompass the white matter of the posterior region of the inferior and middle frontal gyri. The temporal region of interest was defined in the white matter of the posterior part of the superior and middle temporal gyri (Fig. 1) [Forkel et al., 2014]. We extracted the median FA value along the reconstructed tract in both hemispheres as a measure of the white-matter microstructure [Beaulieu, 2002; López-Barroso et al., 2013].

Tractography of the Cortico-Spinal Tracts

To act as control regions, the left and right cortico-spinal tracts were also delineated. From the T2-weighted template, we back-projected a seed-region (an axial delineation of the pons) and two inclusion regions (the posterior limbs of the internal capsule and two axial-planes at the level of the primary motor and somatosensory cortices). We then extracted the median FA value along the reconstructed tract in both hemispheres.

Tractography of the Superior Longitudinal Fasciculi

To reconstruct the superior longitudinal fasciculi bilaterally we back-projected a seed-region (an axial plane delineating the parietal cortex) and an inclusion region (a coronal plane delineating the white matter area anterior of the motor cortex) [de Schotten et al., 2011]. We then extracted the median FA value along the reconstructed tract in both hemispheres.

STATISTICAL ANALYSIS

To address the microstructural effect of neonatal development and early environmental factors linked to premature delivery, we used a general linear model (GLM) to test the linear association between arcuate fasciculi FA, cortico-spinal tracts FA, and global white-matter median FA, with (1) PMA at scan (covaried for GA at birth); and (2) GA at birth (covaried for PMA at scan). The number of days of ex-utero life was highly correlated with PMA at scan and GA at birth (Pearson's correlation coefficient of postnatal age respectively with PMA and GA: $r = 0.79$; $P < 10^{-5}$; $r = -0.90$; $P < 10^{-5}$) and so we did not include this as a covariate in the model.

The primary goal of this study was to assess the role of the direct segments of the arcuate fasciculi in the early acquisition of linguistic function. To do this, we tested whether intersubject differences in composite linguistic skills at two years were associated with term equivalent FA of the left and right direct segments of the arcuate fasciculi.

We removed the effect of confound variables prior to the analysis; these were PMA (for the FA measures) and socioeconomic score (for linguistic skill measures). All features were standardized in the training sets to have zero mean and unit variance and the same transformation was then applied to the testing sets.

To test whether FA values of the left and right arcuate fasciculus was associated with composite linguistic skills at 2 years we first used cross-validated Ordinary Least Squares (OLS) regression. However, coefficient estimates for OLS rely on the independence of the model terms and in this case the measured FA in left and right arcuate fasciculus were highly correlated ($r = 0.58$; $P < 10^{-5}$). To overcome this, we used cross-validated Ridge regression (a linear least squares variant with L_2 regularization) and Partial Least Squares (PLS) regression. PLS is particularly suitable in cases where predictors are highly correlated or

even collinear, that is, where standard regression is not appropriate [Hotelling, 1936; Wegelin, 2000]. The approach identifies linear combinations of the independent variables that optimally predict corresponding combinations of the dependent variables [Rosipal and Krämer, 2006]. Here, it was applied with mode A and deflation mode canonical [Wegelin, 2000].

We used leave-one-out cross-validated PLS to assess whether intersubject differences in linguistic abilities at 2 years of age were associated with term equivalent FA of the left and right arcuate fasciculi. At each training iteration, the data for $n-1$ subjects were used to train a PLS model; the learnt link was then used to generate the linguistic score for the left-out subject. Following all iterations, the correlation between PLS FA scores and PLS language scores was assessed. We then extracted the PLS relative loadings of involvement averaged across all cross-validation folds; the mean and standard deviation (SD) of these parameters were extracted to assess model stability.

As a control, we also used the same cross-validated pipeline to test whether individual-differences in linguistic performance were associated with left and right cortico-spinal tracts FA, and left and right superior longitudinal fasciculus FA.

To test whether early environmental influences associated with preterm birth or global white-matter volume [Northam et al., 2012] were driving the identified brain-behavior link in a dose-dependent fashion, we calculated the partial correlation between PLS FA scores and PLS language scores adjusting for GA at birth, global white matter volume, and sex.

Statistical significance was determined with nonparametric permutation testing (10,000 permutations) with correction for the Family wise error (FWE) rate [Winkler et al., 2014]. All analysis were performed using MATLAB (R2015b, The MathWorks, Natick, MA) and Scikit-learn [Pedregosa et al., 2011].

RESULTS

Neurodevelopmental Assessment

At 2 years of age, the mean scores of the BSID-III composite language and cognitive abilities were respectively 90 (SD ± 16.20) and 92 (SD ± 11.85), with a correlation between the two of $r = 0.79$; $P = 10^{-5}$. No significant correlation was found between PMA at scan and composite language score. A trend toward significance was found between GA at birth and composite language score ($r = 0.21$; $P = 0.09$); a significant correlation was found between socioeconomic score (measured as the English Index of Multiple Deprivation) and composite language score ($r = -0.28$; $P = 0.03$).

Impact of Prematurity on the Arcuate Fasciculus Microstructure

During the term equivalent period, prominent development occurred in the left and right arcuate fasciculi microstructure (respectively, FWE corrected P-values = 0.0002 and 0.0013); in the cortico-spinal tracts (respectively left and right, FWE corrected P-values = 0.0001 and 0.0016); and in the superior longitudinal fasciculus (respectively left and right, FWE corrected P-values = 0. 0007 and 0.0014). Increased prematurity at birth was associated with significantly lower term equivalent FA of the left arcuate fasciculus (FWE corrected P-value = 0.0130) and a trend toward lower FA in right arcuate fasciculus (FWE corrected P-values = 0.0612; Table II). We also found no significant difference between the left and right arcuate fasciculi in terms of term equivalent FA (Wilcoxon signed rank test: Zval = 0.07; $P = 0.94$) or tract length (corrected for brain volume; Wilcoxon signed rank test: Zval = 0.01; $P = 0.99$).

TABLE II. The impact of degree of prematurity on white matter microstructure

	PMA (cov GA)	GA (cov PMA)
Left arcuate FA	0.0002	0.0130
Right arcuate FA	0.0013	0.0612
Left cortico-spinal FA	0.0001	0.3448
Right cortico-spinal FA	0.0016	0.8370
Left superior longitudinal FA	0.0007	0.9995
Right superior longitudinal FA	0.0004	0.5590

We assessed the effect of age at scan and gestational age at birth on arcuate fasciculi, cortico-spinal tracts, and superior longitudinal fasciculi FA. Showing FWE corrected P-values from GLM testing (10,000 permutations). A: Between 39 and 46 postmenstrual weeks, significant development (measured by PMA at scan covaried GA at birth) occurs in the arcuate fasciculi, cortico-spinal tract, and superior longitudinal fasciculi microstructure. B: Increased prematurity at birth (measured by GA at birth covaried PMA at scan) is significantly associated with lower term equivalent FA of left arcuate fasciculus and a nonsignificant trend is seen in the right arcuate fasciculus.

Term Equivalent Arcuate Fasciculus Microstructure Is Associated with Intersubject Differences in Linguistic Skills

Although all cross-validated regression analyses identified statistically significant brain-behavior associations, the PLS regression model achieved greater nonparametric statistical significance when compared with OLS and Ridge regression (Table III). The cross-validated PLS analysis highlighted a statistically significant association between PLS FA scores and PLS language scores ($r = 0.36$; FWE–corrected P-value = 0.0110; Fig. 2). Across folds, the PLS mode accounted for 72% of variance in the arcuate fasciculi FA. The mean of the identified PLS loadings (0.6650 for left and 0.7736 for right) was two orders of magnitude higher than their SD (0.0059 and 0.0099), highlighting strong model stability. The overall strong

TABLE III. Relationship between linguistic skills at 2 years and FA of the left and right arcuate fasciculi at term equivalent

	Arcuate fasciculi FA		Cortico-spinal tracts FA		Superior Longitudinal fasciculi FA	
	r	FWE-corrected *P*-value	*r*	FWE-corrected *P*-value	*r*	FWE-corrected *P*-value
OLS	0.31	0.0275	−0.06	0.4839	−0.02	0.4325
Ridge	0.29	0.0305	−0.04	0.4556	−0.01	0.4166
PLS	0.36	0.0110	0.11	0.2785	0.16	0.2697

Showing rho correlation coefficient between FA at term equivalent and language scores at two years across different regression models and respective FWE-corrected *P*-values. The cross-validated PLS regression demonstrated greater nonparametric statistical significance values. However, no statistically significant association was found when testing the link between linguistic scores and FA of the cortico-spinal tracts or FA of the superior longitudinal fasciculus

positive PLS loadings indicates that children who developed higher linguistic performance at two years were those with higher FA along both the left and right arcuate fasciculi at term equivalent age.

The identified relationship remained significant when tested using partial correlation while adjusting for gestational age at birth, sex, and global white matter volume ($r = 0.32$, FWE–corrected P-value = 0.0230). We then quantified the independent contribution of each variable in the relationship with language abilities (Table IV). This analysis confirmed that the only significant contribution was arcuate fasciculi FA (FWE-corrected P-value = 0.0226).

To determine whether efficient linguistic abilities at 2 years were related to higher FA in both arcuate fasciculi, we tested the alternative hypothesis that lateralization in the arcuate fasciculi FA would be associated with later linguistic abilities. We found no significant association between the degree of asymmetry in the arcuate fasciculus microstructure [(Left FA − Right FA)/(Left FA + Right FA)] and composite linguistic skills at 2 years (GLM testing with 10,000 permutations: positive contrast FWE-corrected P-value = 0.8918; negative contrast FWE-corrected P-value = 0.1129).

When cognitive scores at 2 years were added to the model as an additional response variable, intersubject differences in linguistic and cognitive abilities remained associated with term-equivalent FA of left and right arcuate fasciculus ($r = 0.37$; FWE–corrected P-value = 0.0148). Higher linguistic and cognitive performance at two years of age were linked with higher FA along both the left and right arcuate fasciculi at term equivalent age. Across folds,

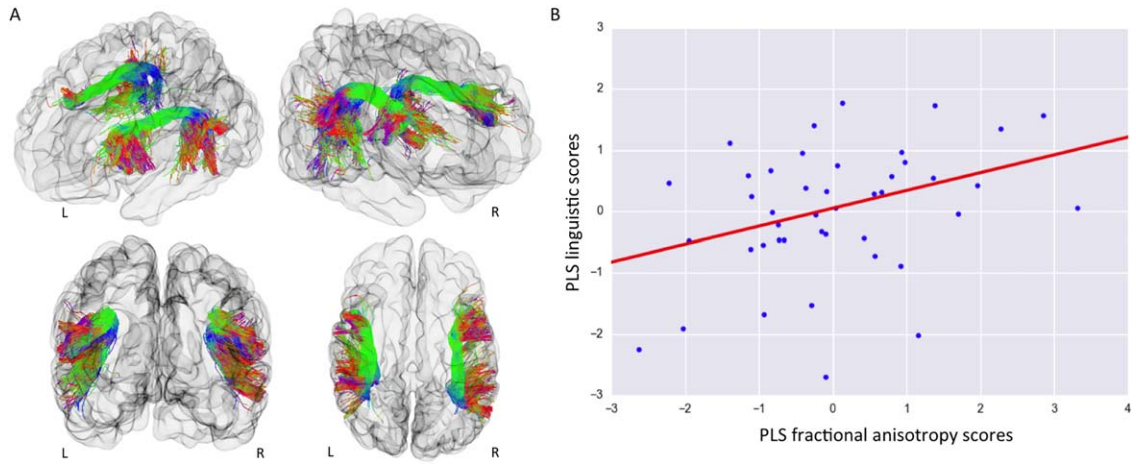

Figure 2.

Intersubject differences in linguistic performance at two years were associated with term equivalent FA of the left and right arcuate fasciculus independently of degree of prematurity. A: Visualization of an infant brain and the reconstructed arcuate fasciculi from left-frontal; right-frontal; frontal and top view. The tracts are colored by direction: green for anterior-posterior; red for left-right; blue for superior-inferior. B: Using cross-validated partial-least-square regression, one statistically significant mode of brain-behavior covariation between PLS FA scores and PLS language scores was identified ($r = 0.36$; FWE–corrected P-value = 0.0110). Term equivalent FA of the left and right arcuate fasciculi was associated with individual differences in composite linguistic skills in early childhood. This link was still present even when controlling for degree of premature delivery measured by GA at birth ($r = 0.32$, FWE–corrected P-value = 0.0230).

TABLE IV. Independent contribution of each variable in the identified relationship with language abilities

Variables	FWE-corrected *P*-value
PLS FA scores arcuate fasciculus	0.0226
Gestational age	0.3712
Sex	0.1174
White-matter volume	0.2694

The relation between arcuate fasciculus FA and linguistic skills at two years remained significant after correction for gestational age at birth, sex, and global white matter volume (partial correlation $r = 0.32$, FWE–corrected *P*-value = 0.0230). Here, we used a GLM to assess the independent contribution of each predictor in the relationship with linguistic skills. Only the arcuate fasciculus FA was significantly associated with later language abilities, suggesting that the identified relationship was not driven by confounds of interest.

the PLS mode accounted for 72 and 71% of variance respectively in X and Y space. High model stability in PLS loadings was highlighted also in this case (Fig. 3, Table V).

Intersubject Differences in Linguistic Skills Are Not Associated with FA of the Cortico-Spinal Tract or Superior Longitudinal Fasciculus at Term Equivalent Age

To test whether the identified relationship between term-equivalent microstructure and linguistic abilities at two years of age was specific for arcuate fasciculus FA, we also tested the relationship with two other major white matter pathways: the cortico-spinal tracts (which are known to be involved in motor function) and the superior longitudinal fasciculi, (a cortico-cortical tract known to be involved in visual-spatial attention and visual-spatial working memory [de Schotten et al., 2011; Vestergaard et al., 2011].

TABLE V. PLS loadings in the initial sets of variables

		PLS loading
X space:		
	FA left arcuate fasciculus	0.66 ± SD 0.006
	FA right arcuate fasciculus	0.78 ± SD 0.009
Y space:		
	Linguistic skills	0.71 ± SD 0.003
	Cognitive skills	0.71 ± SD 0.002

Showing the PLS loadings of involvement in the identified link between the left and right arcuate fasciculus microstructure, and linguistic and cognitive performance. Mean PLS loadings of involvement ± SD averaged across folds. The PLS mode accounted for 72 and 71% of variance, respectively, in X and Y space. The small SDs of the estimated PLS loadings highlight strong model stability

Linguistic skills at two years of age were not significantly associated with term-equivalent FA within either the cortico-spinal tracts ($r = 0.11$, FWE–corrected *P*-value = 0.2785; Fig. 4) or the superior longitudinal fasciculi ($r = 0.16$, FWE–corrected *P*-value = 0.2697). Of interest, FA within the superior longitudinal fasciculi was significantly associated with later general cognitive abilities ($r = 0.32$, FWE–corrected *P*-value = 0.0390). There was no significant relationship between FA of the cortico-spinal tracts and later cognition; $r = 0.12$, FWE–corrected *P*-value = 0.3339).

DISCUSSION

Infants demonstrate linguistic abilities at birth, including discriminating close phonemes [Dehaene-Lambertz and

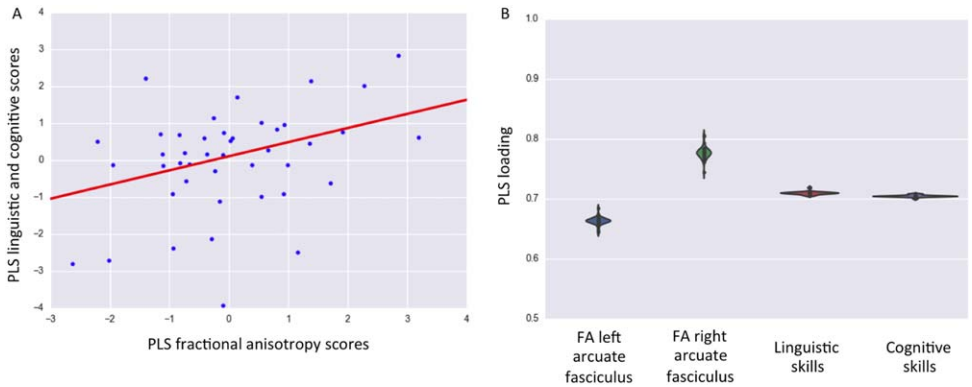

Figure 3.

Association with inter-subject differences in linguistic and cognitive performance at two years of age. A: A significant association was identified between PLS FA scores and PLS language and cognitive scores ($r = 0.37$; FWE–corrected *P*-value = 0.0148). B: PLS loadings of involvement with respect to the initial X space (left and right arcuate fasciculi) and Y space (linguistic and cognitive skills). Note the small dispersion around the means highlight strong model stability. Higher composite linguistic and cognitive skills in early childhood were linked to higher FA of the left and right arcuate fasciculi at term equivalent.

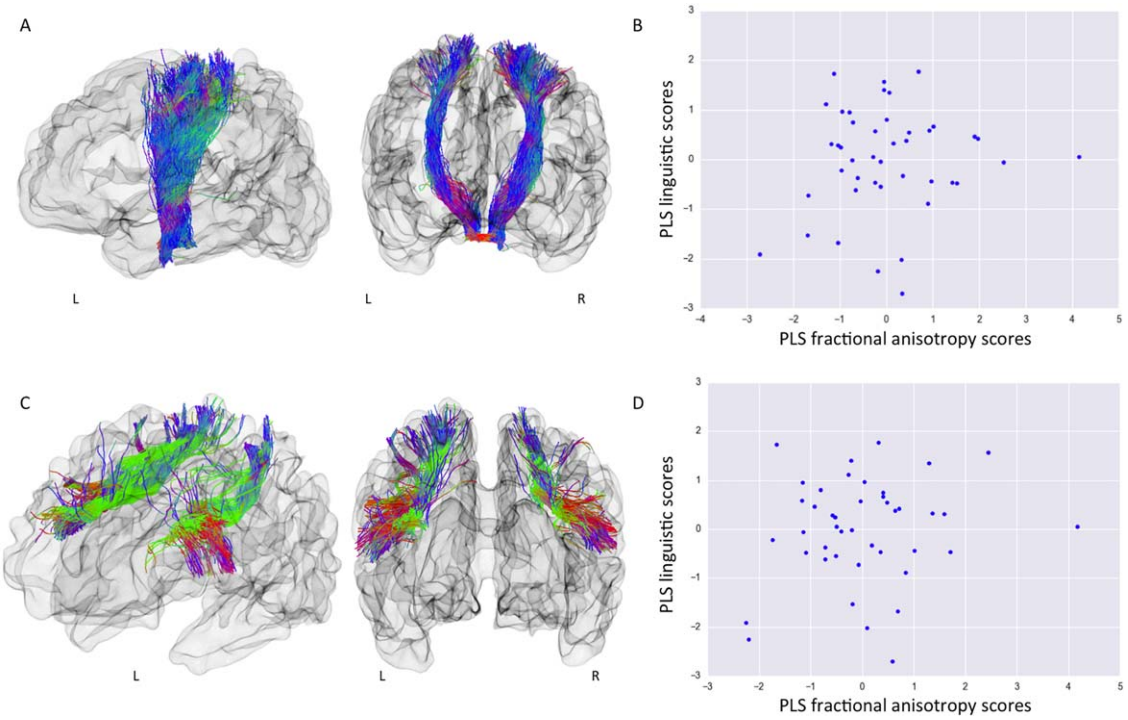

Figure 4.

Term equivalent FA of the cortico-spinal tracts and the superior longitudinal fasciculus is not associated with linguistic abilities at two years. A: Visualization of an infant brain and the reconstructed cortico-spinal tracts from left and frontal view. B: Scatter plot of PLS cortico-spinal tract FA scores versus PLS linguistic scores. Term-equivalent FA of left and right cortico-spinal tracts was not associated with linguistic skills at two years ($r = 0.11$, FWE–corrected P-value $= 0.2785$), or with cognitive scores ($r = 0.12$, FWE–corrected P-value $= 0.3339$). C: Visualization of an infant brain and the reconstructed superior longitudinal fasciculus from left-frontal and frontal view. D: Scatter plot of PLS superior longitudinal fasciculus FA scores versus PLS linguistic scores. Term-equivalent FA of left and right superior longitudinal fasciculus was not associated with linguistic skills at two years ($r = 0.16$, FWE–corrected P-value $= 0.2697$). Of further interest, superior longitudinal fasciculus FA was significantly associated with cognitive scores ($r = 0.32$, FWE–corrected P-value $= 0.0390$).

Pena, 2001] and sentences from different languages [Mehler et al., 2002]. During the first year of postnatal life, rapid learning of the native language is evident and the discovery that the combinatorial properties of language can communicate information represent one of the most remarkable achievements of human learning. Although the underlying neural architecture of language acquisition is believed to be a distinct piece of the biological makeup of the human brain [Jackendoff and Pinker, 2005; Pinker, 1995], the precise neural mechanisms that allow human infants to develop this high-order cognitive function remain unclear [Dehaene-Lambertz and Spelke, 2015; Kuhl, 2010; Skeide and Friederici, 2016]. Preterm born children have impaired linguistic ability when compared with their term-born peers, even in the absence of major disabilities, which can persist as a long-lasting linguistic delay throughout childhood [van Noort-van der Spek et al., 2012]. Studying this population therefore provides an opportunity to test hypotheses concerning infant brain mechanisms linked to language acquisition and to assess the environmental effects of early life exposure.

Noninvasive brain imaging techniques provide an opportunity to assess the neuroanatomical basis of early language acquisition. Diffusion-weighted brain imaging allows the study of white-matter FA, a measure sensitive to the underlying tissue microstructure [Beaulieu, 2002]. In adulthood, the brain architecture which sub-serves language function is relatively well-known [Berwick et al., 2013; Hickok and Poeppel, 2007; Price, 2012], with the arcuate fasciculus [Catani et al., 2005] representing a potential evolutionary marker of human linguistic capability.

This study shows that in preterm infants at the time of normal birth, well before the formal emergence of natural language, the microstructural properties of both the left and right arcuate fasciculi are associated with later linguistic abilities. Previous studies in adulthood and adolescence have linked its microstructural properties to word learning

[López-Barroso et al., 2013]; the development of reading skills [Yeatman et al., 2011, 2012]; sentence comprehension performance [Skeide et al., 2015], and it has been shown to support syntactic processing of language [den Ouden et al., 2012]. We found no significant difference in term equivalent FA and tract-length between the left and right arcuate fasciculi. We also found that symmetry in the left and right arcuate fasciculi FA, rather than asymmetry, was linked to later efficient linguistic abilities. This is in accordance with the language deficiencies reported after both left and right hemispheric lesions in infants [Bates and Roe, 2001] and with the observation that arcuate fasciculus volumetric symmetry is linked to efficient auditory verbal learning in adulthood [Catani et al., 2007]. Previous studies in post-term infants have shown a left hemispheric lateralization for speech processing in the posterior part of the superior temporal region [Baldoli et al., 2015; Dehaene-Lambertz et al., 2002, 2006, 2010], but not for inferior frontal regions [Baldoli et al., 2015; Dehaene-Lambertz et al., 2006]. Indeed, left-lateralization in temporal areas increases during the first months of life [Baldoli et al., 2015; Perani et al., 2011; Shultz et al., 2014]. This bilateral linkage may also be due to the involvement of right frontal regions, which are also activated when infants listen to speech [Dehaene-Lambertz et al., 2002, 2010], and are involved in attention, stimulus selection, and response to novelty. These are important processes for infants to comprehend social world requests, to communicate wants and needs, and to produce combinatorial-grammatical sentences by the age of two years.

We may speculate on the role of the arcuate fasciculi during the first stages of language acquisition. It provides a direct link between speech production and perception and an intracerebral mechanism for the ability at birth to imitate simple articulatory movements such as opening the mouth or protusing the lips is evident from birth [Meltzoff and Moore, 1977]. Infants progressively converge toward recognizable patterns of verbal production [Kuhl and Meltzoff, 1996] and may benefit from the verbal buffer provided by the dorsal pathway to memorize and analyze speech segments [Dehaene-Lambertz et al., 2006]. The relationship between linguistic skills at 2 years and its microstructure confirm that the arcuate is a key element during the first stages of language learning.

Premature birth is associated with a long lasting signature on whole-brain architecture [Ball et al., 2012, 2014; Counsell et al., 2003; Nosarti et al., 2002; Salvan et al., 2014] and later neurodevelopment [Delobel-Ayoub et al., 2009; Johnson et al., 2009; Marlow et al., 2005; Northam et al., 2012]. While the absence of a direct comparison with term control infants limits our ability to assess the full impact of premature birth, we found that increasing prematurity at birth affects arcuate fasciculus microstructure but, in the absence of severe neonatal brain injury, only minimally modulates the identified link with later linguistic skill. Although previous behavioral studies have concluded that many of the language deficits in preterm-born children are more likely a result of general cognitive problems rather than a specific language impairment [Barre et al., 2011; Wolke and Meyer, 1999]; here, we show that the linguistic impairment in preterm born children may result from the microstructural alteration of a fundamental brain language structure.

Of importance, our results support key specific involvement of the arcuate fasciculus in language acquisition as we did not find a significant relationship with white matter microstructure in either the superior longitudinal fasciculi or the cortico-spinal tracts. Furthermore, the identified relationship between the arcuate fasciculus and both language and cognition is in agreement with cognitive models of auditory-verbal working memory which predict the presence of an underlying, efficient working memory buffer for language learning and processing [Baddeley, 2003; Baddeley et al., 1998]. At the age of two years, however, measures of complex linguistic skills strongly correlate to domain-general cognitive performance. Therefore, further investigations of specific cognitive domains are needed in our subjects at an older age to distinguish measures of formal intelligence quotient, working-memory, and attention, from phonological, syntactic processing, and semantics.

A potential limitation of this study is the use of FA as a measure of underlying white-matter microstructure. Although we used high angular resolution diffusion-MRI data and CSD based tractography to delineate the arcuate fasciculi, the observed relationship may be, at least in part, related to intersubject differences in the configuration of crossing fibers.

CONCLUSION

In summary, these results validate a neurolinguistic model in which arcuate fasciculus microstructure shortly after birth plays a role in early language acquisition. We have shown that a brain-behavior mode of covariation links linguistic performance in early childhood to a specific structure in the infant brain, which is known to support complex language function in adulthood. The microstructure of the arcuate fasciculus at around the time of normal birth underpins linguistic development at 2 years of age independent of the extreme environmental influences caused by premature extrauterine life.

ACKNOWLEDGMENTS

The authors are grateful to the families, clinicians, and investigators who made the Eprime study possible, particularly Denis Azzopardi, Mary Rutherford, and Maggie Redshaw. The views expressed are those of the authors and not necessarily those of the NHS, the NIHR, or the Department of Health.

REFERENCES

Alexander MP, Naeser MA, Palumbo CL (1987): Correlations of subcortical lesions sites and aphasia profiles. Brain 110: 961–988.

Andersson JLR, Sotiropoulos SN (2016): An integrated approach to correction for off-resonance effects and subject movement in diffusion MR imaging. Neuroimage 125:1063–1078.

Andersson JLR, Skare S, Ashburner J (2003): How to correct susceptibility distortions in spin-echo echo-planar images: Application to diffusion tensor imaging. Neuroimage 20:870–888.

Avants BB, Epstein CL, Grossman M, Gee JC (2008): Symmetric diffeomorphic image registration with cross-correlation: Evaluating automated labeling of elderly and neurodegenerative brain. Med Image Anal 12:26–41.

Baddeley A (2003): Working memory: Looking back and looking forward. Nat Rev Neurosci 4:829–839.

Baddeley A, Gathercole S, Papagno C (1998): The phonological loop as a language learning device. Psychol Rev. 105:158–173.

Baldoli C, Scola E, Della Rosa PA, Pontesilli S, Longaretti R, Poloniato A, Scotti R, Blasi V, Cirillo S, Iadanza A, Rovelli R, Barera G, Scifo P (2015): Maturation of preterm newborn brains: A fMRI–DTI study of auditory processing of linguistic stimuli and white matter development. Brain Struct Func 220: 3733–3751.

Ball G, Boardman JP, Rueckert D, Aljabar P, Arichi T, Merchant N, Gousias IS, Edwards AD, Counsell SJ (2012): The effect of preterm birth on thalamic and cortical development. Cereb Cortex 22:1016–1024.

Ball G, Aljabar P, Zebari S, Tusor N, Arichi T, Merchant N, Robinson EC, Ogundipe E, Rueckert D, Edwards AD, Counsell SJ (2014): Rich-club organization of the newborn human brain. Proc Natl Acad Sci U S A 111:7456–7461.

Barre N, Morgan A, Doyle LW, Anderson PJ (2011): Language abilities in children who were very preterm and/or very low birth weight: A meta-analysis. J Pediatr 158:766–774.

Bassi L, Ricci D, Volzone A, Allsop JM, Srinivasan L, Pai A, Ribes C, Ramenghi LA, Mercuri E, Mosca F (2008): Probabilistic diffusion tractography of the optic radiations and visual function in preterm infants at term equivalent age. Brain 131: 573–582.

Bates E, Roe K (2001): A vJ Language Development in Children with Unilateral Brain Injury. Handb Dev Cogn Neurosci 281.

Bayley N (2006): *Bayley Scales of Infant and Toddler Development: Technical Manual*. 3rd ed. San Antonio TX: Harcourt Assessment.

Beaulieu C (2002): The basis of anisotropic water diffusion in the nervous system–a technical review. NMR Biomed 15:435–455.

Benson DF, Sheremata WA, Bouchard R, Segarra JM, Price D, Geschwind N (1973): Conduction aphasia: A clinicopathological study. Arch Neurol 28:339.

Berman JI, Glass HC, Miller SP, Mukherjee P, Ferriero DM, Barkovich AJ, Vigneron DB, Henry RG (2009): Quantitative fiber tracking analysis of the optic radiation correlated with visual performance in premature newborns. Am J Neuroradiol 30:120–124.

Berwick RC, Friederici AD, Chomsky N, Bolhuis JJ (2013): Evolution, brain, and the nature of language. Trends Cogn Sci 17:89–98.

Brauer J, Anwander A, Perani D, Friederici AD (2013): Dorsal and ventral pathways in language development. Brain Lang 127: 289–295.

Catani M, Jones DK, Ffytche DH (2005): Perisylvian language networks of the human brain. Ann Neurol 57:8–16.

Catani M, Allin MPG, Husain M, Pugliese L, Mesulam MM, Murray RM, Jones DK (2007): Symmetries in human brain language pathways correlate with verbal recall. Proc Natl Acad Sci 104:17163–17168.

Counsell SJ, Allsop JM, Harrison MC, Larkman DJ, Kennea NL, Kapellou O, Cowan FM, Hajnal JV, Edwards AD, Rutherford MA (2003): Diffusion-weighted imaging of the brain in preterm infants with focal and diffuse white matter abnormality. Pediatrics 112:1–7.

Damasio H, Damasio AR (1980): The anatomical basis of conduction aphasia. Brain 103:337–350.

Dehaene-Lambertz G, Pena M (2001): Electrophysiological evidence for automatic phonetic processing in neonates. Neuroreport. 14:3155–3158.

Dehaene-Lambertz G, Spelke ES (2015): The Infancy of the Human Brain. Neuron 88:93–109.

Dehaene-Lambertz G, Dehaene S, Hertz-Pannier L (2002): Functional neuroimaging of speech perception in infants. Science 298:2013–2015.

Dehaene-Lambertz G, Hertz-Pannier L, Dubois J, Mériaux S, Roche A, Sigman M, Dehaene S (2006): Functional organization of perisylvian activation during presentation of sentences in preverbal infants. Proc Natl Acad Sci U S A 103:14240–14245.

Dehaene-Lambertz G, Montavont A, Jobert A, Allirol L (2010): Language or music, mother or Mozart? Structural and environmental influences on infants' language networks. Brain Lang. 2:53–65.

Delobel-Ayoub M, Arnaud C, White-Koning M, Casper C, Pierrat V, Garel M, Burguet A, Roze J-C, Matis J, Picaud J-C (2009): Behavioral problems and cognitive performance at 5 years of age after very preterm birth: the EPIPAGE Study. Pediatrics 123:1485–1492.

Dubois J, Poupon C, Thirion B, Simonnet H, Kulikova S, Leroy F, Hertz-Pannier L, Dehaene-Lambertz G (2015): Exploring the early organization and maturation of linguistic pathways in the human infant brain. Cereb Cortex bhv082.

Forkel SJ, De Schotten MT, Dell'Acqua F, Kalra L, Murphy DGM, Williams SCR, Catani M (2014): Anatomical predictors of aphasia recovery: A tractography study of bilateral perisylvian language networks. Brain 137:2027–2039.

Geschwind N (1965): Disconnexion syndromes in animals and man. Brain 88:585.

Groppo M, Ricci D, Bassi L, Merchant N, Doria V, Arichi T, Allsop JM, Ramenghi L, Fox MJ, Cowan FM (2014): Development of the optic radiations and visual function after premature birth. Cortex 56:30–37.

Hickok G (2012): Computational neuroanatomy of speech production. Nat Rev Neurosci 13:135–145.

Hickok G, Poeppel D (2007): The cortical organization of speech processing. Nat Rev Neurosci 8:393–402.

Hotelling H (1936): Relations between two sets of variates. Biometrika 28:321–377.

Hüppi PS, Maier SE, Peled S, Zientara GP, Barnes PD, Jolesz FA, Volpe JJ, Huppi PS, Maier SE, Peled S, Zientara GP, Barnes PD, Jolesz FA, Volpe JJ (1998): Microstructural development of human newborn cerebral white matter assessed in vivo by diffusion tensor magnetic resonance imaging. Pediatr Res 44:584–590.

Jackendoff R, Pinker S (2005): The nature of the language faculty and its implications for evolution of language (Reply to Fitch, Hauser, and Chomsky). Cognition 97:211–225.

Johnson S, Fawke J, Hennessy E, Rowell V, Thomas S, Wolke D, Marlow N (2009): Neurodevelopmental disability through 11

years of age in children born before 26 weeks of gestation. Pediatrics 124:e249–e257.
Kuhl PK (2010): Brain Mechanisms in Early Language Acquisition. Neuron 67:713–727.
Kuhl P, Meltzoff A (1996): Infant vocalizations in response to speech: Vocal imitation and developmental change. J Acoust Soc. 100:2425–2438.
Liberman AM, Mattingly IG (1985): The motor theory of speech perception revised. Cognition 21:1–36.
López-Barroso D, Catani M, Ripollés P, Dell'Acqua F, Rodríguez-Fornells A, de Diego-Balaguer R (2013): Word learning is mediated by the left arcuate fasciculus. Proc Natl Acad Sci U S A 110:13168–13173.
Luu TM, Vohr BR, Schneider KC, Katz KH, Tucker R, Allan WC, Ment LR (2009): Trajectories of receptive language development from 3 to 12 years of age for very preterm children. Pediatrics 124:333–341.
Luu TM, Vohr BR, Allan W, Schneider KC, Ment LR (2011): Evidence for catch-up in cognition and receptive vocabulary among adolescents born very preterm. Pediatrics 128:313–322.
Makropoulos A, Gousias IS, Ledig C, Aljabar P, Serag A, Hajnal JV, Edwards AD, Counsell SJ, Rueckert D (2014): Automatic whole brain MRI segmentation of the developing neonatal brain. IEEE Trans Med Imaging 33:1818–1831.
Marlow N, Wolke D, Bracewell MA, Samara M (2005): Neurologic and developmental disability at six years of age after extremely preterm birth. N Engl J Med 352:9–19.
Mehler J, Jusczyk P, Lambertz G, Halsted N, Bertoncini J, Amiel-Tison C (2002): A precursor of language acquisition in young infants. Psycholinguist Crit Concepts Psychol 4:25.
Meltzoff A, Moore M (1977): Imitation of facial and manual gestures by human neonates. Science. 198:75–78.
van Noort-van der Spek IL, Franken M-CJP, Weisglas-Kuperus N (2012): Language Functions in Preterm-Born Children: A Systematic Review and Meta-analysis. Pediatrics 129:745–754.
Northam GB, Liégeois F, Tournier J-D, Croft LJ, Johns PN, Chong WK, Wyatt JS, Baldeweg T (2012): Interhemispheric temporal lobe connectivity predicts language impairment in adolescents born preterm. Brain 135:3781–3798.
Nosarti C, Al-Asady MHS, Frangou S, Stewart AL, Rifkin L, Murray RM (2002): Adolescents who were born very preterm have decreased brain volumes. Brain 125:1616–1623.
den Ouden D-B, Saur D, Mader W, Schelter B, Lukic S, Wali E, Timmer J, Thompson CK (2012): Network modulation during complex syntactic processing. Neuroimage 59:815–823.
Paldino M, Hedges K, Golriz F (2016): The Arcuate Fasciculus and Language Development in a Cohort of Pediatric Patients with Malformations of Cortical Development. Am J. 37:169–175.
Pedregosa F, Varoquaux G, Gramfort A, Michel V, Thirion B, Grisel O, Blondel M, Prettenhofer P, Weiss R, Dubourg V (2011): Scikit-learn: Machine learning in Python. J Mach Learn Res 12:2825–2830.
Perani D, Saccuman MC, Scifo P, Anwander A, Spada D, Baldoli C, Poloniato A, Lohmann G, Friederici AD (2011): Neural language networks at birth. Proc Natl Acad Sci U S A 108:16056–16061.
Petrides M, Pandya DN (1984): Projections to the frontal cortex from the posterior parietal region in the rhesus monkey. J Comp Neurol 228:105–116.
Pinker S (1995): The language instinct: The new science of language and mind, Vol. 7529. UK: Penguin.
Price CJ (2012): A review and synthesis of the first 20years of PET and fMRI studies of heard speech, spoken language and reading. Neuroimage 62:816–847.
Rilling JK, Glasser MF, Preuss TM, Ma X, Zhao T, Hu X, Behrens TEJ (2008): The evolution of the arcuate fasciculus revealed with comparative DTI. Nat Neurosci 11:426–428.
Rilling JK, Glasser MF, Jbabdi S, Andersson J, Preuss TM (2011): Continuity, divergence, and the evolution of brain language pathways. Front Evol Neurosci 3:
Rose SE, Hatzigeorgiou X, Strudwick MW, Durbridge G, Davies PSW, Colditz PB (2008): Altered white matter diffusion anisotropy in normal and preterm infants at term-equivalent age. Magn Reson Med 60:761–767.
Rosipal R, Krämer N (2006): Overview and recent advances in partial least squares. In: Saunders C, Grobelnik M, Gunn S, Shawe-Taylor J, editors. *Subspace, Latent Structure and Feature Selection Techniques*. New York: Springer. pp 34–51.
Salvan P, Froudist Walsh S, Allin MPG, Walshe M, Murray RM, Bhattacharyya S, Mcguire PK, Williams SCR, Nosarti C (2014): Road work on memory lane-Functional and structural alterations to the learning and memory circuit in adults born very preterm. Neuroimage. 114:152–161.
Schmahmann JD, Pandya DN, Wang R, Dai G, D'Arceuil HE, de Crespigny AJ, Wedeen VJ (2007): Association fibre pathways of the brain: Parallel observations from diffusion spectrum imaging and autoradiography. Brain 130:630–653.
de Schotten MT, Dell'Acqua F, Forkel SJ, Simmons A, Vergani F, Murphy DGM, Catani M (2011): A lateralized brain network for visuospatial attention. Nat Neurosci 14:1245–1246.
de Schotten MT, Dell'Acqua F, Valabregue R, Catani M (2012): Monkey to human comparative anatomy of the frontal lobe association tracts. Cortex 48:82–96.
Shultz S, Vouloumanos A, Bennett R (2014): Neural specialization for speech in the first months of life. Developmental. 17:766–774.
Skeide M, Friederici A (2016): The ontogeny of the cortical language network. Nat Rev Neurosci. 17:323–332.
Skeide MA, Brauer J, Friederici AD (2015): Brain functional and structural predictors of language performance. Cereb Cortex bhv042.
Smith SM, Jenkinson M, Woolrich MW, Beckmann CF, Behrens TEJ, Johansen-Berg H, Bannister PR, De Luca M, Drobnjak I, Flitney DE (2004): Advances in functional and structural MR image analysis and implementation as FSL. Neuroimage 23: S208–S219.
Smith RE, Tournier J-D, Calamante F, Connelly A (2012): Anatomically-constrained tractography: Improved diffusion MRI streamlines tractography through effective use of anatomical information. Neuroimage 62:1924–1938.
Smith RE, Tournier J-D, Calamante F, Connelly A (2015): SIFT2: Enabling dense quantitative assessment of brain white matter connectivity using streamlines tractography. Neuroimage 119: 338–351.
Toulmin H, Beckmann CF, O'Muircheartaigh J, Ball G, Nongena P, Makropoulos A, Ederies A, Counsell SJ, Kennea N, Arichi T, Tusor N, Rutherford MA, Azzopardi D, Gonzalez-Cinca N, Hajnal JV, Edwards AD (2015): Specialization and integration of functional thalamocortical connectivity in the human infant. Proc Natl Acad Sci U S A 201422638.
Tournier J-D, Calamante F, Gadian DG, Connelly A (2004): Direct estimation of the fiber orientation density function from diffusion-weighted MRI data using spherical deconvolution. Neuroimage 23:1176–1185.
Tournier J-D, Calamante F, Connelly A (2007): Robust determination of the fibre orientation distribution in diffusion MRI: Non-negativity constrained super-resolved spherical deconvolution. Neuroimage 35:1459–1472.

Tournier JD, Calamante F, Connelly A (2012): MRtrix: Diffusion tractography in crossing fiber regions. Int J Imaging Syst Technol 22:53–66.

Vestergaard M, Madsen KS, Baaré WFC, Skimminge A, Ejersbo LR, Ramsøy TZ, Gerlach C, Åkeson P, Paulson OB, Jernigan TL (2011): White Matter Microstructure in Superior Longitudinal Fasciculus Associated with Spatial Working Memory Performance in Children. J Cogn Neurosci 23:2135–2146.

Wegelin JA (2000): "A Survey of Partial Least Squares (PLS) Methods, with Emphasis on the Two-Block Case," technical report, Dept. of Statistics, Univ. of Washington.

Wilson B, Sundaram S, Huq A, Jeong J (2011): Abnormal language pathway in children with Angelman syndrome. Pediatric. 44:350–356.

Winkler AMA, Ridgway GRG, Webster MA, Smith SSM, Nichols TE (2014): Permutation inference for the general linear model. Neuroimage 92:381–397.

Wolke D, Meyer R (1999): Cognitive status, language attainment, and prereading skills of 6-year-old very preterm children and their peers: The Bavarian Longitudinal Study. Dev Med Child Neurol 41:94–109.

Yeatman JD, Dougherty RF, Rykhlevskaia E, Sherbondy AJ, Deutsch GK, Wandell BA, Ben-Shachar M (2011): Anatomical properties of the arcuate fasciculus predict phonological and reading skills in children. J Cogn Neurosci 23:3304–3317.

Yeatman JD, Dougherty RF, Ben-Shachar M, Wandell BA (2012): Development of white matter and reading skills. Proc Natl Acad Sci U S A 109:E3045–E3053.